Stimulation-specific effects of low intensity repetitive magnetic stimulation on cortical neurons and neural circuit repair in vitro (studying the impact of pulsed magnetic fields on neural tissue)

Stephanie Grehl

THE UNIVERSITY OF WESTERN AUSTRALIA

UPMC SORBONNE UNIVERSITÉS

Stimulation-Specific Effects of Low Intensity Repetitive Magnetic Stimulation On Cortical Neurons and Neural Circuit Repair *In Vitro*

(Studying the impact of pulsed magnetic fields on neural tissue)

Les Effets de la Stimulation Magnétique Répétée de Faible Intensité sur les Neurones Corticaux et sur la Réparation des Circuits Neuronaux *in vitro*

(Une étude de l'impact des champs magnétiques pulsés sur le tissu nerveux)

Par **Stephanie Grehl** *(MSc)*

Thèse de doctorat de Neurosciences

Dirigée par Dr Jennifer RODGER et Pr Rachel SHERRARD

Présentée et soutenue publiquement le 17th June 2014

Devant un jury composé de :

TOMKINS Joseph Prof	Président
HOOL Livia, Prof	Examiner
BATES Krityn A/Prof	Examiner
RODGER Jennifer, A/Prof	Directrice de Thèse
SHERRARD Rachel Prof	Directrice de Thèse

The University of Western Australia

School of Animal Biology
Exp & Regen Neuroscience

Université Pierre et Marie Curie

École doctorale Cerveau-Cognition-Comportement
UMR8256 Biological Adaptation and Ageing
Dév Reparation et Vieillissement Cérébral

This thesis is presented for the joint degree of Doctor of Philosophy of the University of Western Australia, and Université Pierre et Marie Curie, France

Stephanie Grehl

The School of Animal Biology, UWA
L'Ecole doctorale Cerveau-Cognition-Comportement (ED3C), UPMC

STIMULATION-SPECIFIC EFFECTS of low intensity repetitive magnetic stimulation on CORTICAL NEURONS and NEURAL CIRCUIT REPAIR *in vitro.*

Abstract

Electromagnetic fields are widely used to non-invasively stimulate the human brain in clinical treatment and research. Repetitive transcranial magnetic stimulation (rTMS) in humans is applied with maximal high-intensity fields of ~1-2.5 Tesla (T), however the coils used induce currents both at the site of maximum stimulation and in surrounding brain regions, albeit at lower intensities. Importantly, low intensity repetitive transcranial magnetic stimulation in humans (mT range) modifies cortical function, brain oscillations and is beneficial for the treatment of depression. While the effects of magnetic stimulation have been suggested to vary according to frequency and intensity, mechanisms called into action by these parameters and adjacent low-intensity subthreshold stimulation remain unknown.

We investigated the effects of different low intensity repetitive magnetic stimulation (LI-rMS) parameters (10-13 mT) *in vitro* and describe key aspects of custom tailored LI-rMS delivery for the *in vitro* setting. We applied LI-rMS at different frequencies to primary cortical cultures for 4 days and assessed survival and morphological changes. To understand underlying mechanisms, we measured intracellular calcium flux during LI-rMS and subsequent changes in gene expression. Our results show stimulation-specific effects of LI-rMS. In cortical cultures, straight high frequencies (10 Hz and 100 Hz) affected cell survival, while neuronal outgrowth and branching were inhibited only by 1 Hz stimulation. Moreover, all frequencies induced calcium release from intracellular stores and induced stimulation-specific changes in expression of genes related to apoptosis and neurite outgrowth.

Further, we investigated the effects of LI-rMS on neural circuit repair. In organotypic murine hindbrains the cerebellum was denervated then stimulated for 2 weeks and neuronal reinnervation and survival was assessed. To understand underlying mechanisms, we measured changes in gene expression and acute cellular activation after a single LI-rMS session. We show that, LI-rMS did not reduce Purkinje cell survival within the olivo-cerbellar explant, while patterned-high-frequency stimulation increased cerebellar c-fos expression and induced Purkinje cell reinnervation.

Stimulation-induced reinnervation was associated with changes in brain derived neurotrophic factor (BDNF) gene expression.

In addition, we identified the parameters required to build a stimulation system that is tailored for our *in vitro* explant culture requirements. Here we demonstrate and discuss the creation and optimization of an automated and adjustable multi-target stimulation system that can deliver a high range of LI-rMS frequencies to organotypic cultures.

Taken together, we show for the first time an underlying mechanism of cellular activation at stimulation levels below neuronal firing. Our results highlight the biological importance of LI-rMS either on its own or as a contributor to the effects of rTMS. Further understanding of the fundamental effects of LI-rMS on biological tissue is essential to better tailor future therapeutic application of rTMS and explore the therapeutic potential of LI-rMS.

Keywords: Magnetic stimulation, rTMS, rMS, EMF, low intensity, cortical neurons, neuronal network, gene expression, *in vitro*, coil design, device design, LI-rMS

Table of contents

List of Figures

CHAPTER 1

CHAPTER 2

CHAPTER 3

CHAPTER 4

APPENDIX

List of Tables

Abbreviations

AChE	acetylcholinesterase
AF	alexa fluor
AMPA	α-amino-3-hydroxy-5-methyl-4-isoxazolepropionic acid
AraC	cytosine d-D-arabinofuranoside
$\vec{B}$	magnetic field
BDNF	brain derived neurotrophic factor
BHFS	biomimetic high frequency stimulation
Ca^{2+}	calcium
CaBP	calbindin
CaMKII	calmodulin-dependent protein kinase II
cAMP	cyclic adenosine monophosphate
cDNA	complementary deoxyribonucleic acid
CER	cerebellum
CF	climbing fibre
c-fos	FBJ murine osteosarcoma oncogene
CNS	central nervous system
CREB	cAMP response element-binding protein
DAG	diacylglycerol
DIV	day(s) in vitro
Dx	denervation
E	embryonic
$\vec{E}$	electric field
EMF	electromotive force
ER	endoplasmic reticulum
ERK	extracellular signal-regulated kinase
ex - em	excitation - emission
FA	analysed field
GABA	gamma-aminobutyric acid
GAD	glutamic acid decarboxylase
HCN	hyperpolarization-activated cyclic nucleotide
Hz	Hertz
ION	inferior olive nucleus
IP3(R)	inositol 1,4,5-trisphosphate (receptor)
KO	knockout
LI	low intensity

LTD/P	long term depression / potentiation
M (n/µ)	molar (nano / micro)
MAPK	mitogen-activated protein kinase
MEP	motor evoked potentials
NMDA	N-methyl-D-aspartate
NO	nitric oxide
P	postnatal
p75/LNGFR	low-affinity nerve growth factor receptor
Pax3	paired box 3
PBS	phosphate buffered saline
PC	Purkinje cell
PI	propidium iodide
PI3K	phosphoinositide 3-kinase
PKA	protein kinase A
PKB/Akt	protein kinase B
PKC	protein kinase C
PLC	phospholipase C
PSA-NCAM	polysialylated - neural cell adhesion molecule
PV	parvalbumin
Px	pedunculotomy
RL	resistor inductor
rMS	repetitive magnetic stimulation
RMT	resting motor threshold
RNA	ribonucleic acid
ROS	reactive oxygen species
RT	room temperature
RyR	ryanodine receptor
ST8SiaII/Sia2	ST8 alpha-N-acetyl-neuraminide alpha-2,8-sialyltransferase 2
ST8SiaIV/Sia4	ST8 alpha-N-acetyl-neuraminide alpha-2,8-sialyltransferase 4
SYN	synaptophysin
T (m)	Tesla (milli)
TBS (i/c)	theta burst stimulation (intermittent / continuous)
TMS (sp/r)	transcranial magnetic stimulation (single pulse / repetitive)
TrkB	kinase receptor type B
TRP	transient receptor potential
VGCC	voltage-gated calcium channels
VGLUT (1/2)	marker vesicular glutamate transporter (1 / 2)

Acknowledgements

First, I would like to thank my supervisors for their guidance and support throughout this thesis. My sincere gratitude goes to Assoc/Prof Jennifer Rodger at UWA for giving me this and many other opportunities, for all the support and teaching over the years and especially for the tireless provision of feedback on all my work and to Prof Rachel Sherrard at UPMC for all her support, especially for endlessly pushing me to further my written and verbal communication skills and her needle-sharp dissection of my work. I am deeply thankful to Prof Livia Hool for sharing her expertise with me and all the feedback and words of encouragement and W/Prof Sarah Dunlop for the detailed feedback on my writing and support at even the busiest of times.

I am deeply grateful to Marissa Penrose who has taught me so many techniques and has helped in so many matters big and small and to Dr Helena Viola for teaching me and sharing with me her extensive calcium imaging expertise. I would like to thank Juan Sebastián Jara and Natalie Morellini for their technical assistance and for many many laughs under the hood and all the staff and students at EaRN and especially my fellow office mates for creating such a positive, supportive and above all fun and enthusiastic atmosphere. I deeply thank my family and friends for always believing in me and for never losing patience for missing so many big and small events throughout the years and above all David without whom this thesis would not have been possible.

This work was made possible under the French-Australian PhD cotutelle Program. Funding was provided by the Australian Research Council (ARC), Neurotrauma Research Program (NRP) and French National Center for Scientific Research (CNRS) PICS grants. Moreover, I would like to thank the School of Animal Biology, UWA for providing me over the period of this thesis with a scholarship for International Research Fees (SIRF), contributing to the living allowance stipend, and support with PhD completion.

Statement of **candidate contribution**

THE UNIVERSITY OF
WESTERN AUSTRALIA

DECLARATION FOR THESES CONTAINING PUBLISHED WORK AND/OR WORK PREPARED FOR PUBLICATION

The examination of the thesis is an examination of the work of the student. The work must have been substantially conducted by the student during enrolment in the degree.

Where the thesis includes work to which others have contributed, the thesis must include a statement that makes the student's contribution clear to the examiners. This may be in the form of a description of the precise contribution of the student to the work presented for examination and/or a statement of the percentage of the work that was done by the student.

In addition, in the case of co-authored publications included in the thesis, each author must give their signed permission for the work to be included. If signatures from all the authors cannot be obtained, the statement detailing the student's contribution to the work must be signed by the coordinating supervisor.

This thesis contains published work and/or work prepared for publication, **some of which has been co-authored**. The bibliographical details of the work and where it appears in the thesis are outlined below.
The student must attach to this declaration a statement for each publication that clarifies the contribution of the student to the work. This may be in the form of a description of the precise contributions of the student to the published work and/or a statement of percent contribution by the student. This statement must be signed by all authors. **If signatures from all the authors cannot be obtained, the statement detailing the student's contribution to the published work must be signed by the coordinating supervisor**.

1. Grehl, S., Viola, H. M., Fuller-Carter, P. I., Carter, K. W., Dunlop, S. A., Hool, L. C., Sherrard, R.M., Rodger, J. (2015). Cellular and Molecular Changes to Cortical Neurons Following Low Intensity Repetitive Magnetic Stimulation at Different Frequencies. *Brain Stimulation, 8*(1), 114-123. (Appendix E)

   SG contribution: 85 %

2. Grehl S., Martina D., Rodger J. & Sherrard RM. (2015). Optimizing *in vitro* magnetic stimulation: A simple, adjustable and cost-efficient stimulation device that can be tailored to different experimental requirements. *Results compiled for publication.*

   SG contribution: 70 %

3. Grehl S., Goyenvalle C., Dunlop SA., Rodger J. & Sherrard RM. (2015). Low intensity repetitive magnetic stimulation induces olivo-cerebellar reinnervation. *Results compiled for publication.*

   SG contribution: 95 %

Student Signature

S.GREHL (pasted electronic signature)

Coordinating Supervisor Signature

J.RODGER (pasted electronic signature)

Chapter 1

1 GENERAL INTRODUCTION

1.1 Stimulating the brain

1.1.1 A History

Electric stimulation of the human body has a long tradition. One of the first demonstrations was in the 1700s by Galvani, where he showed that electric stimulation can induce responses in isolated frog nerves and muscles (Galvani, 1791). This sparked intensive interest into the electrical excitability of biological tissues, leading to the discovery of muscle activation via electric stimulation of different areas of the motor cortex (Carlson & Devinsky, 2009). Pioneers in this field were Fritsch and Hitzig, two neuroscientists who demonstrated for the first time that electric stimulation in animals can reveal basic motor cortex maps and generate contralateral muscle activation (Carlson & Devinsky, 2009). These experiments paved the way to a wide application of electric stimulation in both diagnostic and therapeutic research.

At a similar time-period, Michael Faraday first described in 1831 the phenomenon of electromagnetic induction, predicting how a changing magnetic field would interact with an electric circuit to produce an electromotive force (EMF) (Walsh, 2003). This sparked extensive research into the effects of changing magnetic fields on nerve tissue. Magnusson and Stevens in 1914 (Walsh, 2003) discovered the induction of phosphenes in the subjects' visual perception and this was followed by Kolin and colleagues in 1959 showing that these visual perceptions could be reliably induced with the application of alternating magnetic fields in other locations than the retina,

namely around the occipital cortex (Walsh, 2003). Kolin and colleagues then proceeded to demonstrate for the first time magnetic activation of nervous tissue in an isolated frog muscle *in vitro* (Walsh, 2003), leading to wide research into the activation of nerves and muscle *via* the application of alternating magnetic fields. However, principally due to technological difficulties of producing strong and fast enough changing magnetic fields, it was not before 1985 that Barker, Jalinous, & Freeston were able to show for the first time hand muscle activation as a result of human motor cortex stimulation with alternating magnetic fields. This caused a surge of clinical and experimental interest into the application of transcranial magnetic stimulation (TMS), in particular because in contrast to electric stimulation, TMS application is non-painful and not attenuated by hair, tissue or bone. The secondary current created in the underlying cortex as a result of the changing magnetic field, deteriorates only as a function of distance and time from the initial point of stimulation (Cracco, Cracco, Maccabee, & Amassian, 1999; Pascual-Leone, Bartres-Faz, & Keenan, 1999; Pascual-Leone, Walsh, & Rothwell, 2000; Walsh & Rushworth, 1999) and as a consequence, brain tissue can be stimulated over discrete areas and for finite times, increasing focality of the stimulation. Since the year of its first application, interest in TMS has increased exponentially and it is currently widely applied as a non-invasive method for brain stimulation in experimental and clinical settings.

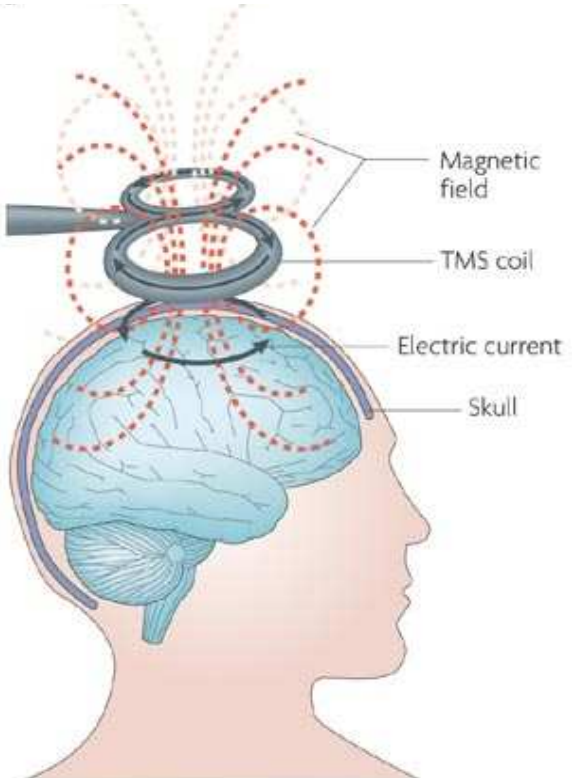

Figure 1.1 Overview of electromagnetic induction in TMS. A pulsed (time varying) primary current inside the coil creates a changing (time varying) magnetic field. Which induces an electric field, that creates a secondary electric current in conductive brain tissue in an opposite direction to the primary current. Image adapted from Ridding & Rothwell (2007).

1.2 Electromagnetic principles

Based on the principle of electromagnetic induction, a pulsed primary electric current flowing in one direction creates a magnetic field perpendicular to that primary current (Pascual-Leone et al., 2000; Walsh & Rushworth, 1999). This varying magnetic field in turn induces a perpendicular electric field, which can create a secondary electric current of opposite direction to the primary current in a nearby conductor (Wassermann et al., 2008). Hence, TMS is sometimes described as 'carrying' an electric current to the cortex (Siebner, Hartwigsen, Kassuba, & Rothwell, 2009) (Fig 1.1).

It has been widely suggested that magnetic stimulation, or more precisely the created secondary current, changes the membrane potential of a neuron and thus its excitability (Di Lazzaro et al., 2003; Wassermann et al., 2008). For this to occur, a flow of electric charge across the membrane is required, where the relevant parameter for effective membrane depolarization is the total amount of charge transferred across the membrane (Pell, Roth, & Zangen, 2011). The amount of charge depends on several factors, such as strength and direction of the induced electric field and the biological structure's inherent conductivity. Specifically, to have an effect on a cell membrane, the induced electric field needs to produce a gradient change of electric charge at some point of the neuron (Fig 1.2) (Bailey, Karhu, & Ilmoniemi, 2001; Di Lazzaro et al., 2003; Radman, Ramos, Brumberg, & Bikson, 2009; Ruohonen & Ilmoniemi, 1999; Siebner et al., 2009). It has been widely suggested that long structures such as axons are more likely to be affected in a uniform electric field, where the precise effect depends on several different geometrical factors such as axon size, bending and branching (Fatemi-Ardekani, 2008; Ruohonen & Ilmoniemi, 1999). In contrast cell bodies are suggested to be more likely directly activated in response to gradient changes along the soma membrane as a result of a non-uniform electric field (McIntyre & Grill, 2002). However, recently it was proposed that this mechanism is more applicable to relatively long and thick peripheral axons, while central nervous system (CNS) neurons with their relatively short and thin axons are suggested to show strongest depolarization responses at their larger cell somata, increasing with increasing diameter (Pashut et al., 2011). However, to date no experimental studies have been able to directly record membrane potential changes in different cells in response to TMS induced electric field parameters.

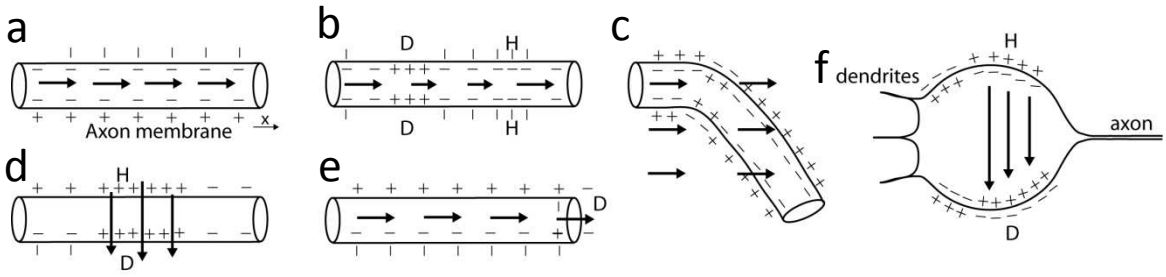

Figure 1.2 Illustration of possible activation mechanism of magnetic stimulation by gradient changes to membrane potentials. a) A uniform electric field (black arrows) flowing parallel to the axon does not result in gradients along the axon and hence no membrane potential changes occur. b) A non-uniform electric field induces partial membrane potential changes. c) An uniform electric field along a bending axon (spatial variation) causes strong membrane potential changes. d) An electric field perpendicular to an axon results in strong membrane potential changes. e) An electric field induces change at axonal terminals and f) A non-uniform field at a relative larger soma, induces partial membrane potential changes. D and H represent depolarization and hyper-polarization, respectively. Strong membrane depolarization through b, c, d, e or f are suggested to be able to generate action potentials. Figure partially adapted from Ruohonen & Ilmoniemi (1999).

1.3 Stimulation parameters

One major parameter that influences the direction and amplitude of the induced electric field is how fast the magnetic field changes over time, which occurs during the rise-time and fall-time of the magnetic pulse as defined by the Maxwell-Faraday equation:

$$\nabla \mathrm{x}\, \mathrm{E} = -\frac{\partial \vec{B}}{\partial \mathrm{t}} \qquad \text{(Jackson, 1962)}$$

Where ∇ is the curl operator, E the electric field and $\vec{B}$ the magnetic field with time *t*. Thus, the amplitude of the induced electric field is dependent not only on the amplitude of the magnetic field, but also how fast it changes in its amplitude over time.

1.3.1 The stimulator output

To be able to produce a changing magnetic field, a stimulator that holds an electrical charge is needed in addition to a stimulation coil through which the electric current can flow to produce a magnetic pulse (Wassermann et al., 2008).

The stimulator consists of a power source, a capacitor (to store the current) and a switch that determines when the current flows into the coil (Wassermann et al., 2008). Commercially available stimulation devices are based on oscillatory circuits and produce exclusively sinusoidal pulses (Goetz et al., 2012; Goetz et al., 2013b). This means that rise- and fall-time of the pulse are fixed and cannot be controlled by the user, limiting the control of stimulation strength to adjustments in magnetic field amplitude. However, these stimulator set-ups are very energy inefficient, with only about 1 % of the electric pulse energy transferred to the target (Hsu, Nagarajan, & Durand, 2003). The high losses of energy lead to heating of the coil with increasing pulse number (Goetz et al., 2013b).

Stimulators can generate either a monophasic pulse whereby pulse oscillation is damped by a resistor, or a biphasic/polyphasic pulse where current flow is interrupted after ≥ one full cycle (Fig 1.3A) (Goetz et al., 2012; Goetz et al., 2013b). In a monophasic pulse, current flows through the coil for one quarter-cycle of the sine-wave (Wassermann et al., 2008). A biphasic pulse is terminated after one full sine-wave cycle (4 quarter cycles), while the polyphasic pulse consists of more than one full cycle (Kammer, Beck, Thielscher, Laubis-Herrmann, & Topka, 2001; Wassermann et al., 2008). Quarter cycle duration can range between 70-100 μs, however optimal durations have not been systematically investigated (Wassermann et al., 2008). However, a recent study modelling membrane depolarization of CNS neurons in

response to single TMS pulses, suggested total pulse oscillation to be optimal around 400 µs (Pashut et al., 2011). Nonetheless, it has to be taken into account that different stimulator and coil systems produce slightly different current characteristics (Fig 1.3B) that can have different experimental outcomes (Kammer et al., 2001).

In general, monophasic and bi/polyphasic pulses are known to have different neuromodulatory effects (Arai et al., 2005; Maccabee et al., 1998; Sommer et al., 2006; Sommer, Lang, Tergau, & Paulus, 2002). Monophasic pulses are suggested to influence neuronal axons that lie in one spatial domain of the uni-directional induced electric current and are suggested to activate similar neuronal populations (Arai et al., 2005). Thus, effects of monophasic pulses are more sensitive to the magnetic field direction in relation to the target (Wassermann et al., 2008). In contrast, bi/polyphasic pulses can excite neuronal axons that lie in both spatial domains, due to induced current inversion in the second/following quarter cycle phases (Wassermann et al., 2008). Hence these pulses are thought to activate different neuronal populations (e.g. facilitatory and inhibitory) leading to possible opposite or cancelling of overall effects (Arai et al., 2005). Research suggest that bi/polyphasic pulses are more powerful in single stimuli application while monophasic pulses have been shown to induce stronger neuromodulatory effects in repeated applications at the same stimulation intensity, due to possible summation from repeated activation of a homogenous neuronal subpopulation (Arai et al., 2005; Sommer et al., 2006; Sommer et al., 2002).

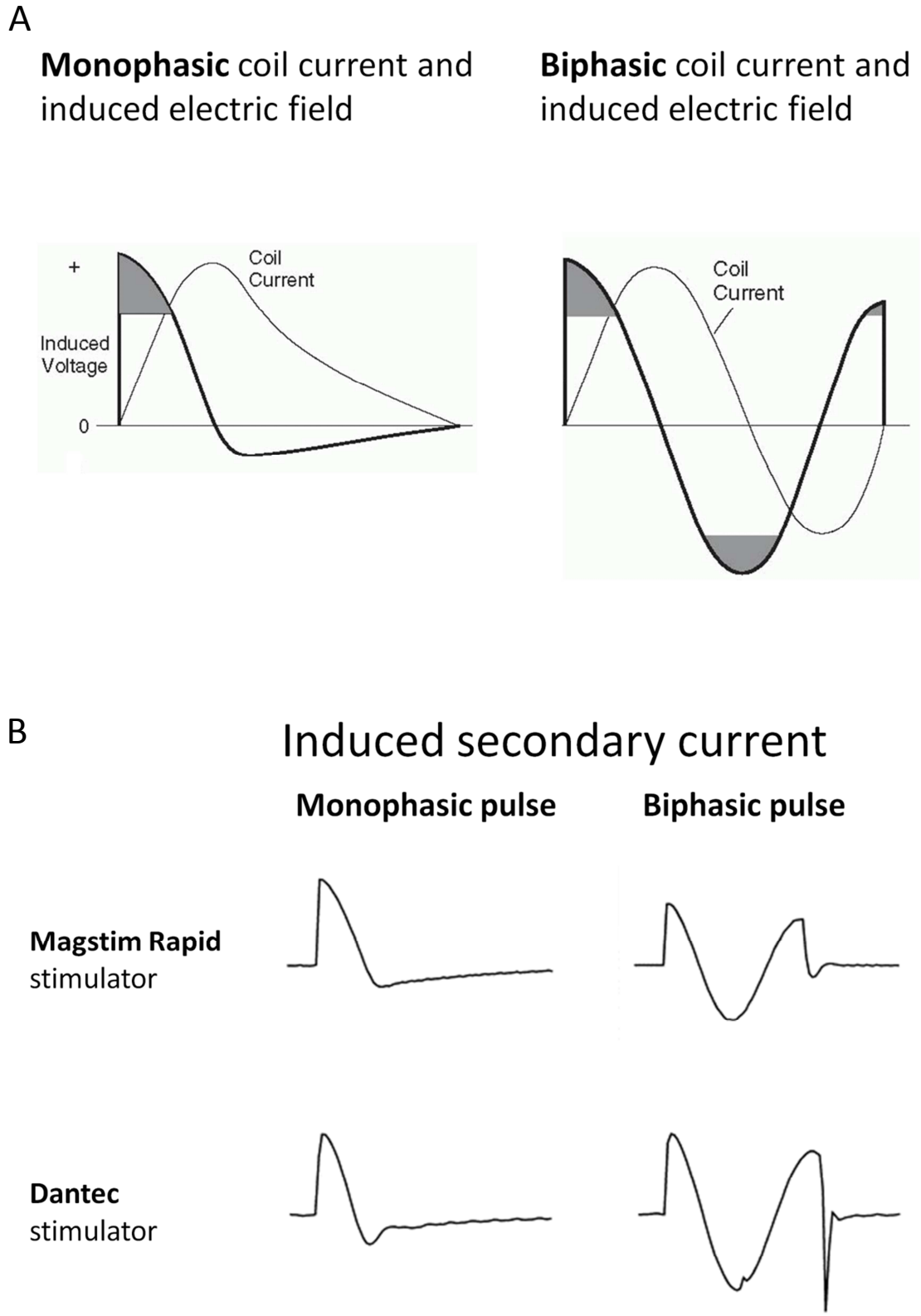

Figure 1.3 Illustration of induced electric field and secondary current produced by monophasic or biphasic pulse form. A) Schematic illustration of the current in a stimulation coil and its associated induced electric field voltage in a nearby conductor during either a monophasic or biphasic pulse. Figure adapted from Wassermann, et al., (2008). B) Illustration of the induced secondary current in a nearby conducting pick-up coil resulting from two different commercially available stimulators and figure-of-eight shaped coils at the same level of stimulator output. Figure adapted from Kammer, et al. (2001).

However, current pulse forms are based more on availability than consideration for optimal neuronal activation (Goetz et al., 2013b). Considering this and energy efficiency, the exploration of alternative pulse forms is necessary and might be advantageous. A few studies so far have used different experimental waveforms (Havel et al., 1997; Sommer et al., 2006). Recently, one group (Peterchev, Murphy, & Lisanby, 2011) showed that the implementation of a new stimulator set-up with a near-triangular waveform generation increased energy efficiency and decreased coil heating, while inducing strong membrane depolarisation (Peterchev et al., 2011). Other waveform optimization proposals have been put forward with a variety of novel stimulator designs under development (Goetz, Helling, & Weyh, 2013a; Goetz et al., 2012; Goetz et al., 2013b).

1.3.2 Coil design

TMS coils consist of a conducting wire, usually copper, which is surrounded by an insulating plastic (Pascual-Leone et al., 1999) and held over the subject's head. For human TMS application there are several coil designs, the two most commonly used being a classic round coil design or the figure-of-eight shaped coil (Fig 1.4) (Cohen et al., 1990; Hallett, 2007). Different coil designs produce differently shaped magnetic fields, determining the location or area of strongest stimulation point, total area stimulated and stimulation depth (Deng, Lisanby, & Peterchev, 2013; Lang et al., 2006).

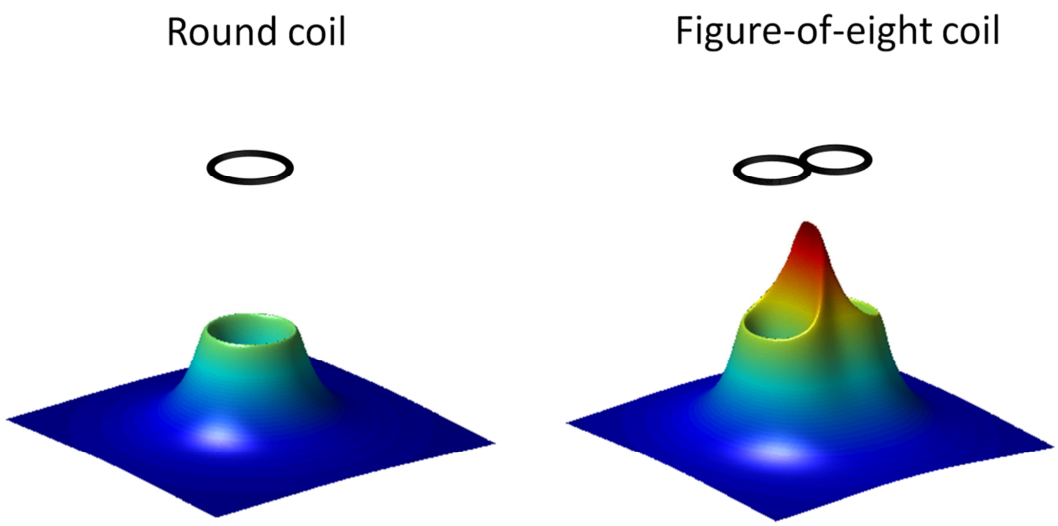

Figure 1.4 Shape of stimulation coils and their associated magnetic field. Classic round shaped coil with its associated magnetic field, showing strongest field intensities under the edges of the coil. A figure of eight coil with it associated magnetic field, with strongest field intensities under the central intersection of the two adjacent coil loops.

In human TMS application, commercially available stimulator coils generally produce a maximal magnetic field strength of 1-2.5 Tesla (T) (Rossini et al., 1994). The strength of stimulus decreases with increasing distance from the coil and maximal point of stimulation (Thielscher & Kammer, 2002), leaving regions surrounding the focal point to also receive stimulation but at increasingly lower intensities (Fig 1.4) (Cohen et al., 1990; Deng et al., 2013; Thielscher & Kammer, 2002).

1.3.3 Stimulation intensity

Measurement of the outcome of human TMS is difficult, with direct, objective measurements being limited to the induction of muscle twitches via activation of upper motor neurons in the primary motor cortex. Eliciting such muscle twitches

requires stimulation above the threshold of neuronal activation of action potential firing (suprathreshold stimulation) (Pell et al., 2011). Motor evoked potentials (MEP) can be recorded from muscles following direct stimulation of the motor cortex. The MEP amplitude is an indication of changes in corticospinal excitability of the targeted area, whereby MEP amplitude increases with increasing stimulation intensity (Rothwell, Day, Thompson, Dick, & Marsden, 1987). The stimulation intensity required to induce muscle twitches in a resting muscle is expressed relative to the resting motor threshold (RMT) or in an active muscle relative to the active motor threshold (AMT), and is the percentage of stimulator output that is required to systematically produce MEPs (Fitzgerald, Fountain, & Daskalakis, 2006; Rothwell et al., 1987). The RMT is commonly used as guideline of excitability threshold for stimulation of cortical areas other than the motor cortex and as a standardization tool for inter-subject stimulation intensity (Fitzgerald et al., 2006; Rossini et al., 1999). However, validity of applying this method to identify stimulation intensity to non-motor cortex areas is disputed, due to inter-subject and inter-region anatomical and excitation variability, in addition to the influence of internal states such as arousal and attention (Cuypers, Thijs, & Meesen, 2014; Roy Choudhury et al., 2011).

Stimulation intensity of TMS is commonly applied around 80-120 % RMT or AMT and hence is only described as a relative measure of stimulator output. This also means that the strongest point of stimulation is applied around the threshold of action potential firing with induced electric fields of approximately 100 - 150 V/m at the maximal point of stimulation in cortical areas (Salinas, Lancaster, & Fox, 2009; Thielscher & Kammer, 2004).

1.3.4 Temporal pulse spacing (frequency)

TMS can be applied in two ways. Firstly, single pulse TMS (spTMS, 1-2 pulses, depending on the protocol) aims to test cortical excitability or influence ongoing neuronal activity. Effects of spTMS are short lasting (millisecond (ms) range), meaning they do not extend after stimulation has ceased ('online' effects) (Wassermann et al., 2008). Secondly, TMS can be applied in repetitive pulse trains (rTMS). rTMS has shown changes to cortical excitability that last beyond the actual stimulation time ('offline' effects) up to 45 minutes after stimulation has ceased, depending on the applied rTMS protocol (Fitzgerald et al., 2006; Huang, Edwards, Rounis, Bhatia, & Rothwell, 2005).

An important factor in rTMS application is how often and for how long the magnetic pulse is delivered. The temporal spacing of the pulse (frequency) is the most extensively studied and manipulated parameter of magnetic stimulation, though the length of the pulse has not been investigated due to inherent stimulator limitations (Goetz et al., 2013b). Generally, in human stimulation, high frequencies ≥ 3 Hz are considered to increase cortical excitability (Berardelli et al., 1998; Fitzgerald et al., 2006), while straight frequencies ≤ 1 Hz decrease cortical excitability (Fitzgerald et al., 2006; Lang et al., 2006). However, patterned stimulation frequencies based on endogenous patterns of brain activity, such as theta-burst stimulation, have been shown to have either excitatory or inhibitory effects (Hoogendam, Ramakers, & Di Lazzaro, 2010; Huang et al., 2005) and effects seem to be sensitive to variation in magnetic field intensity (Huang & Rothwell, 2004) and total length of stimulation (Gamboa, Antal, Moliadze, & Paulus, 2010).

1.4 TMS application

The potential for TMS to induce long-term modulation of brain activity has driven much research into its application for therapeutic purposes. rTMS has been delivered in a wide range of neurological conditions, such as stroke, epilepsy, Parkinson's disease and tinnitus, in addition to psychiatric disorders such as depression, schizophrenia, bipolar and posttraumatic stress disorder, as well as pain syndromes such as migraine and chronic pain (Schulz, Gerloff, & Hummel, 2013; Wassermann et al., 2008).

Improvements to neurological and psychological conditions after rTMS applications have been shown to last up to months (Wassermann et al., 2008). However, to date reported results are highly variable, with studies regularly failing to reproduce published effects or even demonstrating conflicting results. Thus in recent years, the viability of rTMS as a therapeutic tool has increasingly come under scrutiny (Platz & Rothwell, 2010; Ridding & Rothwell, 2007; Wassermann & Zimmermann, 2012). This suggests that current rTMS protocols are sub-optimal and do not account sufficiently for variability between protocols and patients. Currently, it is impossible to control for such variability beyond basic measures such as RMT adjustments (Cuypers et al., 2014; Fitzgerald et al., 2006; Roy Choudhury et al., 2011). One possible factor involved is that even though rTMS has been applied for almost two decades in the clinical setting, it is one of the few therapeutic tools that has been employed without preceding fundamental animal research. Fundamental investigation of the effects of rTMS in humans is limited to non-invasive methods and not much is known to date about the brain mechanisms underlying rTMS effects.

1.5 Underlying biological mechanism of rTMS

1.5.1 Mathematical modelling

Estimating inherent conductive properties of the biological tissue in connection with the effect of the induced electric current is limited. Attempts have been made to model the induced electric currents after TMS application (Bijsterbosch, Barker, Lee, & Woodruff, 2012; Salinas et al., 2009), assuming different head models and inherent tissue conductivity/impedance (Wagner et al., 2014). Researchers also have attempted to model the basic mechanism of interaction between electromagnetic stimulation and neurons (Dmochowski et al., 2012; Joucla & Yvert, 2012; Modolo, Thomas, & Legros, 2013; Pashut et al., 2011). These models are largely based on Hodgkin and Huxley's theory of neuron excitability (Hodgkin & Huxley, 1952), with Roth's peripheral nerve model being one of the most well-known electrophysiological models for predicting TMS effects on biological tissue (Fatemi-Ardekani, 2008; Roth & Basser, 1990). Modelling magnetic stimulation effects is highly valuable in providing experimental predictions to guide fundamental experimental research into magnetic stimulation effects. However, to date these computational models predict effects based on particular biological assumptions, limiting the complexity of factors taken into account. To confirm predictions, systematic investigation of magnetic stimulation effects in living biological tissue is needed (Schulz et al., 2013; Wagner et al., 2014).

1.5.2 rTMS in animal models

A slowly increasing base of studies of *in vivo* and *in vitro* models has investigated the functional, anatomical and molecular effects of rTMS in healthy and diseased animal brain tissue. In animal models of CNS injury, repeated application of rTMS has been

shown to have beneficial functional outcomes over a range of frequencies. Daily rTMS application of low (0.5 Hz) and high frequencies (10 Hz) increase functional recovery after ischemic stroke (Wang, Geng, Tao, & Cheng, 2010; Yoon, Lee, & Han, 2011; Zhang, Mei, Liu, & Yu, 2007). Frequencies above 20 Hz increase neuronal survival (Gao et al., 2010; Yoon et al., 2011) and modulate gene expression (Wang et al., 2010; Yoon et al., 2011; Zhang et al., 2007). Improvement of functional outcomes was also observed in animal models of visual neglect after 10 days of 10 Hz application (Afifi, Jarrett Rushmore, & Valero-Cabré, 2013) and epilepsy, decreasing the severity of epileptic attacks during simultaneous 1 Hz stimulation (Yadollahpour, Firouzabadi, Shahpari, & Mirnajafi-Zadeh, 2014). It has been suggested that long-term effects of rTMS application are based on changes in cortical excitability and resulting modification of brain plasticity (Schulz et al., 2013; Wassermann et al., 2008; Wassermann & Zimmermann, 2012).

1.5.3 Cortical excitability – Neuroplasticity

rTMS has been shown to induce changes in cortical excitability beyond the duration of actual stimulation, for up to 45 minutes after stimulation has ceased (Huang et al., 2005). In animals, rTMS has also been shown to alter cortical excitability in a frequency dependent manner. Consistent with human rTMS effects, low frequency rTMS reduced (Muller et al., 2014) and high frequency increased (Aydin-Abidin, Moliadze, Eysel, & Funke, 2006) cortical excitability, in the rodent and feline cortex respectively. However, some discrepancies with human studies were also observed, for example, the reduction in visual evoked potentials in the feline visual cortex after 5-20 min of rTMS was stronger after 3 Hz in contrast to 1 Hz stimulation (Aydin-Abidin et al., 2006).

The reasons for these differences remain poorly understood and emphasize the need for more basic animal studies.

The physiological mechanisms of how rTMS alters cortical excitability are largely unknown, but it has been widely suggested that changes in brain plasticity might underlie rTMS effects (Huerta & Volpe, 2009; Pascual-Leone, 2006). Neuroplasticity can be defined as the intrinsic ability of the nervous system to alter structural and functional neural circuits in response to environmental input and/or brain injury that disrupts the current homeostasis of network activity (Kleim, 2011; Pascual-Leone et al., 2011). The system strives to re-establish a homeostasis of network activity through changes at the cellular and molecular level, with or without anatomical adjustments, and leading to functional modifications (Fig 1.5) (Butz, Wörgötter, & van Ooyen, 2009).

1.5.4 LTP-LTD

It has been suggested for some time that changes in neuroplasticity underlie mechanisms similar to long term potentiation (LTP) and long term depression (LTD) (Thickbroom, 2007). LDP/D is a long-lasting enhancement/inhibition in signal transmission between two neurons that results from specific patterns of stimulation in the pre- and postsynaptic neuron. There are several theories of LTP/LTD induction: 1) Hebbian LTP/LTD, requiring simultaneous pre- and postsynaptic depolarization (Wigström & Gustafsson, 1986). Non-Hebbian LTP/LTD, requiring particular high-frequency firing pattern in the mossy fibre hippocampal pathway (Urban & Barrionuevo, 1996). And anti-Hebbian LTP/LTD requiring simultaneous pre-synaptic depolarization with post-synaptic hyperpolarization (Kullmann & Lamsa, 2008).

It has been known for several years that high frequency rTMS (15 Hz) increases neuronal sensitivity to LTP induction via electric stimulation *in vitro* (Ahmed & Wieraszko, 2006). However only recently has it been confirmed that a single session of 10 Hz repetitive magnetic stimulation *in vitro* (rMS) induces changes in structural plasticity of postsynaptic dendritic spines in addition to changes in synaptic plasticity of Ca1 pyramidal neurons (Vlachos et al., 2012). These changes were correlated with increases in GluA1 α-amino-3-hydroxy-5-methyl-4-isoxazolepropionic acid (AMPA) receptor subunit expression, which in turn were dependent on N-methyl-D-aspartate (NMDA) receptor activation (Vlachos et al., 2012). NMDA receptor involvement is in accordance with studies in humans showing that the effects of 10 Hz rTMS could be blocked with administration of NMDA antagonists ketamine (Ciampi de Andrade, Mhalla, Adam, Texeira, & Bouhassira, 2014) and lamotrigine (Ziemann et al., 2008). NMDA receptor activation has been shown to require concurrent depolarization of the cellular membrane in accordance with Hebbian LTP (Ciampi de Andrade et al., 2014). Direct evidence for neuroplasticity and LTD like effects of low-frequency rTMS is still lacking, although long-term suppression of NMDA dependent cortical excitability has been confirmed using MEP measurements in rats (Muller et al., 2014). A key consequence of NMDA (and to a lesser extent, AMPA) receptor activation during LTP and LTD is a change in intracellular calcium, an important and versatile intracellular signalling molecule (Berridge, Lipp, & Bootman, 2000). As a result, modulation of intracellular calcium levels has been widely suggested to be involved in short-term and long-term effects of rTMS (Fung & Robinson, 2013; Thickbroom, 2007).

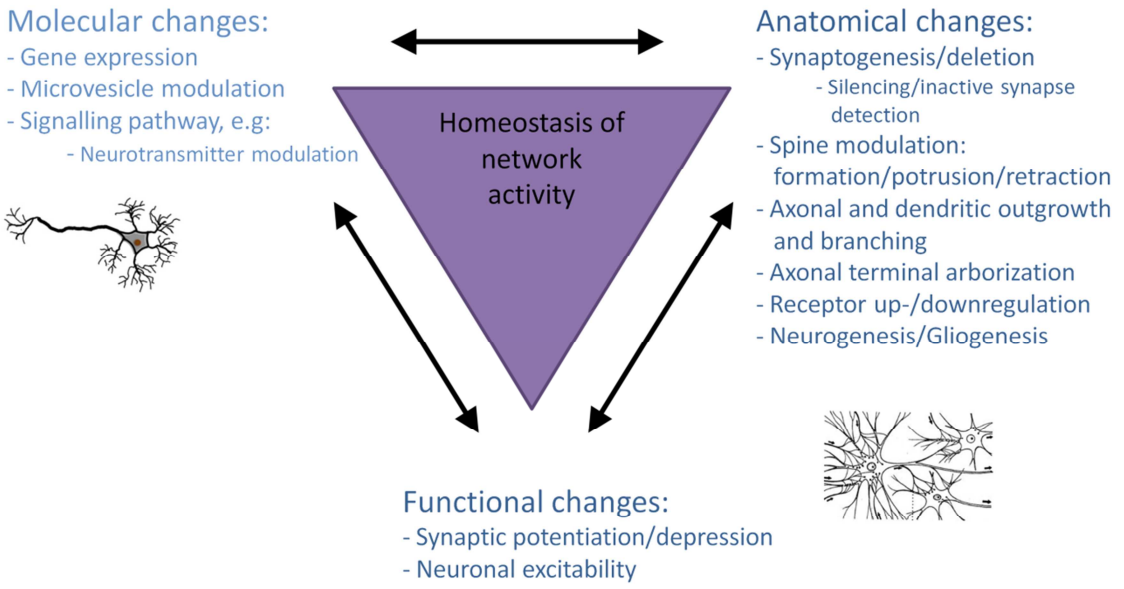

Figure 1.5 Overview of plasticity related changes classified into molecular, anatomical and functional modulation. Driven by the system to establish a homeostasis of network activity in response to environmental input or brain injury (Butz et al., 2009). Light blue indicates changes occurring at the single cell level, dark blue indicates changes at the network level.

1.5.5 Calcium hypothesis

Effects of magnetic stimulation have been hypothesized to underlie activity-dependent mechanism based on changes in intracellular calcium concentration. Increase in intracellular calcium activates second messenger type signalling and gene expression underlying molecular, anatomical or functional plasticity (Fung & Robinson, 2013; Thickbroom, 2007). The two major mechanisms that can result in changes in intracellular calcium levels are either calcium influx from the extracellular milieu or release from intracellular stores. Because high intensity stimulation can depolarize the membrane to the extent of action potential induction, calcium influx from extracellular milieu is considered fundamental in rTMS mechanisms. Voltage-gated ion channels

such as voltage-gated sodium channels, voltage-gated calcium channels (VGCC) and transient receptor potential (TRP) channels open in response to sufficient membrane potential changes (Alberts et al., 2002). Activation of voltage gated ion channels is induced via ligand-binding to receptors such as AMPA and NMDA, resulting in opening of voltage-gated sodium channels and influx of sodium ions. This leads to further membrane depolarization and voltage-gated ion channel opining, resulting in influx of calcium ions to the intracellular milieu with many signalling consequences including second messenger activation and regulation of gene expression (Fung & Robinson, 2013; Thickbroom, 2007). Hence, NMDA receptor activation provides a feasible candidate mechanism underlying high intensity TMS effects.

1.5.6 State dependent effects

It has been shown that possible underlying neuroplasticity effects of rTMS are state dependent (Gersner, Kravetz, Feil, Pell, & Zangen, 2011). rTMS stimulation in rodents, delivered daily for 2 weeks (20 Hz), increased synaptic plasticity while the same stimulation decreased Glu1 subunit expression in anesthetized animals. Interestingly, 1 Hz stimulation failed to induce LTD like effects in either awake or anaesthetised groups (Gersner et al., 2011). In contrast, other studies have reported LTD like effects of cortical excitability in anesthetized rats after 1 Hz stimulation, however effects on awake animals were not investigated (Muller et al., 2014). These experiments highlight the importance of systematic control and investigation of parameters in animal and *in vitro* models to systematically unravel the effects of magnetic stimulation on cellular and molecular mechanism.

1.5.7 Involvement of neuronal subclasses

It has been suggested that TMS affects various neuronal types differently, depending on frequency and underlying brain state. The patterned frequency theta burst stimulation (TBS) has been in focus of investigations because of its strong and composite effects on human cortical excitability (Gamboa et al., 2011; Huang et al., 2005; Stagg et al., 2009), in addition to the widely employed 'classic' straight frequencies of 1 Hz (inhibitory protocol) and 5-20 Hz (excitatory protocol). TBS has been shown to have opposite effects on cortical excitability, depending on whether it is applied in a continuous stream (cTBS) or in an intermittent pattern (iTBS), decreasing or increasing cortical excitability, respectively (Huang et al., 2005). The underlying mechanisms are still unclear, however previous research suggests that mostly pyramidal neuron axons, and to a lesser extent interneuron axons, are stimulated by TMS (Di Lazzaro et al., 2004), depending on axonal length, though the precise involvement of neuronal subgroups is still unclear (Meyer, Wolf, & Gross, 2009). Moreover, some evidence suggests the involvement of inhibitory interneuron subpopulations in long-term TBS effects (Funke & Benali, 2011). Investigation of interneuron classes in the rat neocortex revealed a primary effect on calcium dependent interneurons after a single dose of TBS. iTBS reduced the number of parvalbumin expressing (PV) interneurons, while 1 Hz and cTBS principally suppressed number of calbindin (CaBP) expressing interneurons, without increasing cell death (Benali et al., 2011). Interestingly, the duration of suppression differed per interneuron subclass, CaBP expression was reduced up to one day, but suppression of PV expression levels was recorded up to one week after the last stimulation (Benali et al., 2011).

These effects of iTBS have been shown to be NMDA receptor dependent. Administration of an NMDA receptor antagonist rapidly blocked iTBS effects on PV expressing interneurons, while higher concentrations of the antagonist were required to inhibit rTMS effects on CaBP expressing interneurons (Labedi, Benali, Mix, Neubacher, & Funke, 2014).

Subclass activation of neurons via TMS application has also been shown in *in vitro* neuronal cultures. Single or repeated pulses on average strongly activated ~20-30 % of total neurons in the culture (Meyer et al., 2009; Rotem & Moses, 2008). Stimulation at patterned, high frequencies suppressed firing rate with increasing number of pulses, and this response was also shown to be reversible by administration of NMDA receptor antagonists (Meyer et al., 2009).

Taken together, studies suggest that rTMS activates neuronal subclasses differentially, where different interneuronal subclasses activation was dependent on frequency and NMDA receptors activity. However, it is still unclear to what extent neuronal sensitivity or electric current properties play a role in neuronal subclass activation. There is some evidence that effects may be partially waveform-specific and thus dependent on the direction and intensity of created electric current (Arai et al., 2005; Sommer et al., 2006; Sommer et al., 2002). To be able to even partially estimate the effects of electric currents inside the brain and extrapolate between studies, careful control of induced electric field parameters is necessary.

1.5.8 Frequency effects on further signalling pathways

In addition to activation of ion channel-linked receptors, such as NMDA and AMPA, rTMS has also been suggested to activate different signalling pathways based on G

protein-coupled and enzyme linked receptors (see also Fig 1.6). One signalling cascade triggered by G protein-coupled receptor activation is the Phospholipase C (PLC) pathway (Neves, Ram, & Iyengar, 2002). Activation of PLC leads to increased amounts of diacylglycerol (DAG) in the membrane and inositol 1,4,5-trisphosphate (IP3). IP3 diffusion through the cytosol activates IP3 receptors in the endoplasmic reticulum (ER), resulting in release of intracellular calcium from intracellular stores in the endoplasmic reticulum and influence mitochondrial calcium uptake (Santo-Domingo & Demaurex, 2010; Valsecchi, Ramos-Espiritu, Buck, Levin, & Manfredi, 2013), modulating intracellular calcium levels. Increases in intracellular calcium concentrations start further intracellular signalling cascades (Neves et al., 2002). In addition, calcium and DAG activate protein kinase C (PKC), which subsequently phosphorylates other molecules, further activating different signalling cascades (Tanaka & Nishizuka, 1994).

Another signalling cascade triggered by G protein activation is the Cyclic adenosine monophosphate (cAMP) dependent signalling pathway (Freedman et al., 1995), involved in the activation of protein kinases (Valsecchi et al., 2013). cAMP has also been shown to regulate the function of other ion membrane channels such as the HCN (Hyperpolarization - activated cyclic nucleotide-gated) channels, that serve as non-selective ligand-gated cation channels, suggested to also be involved in TMS mediated effects (Pell et al., 2011). Higher frequency rTMS (5 Hz) has been shown to upregulate cAMP (Hellmann et al., 2012). A different study showed activation of mitogen-activated protein kinase (MAPK)/ extracellular signal-regulated kinase (ERK) and phosphoinositide pathways after low frequency stimulation (1 Hz), upregulating MAPK/ ERK and phosphoinositide 3-kinase (PI3K)/protein kinase B (PKB-Akt) expression (Ma et al., 2013). Activation of cAMP and protein kinase A (PKA) pathway

has been shown to be crucial for axonal repair of the optic nerve (Hellström & Harvey, 2014).

Frequency-specific effects were also shown for TBS (continuous and intermittent), modulating GABA-synthesizing enzymes glutamic acid decarboxylase (GAD) 65 and GAD67. GAD65 showed a fast increase, followed by a slower, longer lasting decrease in GAD67 (Hoppenrath & Funke, 2013; Volz, Benali, Mix, Neubacher, & Funke, 2013). However, responses largely reversed after two or more repeated applications (1-7 days) (Trippe, Mix, Aydin-Abidin, Funke, & Benali, 2009). These responses have been shown to be dose dependent in a non-linear manner: 600 pulses of iTBS induced higher expression increase than 600 pulses of cTBS. However, cTBS required fewer pulses (600) than iTBS (1200) to induce significant reductions of GAD67. Frequency and dose dependency was also shown for the expression of the synaptic marker vesicular glutamate transporter 1 (VGLUT1), which increased with increasing number of stimuli (> 1200), and was more strongly upregulated after iTBS than cTBS application (Volz et al., 2013). GAD65 and GAD67 are regulated via phosphorylation (Wei, Davis, Wu, & Wu, 2004), where GAD65 is activated by phosphorylation (via PKA activation), but GAD67 is inhibited by phosphorylation (via PKC) (Wei et al., 2004). However, even though rTMS has been shown to modulate PKA/PKC activation, it remains unknown whether rTMS affects phosphorylation of these enzymes in addition to their expression level.

1.5.8.1 Downstream activation – converging pathways

Increase of intracellular calcium levels that activate different signalling pathways such as cAMP and protein kinase signalling, can further result in the activation of CREB, a

cellular transcription factor (Kornhauser et al., 2002). CREB has been shown to be upregulated after 1 Hz stimulation (Hellmann et al., 2012). This response was diminished by the administration of lithium a classical inhibitor of the phosphoinositide pathway (Becchetti & Whitaker, 1997), while ketamine, a blocker of NMDA receptor activity, enhanced cAMP/CREB expression (Hellmann et al., 2012).

CREB has been shown to play an important role in neuroplasticity and regulates gene expression of early response genes and growth factors, such as c-fos and BDNF (Ginty, Bonni, & Greenberg, 1994; Kornhauser et al., 2002; Tao, Finkbeiner, Arnold, Shaywitz, & Greenberg, 1998).

1.5.8.2 Early response gene activation

Increases in intracellular calcium activate second messenger type signalling and can modulate gene expression. Investigation of enzyme and gene expression in addition to calcium binding interneuron subclasses revealed that straight and patterned rTMS frequencies modulated early response genes c-fos and zif268 in a frequency dependent manner (Hoppenrath & Funke, 2013; Trippe et al., 2009). Both genes are suggested to be involved in synaptic plasticity, where c-fos expression is activated after recent neuronal activity (Fleischmann et al., 2003; Knapska & Kaczmarek, 2004). c-fos expression was most strongly increased after 1 Hz stimulation, while zif268 was more strongly upregulated after stimulation with 10 Hz, iTBS or cTBS. Other studies have also shown an increase in c-fos expression after single application of low intensity stimulation *in vivo* at 0.5-1 Hz (Hausmann, Marksteiner, Hinterhuber, & Humpel, 2001; Trippe et al., 2009) and repeated application for 7-28 days (Zhang et al., 2007). However, c-fos was not upregulated in cultured rodent prefrontal cortex slices after

one single 20 Hz stimulation (Hausmann et al., 2001), but did increase in some layers of the rodent cortex after repeated daily stimulation for 14 days *in vivo* (Hausmann, Weis, Marksteiner, Hinterhuber, & Humpel, 2000). In contrast, another group found a increase in c-fos in mouse cortex after a single 20 Hz stimulation, but a decrease after repeated application for 20 days (Ikeda, Kurosawa, Uchikawa, Kitayama, & Nukina, 2005). Such variation in results might be partially based on the differences between studies in the chosen animal models (mice, rats, *in vivo, in vitro*) and stimulation parameters (waveform, intensity, magnetic field direction), as well as stimulation duration and detection methods of c-fos. These differences highlight the difficulty of comparing and interpreting outcomes across various rTMS studies *in vivo* and *in vitro* and the need for systematic investigation of magnetic stimulation effects on the cellular level.

1.5.8.3 BDNF regulation

BDNF is a member of the neurotrophin family and provides trophic (survival and growth) support to sensory and sympathetic neurons (Binder & Scharfman, 2004). BDNF is widely expressed in the CNS (Lu, Nagappan, Guan, Nathan, & Wren, 2013) and is crucial for normal brain development and in the adult system, where its major role is to enhance synaptic transmission, synaptic plasticity and promote synaptic growth (Lu et al., 2013). CREB upregulation increases the synthesis of BDNF protein in the endoplasmic reticulum. BDNF is then stored in dense-core vesicles of nerve terminals until secretion into extracellular domain (Bramham & Messaoudi, 2005; Lu et al., 2013). Extracellular BDNF is a ligand for high affinity tyrosine kinase receptor type B (TrkB) a member of the enzyme linked receptor family and low-affinity nerve growth factor receptor (LNGFR or better known as p75 receptor) a member of the tumor

necrosis factor receptor family (Bramham & Messaoudi, 2005; Lu et al., 2013). Activation of the TrkB receptor initiates further signalling pathways, such as MAPK/ERK and PKC protein kinase pathways (Bramham & Messaoudi, 2005), which influence neurite outgrowth, cellular differentiation and neuronal survival (Fig 1.6) (Bramham & Messaoudi, 2005; Harvey, Ooi, & Rodger, 2012). The p75 receptor is involved in survival/apoptosis related pathway activation, but also functions to potentiate the effects of TrkB activation (Fig 1.6) (Bramham & Messaoudi, 2005). Recent studies suggest an important role of BDNF in the induction of LTP *via* activation of the immediate early gene encoding Arc (Binder & Scharfman, 2004). Given these effects of BDNF-TrkB activation, it has been widely investigated as a suitable candidate in mediating brain repair after injury, especially in the adult CNS (Lu et al., 2013).

Many studies have shown modulation of BDNF expression after TMS. One study has shown an increase in the expression of BDNF after a single rTMS session of 20 Hz but not after 1 Hz (Gersner et al., 2011), while repeated sessions of low frequency stimulation (0.5 Hz) did increase BDNF expression after 5 days (Ma et al., 2013), 7-21 days (Zhang et al., 2007) and 6 weeks (Wang et al., 2010; Wang et al., 2011). Moreover, repeated rTMS stimulation for 11 weeks at high intensity and frequency (20 Hz) showed significant, brain area dependent upregulation of BDNF in the healthy rat (Muller, Toschi, Kresse, Post, & Keck, 2000b). However, a recent study showed that even though two different high intensities (1.14 T and 1.55 T) of 1 Hz stimulation both upregulated BDNF and TrkB receptor expression (Ma et al., 2013), these increases did not correlate simply with increases in markers of neuroplasticity. In fact, the expression of neuroplasticity markers was inversely correlated with intensity, where the lower intensity (1.14 T) increased dendritic and axonal arborization, synapse

density, synaptophysin (SYN), growth associated protein 43 (GAP43) and post-synaptic-density 95 (PSD95) (Ma et al., 2013), and the higher intensity (1.55 T) increased neuronal apoptosis, reduced dendritic and axonal arborization, decreased synapses and disordered synaptic structure (Ma et al., 2013).

Overall, data obtained from animal studies suggest profound effects of rTMS on signalling cascades underlying molecular and cellular changes and suggest involvement of signalling pathways *via* G protein-coupled and enzyme binding receptor activation, in addition to modulating ionotropic channel activity. Furthermore, it is apparent that rTMS effects do not show a simple linear and cumulative effect and careful investigation is needed to better understand and tailor clinical applications. Longer durations and higher intensities of rTMS stimulation do not necessarily increase the strength of effects and might even result in detrimental outcomes. These studies outline the complex effects of frequency and timing (depending on number of pulses, inter-pulse/ inter-train intervals and stimulation intensities) and difficulty in comparing outcomes between different studies. Hence, to date the underlying neurobiological effects of TMS are only partially understood (Pashut et al., 2011).

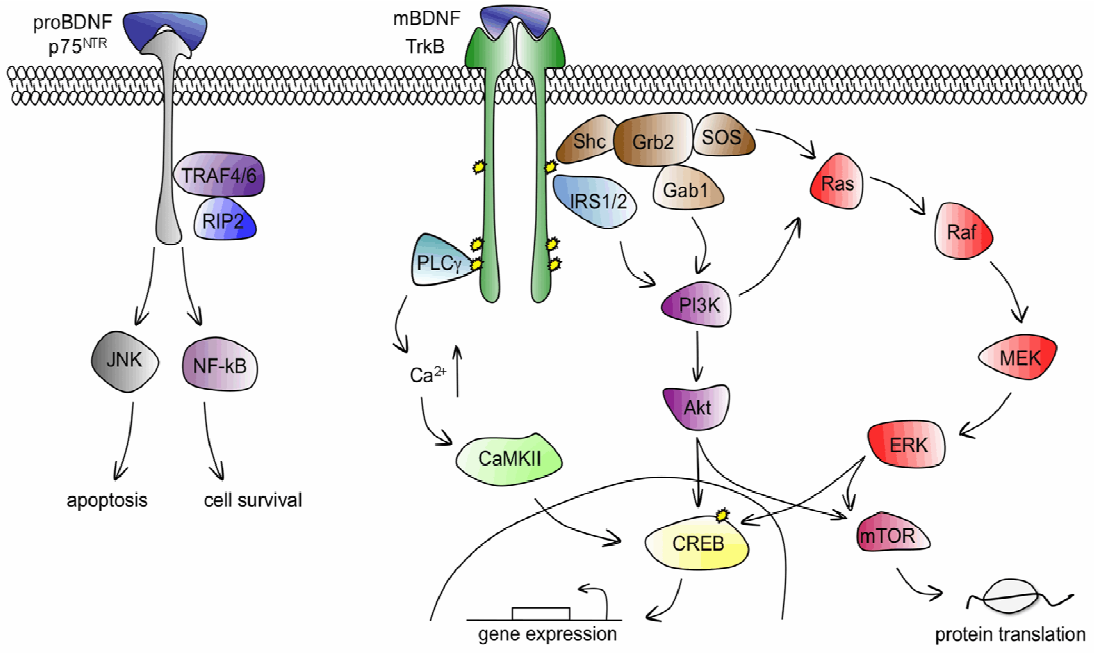

Figure 1.6 BDNF receptor and signalling pathways. BDNF binds TrkB with high affinity and activates three main signalling pathways: Phospholipase C (PLC), PI3K and ERK cascades, PLC increases intracellular Ca^{2+} levels and leads to the activation of calmodulin-dependent protein kinase II (CaMKII) to phosphorylate CREB. PI3K signalling cascades activate PKB-Akt, upstream of CREB. ERK phosphorylation leads directly to CREB phosphorylation. BDNF binds $p75^{NTR}$ with low affinity, leading to activation of apoptosis or cell survival signalling cascades. Image and text from Cunha, Brambilla, & Thomas (2010).

1.6 Low intensity (LI) magnetic stimulation

As discussed above, stimulation intensity in humans is based on threshold measurements of cortical excitability. Coils are therefore designed to produce a maximal centre of high intensity at a focal point. However, this focal centre is surrounded by a weaker magnetic field (Deng et al., 2013; Trillenberg et al., 2012), such that a large volume of adjacent cortical and sub-cortical regions is also stimulated, albeit at a lower intensity (Cohen et al., 1990; Deng et al., 2013). Effects of

surrounding magnetic fields are often regarded as negligible and most research has been focussed on high intensity stimulation.

Nonetheless, LI-rTMS in humans (in the mT range) has been shown to modify cortical function (Capone et al., 2009; Robertson et al., 2010), brain oscillations (Cook, Thomas, & Prato, 2004), analgesic pain response (Shupak, Prato, & Thomas, 2004) and to be beneficial for the therapeutic treatment of depression (Martiny, Lunde, & Bech, 2010). Moreover, studies in rats show improvement of function and neuronal survival after high frequency LI-rTMS following traumatic brain injury (20 Hz, 0.1-0.5 mT) (Yang et al., 2012) and Huntington's disease (60 Hz, 0.6 mT) (Tasset et al., 2012). However, no improvement has been found in a rat model of ischemic stroke, applying high and low frequency stimulation (20 Hz + 1 Hz or 20 Hz + patterned high frequency, 8 mT) (Bates, Clark, Meloni, Dunlop, & Rodger, 2012). In contrast, a wide range of studies investigating LI-rTMS effects on peripheral sciatic nerve damage, showed promotion of peripheral nerve regeneration and function in the rat (De Pedro et al., 2005; Markov, 2007; Siebner & Rothwell, 2003; Walker et al., 1994), but not in the mouse (Baptista et al., 2009). Furthermore, LI-rTMS has also been shown to alter the structure and function of abnormal neural circuits (Rodger, Mo, Wilks, Dunlop, & Sherrard, 2012).

1.6.1 Frequency-specific effects - underlying mechanisms

Mechanisms underlying LI-effects are still unknown. Investigation of LI repetitive magnetic stimulation *in vitro* (LI-rMS), employing central and nervous system cell cultures has shown pronounced but variable effects.

LI-rMS has been shown to modulate neuroplasticity related mechanisms such as increasing myelin repair (Gunay & Mert, 2011; Sherafat et al., 2012), modulating cAMP

expression (Hogan & Wieraszko, 2004) and neuronal survival (Boland, Delapierre, Mossay, Dresse, & Seutin, 2002; Di Loreto et al., 2009; Kaszuba-Zwoinska J et al., 2010; Stratton, Lange, & Inal, 2013; Yang et al., 2012). Interestingly, among the same exposure system (50 Hz, 45 mT), LI-rMS increased cell death at high cellular densities, while at lower densities it was shown to prevent stress induced apoptosis (Juszczak, Kaszuba-Zwoinska, & Thor, 2012; Kaszuba-Zwoinska J et al., 2010).

1.6.1.1 Neuroplasticity - Calcium signalling

LI-rMS has frequency-specific effects on structural plasticity, increasing neurite outgrowth after repeated application of 7 and 10 Hz, but not 4 and 12 Hz (6.4 mT) (Hernández-Hernández, Cruces-Solis, Elías-Viñas, & Verdugo-Díaz, 2009). At high frequencies (50/60 Hz) LI-rMS has been shown to alter calcium signalling (Barbier, Veyret, & Dufy, 1996; Grassi et al., 2004; McCreary, Dixon, Fraher, Carson, & Prato, 2006; Morabito et al., 2010b; Morgado-Valle, Verdugo-Díaz, García, Morales-Orozco, & Drucker-Colín, 1998; Piacentini, Ripoli, Mezzogori, Azzena, & Grassi, 2008), suggesting the applicability of the calcium-dependent activation hypothesis to low intensity rMS effects, as for high intensity (Fung & Robinson, 2013). Some groups reported changes in intracellular calcium originating from voltage gated calcium channels (VGCC; 50 Hz, 0.05-1 mT) (Barbier et al., 1996; Grassi et al., 2004; Piacentini et al., 2008), while another group (60 Hz, 0.7 mT) found L-type calcium channels to be involved (Morgado-Valle et al., 1998). However, another group showed increasing intracellular calcium concentrations by release from intracellular stores and not influx from the extracellular milieu after high frequency (50 Hz, 3 mT) LI-rMS (Aldinucci et al., 2000; Pessina et al., 2001). In addition, LI-rMS decreased mitochondrial membrane potential, suggested to be involved in the observed changes of free intracellular calcium levels (Morabito et

al., 2010b). Mitochondria, as well as the endoplasmic reticulum, are two organelles involved in storage and regulation of intracellular calcium levels (Berridge et al., 2000).

1.6.1.2 Intracellular signalling

Increases in intracellular calcium trigger different intracellular signalling events, such as cAMP and protein kinase signalling. Investigating expression of cAMP in hippocampal slices, one study found low frequency dependent effects at 15 mT, where 0.16 Hz but not 0.5 Hz increased cAMP concentrations (Hogan & Wieraszko, 2004). Studies report increases in cAMP, PKA and ERK 1/2 second messengers (Yong, Ming, Feng, Chun, & Hua, 2014) after high frequency stimulation at lower intensities (15 Hz, 1 mT) and decreases in PKB-Akt and P13K (50 Hz, 1 mT). This suggests a possible involvement of signalling pathways based on G protein-coupled and enzyme linked receptors activation in the effects of LI-rMS at subthreshold intensity (no action potential firing).

Low intensity magnetic stimulation has been shown to have further downstream signalling effects, such as regulation of gene expression, both *in vivo* and *in vitro*. Rats exposed to LI-rTMS for 7 days (60 Hz, 2 mT) have shown modulation of nitric oxide (NO) in several brain areas (Cho et al., 2012). Nitric oxide, an essential neurotransmitter, has been shown to be primarily regulated by increases in intracellular Ca^{2+} through calmodulin (CAM) binding and is involved in the regulation of synaptic plasticity but can mediate neurotoxicity at excess levels (Cho et al., 2012; Mungrue & Bredt, 2004).

In addition, stimulation of cortical neurons at 50 Hz (1 mT) for 7 days protected cells from increased levels of reactive oxygen species (ROS), a marker of cellular stress (Halliwell & Whiteman, 2004) *via* modulation of survival promoting genes including

BDNF, TrkB, IL1 and the antioxidant enzyme Glutathione (GSH) (Di Loreto et al., 2009). However, reported effects of LI-rMS on ROS are variable, with some studies reporting increased levels after high frequency stimulation (50 Hz) and others showing no effect (Frahm, Mattsson, & Simkó, 2010; Mattsson & Simkó, 2012; Morabito, Guarnieri, Fanograve, & Mariggi, 2010a).

LI-rMS has also shown effects on microvesicle release. Microvesicles play an important role in intercellular communication and can transport RNA and proteins between cells (Muralidharan-Chari, Clancy, Sedgwick, & D'Souza-Schorey, 2010). High frequency LI-rMS has been reported to increase microvesicle release (10 Hz, 0.3 μT) (Stratton et al., 2013) and downregulate expression of clathrin and adaptin, proteins involved in microvesicle formation (50 Hz, 1 mT) (Frahm et al., 2010).

1.6.2 In conclusion

Taken together, these results suggest profound effects of low intensity magnetic stimulation on biological mechanisms in the mT range (Di Lazzaro et al., 2013), with these effects being dependent on cell type, brain area, stimulation intensity and frequency. This is especially important, because as described earlier, magnetic stimulation is applied at heterogeneous intensities with peri-focal lower intensities along the field of the coil (Deng et al., 2013), thus these studies suggest that effects should not be disregarded simply because of the subthreshold nature of LI-rTMS.

However, to date the exact effects of LI-rTMS and especially different frequencies on biological mechanisms remain largely unclear. Generalizability of results obtained from the principal body of research remains difficult due to the employment of different rMS delivery systems and especially different experimental models, with relatively few

studies using models of the healthy central nervous system. Furthermore, no systematic investigation of the effects of rMS at different frequencies has been conducted. Hence, cellular and molecular mechanisms underlying effects of LI-rMS at different frequencies in normal CNS tissue remain unknown.

Thus, a systematic investigation of low intensity repetitive stimulation at different frequencies at the neuronal and neural circuit level is essential to better understand the underlying biological mechanisms of magnetic stimulation effects in the central nervous system. Identification of the fundamental effects of magnetic stimulation is essential to direct further research more efficiently into more complex systems and ultimately interpretation and better tailoring of magnetic stimulation results obtained in the clinic. Moreover, the first promising explorations of LI-rTMS in the clinic (Martiny et al., 2010), together with the unlikelihood of side-effects such as seizures following the subthreshold low intensities associated with LI-rTMS, makes LI-rTMS a desirable therapeutic and research tool (Di Lazzaro et al., 2013; Martiny et al., 2010), either on its own or as a contributor to the effects of rTMS and merit exploration.

1.7 AIMS

The effects of different rMS frequencies on biological mechanisms

A. Investigating the effects of LI-rMS on single neurons at a range of different frequencies: anatomical and molecular changes.
B. Investigating the effects of LI-rMS on neural circuits at a range of frequencies: anatomical and molecular changes
C. Optimizing custom-tailored LI-rMS delivery to *in vitro* set-ups.

1.7.1 Advantages of in vitro systems

In order to address these aims, we chose *in vitro* LI-rMS because *in vitro* systems have the advantage of offering precise control and isolation of experimental variables, increasing standardization and reproducibility of results. Environmental influences such as temperature and physiological conditions such as cell type can be tightly controlled and defined, reducing experimental variation (Reichert, 2008). Furthermore, they provide better control of the magnetic stimulation parameters, such as induced electric field properties. Hence *in vitro* systems can provide vital insight into the complex, often contradictory results observed in magnetic stimulation research (Basham, Zhi, & Wentai, 2009). Furthermore, neurons in culture have the advantage of being more accessible for experimental techniques such as real-time and intracellular imaging. Usage of murine tissue as a model organism has the advantage of anatomical, physiological and genetic similarities to humans, while being reproducible, cost–efficient and widely applied in experimental research (Nguyen & Xu, 2008). Mouse models have been shown to be easily comparable and particularly applicable to human

disease research (Nguyen & Xu, 2008) and provide an optimal tool for fundamental investigation of biological mechanisms.

1.7.2 Rationale of aims and experimental models

A. The effects of LI-rMS on the individual neuron

Single cell cultures are an excellent and widely applied tool to study cellular and molecular mechanisms of a particular cell type, such as neurite extension, molecular modulation and cell survival (Meberg & Miller, 2003).

Cells of primary cultures, which are cultures derived directly from the tissue of an organism, have the advantage to commonly display the *in vivo* cellular properties of their origin (Robert, Cloix, & Hevor, 2012), while providing the opportunity to observe and manipulate them in a far less complex environment than the *in vivo* setting (Beaudoin et al., 2012). Primary cultures of cortical neurons derived from rodent tissue are extensively and routinely employed to study such neuronal mechanisms (Meberg & Miller, 2003). Neurons derived from postnatal (P0-P1) cortical tissue can be dissociated and grown in culture. This technique results in a culture comprised of a high number of neurons, plus an additional small number of non-neuronal cells such as glial cells (Beaudoin et al., 2012). Glial cells maintain homeostasis, form myelin, and provide support and protection for neurons in the CNS (Jessen & Mirsky, 1980). Presence of glial cells in *in vitro* systems has been shown to be advantageous to the normal development of neuronal cells (Hatten, 1985). However, reproduction of glial cells by cell division (proliferation) results in extensive expansion and covering of culture populations, which can be undesirable for single neuronal cell analysis *in vitro.* Proliferation can easily be avoided by the addition of proliferation inhibitor cytosine d-

D-arabinofuranoside (AraC), which is routinely applied in postnatal neuronal cultures (Beaudoin et al., 2012). Sparse seeding and short-term culturing results in neuronal cultures that do not form synaptic connections and allow visualization of individual neurons and their processes. This has the advantage of yielding a relatively pure but slightly mixed neuronal culture more similar to the *in vivo* environment while giving the opportunity to investigate the single neuron.

In addition, primary cortical cultures have been shown to be mainly comprised of GABAergic neurons (Thomas, 1985). Based on previous *in vivo* studies showing the activation of inhibitory neuronal subpopulation (Funke & Benali, 2011), primary cortical cell cultures are particularly appropriate to investigate the biological effects of rMS on the single neuron level.

Here we systematically investigate the effects of a range of LI-rMS frequencies on neuronal survival, morphology and gene expression changes in single cortical cultures.

B. The effects of LI-rMS on neuronal circuit repair

Injury to the central nervous system resulting from traumatic brain injury, stroke or degenerative disease can lead to severe and lasting cognitive and functional deficits as repair of the adult mammalian brain after lesion is limited or unspecific (Fitzgerald & Fawcett, 2007; Nudo, 2013).

While the exact underlying mechanisms are still unknown (Müller-Dahlhaus & Vlachos, 2013), studies have shown that neurorehabilitation can be enhanced by promoting structural and functional neuroplasticity (Lee, Lin, Robertson, Hsiao, & Lin, 2004; Li et al., 2004). Many current treatments aim to promote neuroplasticity to either restore

the lesioned system, recruit non-affected brain areas and/or retrain non-affected brain areas to perform new functions (Kleim, 2011), which can occur *via* axonal regeneration, heterologous terminal sprouting and/or collateral reinnervation.

It has been shown that cortical activity at the site of the lesion is crucial to achieve even limited functional improvement (Nudo, 2013). rTMS has the advantage of being able to non-invasively affect the brain, providing a mechanism to directly target cortical activity. However, because the precise effects of rTMS on the injured central nervous system are largely unknown, tailoring of stimulation to particular injury requirements remains unfeasible.

To examine the effects of LI-rMS on neuroplasticity after injury, this thesis assesses the effects of different low intensity magnetic stimulation frequencies on neural circuit repair using an *in vitro* mouse olivo-cerebellar projection model of axonal injury (Letellier, Wehrlé, Mariani, & Lohof, 2009). This model has been thoroughly characterized in our laboratories (Dixon et al., 2005; Dixon & Sherrard, 2006; Fournier, Lohof, Bower, Mariani, & Sherrard, 2005; Letellier et al., 2007; Lohof, Mariani, & Sherrard, 2005; Willson, Bower, & Sherrard, 2007; Willson, McElnea, Mariani, Lohof, & Sherrard, 2008) and has the advantage of being organized with precise topography, displaying a one to one relationship between the afferent climbing fibre (CF) axons and the target Purkinje cell (PC) (Eccles, Ilinas, & Sasaki, 1966; Fournier et al., 2005; Lohof et al., 2005). It has been optimized *in vitro* (Letellier et al., 2009) to closely resemble the *in vivo* system and is thus highly suitable to investigate and optimize LI-rMS parameters.

B.1 The cerebellum, cerebellar cortex and olivary nucleus circuit

The cerebellum consists of two lateral hemispheres and a central vermis (Apps & Garwicz, 2005). The cerebellar cortex has three cortical layers (Fig 1.7B), containing two major types of neurons (the Purkinje cells and granule cells), in addition to three major types of interneurons. The cerebellar circuit comprises three major types of axons: the climbing fibres (CF, ascending from neurons in the olivary nucleus), mossy fibres (indirect input from the cerebral cortex) and parallel fibres (granule cell axons). Except for excitatory, glutamatergic granule cells, all other cells form GABAergic synapses (Apps & Garwicz, 2005).

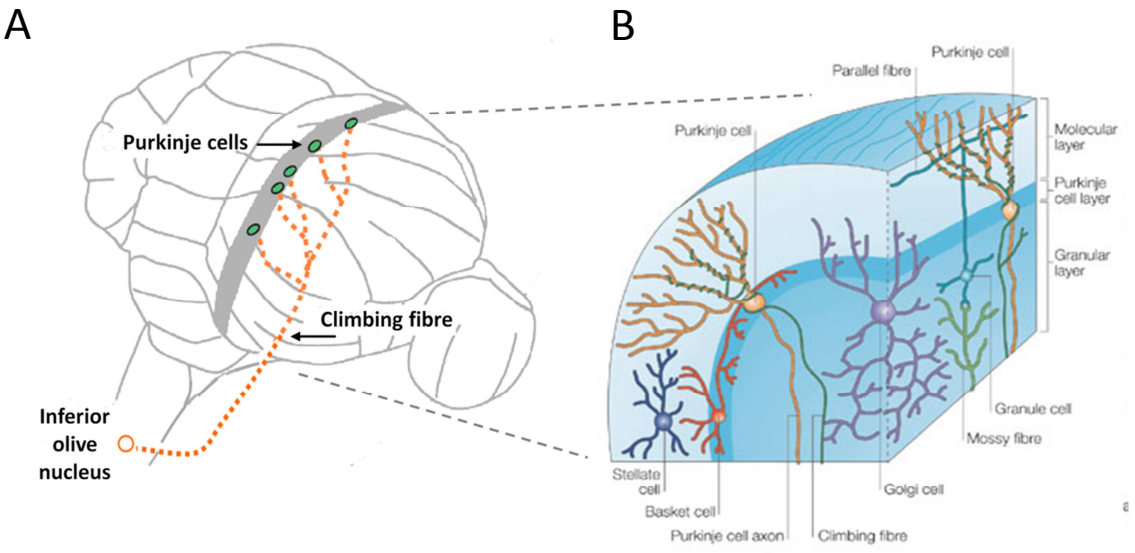

Figure 1.7 Schematic view of the olivo-cerebellar pathway. Showing the whole cerebellum and brainstem (A) and the layers of the cerebellar cortex (B). Five major neuronal cell types are involved in the cerebellar circuit: neuron: granule cell + Purkinje cell and interneurons: golgi cell, stellate cell and basket cell. With three major fibres: climbing fibre, mossy fibre and parallel fibre. Except for excitatory granule cells (glutamate), all other cells are GABAergic. A) adapted from Letellier-personal communication, B) adapted from Apps & Garwicz (2005).

The granule layer is the most interior layer and derives its name from the high amount of small densely packed granule cells. The Purkinje cell layer lies in between the granular layer and the most exterior situated molecular layer (Fig 1.7B). Large cell bodies of the PCs make up the Purkinje cell layer, with their planar dendritic trees extending into the molecular layer. The thin unmyelinated axons of the granule cells rise through the Purkinje cell layer into the molecular cell layer, where they synapse into parallel fibres. Parallel fibres pass through the dendritic tree of Purkinje cells forming intermittent synapses onto every 3rd-5th PC (Apps & Garwicz, 2005). In the mature cerebellar system, CFs arise exclusively from the contralateral inferior olive located in the caudal brain (Fig 1.7A). The climbing fibres directly synapse onto PCs, where in the mature system each PC only receives input from one CF (De Zeeuw et al., 1998). PCs project axons to the deep cerebellar nuclei, situated in the central white matter of the cerebellum. Axons from the cerebellar nuclei in turn project to the thalamus or motor tracts (Apps & Garwicz, 2005). PCs are the sole output neurons of the cerebellar cortex to circumscribed regions of the cerebellar nuclei and thereby forming discrete, topographical, neuronal cerebellar circuits (Apps & Garwicz, 2005).

The inferior olive nucleus is the largest nucleus situated in medulla oblongata in the lower portion of the brain stem. The inferior olive comprises two types of neurons, in addition to a very small subpopulation of interneurons (De Zeeuw et al., 1998). Both neuronal types are assumed to be projection neurons, sending axonal climbing fibres to the cerebellar cortex where they terminate in 5-7 PCs (De Zeeuw et al., 1998).

B.2 Olivo-cerebellar development

Development of the cerebellum occurs both prenatally (embryonic, E) and postnatally (P). Migration of granular precursor cells starts around E13 and migration of mature granule cells to the cerebellar granule layer is completed around P20 (Komuro et al., 2013). Purkinje cells formation and migration to the Purkinje cell layer in the cerebellar cortex occurs around E13-E17 (Yuasa, Kawamura, Ono, Yamakuni, & Takahashi, 1991). Inferior olivary neurons complete migration to the olivary nucleus around E17 (De Zeeuw et al., 1998). Olivary neuron axons project to the cerebellar cortex after crossing the midline in the medulla, move through the inferior cerebellar peduncle, extend further through the granular layer of the cerebellar cortex to synapse onto PCs in the Purkinje cell layer. Olivary neuron axons become CFs by branching just before reaching the cerebellar cortex (Watanabe & Kano, 2011), leading to a precise parasagittal topography (Sugihara, 2005).

Formation of CF-PC synapse occurs in 4 stages of progressing synapse elimination (Watanabe & Kano, 2011). Multiple CFs initially form synapses with multiple PCs, which then get progressively removed. The early synaptic pruning phase (P7-11) is driven *via* P/Q-type-VGCC activation in the PC. The late synaptic pruning phase (P12-17) is driven by metabotropic GluR1 receptor signalling pathways (Gaq–PLCb4–PKCc) to result in monoinnervation of each PC by one CF at P20 (Watanabe & Kano, 2011).

B.3 Olivo-cerebellar injury

The olivo-cerebellar pathway model is an established model of reinnervation and neural circuit repair (Reeber, White, George-Jones, & Sillitoe, 2013). Unilateral transaction of the olivo-cerebellar pathway (Pedunculotomy (Px)) at the cerebellar

peduncle results in degeneration of the contralateral inferior olive. In the early development stages (< P10) the remaining inferior olive spontaneously regrows new CFs to reinnervate the denervated PCs (Sugihara, Lohof, Letellier, Mariani, & Sherrard, 2003). After the early developmental period, structural plasticity decreases with no spontaneous reinnervation observed *in vivo* for Px at P10 or later (Sherrard, Letellier, Lohof, & Mariani, 2013). However, it has been shown that similar reinnervation can be induced with the neurotrophic factor BDNF, also at later stages of development, with the same parasagittal order (Dixon & Sherrard, 2006; Willson et al., 2008), but *via* direct CF-PC mono-innervation (Letellier et al., 2007). BDNF induced reinnervation has been shown to provide functional and cognitive benefits in rats (Willson et al., 2007; Willson et al., 2008). The olivo-cerebellar pathway model has been optimized and clearly defined *in vitro* (Chedotal, Bloch-Gallego, & Sotelo, 1997; Letellier et al., 2009) which has been shown to reproduce the normal stages of CF-PC development (Letellier et al., 2009).

B.4 Molecules involved in reinnervation

Brain derived neuroptrophic factor (BDNF), which is important for neuronal survival, outgrowth, differentiation and synapse formation (see section 1.5.8.3) has also been shown to be involved in cerebellar and olivary development. Expression of its receptor TrkB is highest during CF-PC synaptogenesis and then steadily decreases with the increasing maturation of the olivo-cerebellar system (Sherrard et al., 2009).

Investigation of underlying molecular mechanisms shows that spontaneous reinnervation in early developmental stages and induced reinnervation *via* BDNF treatment at later stages is dependent on polysialylated neural cell adhesion molecule

(PSA-NCAM) activation, a growth-permissive cell surface molecule (Sherrard et al., 2013). PSA-NCAM is known to be involved in neuroplasticity (Rutishauser, 2008) and is extensively expressed in the developing cerebellum of the healthy rodent system (Bonfanti, 2006; Ponti, Peretto, & Bonfanti, 2006). PSA-NCAM can affect ligand-receptor binding and it has been shown to facilitate BDNF-TrkB interaction (Muller et al., 2000a) and to regulate p75 receptor expression (Gascon, Vutskits, Jenny, Durbec, & Kiss, 2007). In models of CNS injury, PSA-NCAM expression has been shown to change in association with neurite sprouting and reactive gliosis (Bonfanti, 2006). After PC axotomy in the adult cerebellum, PSA-NCAM was expressed in astrocytes near PC sprouts during the period of axonal sprouting (Dusart, Morel, Wehrlé, & Sotelo, 1999). This suggests an essential role of PSA-NCAM in axonal regeneration, possibly by inhibiting cell-cell adhesion to allow axonal outgrowth, although the exact mechanism remains unclear (Bonfanti, 2006).

NCAM function is strongly influenced by polysialylation. Addition of polysialic acid (PSA) to NCAM decreases the amount of receptor binding between adjacent cells (Bonfanti, 2006). PSA binding to NCAM is mediated *via* two Golgi-associated polysialyltransferases, ST8SiaIV (Sia4) and ST8SiaII (Sia2) (Angata & Fukuda, 2003). Studies suggest that Sia2 expression is regulated *via* cAMP-CREB pathway activation and is one of the target genes of the transcription factor Pax3 (Angata & Fukuda, 2003; Mayanil et al., 2001). Furthermore, it has been shown that Pax3 expression increases in NCAM polysialylation (Mayanil et al., 2000). Taken together, these molecules (BDNF, PSA-NCAM/Sia and Pax3) are compelling candidate genes to be involved in CF-PC reinnervation.

B.5 Cerebellar rTMS

A number of studies have shown the possibility of exciting cortico-cerebellar circuits by rTMS (Koch, 2010; Pope & Miall, 2014; Schmahmann & Caplan, 2006). It has been proposed that cerebellar stimulation activates Purkinje cells in the cerebellar cortex, leading to inhibition of thalamic and motor tract projections (Koch, 2010; Pope & Miall, 2014). One study showed an effect of cerebellar TBS (i and c) on MEP amplitude and short/long intracortical inhibition (S/LICI), suggested to reflect long-lasting modulation of motor cortex excitability *via* cerebellar-thalamic-cortical pathways, targeting GABAergic interneurons (Koch, 2010; Koch et al., 2008). Furthermore, direct application of rTMS applied to the cerebellum has been shown to have a variety of effects, such as increasing cortico-spinal excitability (Gerschlager, Christensen, Bestmann, & Rothwell, 2002), increasing oscillatory theta-wave activity (Schutter & van Honk, 2006) and improving symptoms of spino-cerebellar ataxia (Shimizu et al., 1999). A recent *in vivo* study showed modulation of molecules related to neural plasticity after high frequency rTMS in rats (Lee, Oh, Kim, & Paik, 2014). Moreover, cerebellar rTMS has been shown to have a high potential as a therapeutic tool (Koch, 2010). However, currently cerebellar rTMS is technically challenging, due to increased discomfort from involuntary muscle contractions at high intensities, which is preventable at lower intensities.

A very limited number of studies have investigated effects of low intensity magnetic stimulation in the cerebellum. At higher frequencies (50/60 Hz), LI-rMS was shown to increase membrane currents *via* activation of the cAMP/PKA pathway in cerebellar granule cells *in vitro* (He et al., 2013), to affect acetylcholinesterase (AChE) activity in

cerebellar synaptosomal membranes *in vitro* (Ravera et al., 2010) and to modulate ROS expression in the mouse cerebellum *in vivo* (Chu et al., 2011) .

Here we use an established model of axonal injury in the olivocerbellar circuit to investigate the effects of a range of LI-rMS stimulation frequencies on neural-circuit repair, candidate gene expression and activation of cellular population.

C. Custom tailoring LI-rMS delivery to the *in vitro* set-up

Models of TMS induced electric fields in the human brain (Bijsterbosch et al., 2012; Salinas et al., 2009) have shown that the induced electric field and efficiency of stimulation are determined by the relative sizes of the coil and brain (Deng et al., 2013; Weissman, Epstein, & Davey, 1992). Thus, when human devices are used in animal research, the discrepancy between large coils and small *in vivo* or *in vitro* targets results in induced electric fields which differ from those induced in the human brain. Effects are often distributed over a large area of the target, e.g. the whole animal head/body or overlapping multiple culture wells, limiting efficiency and definition of stimulation delivery. Hence, stimulation coils for animal and *in vitro* research should be tailored to specific experimental requirements.

Some groups have started to address the importance of coil size and stimulation focus by developing small stimulation devices for specific animal models (Bonmassar et al., 2012; Park et al., 2013; Rotem et al., 2014; Tischler et al., 2011). In high intensity stimulation research there is the issue that with decreasing coil size the thermal and mechanical stress increases to maintain stimulation intensity. Some groups have incorporated complex cooling devices and/or coil designs to deal with these problems (Bonmassar et al., 2012; Rotem et al., 2014; Tischler et al., 2011). However, one

advantage of lower intensity magnetic stimulation is that stimulation intensities can be reached without excessive stress on the stimulation device, as has been demonstrated recently in our laboratory *via* the construction of a small animal coil to investigate the effects of low intensity magnetic fields in the mT range in a mouse model of abnormal neuronal connections (Rodger et al., 2012).

Additionally, because of increased control possibilities of experimental parameters *in vitro*, a homogenous magnetic field is generally achieved *via* application of Helmholtz coil systems (Di Loreto et al., 2009; Morabito et al., 2010a; Stratton et al., 2013). These consist of two or more solenoid coils along the same axis (Bronaugh, 1995), where the target is placed within that axis, generally along the central, homogenous magnetic field depending on the *in vitro* requirements. Nonetheless, due to their relatively large space requirements, Helmholtz systems are not always ideal, nor cost-efficient to apply in the limited space of an incubator and to some kinds of culture plates, especially, if multiple, simultaneous stimulation is desired. To be able to have multiple, simultaneous coils at close proximity, their effects on each other and neighbouring tissue have to be taken into careful consideration for the development of a multi-channel system (Han, Chun, Lee, & Lee, 2004). Hence, custom-tailored stimulation devices for multi-target stimulation are needed to optimize rMS *in vitro* and increase comparability of results.

A key aspect of this thesis was to identify the parameters required to build a stimulation system that is tailored for organotypic culture. In addition, we demonstrate the creation of an automated and adjustable stimulation system that can deliver a high range of LI-rMS frequencies adapted to the specific requirements of our *in vitro* organotypic culture.

Chapter 2

2 Investigating the effects of LI-rMS on single neurons at a range of different frequencies: anatomical and molecular changes

Chapter 1 outlines the increasing scientific base of the biological importance of low intensity magnetic stimulation effects. In particular, because initial studies indicate that LI-rTMS has therapeutic benefits and low intensity stimulation forms a peri-focal by-field of human rTMS, the effects of LI-rTMS merit systematic investigation. To understand the long-term effects of LI-rTMS at a brain systems level (such as cortical excitability), it is necessary to perform fundamental investigation of effects at the cellular and molecular level in CNS tissue. A small number of studies have started to investigate these effects; however comparison between studies is difficult due to high variability of experimental models, in particular the stimulation parameters used. A systematic investigation of the effects of different frequencies on a range of biological parameters at the single cell level, after both single or multiple stimulation sessions, has not been carried out.

Here we investigate the effects of LI-rMS on anatomical and molecular changes in single neurons at a range of different frequencies. We applied different LI-rMS to primary cortical cultures in order to systematically investigate the effects of single and multiple LI-rMS, with the help of a small custom-build magnetic stimulation device that was tailored for the specific *in vitro* set-up, to deliver a defined magnetic field in the tissue of interest.

We applied four consecutive stimulation sessions per frequency and quantified survival of different cell populations and changes in neuronal morphology. We then sought insight into the underlying mechanisms involved in these long-term effects, and investigated modulation of intracellular calcium in real time during stimulation.

Consistent with a wide range of studies, both in high and low intensity literature, we showed that intracellular calcium was increased by LI-rMS. We also applied pharmacological agents to demonstrate for the first time that the source of intracellular calcium changes resulted from intracellular stores. We showed that a single session of LI-rMS induced changes in the expression of genes involved in downstream calcium signalling cascades and that these changes were stimulation-specific and consistent with the changes in cellular viability observed after repeated stimulation.

Article 1

Grehl, S., Viola, H. M., Fuller-Carter, P. I., Carter, K. W., Dunlop, S. A., Hool, L. C., Sherrard, R.M., Rodger, J. (2015). Cellular and Molecular Changes to Cortical Neurons Following Low Intensity Repetitive Magnetic Stimulation at Different Frequencies. *Brain Stimulation, 8* (1), 114-123. (Appendix E)

SG contribution: 85 %

Cellular and molecular changes to cortical neurons following low intensity repetitive magnetic stimulation at different frequencies

Stephanie Grehl (1,4), Helena Viola (2), Paula I Fuller-Carter (1), Kim W Carter (3),

Sarah A Dunlop (1), Livia Hool (2), Rachel M Sherrard*(2,4), Jennifer Rodger* (1)

School of Animal Biology (1) and Anatomy, Physiology and Human Biology (2) , Telethon Institute for Child Health Research, Centre for Child Health Research, University of Western Australia, Perth, Australia (3) and Sorbonne Universités, UPMC Univ Paris 06 & CNRS, UMR 8256 Adaptation Biologique et Vieillissement, Paris, France (4).

** These two are co-senior authors*

Corresponding author:

A/Prof Jennifer Rodger

Experimental and Regenerative Neurosciences M317

School of Animal Biology

University of Western Australia

35 Stirling Highway

Crawley WA 6009

email: jennifer.rodger@uwa.edu.au

INTRODUCTION

Repetitive transcranial magnetic stimulation (rTMS) is used in clinical treatment to non-invasively stimulate the brain and promote long-term plastic change in neural circuit function (Pell et al., 2011; Thickbroom, 2007), with benefits for a wide range of neurological disorders (Adeyemo, Simis, Macea, & Fregni, 2012; Daskalakis, 2014; George, Taylor, & Short, 2013). In addition, there is increasing evidence that low intensity magnetic stimulation (LI-rTMS) may also be therapeutic, particularly in mood regulation and analgesia (Di Lazzaro et al., 2013; Martiny et al., 2010; Robertson et al., 2010). Nonetheless, clinical outcomes of rTMS and LI-rTMS are variable (Wassermann & Zimmermann, 2012) and greater knowledge of the mechanisms underlying different stimulation regimens is needed in order to optimise these treatments.

Investigating the mechanisms of both high and low intensity rTMS is important because most human rTMS protocols deliver a range of stimulation intensities across and within the brain. Human rTMS is most commonly delivered using butterfly figure-of-eight shaped coils (Fatemi-Ardekani, 2008; Thielscher & Kammer, 2004) to produce focal high-intensity fields that depolarise neurons in a small region of the cortex underlying the intersection of the 2 loops (Fatemi-Ardekani, 2008; Thielscher & Kammer, 2004), which in turn can modulate activity in down-stream neural centres (Aydin-Abidin, Trippe, Funke, Eysel, & Benali, 2008; Valero-Cabré, Payne, Rushmore, Lomber, & Pascual-Leone, 2005). However, this stimulation focus is surrounded by a weaker magnetic field such that a large volume of adjacent cortical and sub-cortical tissue is also stimulated, albeit at a lower intensity that is below activation threshold (Cohen et al., 1990; Deng et al., 2013). While the functional importance of this para-

focal low-intensity stimulation in the context of human rTMS is unclear, low-intensity magnetic stimulation on its own modifies cortical function (Capone et al., 2009; Robertson et al., 2010) and brain oscillations (Cook et al., 2004). Moreover, animal and *in vitro* studies demonstrate that low-intensity stimulation alters calcium signalling (Pessina et al., 2001; Piacentini et al., 2008), gene expression (Mattsson & Simkó, 2012), neuroprotection (Yang et al., 2012) and the structure and function of neural circuits (Makowiecki, Harvey, Sherrard, & Rodger, 2014; Rodger et al., 2012). However, the mechanisms underlying outcomes of low-intensity magnetic stimulation, particularly in conjunction with different stimulation frequencies, have not been investigated.

To address this, we undertook a systematic investigation of the fundamental morphological and molecular effects of five repetitive low intensity magnetic stimulation (LI-rMS) protocols in a simple *in vitro* system with defined magnetic field parameters. We show for the first time that LI-rMS induces calcium release from intracellular stores. Moreover, we show specific effects of different stimulation protocols on neuronal survival and morphology and associated changes in expression of genes mediating apoptosis and neurite outgrowth. Taken together, our data demonstrate that even low intensity magnetic stimulation induces long-term modifications to neuronal structure, which might have implications for understanding the effects of high-intensity human rTMS in the whole brain.

METHODS

Animals

C57Bl/6j mice pups were sourced from the Animal Resources Centre (Canning Vale, WA, Australia). Experimental procedures were approved by the UWA Animal Ethics Committee (03/100/957).

Tissue culture

To investigate changes in neuron biology following LI-rMS stimulation, we used neuronal enriched cultures from postnatal day 1 mouse cortex. Pups were euthanased by pentobarbitone sodium (150 mg/kg i.p.), decapitated and both cortices removed. Pooled cortical tissue was dissociated and prepared following standard procedures (Meloni, Majda, & Knuckey, 2001). Cells were suspended in NB media (Neurobasal-A, 2 % B27 (Gibco®), 0.6 mg/ml creatine, 0.5 mM L-glutamine, 1 % Penicillin/Streptomycin, and 5 mM Hepes) and plated on round poly-D-lysine coated coverslips at a density of 75000 cells/well (day 0 *in vitro*; DIV 0). On DIV 3, half the culture medium was removed and replaced with fresh media containing cytosine arabinofuranoside (6 µM; Sigma) to inhibit glial proliferation. Cells were grown at 37°C in an incubator (5% CO_2 + 95% air) for 10 days and half the medium was replaced on DIV 6 and 9. To ensure that any experimental effects were not due to either different litters or culture sessions, plated coverslips from each litter were randomly allocated to stimulation groups. The whole culture-stimulation procedure was repeated 3 times.

Repetitive Magnetic Stimulation

LI-rMS stimulation was delivered to cells in the incubator with a custom built round coil (8 mm inside diameter, 16.2 mm outside diameter, 10 mm thickness, 0.25 mm copper wire, 6.1 Ω resistance, 462 turns) placed 3 mm from the coverslip (Fig 2.1A) and driven by a 12 V magnetic pulse generator: a simple resistor-inductor circuit under control of a programmable (C-based code) micro-controller card (CardLogix, USA). The non-sinusoidal monophasic pulse (Peterchev et al., 2011) had a measured 320μs rise time and generated an intensity of 13 mT as measured at the target cells by hall effect (ss94a2d, Honeywell, USA) and assessed by computational modelling using Matlab (Mathworks, USA; Fig 2.1B,C). Coil temperature did not rise above 37^{o}C, ruling out confounding effects of temperature change. Vibration from the bench surface (background) and the top surface of the coil were measured at 10 Hz stimulation using a single-point-vibrometer (Polytec, USA); coil vibration was within vibration amplitude of background (Fig 2.1D).

Stimulation was delivered for 10 continuous minutes per day at 1 of 5 frequencies: 1 Hz, which reduces, or 10 Hz which increases, cortical excitability in human rTMS (Fitzgerald et al., 2006; Hoogendam et al., 2010); we also used 100 Hz, consistent with very low intensity pulsed magnetic field stimulation (Ash et al., 2009; Di Lazzaro et al., 2013), continuous theta burst stimulation (cTBS: 3 pulses at 50 Hz repeated at 5 Hz) showing inhibitory effects on cortical excitability post-stimulation in human rTMS (Gamboa et al., 2011; Huang et al., 2005) or biomimetic high frequency stimulation (BHFS: 62.6 ms trains of 20 pulses, repeated at 9.75 Hz). The BHFS pattern was designed on electro-biomimetic principles (Martiny et al., 2010), based on the main

parameter from our previous studies (Makowiecki et al., 2014; Rodger et al., 2012) which was modelled on endogenous patterns of electrical fields around activated nerves during exercise (patent PCT/AU2007/000454, Global Energy Medicine). The total number of pulses delivered for each stimulation paradigm is shown in Table 1. We chose a standard duration of stimulation of 10 minutes (rather than a standard number of pulses) because studies of brain plasticity reveal that 10 minutes of physical training or LI-rTMS is sufficient to induce functional and structural plasticity (Angelov et al., 2007; Makowiecki et al., 2014; Rodger et al., 2012). For all experiments, controls were treated identically but the coils were not activated. An overview of experiments and summary of experimental design is shown in Fig 2.1E.

Frequency	Total pulses delivered in 10 minutes
1 Hz	600
10 Hz	6,000
100 Hz	60,000
cTBS	7,000
BHFS	120,000

Table 2.1 Total number of pulses delivered during 10 minutes for each frequency.

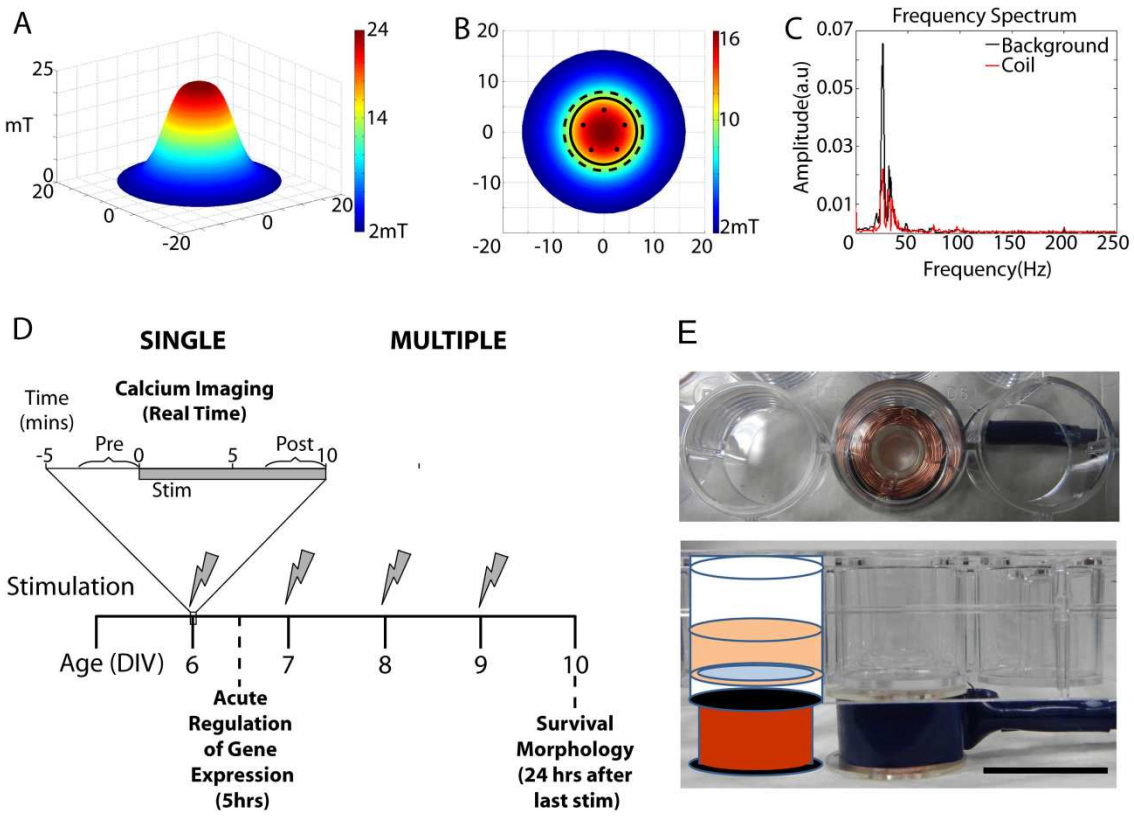

Figure 2.1 Stimulation apparatus and experimental design. A) Matlab software model representing the induced magnetic field at the level of the coil, distance in mm. B) Top view of modelled magnetic field strength at 3 mm from the base of the coil (position of the coverslip). Dashed circle represents the well and solid circle represents the edge of the cover slip (Ø = 13 mm). Black dots show the sampling locations for cell counts and morphological analysis. C) Fourier transform of the frequency spectrum of vibration measurement (mm/s) taken by a single-point-vibrometer placed either on the bench surface (background) or on top of the coil (in place of the culture plate as illustrated in (E). Vibration measured from background surface (black) and the coil (red) confirms that the coil did not generate vibration above background levels. D) Timeline for our experimental design. We delivered multiple sessions of LI-rMS (DIV6-9) to see the cumulative effects on the survival and morphology of single neurons. Then in separate experiments we examined potential mechanisms underpinning these cellular effects by identifying acute changes induced by a single session of LI-rMS: (1) intracellular calcium during stimulation; (2) gene expression 5 hrs after stimulation, an interval necessary for transcriptional changes to have occurred. The inset shows the detailed timeframe for intracellular calcium imaging, and is an example for DIV 6. LI-rMS was delivered for 10 minutes (grey zone). Ratiometric fluorescent values recorded over the last 3 min of stimulation were averaged and reported as a percentage of pre-stimulation baseline. E) photographs of an *in vitro* stimulation coil used in this study. Views are from the top (top panel) and side (bottom panel). The diagram in the bottom panel shows that the coil was placed beneath one well of a 24 well culture dish containing a coverslip (blue) with culture medium (pink). The coil (orange) was located at a distance of 3 mm from the coverslip because of the thickness of the plastic base of the culture dish (white). Note that neighbouring wells did not contain coverslips to avoid interactions of magnetic fields from individual coils (compare extent of magnetic field and coverslip shown in (B). Scale bar (A): 15 mm.

Immunohistochemistry

To investigate the influence of different stimulation frequencies at the cellular level, we used immunohistochemistry to examine neuronal survival and the prevalence of different cell types. Cells plated on glass coverslips were grown in 12 spatially separated wells of a 24 well plate to ensure no overlap of magnetic field. Wells were stimulated for 10 minutes daily from DIV 6-9 and cells were fixed with 4% paraformaldehyde 24 hours after the last stimulation. Mouse anti-active Caspase-3 (1:50, Abcam) and TUNEL (DeadEnd™ Fluorometric TUNEL System, Promega) double labelling were carried out to identify apoptosis. Glia and neurons were labelled with rabbit anti-GFAP (1:500, Dako) or mouse anti-βIII Tubulin (1:500, Covance). Subpopulations of neurons were identified, using rabbit anti-calbindin D-28K (inhibitory and small excitatory neurons; 1:500, Chemicon (Brederode van, Helliesen, & Hendrickson, 1991)) or mouse anti-SMI-32 (excitatory neurons; 1:2000, Covance (DeFelipe, 1997)). Antibody binding was visualised using fluorescently labelled secondary antibodies (Alexa Fluor 546 and Alexa Fluor 488; Invitrogen). Cell nuclei were labelled with either Hoechst (1:1000, Sigma Aldrich) or Dapi (DeadEnd™). Coverslips were mounted with Fluoromount-G.

Histological Analysis

For each experimental group, histological analyses were performed blind to stimulation paradigm on 12-18 images containing cultured cells from 2-3 different litters. Five semi-randomly distributed images per immunostained coverslip were taken from locations underneath the desired magnetic field (13 mT), in order to analyse cells that had received similar stimulation intensity.

We counted cells labelled with the following antibody combinations: βIII Tubulin or GFAP (neurons/glia), Caspase-3 and TUNEL (apoptotic cells), or Calbindin or SMI-32 (inhibitory/excitatory neurons). Raw counts were normalized to the total cells numbers (Hoechst or DAPI labelled) in the analysed field (FA). Cells that were not immunolabelled for either marker were identified as 'other' and included in the total cell count.

Morphometric analysis was undertaken on individually visualized neurons. Calbindin labelled neurons had weakly labelled processes thus neurite morphology could not be reliably distinguished. Thus, only SMI-32 positive cells were analysed. For every cell, the longest neurite was traced and its total length calculated with Image J. To estimate neuronal morphology, fast Sholl analysis (Gutierrez & Davies, 2007) was performed, using an Image-Pro®Plus (Media Cybernetics, Inc.) based macro (M. Doulazmi, UPMC).

Calcium Imaging

To assess the mechanisms underlying LI-rMS effects, we measured real-time changes in intracellular calcium during stimulation. On DIV 6-10, cells were incubated in 1 µM Fura-2AM (Molecular Probes) supplemented media at 37°C for 90-120 min. Immediately prior to experimentation, cells were transferred to Fura-2AM supplemented imaging solution containing: 140 mM NaCl, 5 mM KCl, 2.5 mM $CaCl_2$, 0.5 mM $MgCl_2$, 10 mM Glucose and 10 mM Hepes (pH 7.4). Intracellular calcium was assessed at 37°C as described previously (Viola, Arthur, & Hool, 2007) to evaluate ratiometric change and estimate intracellular concentration $[Ca^{2+}]_i$ (nM). Fura-2 340/380 nm ratiometric fluorescence was captured using a Hamamatsu Orca ER digital

camera attached to an inverted Nikon TE2000-U microscope (ex 340/380 nm, em 510 nm) and analysed by manually tracing cells in MetaMorph® 6.3 (Molecular Devices).

Ratiometric fluorescent values were recorded from 5 min pre-stimulation to 5 min post-stimulation (or control) at 1 minute time intervals. Analyses were made off-line such that the experimenter was blind to stimulation group. Ratiometric fluorescent values were averaged over the last 3 min of stimulation ($\mu_{Main:}$ minutes 8-10), and normalised to the pre-stimulation baseline (μ_{Pre}: minutes 3-5). Percentage Fura-2 ratiometric signal change ($Y_{\%change}$) was calculated ($Y_{\%change} = ((\mu_{Pre} - \mu_{Main})/ \mu_{Main}) * 100$) (Fig 2.1E). Pilot experiments showed that there was no effect of culture age (DIV) on calcium responses, thus data were pooled across days.

Following each experiment, cells were fixed with 4% paraformaldehyde and immunostained for GFAP/βIII Tubulin/Hoechst, as described above, to confirm that imaged cells were neurons. Only data from βIII tubulin-positive neurons were included in the analysis.

To investigate the source of increased intracellular calcium, we assessed alterations in intracellular calcium when neurons were either placed in calcium-free imaging solution, or exposed to thapsigargin (3 μM, SIGMA) to deplete intracellular calcium stores. For calcium-free studies, cells were placed in calcium-free imaging solution (140 mM NaCl, 5 mM KCl, 0.5 mM $MgCl_2$, 10 mM HEPES, 10 mM Glucose, 3 mM EGTA, pH 7.4) immediately prior to experimentation. To confirm that results were not based on changes in ion concentration, in some experiments we compensated for the drop in Ca^{2+} with an equi-molar replacement of Mg^{2+} to keep a constant surface charge effect across the membrane. Results showed no difference between these 2 solutions.

Thapsigargin studies (supplemented 10 min prior to experimentation) were performed in normal 2.5 mM calcium containing imaging solution. All imaging solutions were supplemented with 1 µM Fura-2AM. Cell viability was confirmed with propidium iodide (PI) post-stimulation and cells that were permeable to PI were excluded from subsequent analysis (Appendix A) .

PCR Array

To investigate the molecular events triggered by different frequency stimulation, changes in gene expression were examined in a separate series of cultures following a single stimulation at DIV 6. For each group (3 frequencies plus control), three replicates of ten wells underwent one stimulation session. Five hours after the end of stimulation, total RNA was extracted with Trizol (Life Technologies) followed by purification on RNeasy kit columns (Qiagen). cDNA was transcribed from 200 ng of total RNA using the RT² Easy First Strand cDNA Synthesis Kit (Qiagen). For each sample, 250 ng of cDNA was applied to the Mouse cAMP / Ca^{2+} Signaling Pathway Finder PCR Array and amplified on a Rotorgene 6000. Results were analysed by a researcher (K Carter), who did not know the tissue groupings, on the Qiagen RT^2 Profiler PCR array data analysis (v3.5) using the geometric mean of housekeeping genes glyceraldehyde-3-phosphate dehydrogenase and glucuronidase beta. Normalized mean expression levels (log2(2-ΔCt)) were used to determine differentially expressed genes between each group and control. Changes in gene expression were analysed further in R 3.0.1 using the NMF package (Gaujoux & Seoighe, 2010), Ingenuity Pathways Analysis (IPA) and WebGestalt (Zhang, Kirov, & Snoddy, 2005).

Statistical analysis

Data from all groups were explored for outliers and normal distribution with SPSS Statistics 20 (IBM). For cell survival and calcium imaging experiments, effects of frequency were analysed with One-way Analysis of Variance (Kruskal-Wallis; H) and Mann-Whitney (U) pairwise comparisons with Bonferroni-Dunn correction where appropriate. Neurite length data was analysed with Univariate ANOVA (F). Gene expression levels from the PCR array were compared by two sample *t*-test. All values are expressed as mean ± SEM and considered significant at $p < 0.05$.

RESULTS

We delivered multiple sessions of LI-rMS (DIV6-9) to see the cumulative effects on the survival and morphology of single neurons. We then examined potential mechanisms underpinning these cellular effects by identifying acute changes induced by a single session of LI-rMS: (1) intracellular calcium during stimulation; (2) gene expression 5 hrs after a single stimulation session, an interval necessary for transcriptional changes to have occurred. The experimental design is summarized in Fig 2.1E.

rMS stimulation-specific effects on neuronal survival and morphology

We first investigated whether low intensity LI-rMS had deleterious effects and induced apoptosis by counting cells double labeled for Caspase-3 and TUNEL ($N_{\text{fields analyzed (FA)}}$: Control = 22; 1 Hz = 10; 10 Hz = 10; 100 Hz = 9; cTBS = 10; BHFS = 10). While the great majority of cells (about 90%) continued growing normally, there was a small but significant increase of apoptotic cells in cultures stimulated at 10 Hz (11.11 % ± 1.84) and 100 Hz (11.08 % ± 1.79) compared to unstimulated controls (4.3 % ± 0.9; $p = 0.036$

and 0.044 respectively, Fig 2.2A). In contrast, stimulation by 1 Hz and complex frequencies did not significantly alter apoptosis (~ 4-7 % cells in each group). Because stimulation at 100 Hz did not induce more apoptosis than 10 Hz, it was not investigated further.

We next evaluated whether different LI-rMS patterns altered the proportions of neurons and glia in primary cortical cultures (N_{FA}: Control = 19; 1 Hz = 18; 10 Hz = 18; cTBS = 18; BHFS = 15). The ratio of neurons-to-glia following stimulation at any frequency was no different from unstimulated control cultures (Fig 2B,C), suggesting that the small amount of apoptosis (~4-7 %) involved all cell types equally. On average, pooled across all frequencies, we observed 85.6 % ± 1.1 neurons, 5.1 % ± 1.3 glia and 9.3 % undefined cells in our cultures.

Because some studies have shown that magnetic fields differentially affect inhibitory and excitatory neurons (Benali et al., 2011; Meyer et al., 2009) we quantified the proportions of two neuronal populations: calbindin D-28K-positive neurons, which are predominantly inhibitory (Brederode van et al., 1991), and SMI-32-labelled excitatory neurons (N_{FA}: Control = 24; 1 Hz = 13; 10 Hz = 25; cTBS = 16; BHFS = 14). The higher proportion of inhibitory neurons in early postnatal cultures is in line with previous studies (Alho, Ferrarese, Vicini, & Vaccarino, 1988). Only 1 Hz stimulation altered the relative proportions by increasing that of calbindin positive neurons ($p = 0.001$), from 81.6 % ± 1.8 in control cultures to 92.2 % ± 1.7, while decreasing the percentage of SMI-32 positive neurons ($p = 0.029$), from 4.1 % ± 0.8 in control cells to 0.8 % ± 0.3 (Fig 2.2 D,E).

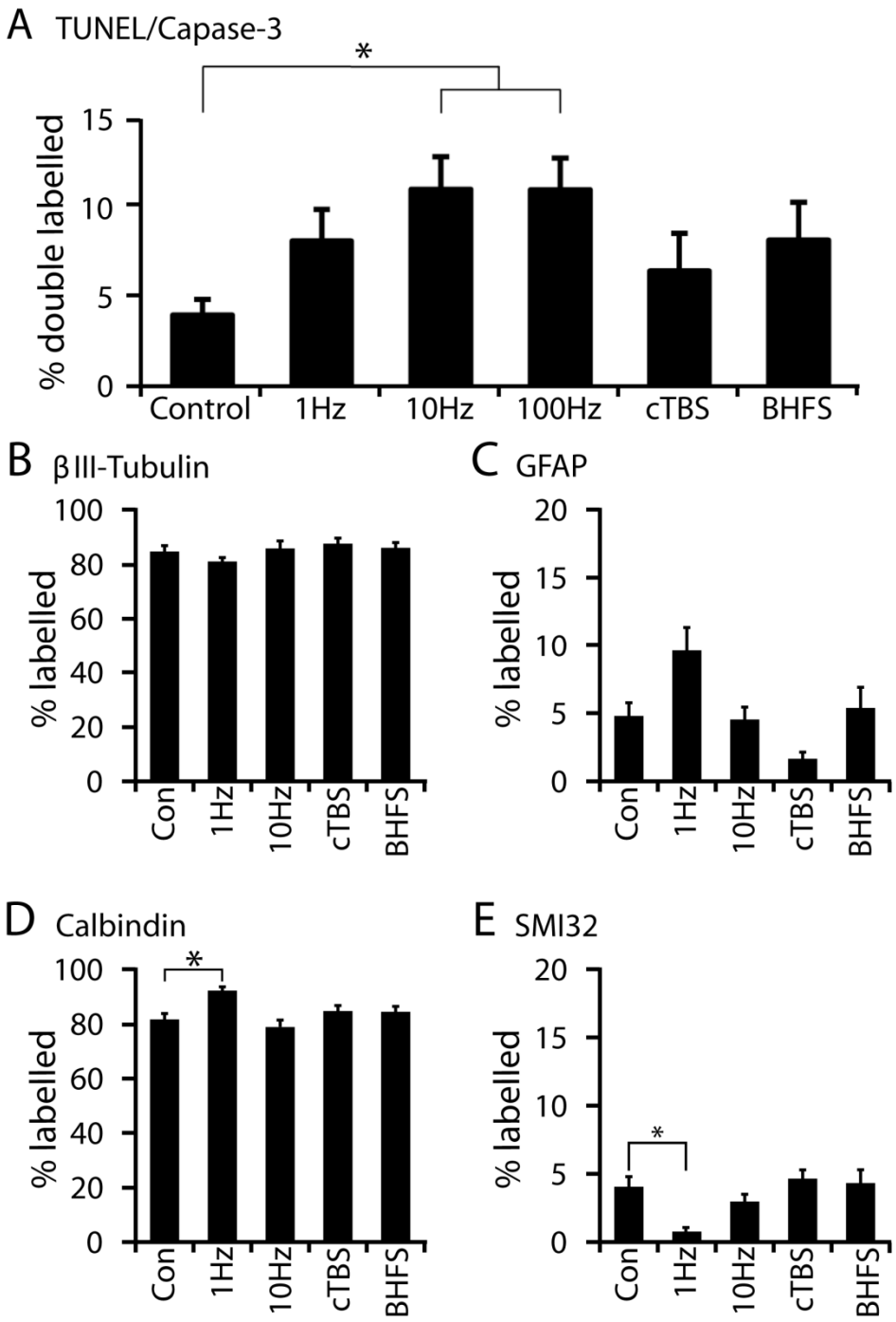

Figure 2.2 Cell survival and neuronal subpopulations. A) Percentage cells double labeled for Caspase-3 and TUNEL were increased following 10 and 100 Hz compared to unstimulated controls (H = 14.32, p = 0.014. Pairwise comparisons Control-10 Hz: U = -23.832, p = 0.036 and Control-100 Hz: U = -24.237, p = 0.044). B,C) Percentage cells that were labeled with βIII Tubulin (neurons; B) or GFAP (glia; C) (Neuron: H = 5.93, p = 0.204, Glia: H = 14.53, p = 0.006. Pairwise comparisons (U): no significant difference to Control). D,E) Percentage cells that were labeled with Calbindin (D) or SMI-32 (E). 1 Hz increased the proportion of calbindin positive inhibitory neurons and decreased SMI-32 positive glutamatergic neurons compared to unstimulated controls (H = 21.103, p = 0.000. Pairwise comparisons Control-1 Hz: U = -35.94, p = 0.001. SMI-32: H = 15.19, p = 0.004. Pairwise comparisons Control-1 Hz: U = 26.71, p = 0.029). Error bars are standard error of the mean.

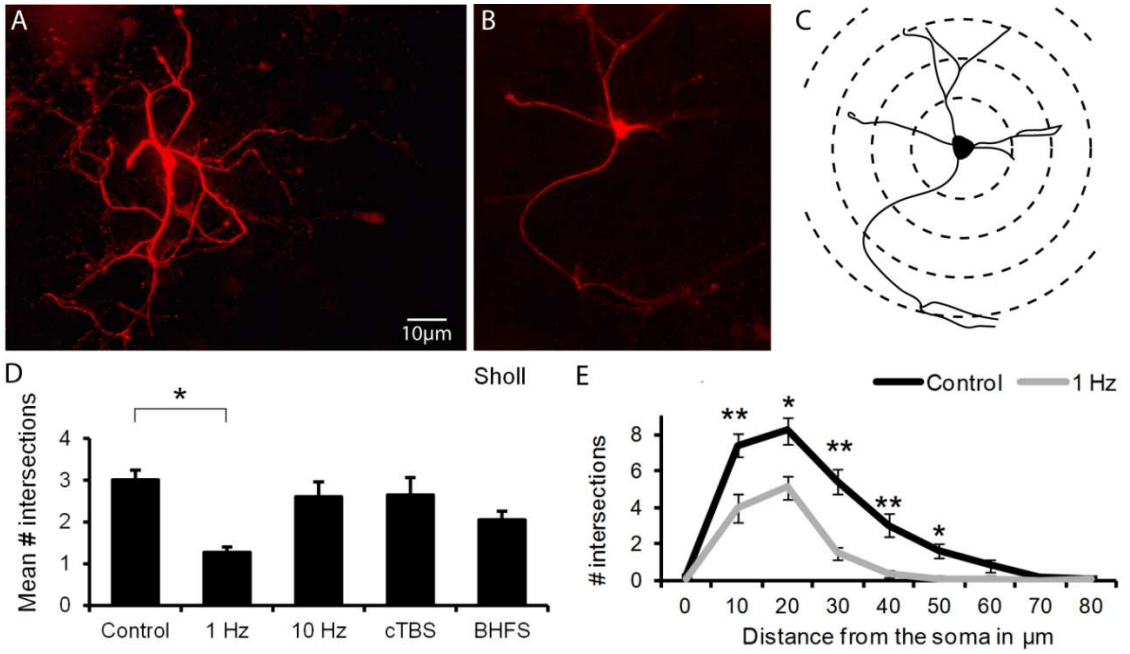

Figure 2.3 LI-rMS has stimulation pattern-specific effects on neuronal morphology. A,B) Representative neuronal morphology from control (A) and 1 Hz (B) stimulation. C) diagram illustrating Sholl analysis. D) mean number of dendrite intersections per neuron following LI-rMS (4 days, 10 min per day) at different frequencies ($H = 17.84$, $p = 0.001$. Pairwise comparisons Control-1 Hz: $U = 30.771$, $p = 0.001$). E) Number of intersections per concentric Sholl circle from 10-80 µm from the soma are decreased in 1 Hz stimulated samples compared to unstimulated controls (10 µm: $U = 7.13$, $p = 0.008$, 20 µm: $U = 5.94$, $p = 0.015$, 30 µm: $U = 7.86$, $p = 0.005$, 40 µm: $U = 6.84$, $p = 0.009$, 50 µm: $U = 5.29$, $p = 0.021$). Error bars are standard error of the mean.

This reduction in number of SMI-32 positive cells (3.3 %) is within the 4-7 % cell death observed in control and 1 Hz stimulated cultures (Fig 2.2A) and suggests that LI-rMS at 1 Hz slightly impaired survival of SMI-32 positive excitatory neurons without increasing apoptosis overall.

We then investigated neurite branching and outgrowth from individual SMI-32 positive neurons (N: Control = 24; 1 Hz = 8; 10 Hz = 14; cTBS = 7; BHFS = 11). Stimulation at 1 Hz significantly reduced neurite branching and outgrowth by 60% compared to control

neurons (Fig 2.3A-E; p = 0.001). Sholl analysis revealed that changes occurred 10-50 µm from the soma (Fig 2.3E). However, the length of the longest neurite of each SMI-32 positive neuron was not significantly different between stimulation frequencies (F = 0.936, p = 0.45).

LI-rMS releases calcium from intracellular stores

To identify mechanisms that may explain these morphological and cell survival data, we examined changes in intracellular calcium during stimulation. Compared to unstimulated controls, each of 10 Hz, cTBS and BHFS stimulation significantly increased Fura-2 ratiometric fluorescence ($p < 0.001$; Fig 2.4A) by 11–13 % (Control: 2.1 % ± 0.8; 10 Hz: 13.4 % ± 2.3; cTBS: 15.0 % ± 2.6 and BHFS: 15.1 % ± 2.0). This is equivalent to an average change in intracellular Ca^{2+} from 34.31 nM ± 7.44 in control to 414.77 nM ± 41.52 after 10 min stimulation, a rise which is in the range of increased Ca^{2+} concentration following action potential induction (Helmchen, Borst, & Sakmann, 1997; Liao & Lien, 2009). In contrast, 1 Hz stimulation induced an intermediate increase (8.3 % ± 1.1) in Fura-2 ratiometric fluorescence which was not significantly different from either unstimulated control or other stimulation frequencies (Fig 2.4A). No impact on neuronal viability was observed following a single session of LI-rMS stimulation (data not shown).

To determine whether the increase in intracellular calcium originated from the extracellular milieu or intracellular stores, we stimulated neurons either in calcium-free imaging solution, or after thapsigargin treatment (Fig 2.4B). Because of apparent equivalence of effect for cTBS and BHFS stimulation in previous experiments, pharmacological tests were carried out on 1 Hz, 10 Hz and BHFS frequencies.

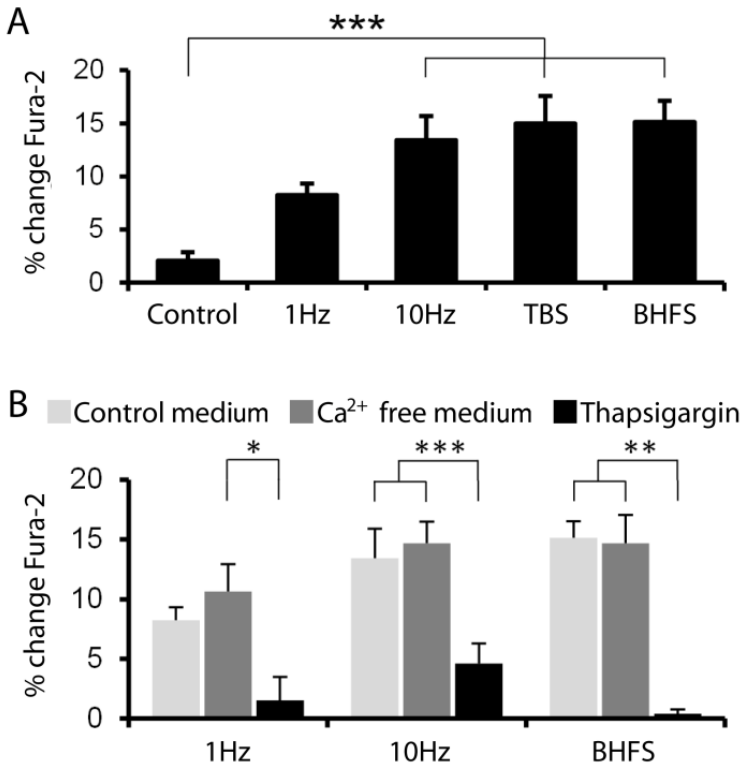

Figure 2.4 LI-rMS induces Ca^{2+} release from intracellular stores. Alterations in Fura-2 340/380 nm ratiometric fluorescence (% change Fura-2) in cortical neurons after a single 10 min stimulation with 1 Hz, 10 Hz, cTBS and BHFS frequencies. A) LI-rMS at each of 10 Hz, cTBS and BHFS increased intracellular calcium compared to unstimulated controls, while 1 Hz only generated an intermediate rise (H = 20.7, p = 0.000. Pairwise comparisons Control-10 Hz: U= -27.97, p = 0.007; Control-cTBS : U = -32.48, p = 0.001; Control-BHFS : U = -38.03, p = 0.000). B) LI-rMS induced similar increase in Fura-2 ratiometric fluorescence in normal imaging and calcium-free media but not in thapsigargin supplemented (H = 20.89, p = 0.000. Pairwise comparisons Normal-Thapsigargin: U = 23.6, p = 0.000; Ca2+ free – Thapsigargin: U = 31.39, p = 0.000). Error bars are standard error of the mean.

For all frequencies, the increase in neuronal Fura-2 ratiometric fluorescence under calcium-free conditions was not significantly different from that in normal imaging media (1 Hz: 10.7 % ± 2.5; 10 Hz: 14.7 % ± 1.8 and BHFS: 14.7 % ± 1.7). In contrast, exposure of cells to thapsigargin resulted in strong attenuation of the Fura-2 signal during stimulation at all frequencies ($p < 0.05$; 1 Hz: 1.5 % ± 1.4, 10 Hz: 4.6 % ± 2.4 and BHFS: 0.4 % ± 0.4). These data indicate that LI-rMS stimulation induces release of Ca^{2+} from intracellular stores rather than influx from the extracellular milieu (Fig 2.4B).

LI-rMS changes expression of genes implicated in neuronal survival

To further understand how LI-rMS may lead to changes in cell survival and morphology, we examined the immediate up-and down-regulation of genes associated with Ca^{2+} signaling, five hours after a single session of stimulation at different frequencies (Appendix B). We identified 16 genes (Table 2.2; Fig 2.5A) for which expression changes were significantly different from unstimulated controls ($p < 0.05$) in at least one of the three experimental groups (Fig 2.5B).

Enrichment analysis on these 16 genes in IPA and gene ontology terms (Webgestalt; supplementary Table 1, Appendix E) revealed that 15 of the 16 genes were significantly associated with two major biofunctions: 1) cell survival and apoptosis and 2) cell morphology and migration (Fig 2.5C). The remaining gene, slc18a1 encodes a vesicular monoamine transporter and was significantly increased following stimulation with 10 Hz.

All LI-rMS frequencies induced changes in genes situated within neuronal survival or apoptosis pathways (Fig 2.6A,B), of which some were common to all frequencies (ENO2 and CRH), and others pattern-specific (Figs 2.5B, 2.6A,B; Table 2.2). 10 Hz stimulation, which was associated with apoptosis, upregulated pro-apoptotic genes (e.g. Pmaip1/Noxa, and BRCA1) and downregulated anti-apoptotic genes (e.g. JunD). In addition, stimulation by frequencies which did not induce apoptosis resulted in pro-survival changes to gene expression (eg. 1 Hz upregulated hexokinase and BHFS downregulated cdk5 and Sod2). These data also show that although all our LI-rMS paradigms altered intracellular Ca^{2+}, the downstream effects on gene expression were specific for each stimulation frequency and rhythm.

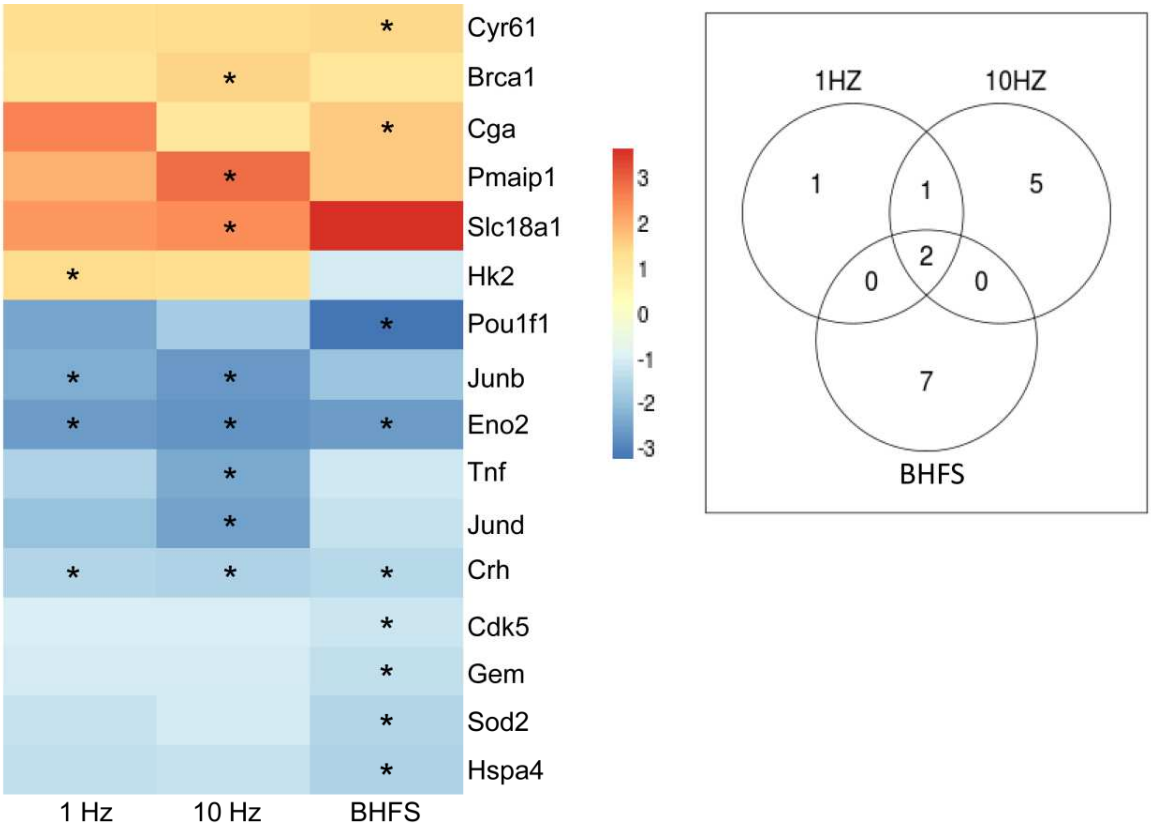

C

Molecules in Network	Focus Molecules	Top Functions
Brca1, Cdk5, Cga, Crh, Cyr61, Eno2, Gem, Hk2, Hspa4, Junb, Jund, Pmaip1, Pou1f1, Slc18a1, Sod2, Tnf, TSHB, GH2, Crhr	15	Cell Death and Survival, Cell Cycle, Cellular Development, Endocrine System Disorders, Cellular Growth and Proliferation, Hematological System Development and Function
Slc18	1	Cell-To-Cell Signaling and Interaction, Nervous System Development and Function, Cellular Growth and Proliferation

Figure 2.5 Changes in gene expression following different LI-rMS stimulation protocols. A) Heat map showing changes in expression (log_2 fold change) of the 16 genes that were significantly (asterisks) regulated following LI-rMS stimulation at one or more frequencies. B) Venn diagram showing number of changes in gene expression that are common to all frequencies and those that are specific to individual frequencies. C) Biofunctions of the 16 modulated genes as identified in Ingenuity Pathway analysis.

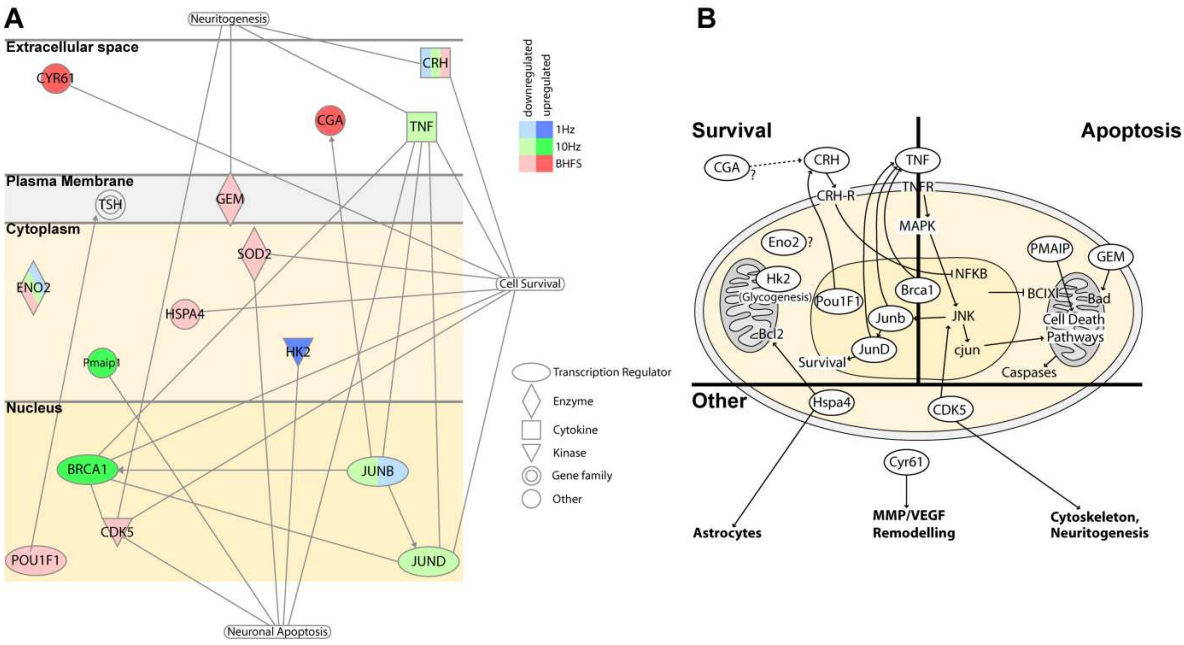

Figure 2.6 Representations of the relationships between 15 genes that were significantly regulated following LI-rMS stimulation. A) Pathway diagram obtained from Ingenuity Pathway Analysis showing the relationship between the genes examined following LI-rMS (blue = 1 Hz; green = 10 Hz and red = BHFS). Dark shading indicates upregulation and light shading indicates downregulation. B) Regulated genes (in ovals) are situated within the cell survival and cell death pathways (see also Table 2.2 and Fig 2.5C). Non-regulated genes are included to provide context.

ID	Entrez Gene Name	1Hz p-value	1 Hz Log FC	10 Hz p-value	10Hz Log FC	BHFS p-value	BHFS Log FC	Location	Type(s)
Brca1	breast cancer 1, early onset	0.27	1.200	**0.03**	**1.530**	0.62	1.070	Nucleus	transcription regulator
Cdk5	cyclin-dependent kinase 5	0.75	-1.030	0.68	-1.040	0.03	-1.220	Nucleus	kinase
Cga	glycoprotein hormones, alpha polypeptide	0.20	2.620	0.75	1.050	**0.04**	**1.640**	Extracellular Space	other
Crh	corticotropin releasing hormone	0.01	-1.540	0.03	-1.620	0.003	-1.500	Extracellular Space	cytokine
Cyr61	cysteine-rich, angiogenic inducer, 61	0.19	1.290	0.06	1.370	**0.03**	**1.410**	Extracellular Space	other
Eno2	enolase 2 (gamma, neuronal)	0.04	-2.590	0.03	-2.740	0.03	-2.560	Cytoplasm	enzyme
Gem	GTP binding protein overexpressed in skeletal muscle	0.85	-1.050	0.33	-1.110	0.02	-1.330	Plasma Membrane	enzyme
Hk2	hexokinase 2	**0.04**	**1.360**	0.14	1.280	0.57	-1.090	Cytoplasm	kinase
Hspa4	heat shock 70kDa protein 4	0.09	-1.350	0.08	-1.280	0.04	-1.610	Cytoplasm	other
Junb	jun B proto-oncogene	0.04	-2.330	0.03	-2.670	0.08	-1.860	Nucleus	transcription regulator
Jund	jun D proto-oncogene	0.07	-1.950	0.007	-2.510	0.33	-1.300	Nucleus	transcription regulator
Pmaip1	phorbol-12-myristate-13-acetate-induced protein 1	0.31	1.980	**0.03**	**2.860**	0.30	1.620	Cytoplasm	other
Pou1f1	POU class 1 homeobox 1	0.26	-2.470	0.10	-1.760	0.04	-3.220	Nucleus	transcription regulator
Slc18a1	solute carrier family 18 (vesicular monoamine), member 1	0.37	2.320	**0.04**	**2.480**	0.23	3.650	Plasma Membrane	transporter
Sod2	superoxide dismutase 2, mitochondrial	0.22	-1.310	0.71	-1.090	0.03	-1.580	Cytoplasm	enzyme
Tnf	tumor necrosis factor	0.34	-1.610	0.04	-2.390	0.89	-1.160	Extracellular Space	cytokine

Table 2.2 List of genes that were significantly up or down regulated five hours after a single LI-rMS stimulation at 1Hz (blue), 10 Hz (green) or BHFS (red) frequencies. Fold change (primary colours indicate upregulation and pastels indicate downregulation) and p-values are relative to unstimulated controls.

DISCUSSION

This study used cortical neuron cultures to identify cellular and molecular mechanisms underlying the outcomes of different low intensity magnetic stimulation parameters. Our data show differential effects of specific LI-rMS paradigms on neuronal survival and morphology. Furthermore, evidence for calcium release from intracellular stores and stimulation-specific regulation of gene expression identify a potential cellular and molecular framework for understanding what low intensity magnetic stimulation may contribute to rTMS outcomes in humans.

Paradigm-specific effects on neuronal survival: dose vs rhythm

Our study shows specific effects of different LI-rMS paradigms on neuronal survival, suggesting that the overall stimulation load (pulse number and density) and/or rhythm of pulse delivery may be important. It has recently been proposed that there is no simple dose-dependent cumulative effect of rTMS on the cerebral cortex (Volz et al., 2013). Our data on isolated cortical neurons, showing that several low-intensity stimulation paradigms induce similar changes to intracellular calcium concentration but different patterns of gene expression and cell survival, extend this hypothesis to suggest that pulse rhythm, i.e. the pattern of stimulation frequency, is a primary determinant.

Considering pulse trains delivered at simple frequencies, increasing stimulation load (pulses/unit time) is associated with an increase in intracellular Ca^{2+} and cell death. In the group that received the lowest number of pulses (1 Hz: 600 pulses), there was only an intermediate non-significant increase in intracellular Ca^{2+} and a level of apoptosis

that was within the range observed in control cultures (4 %). Moreover, increasing stimulation load with 10 and 100 Hz (6000 and 60,000 pulses within the 10 min stimulation period), significantly increased intracellular Ca^{2+} and overall cellular apoptosis, consistent with the deleterious effect of prolonged magnetic stimulation to human monocyte leukemia cells (Stratton et al., 2013). Such fundamental biological knowledge will be important to future human rTMS as advances in coil cooling will permit longer stimulation trains without frequent TMS-free pauses seen in current clinical practice (Daskalakis, 2014). In contrast, even higher stimulation load, but delivered with a complex biomimetic frequency (TBS: 7000 and BHFS: 120000 pulses within 10 minutes) did not increase neuronal apoptosis despite rises in intracellular Ca^{2+} similar to those following 10 Hz. This not only confirms the hypothesis that dose and effect are not simply related (Nettekoven et al., 2014; Volz et al., 2013), but suggests that the rhythm with which the pulses are delivered is fundamental to their effect. By mimicking endogenous patterns of neuronal firing, biomimetic complex waveforms may induce more intricate and biologically safe changes compared to simple frequencies (Hoogendam et al., 2010; Martiny et al., 2010). One possible mechanism underlying these observations is frequency- and pattern-specific regulation of calcium buffering proteins (Chard, Bleakman, Christakos, Fullmer, & Miller, 1993; Funke & Benali, 2011; Gilabert, 2012), which is likely to contribute to the complex relationship between stimulation load, regulation of intracellular Ca^{2+} levels and cell viability. Indeed the promising therapeutic outcomes in human patients using TBS, albeit at high intensity (Li et al., 2014; Talelli, Greenwood, & Rothwell, 2007), would appear to support the hypothesis. Thus our data shows a complex interplay between pulse frequency, rhythm and outcome, confirms the recent suggestion that

appropriately designed rTMS protocols may generate highly adaptable therapies to treat a wide range of neurological conditions (Daskalakis, 2014).

The possibility that the effect of LI-rMS is determined by the number and/or rhythm of pulses was supported by our gene expression studies, which show that 1 Hz results in fewer gene-expression changes than 10 Hz and BHFS stimulation and BHFS alters a greater number of genes than 10 Hz. The majority of the regulated genes in our study were associated with cell survival and apoptosis pathways (Fig 2.5C), consistent with evidence for pro-survival (Yang et al., 2012) or pro-apoptotic (Juszczak et al., 2012; Stratton et al., 2013) effects of magnetic fields and our survival data (discussed above). All frequencies in our study downregulated neuron-specific enolase (ENO2) and corticotrophin-releasing hormone (CRH), both of which have neuroprotective properties (Hattori, Takei, Mizuno, Kato, & Kohsaka, 1995; Lezoualc'h, Engert, Berning, & Behl, 2000). However, in addition, we show paradigm-specific regulation of genes within neuronal survival and apoptosis pathways. Increased apoptosis after 10 Hz stimulation was associated with the upregulation of pro-apoptotic (Seo et al., 2003; Thangaraju, Kaufmann, & Couch, 2000) and downregulation of anti-apoptotic genes (Agarwal & Agarwal, 2012; Weitzman, Fiette, Matsuo, & Yaniv, 2000). In contrast, stimulation by frequencies which did not induce apoptosis showed survival-promoting gene expression changes (Vincent et al., 2007; Zhang, Liu, Szumlinski, & Lew, 2012). Given that neuroprotective effects of rTMS remain controversial (Bates et al., 2012), further characterisation of these gene expression changes at the protein and functional level could identify novel neuroprotective therapies for treatment of neurological disorders.

Stimulation-specific effects of LI-rMS on neuronal morphology: implications for reorganisation of cortical circuits

In addition to effects on neuronal survival, our data also shows a stimulation pattern-specific effect on neuronal morphology. 1 Hz stimulation reduced neurite complexity of glutamatergic projection neurons, consistent with a recent study in hippocampal neurons *in vitro* demonstrating that 1 Hz magnetic stimulation reduced dendritic branching and damaged synaptic structure (Ma et al., 2013). This suggests that the intermediate rise in Ca^{2+} following 1 Hz stimulation, although statistically non-significant, has biological relevance. In addition, 1 Hz-induced neurite regression would have the net effect of reducing excitatory connectivity within a cortical circuit, which is consistent with the LTD-like effects of 1 Hz rTMS on the human cortex (Gerschlager, Siebner, & Rothwell, 2001). However, we studied dissociated neurons, with minimal contact between neurites, suggesting that magnetic stimulation may directly alter neuronal structure beyond those changes (e.g. spines) associated with modulation from synaptic signalling (Funke & Benali, 2011; Majewska, Newton, & Sur, 2006; Vlachos et al., 2012).

Although we did not observe morphological changes when applying other frequencies, BHFS upregulated Cyr61, which is involved in the control of dendritic growth and has been associated with reorganisation of neuronal projections (Malik et al., 2013) and in association with longer treatment may contribute to the reorganization of abnormal circuitry induced by LI-rTMS at BHFS frequency (Makowiecki et al., 2014; Rodger et al., 2012).

Intracellular Ca^{2+} increase: mechanism of cortical plasticity?

Changes in intracellular Ca^{2+} in response to magnetic fields have been demonstrated in a range of cells (Huang, Ye, Hu, Lu, & Luo, 2010; McCreary et al., 2006; Pessina et al., 2001). We show here for the first time that in neurons LI-rMS releases Ca^{2+} from intracellular stores. This provides a mechanism for LI-rMS induced cellular and molecular changes that is independent of action potential induction, given that the stimulation was subthreshold, estimated to be 0.4 V/m (Appendix C), which is several orders of magnitude below the ~50 V/m that depolarises neurons (Volz et al., 2013). This concurs with our gene expression data in which markers of synaptic activity and action potential firing (e.g. CREB and BDNF) were not upregulated (Appendix B). Importantly, calcium release from intracellular stores can modulate synaptic plasticity (Hulme, Jones, Ireland, & Abraham, 2012) even without action potential firing and associated calcium influx. Therefore our data provide a mechanism to explain the effects of low intensity magnetic stimulation on cortical neurons (Capone et al., 2009), and provides a cellular and molecular framework for understanding what low intensity magnetic stimulation may add to the altered calcium signalling induced by the high-intensity focus of human rTMS, and thus its potential contribution to human rTMS outcomes.

Elucidation of novel mechanisms: relevance of *in vitro* low intensity LI-rMS to human rTMS

As discussed above, we have identified changes to cell morphology, intracellular calcium flux and gene expression in isolated neurons stimulated by subthreshold low-intensity magnetic pulses. This experimental paradigm is *very different* from the peri-

threshold high-intensity stimulation of whole neural networks in human rTMS; so what do our data contribute? First, our data reveal for the first time a fundamental cellular mechanism of non-depolarising magnetic fields on neurons, which in the *in vivo* context would underlie any trans-synaptic, neural circuit or cell environment responses. This could only be achieved by the application of a defined magnetic field to isolated cortical neurons, thus removing the confounding effects of glial responses and neuronal circuit activity from the observed outcomes. However, neurons that are maintained in culture are relatively immature, albeit fully differentiated, and not integrated within functioning neural networks. Thus their response to magnetic fields may be modified by different receptor and calcium-buffering capacities to adult neurons, especially in the absence of normal glial metabolic regulation and afferent activity. This, in turn, may make these neurons more susceptible to the low-intensity stimulation we induced in a manner that would not occur in the adult human brain even to higher intensity stimulation. Second, we identified potentially deleterious effects of 10 minutes continuous stimulation (slight increase in neuronal apoptosis) even at low intensity. Although such continuous pulse trains are not given in current human rTMS, the concern our data raise has pertinence to potential future human rTMS protocols as advances in coil-cooling technology may remove the requirement for short stimulation trains interspersed with TMS-free pauses. Taken together, our data demonstrate a novel cell-intrinsic mechanism for low intensity magnetic field stimulation of neurons which provides new insights into the structural and functional plastic changes described following low intensity magnetic stimulation (Capone et al., 2009; Di Lazzaro et al., 2013; Makowiecki et al., 2014; Rodger et al., 2012). Importantly, this mechanism may also be evoked during high intensity stimulation,

thus potentially working together with previously described metabolic and synaptic plasticity mechanisms of human rTMS (Allen, Pasley, Duong, & Freeman, 2007; Gersner et al., 2011; Ma et al., 2013; Valero-Cabré et al., 2005; Vlachos et al., 2012).

CONCLUSION

In summary, our data show that magnetic fields of different frequencies and rhythms alter intracellular calcium concentration and gene expression, which are consistent with long term modulation of neuronal survival. The immediate modification of calcium levels and gene expression support the development of long term changes following multiple stimulation sessions. Taken together with our previous study demonstrating that LI-rTMS can induce reorganization of neural circuits *in vivo* (Makowiecki et al., 2014; Rodger et al., 2012) our data indicate that effects of low intensity stimulation as a by-product of high intensity rTMS coils cannot be disregarded. Although, our stimulation parameters did not directly mimic those used in human rTMS, the knowledge about mechanisms underlying the effects of different stimulation paradigms provided by this study will contribute to understanding magnetic stimulation outcomes and optimizing therapeutic application in humans.

ACKNOWLEDGEMENTS

Funded by an Australian Research Council (ARC) Linkage grant LP110100201, the National Health and Medical Research Council (NHMRC) Australia, the Neurotrauma Program (State Government of Western Australia, funded through the Road Trauma Trust Account, but the project does not reflect views or recommendations of the Road

Safety Council) and a French CNRS PICS grant to support the international collaboration. SG is funded by UIS and SIRF grants, University of Western Australia. HV is funded by the National Heart Foundation. KWC is supported by the McCusker Charitable Foundation Bioinformatics Centre. LH is an ARC Future Fellow and honorary NHMRC Senior research fellow, JR is a NHMRC Senior Research Fellow and SAD a NHMRC Principal Research Fellow.

We are grateful to Marissa Penrose and Michael Archer for technical assistance, Rob Woodward and Andrew Garrett for scientific advice and assistance and Mohamed Doulazmi for the fast Sholl Analysis program and scientific advice. Finally we would like to thank Global Energy Medicine Pty Ltd for the donation of stimulation devices.

Chapter 3

3 Optimizing custom-tailored LI-rMS delivery to *in vitro* set-ups. Detailed description of creation and construction for Chapter 4 in vitro experimental requirements.

The effects of magnetic stimulation are suggested to arise from the induced electric field interacting with inductive biological tissue. Chapter 1 describes in detail the parameters involved in producing a particular electric field, such as magnetic pulse intensity, waveform (rise- and fall-time), direction and duration.

The implication is that in order to be able to understand the fundamental effects of magnetic stimulation and compare between studies, magnetic field parameters need to be precisely described and controlled in the experimental setting. In addition, it is important to consider that biological research is fast changing and time-consuming. *In vitro* set-ups (such as culture plates, well size and position of the sample) vary greatly between culture requirements for different tissues/models. This is exemplified with the applicability of our stimulation system for single cell cultures, which externally provided, was not designed to be adjustable to another experimental set-up. However, following effects of LI-rMS on single cell level, the subsequent investigation of LI-rMS effects on neural circuit level results in different experimental culture requirements.

This chapter describes the theory behind LI-rMS delivery systems, such as unique challenges and advantages of the *in vitro* setting. In addition, it describes in detail the computation of one solution to those challenges inherent to our particular *in vitro* requirements. The chapter describes the construction of a complete stimulation device for this particular solution, which is applied in Chapter 4. To increase reproducibility,

the device was specifically designed to be as simple and cost-efficient as possible. In addition to decreased time-consumption and increased applicability between culture set-ups, the device delivered automatized but adjustable stimulation.

Article 2

Grehl S., Martina D., Rodger J. & Sherrard RM. (2015). Optimizing *in vitro* magnetic stimulation: A simple, adjustable and cost-efficient stimulation device that can be tailored to different experimental requirements. *Results compiled for publication.*

SG contribution: 70 %

Optimizing *in vitro* magnetic stimulation:

A simple, adjustable and cost-efficient stimulation device that can be tailored to different experimental requirements

Stephanie Grehl [1,3], David Martina [2], Jennifer Rodger [3] and Rachel M Sherrard [1]

(1) Sorbonne Universités, UPMC Univ Paris 06 & CNRS, IBPS-B2A, UMR 8256 Biological Adaptation and Ageing, (2) Institut Langevin, UMR7587 ESPCI ParisTech & CNRS, INSERM ERL U979, Paris, France. (3) Experimental and Regenerative Neuroscience, School of Animal Biology, the University of Western Australia, Perth, Australia.

Corresponding author:

Prof Rachel M Sherrard

UMR 8256 B2A Biological Adaptation and Ageing

Brain Development, Repair and Aging (BDRA)

Boite 14, University P. and M. Curie

9 Quai St Bernard, 75005, Paris

email: rachel.sherrard@upmc.fr

INTRODUCTION

Transcranial Magnetic Stimulation (TMS) is a powerful method to non-invasively stimulate the human brain. While single or paired pulse TMS is used to investigate the function of specific brain regions, repetitive stimulation (rTMS) at varying frequencies has been shown to modulate neural excitability and synaptic plasticity. TMS and rTMS are therefore key techniques in neurological research and therapy.

Despite magnetic stimulation being used in the diagnosis and treatment of neurological disorders for over two decades (Barker et al., 1985), its cellular effects are still unclear due to the relative paucity of animal and *in vitro* studies. A significant challenge to such investigations is the ability to deliver precisely defined stimulation conditions to animal and *in vitro* models. Magnetic stimulation induces an electric field within the brain tissue, which modulates excitability within neural circuits according to the intensity and/or distribution of its field (Pell et al., 2011). Thus, it is crucial to be able to deliver precisely defined magnetic, and therefore electric, fields to cellular and/or animal models in order to optimise potential therapeutic parameters prior to translation to human patients.

Models of TMS-induced electric fields in the human brain (Bijsterbosch et al., 2012; Salinas et al., 2009) have shown that stimulation efficiency and the induced electric field are determined by the relative sizes of the coil and brain (Deng et al., 2013; Weissman et al., 1992). Thus, when human devices are used in cellular or animal research, the large coils generate electric fields in small *in vivo* or *in vitro* targets that are different to those induced in the human brain, which renders difficult the comparison of outcomes and extrapolation of mechanisms between experimental

paradigms. Moreover, although recent research has started to develop small stimulation devices for cellular and animal models (Bonmassar et al., 2012; Park et al., 2013; Rotem et al., 2014; Tischler et al., 2011), in small coils, stimulation at the high intensities used in the clinic generates significant thermal and mechanical stressors that can directly impact on the target animal/culture tissue (Bonmassar et al., 2012; Tischler et al., 2011). Hence, stimulation coils for animal and *in vitro* research should be tailored to specific experimental requirements.

While high-intensity human rTMS not only induces currents beneath the site of maximum stimulation, it also impacts upon surrounding brain regions at lower (subthreshold) intensities (Cohen et al., 1990; Thielscher & Kammer, 2002). In humans, low-intensity fields modulate cortical function (Capone et al., 2009; Robertson et al., 2010) and brain oscillations (Cook et al., 2004) and are used therapeutically (Martiny et al., 2010; Rohan et al., 2014). They also modulate gene expression (Mattsson & Simkó, 2012), provide neuroprotection (Yang et al., 2012) and reorganise neural circuits, neuronal morphology and molecular signalling (Grehl et al., 2015; Makowiecki et al., 2014; Rodger et al., 2012). To try to understand the mechanisms underlying low-intensity magnetic stimulation, we previously developed small stimulation coils that were scaled to deliver focal low intensity stimulation to dissociated neurons in 24 well plates (15 mm outer diameter (Grehl et al., 2015)). To deepen our understanding of the effects of different stimulation parameters, LI-rMS also needs to be applied to organotypic culture models which retain some complex neural circuits: e.g. hippocampal or cortico-striatal slices and olivocerebellar explants (Chedotal et al., 1997; Hausmann et al., 2001; Hogan & Wieraszko, 2004; Letellier et al., 2009; Vlachos et al., 2012). However, organotypic cultures require different culture conditions,

highlighting the need to establish a reliable and flexible stimulation system that can be tailored to deliver a magnetic field that induces an electric field of predicted intensity and direction at a particular location within each culture dish.

Here we describe the design and construction of such a stimulation device and solve the coil parameters required for the long-term stimulation of organotypic mouse hindbrain explant cultures. We aimed to make the design and execution of this device as simple, cost-effective and adjustable as possible to maximise reproducibility and application for different culture conditions. The wide range of parameters controlled by our fully automated magnetic stimulator and coil system will facilitate comparison of different stimulation protocols in a range of *in vitro* models, contributing to the optimisation of rTMS application in the clinic.

METHODS

Software tools used to solve parameter space

In order to find suitable combinations for coil and device parameters in response to our specific experimental requirements as outlined below, a range of software tools were used. Matlab (MathWorks, USA) was used to compute the magnetic field, electric field and the inductance of the coils. Finite element method open-source software (FEMM, USA) was used in order to validate results obtained with Matlab, to assess coil core choices (air, iron) and model the effect of Mu-metal. It has to be highlighted that FEMM especially has the advantage of being able to simulate a wide range of different configurations, without much prior knowledge of electromagnetics. The design of the

electronic circuit was validated with the use of the open-source software TINA (Texas Instruments, USA).

Requirements for *in vitro* magnetic stimulation

In vitro culture, whether of isolated neurons and glia or neurons within intact circuits of 3-dimensional organotypic explants, has physical restraints that have to be accommodated during magnetic stimulation protocols: sterility, stable temperature of the incubator and constant gas atmosphere (95% air plus 5% CO_2) for maintaining pH. Thus cultures have to be stimulated within the restricted incubator environment, with the coils being outside a closed culture dish, which requires single small coils rather than large Helmholtz solenoids.

Our particular *in vitro* experiments required long-term culture and stimulation of organotypic mouse hindbrain explants cultured on 30 mm Millipore membranes (Millipore, USA) in six-well culture plates (Techno Plastic Products (TPP), Switzerland) and incubated at 35°C in 95% air plus 5% CO_2. The hindbrain explants comprise the brainstem and cerebellum and their associated circuitry (Chedotal et al., 1997; Letellier et al., 2009) and thus are of multi-axial dimensions: 5 x 5 x 1 mm (L x W x H). Since explants on insert membranes are closer to the bottom of the culture plate than the top, to minimize coil-tissue distance, the coils were located directly underneath the culture wells. Distance from the top of the coil to the multi-axial target tissue was 3.5-4.5 mm (1 mm tissue depth) (Fig 3.1).

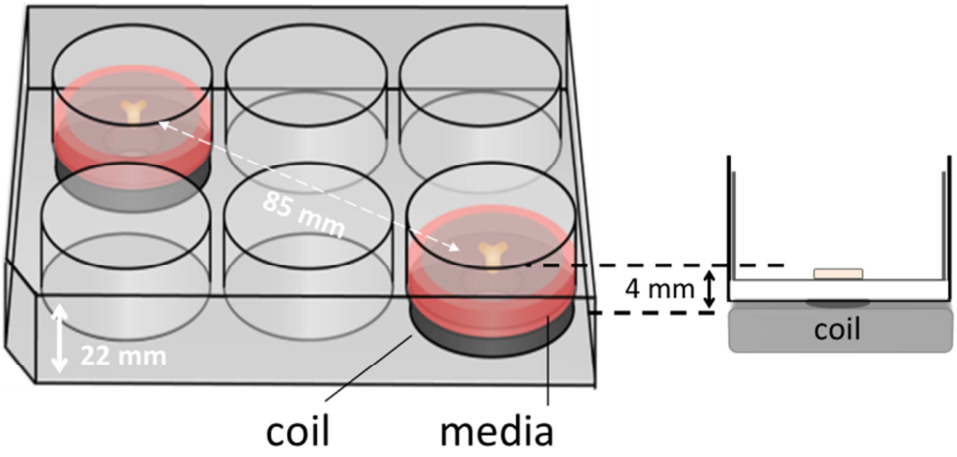

Figure 3.1 Overview of the culture set-up. The total height of the culture plate was 22 mm, resulting in a large difference between distance from the explants to the top (~18 mm) and the bottom (~4 mm). Hence, to produce a homogenous magnetic field at the position of the explants, a circular coil larger than the sample was needed. Organotypic hindbrain samples (orange) were located on a membrane ~4 mm away from the top of the coil, located underneath the culture well.

Requirements for magnetic and induced electric field at the target tissue

A time varying primary current in a coil creates a time varying magnetic field. The Maxwell-Faraday's equation

$$-\frac{d}{dt}\iint \vec{B}\,.\,d\vec{S} = \oint \vec{E}\,.\,d\vec{l} \qquad \text{(Jackson, 1962)}$$

describes how the variation of the flux of the magnetic field over the time induces an electric field, wherein ***B*** is the magnetic field, ***E*** the electric field, ***l*** the contour and ***S*** the surface. The electric field creates a secondary electric current in a nearby conductor (such as brain tissue) in an opposite direction to the primary current. This secondary current shows the same axisymmetric distribution around the axis of the coil as the primary electric current (Battocletti, Macias, Pintar, Maiman, & Sutton,

2000; Tofts, 1990) and has been suggested to interact with cellular processes underlying effects of low intensity magnetic stimulation (Grehl et al., 2015).

As based on Maxwell-Faraday's equation, the amplitude of the induced electric field depends on magnetic field amplitude, how fast it changes over time and its direction (axial components). In the case of a round coil, the induced electric field intensity is maximal when the created magnetic field direction lies parallel to the central axis of the coil. Hence, to systematically investigate the effects of magnetic stimulation parameters on biological tissue, we chose a simple defined parameter space for which we designed the magnetic field to be as vertical and uniform as possible. In order to produce this magnetic field at the explant, the coil diameter had to extend beyond the target sample. Thus for reproducibility of positioning we made the coil size the same as the diameter of the culture well. To estimate the magnetic field homogeneity, we calculated the influence of its different axial (vectorial) components. In an axisymmetric plane, the vectorial magnetic field $\overrightarrow{B}$ is composed of the sum of a vertical field component B_z and a horizontal component B_r, with their directional unit vectors $\overrightarrow{e_r}$ and $\overrightarrow{e_z}$, and can be written as

$$\vec{\mathbf{B}} = \mathbf{B_r}\overrightarrow{\mathbf{e_r}} + \mathbf{B_z}\overrightarrow{\mathbf{e_z}}$$

Based on the symmetry of a circular coil around its central axis, the induced electric field creates secondary current loops parallel to the current in the coil in every conducting material present in the field. However, if free looping of the secondary current is not possible due to presence of conductor boundaries it will produce an accumulation of free charge at the boundaries of the conductor (in this case the edge of the explant tissue), which will create a secondary potential (*phi* ϕ) working in the

opposite direction to the induced electric current. Hence, to limit the effect of accumulation of free charges, our explant tissue was positioned vertically above the centre of the coil (Fig 3.5A).

Magnetic waveform requirements

The waveform of the magnetic pulse has a significant impact on the induced electric field in the target tissue and depends on the pulse rise- and fall-time. Thus, the induced secondary current is proportional to the derivative of the magnetic field in the target over time, so that the faster the rate of change of the magnetic field, the stronger the electric field induced within the target tissue. To have a constant induced electric field, the magnetic field needs to change continuously over time with identical rise and fall-times to produce uniplanar, opposite field directions.

Based on previous *in vivo* parameters (Rodger et al., 2012), we desired a maximal magnetic field strength of 10 mT at the target tissue, with a rise-time of less than 100 µs and pulse length of 300 µs (Grehl et al., 2015). These parameters required a symmetric trapezoidal pulse, a form which is known to improve efficiency of magnetic stimulation (Peterchev et al., 2011), with the same rate of current rise-and fall. However, there is a static magnetic field between rise and fall-times (Fig 3.2), during which no current flows inside the target tissue.

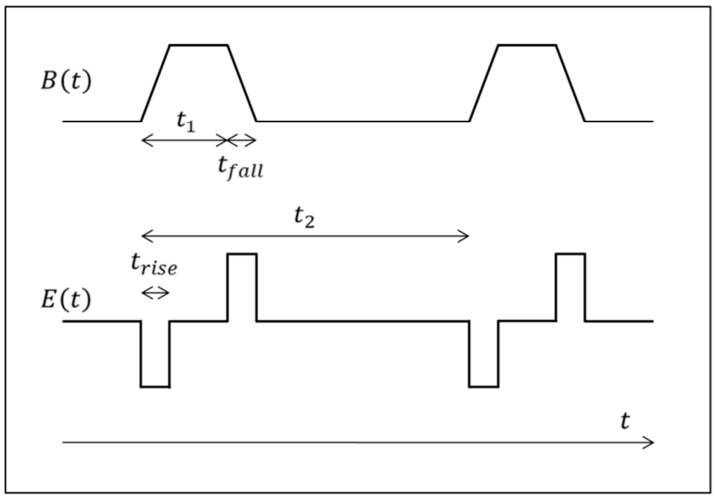

Figure 3.2 Desired magnetic field (B(t)) and the predicted induced electric field inside a conductor (E(t)). Three different temporal domains are specified for this set-up: t_{rise} = rise-time, t_{fall}= fall-time ,t_1 = pulse ON and t_2 = inter-pulse interval (frequency). t_{rise} /t_{down} and t_1 are based on previous experiments and have a value of 100 µs and 300 µs respectively; t_2 is experiment dependent.

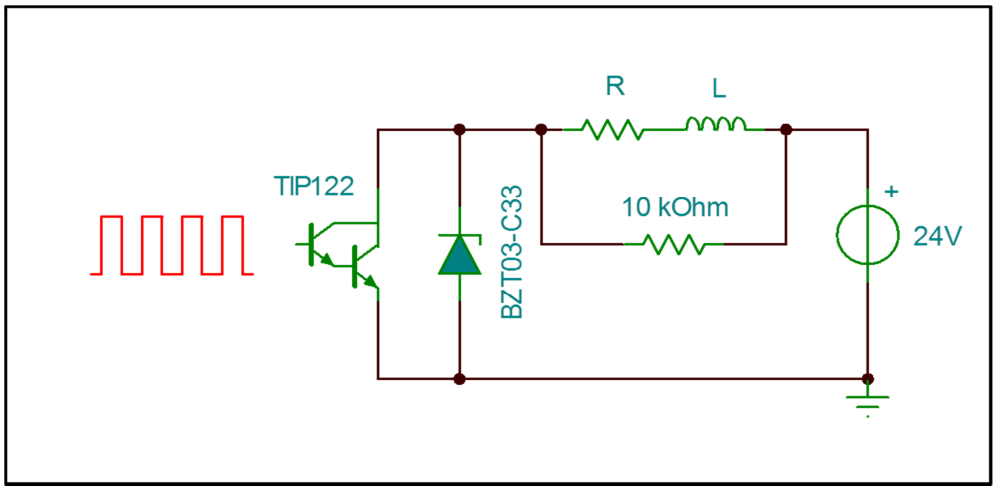

Figure 3.3 Schematic overview of the electronic circuit used to produce the desired current in the coil (L). The microcontroller produces a squared waveform, which triggers the darlington transistor (TIP122) on and off to permit the 24V power source to drive current through the RL circuit at the desired frequency during the desired period. The unidirectional zener diode (BZT03-C33) limits the level of current induced by the coils energy, after the opening of the transistor, to control the fall time.

Generation of the Magnetic field: coil construction and circuit design

To obtain these field parameters an inductor (coil) and electric circuit are required. The simplest appropriate model comprises a resistor-inductor (RL) circuit, in which the properties of one will alter the outcome of the other; thus these 2 components were designed in parallel.

Circuit design and construction

The circuit was created to generate parameters defined by previous experiments, specifically the fast rise-time of the magnetic field (Rodger et al., 2012), as well as to fulfil *in vitro* requirements (no excess heating or vibration). The performance of the resistor-inductor circuit (RL circuit, Fig 3.3), which contains a power supply, an electronic switch to allow the use of large currents, a zener diode and a programmable microcontroller card (Max 32, Chipkit), was simulated in TINA software.

In an RL circuit, the response of the circuit at a voltage step is given by:

$$\mathbf{I(t) = \frac{U}{R}\ (1 - e^{-\frac{t}{\tau}})} \qquad \text{with} \qquad \boldsymbol{\tau} = \frac{\mathbf{L}}{\mathbf{R}}$$

where I(t) is the electric current flowing in the circuit at a time (t), U the value of the voltage step at time t = 0, R the total resistance of the circuit, and Tau (**τ**) is the characteristic time for current to rise within the coil (Fig 3.4), a factor which depends on the inductance L of the coil and total R of the circuit. The two parameters L and R can be chosen as

$$\boldsymbol{t_{rise} = 5\tau = 5\frac{L}{R}}$$

where the field intensity inside the circuit reaches more than 99.9% of its maximum after a time of ~5 Tau (Fig 3.4). The desired rise time (5τ) is defined as the time needed to reach the maximum magnetic field inside the coil and was defined as 100µs in our system according to previous experiments (Rodger et al., 2012).

During the fall-time, the energy stored inside the coil during the rise-time induces a current that powers the circuit through the zener diode. In order to have the same circuit response during this step, the zener diode was used to limit the voltage generated by the coil. Increasing the threshold of the diode allows the stored energy to dissipate faster, leading to an increase in the rate of change of the magnetic field during the fall-time.

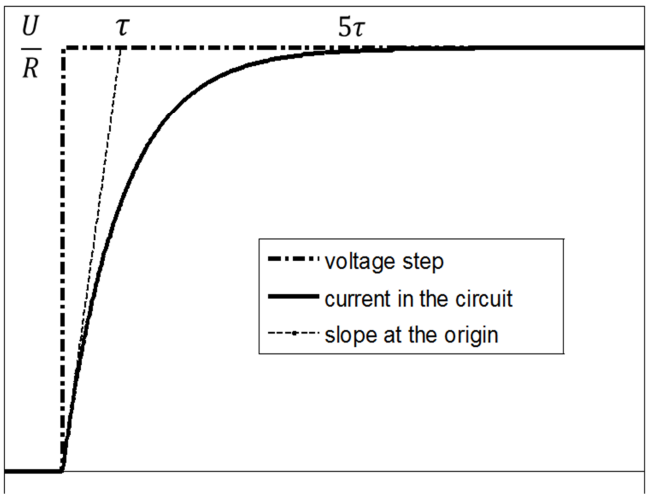

Figure 3.4 Definition of the characteristic time Tau (τ). Current intensity inside the circuit in response to increasing voltage steps reaches more than 99.9% of its maximum after a time of ~5τ.

Activation of the circuit was automatically controlled via the programmable microcontroller card (Max 32, Chipkit), which could be programmed (C-based code) via USB connection to a standard PC, to select the stimulation duration, pulse length, and pulse spacing (frequency). In addition, the time of day and immediate or next day start of stimulation could be programmed with real-time, remote control and feedback options. In order to optimise efficiency of the experimental protocol, the circuit was designed to connect a total of 16 coils, with two coils being activated with same stimulation parameters at any one time; thus allowing up to 8 different coil protocols to be programmed at a given time.

Coil calculation and construction

At the same time, the circuit inductor (coil) had to fulfil the requirements for pulse rise-time and magnetic field intensity and homogeneity, while also conforming to the needs of the *in vitro* culture system (e.g. sterility and temperature). To find a feasible solution, the magnetic field and the coil characteristic for a given geometry and a given current were modelled in Matlab (Battocletti et al., 2000; Queiroz de, 2005; Simpson, Lane, Immer, & Youngquist, 2001).

First, to ensure the best balance between induction efficiency while avoiding magnetic field spillover to other explants within the same culture plate, coil size should not exceed the culture well dimensions, i.e. 30 mm outer diameter. To optimise uniformity of the magnetic field (vertical vectorial component) the inner diameter was set at 10 mm.

Second, total coil temperature (heating/dissipation) must not exceed 35°C, the stable temperature of the incubator environment, and we verified the stability of our coil with a thermocouple sensor. Heat production (Joule effects) in the coil increases with increasing wire resistance and electric current intensity, which in turn is defined by the intensity required to produce the desired vertical magnetic field at the centre of the coil. To avoid the costs and safety issues associated with using high voltages, we chose a standard 24V power supply. Therefore, to balance between the required current intensity (2A) and low internal resistance (large wire diameter) to minimise heating, we chose a wire of 0.4 mm diameter. Coils were wound manually using a custom built winder and chosen parameters are shown in Table 3.1. The base of the coil was made of *Poly methyl methacrylate* (PMMA), a non-conductive and non-magnetic polymer.

Restricted parameters	Outer ⌀	Rise-time	I
	26 mm	**100 µs**	**2 A**

Chosen parameters	**Inner ⌀**	**Height**	**No. Turns**	**Copper Wire ⌀**	**L**	**R**
	10 mm	3.5 mm	119	0.40 mm	224 µH	11.6 Ω

⌀ = diameter, I = electronic circuit current, L = inductance, R = Resistance

Table 3.1 Parameters chosen for this specific in vitro set-up were identifed using a combination of several software programs.

RESULTS

This study created a magnetic stimulation device whose design complied with the following criteria: (1) A device ensuring culture sterility that was compatible with stimulating within an incubator. (2) The outer diameter of the coil ≤ the outer diameter of the culture well. (3) An homogenous field was generated at the target tissue. (4) The generated field strength was similar to previous low intensity stimulation experiments (Grehl et al., 2015; Makowiecki et al., 2014; Rodger et al., 2012). (5) Total coil temperature was kept at culture temperature 35°C. (6) Capability for multiple cultures to be stimulated simultaneously without interfering with each other and (7) stimulation must be automatic and parameters adjustable. Parameters identified as a feasible solution are given in Table 3.1.

Desired magnetic field, waveform and electric field

The magnetic field

Modelling of the predicted magnetic field shows a homogenous magnetic field (Fig 3.5A) at the location of the explant, 4 mm vertically above the base of the coil (1 mm plastic shell + 2.5 mm free distance + 0.5 mm half thickness of the sample). With a value of $\vec{B} = 9.6$ mT at the explant (Fig 3.5B, 3.6A), the vectorial component of the magnetic field $\vec{B}$ at a radius of up to 2.5 mm from the centre of the coil is mainly vertical, B_z (9.6 - 9.27 mT), while the horizontal component B_r approaches 0 (Fig 3.5B).

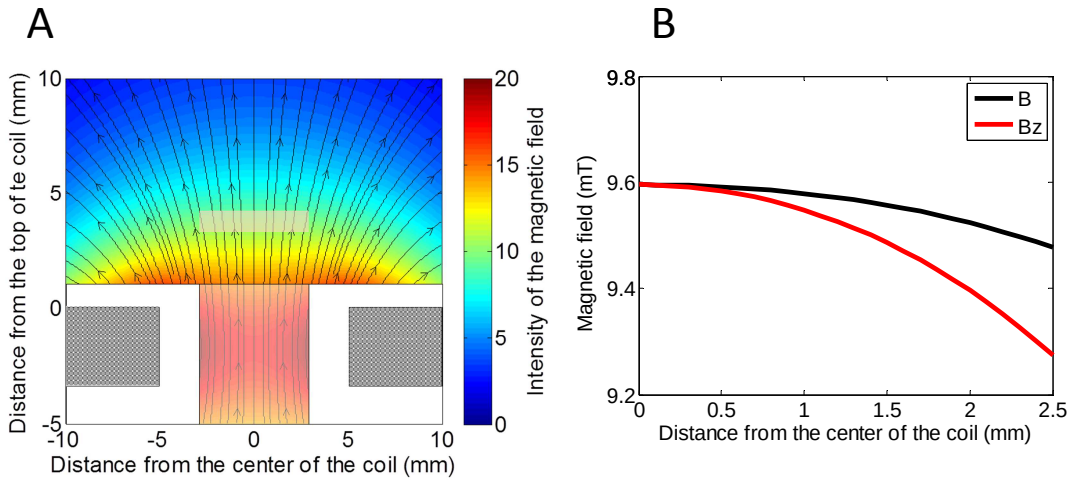

Figure 3.5 A) Modelled overview of the coil and its generated magnetic field. Grey squares at the bottom of the image show a dissected view of the coil wiring. White surround corresponds to the coils' plastic shell. Colours correspond to the magnetic field strength and black arrows to magnetic field direction *B* . The beige block in the centre of the image shows the location of the explant. B) Schematic overview of the different magnetic field components at 4 mm distance from the base of the coil. One can observe that the magnetic field *B* is almost exclusively comprised of the vertical field component *Bz*.

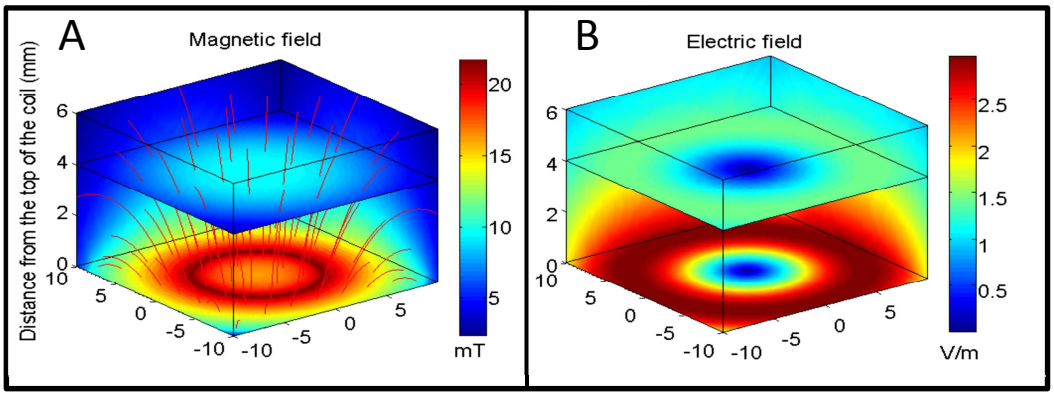

Figure 3.6 A) Modelled overview of magnetic field strength (mT; colours) and direction *B* (red lines) starting at the top of the coil wiring (horizontal plane at 0 mm). B) Modelled overview of the induced electric field from the top of the coil wiring (Horizontal plane at 0 mm). Colours indicate the electric field strength (V/m). A,B: Horizontal plane at 4 mm corresponds to target tissue location.

Hall device measurements (ss94a2d; Honeywell, USA) confirmed the predicted magnetic field strength and pulse waveform (Fig 3.7A) at 4 mm above the base of the coil showing a tight correspondence of modelled (TINA) and measured (Hall effect) pulse shape. This confirms a fast rise-time of < 100 µs with a proportional fall-time after 300 µs.

All coils were systematically tested and showed stability of magnetic field production for simultaneous and multiple activation (two at a time) at different stimulation frequencies.

The induced electric field

The induced electric field was modelled in Matlab and the maximally induced electric field was estimated to be 0.4 Vm^{-1} (Fig 3.6B, 3.7B; (Rohan et al., 2014)). Given that this is at least one order of magnitude below the electric field amplitude reported for neuronal activation within the cerebellum (Chan & Nicholson, 1986), this suggests sub-threshold stimulation of the target biological tissue.

Requirements to prevent eddy currents

Since the culture conditions and duration are common to all biological samples within a given experiment, in our case hindbrain explants, the device was designed to be able to stimulate up to 16 targets (explants) within the same incubator with the same or different stimulation protocols. To achieve this, we had to ensure that a coil did not induce electric fields (eddy currents) in another target located in an adjacent well of the culture plate. We calculated in Matlab and FEMM the minimal distance necessary to simultaneously stimulate different culture wells without interference of adjacent

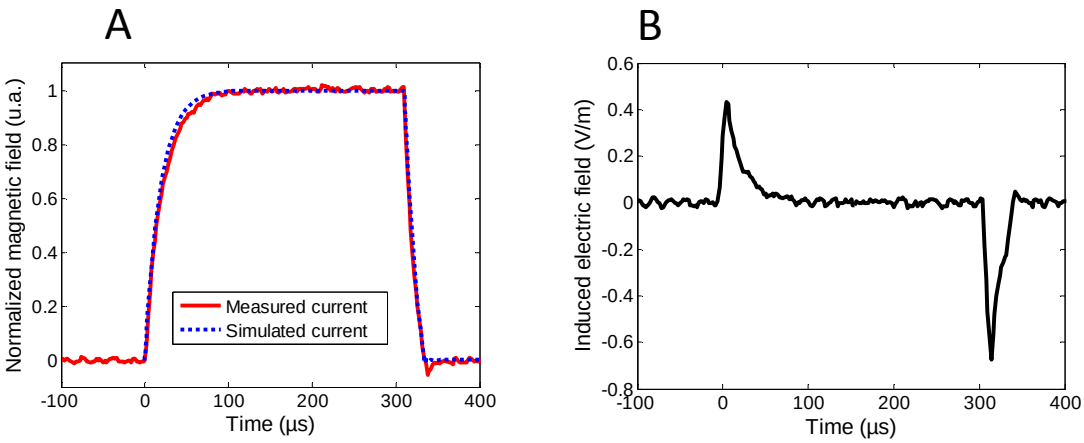

Figure 3.7 A) Single pulse waveform in normalized, arbitrary units (a.u.). Intensity inside the coil modelled in Tina (blue dotted line) and magnetic field strength measured via hall effect (red line), showing a tight correspondence between predicted and measured waveform. B) Calculated, single pulse induced electric field in a round conductor at a radius of 2 mm from the central axis and 4 mm vertically above the top of the coil's wiring.

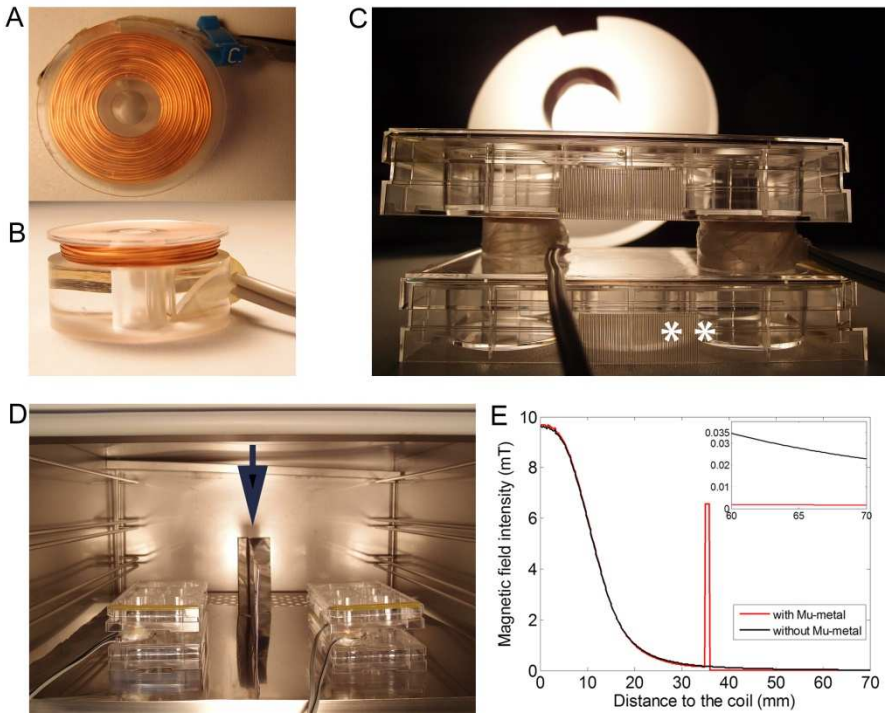

Figure 3.8 Coil set-up and magnetic shielding. A, B) View of a single coil from the top (A) and the side (B). C) View of the coils located on supporting cell plates underneath the tissue (**). Coils were wrapped in Parafilm M (Bemis, USA) to ensure stability and sterility. D) View of the coil set-up within the incubator. A sheet of (min 1mm thickness) of Mu-metal is also placed between adjacent cultures (vertical arrow). To ensure complete shielding also to the top and bottom of different incubator levels, a sheet of Mu-metal is also placed under the supporting cell plates. Mu-metal was never in direct contact with the coils as they were placed on supporting plastic plates (see C). E) Effect of the Mu-metal on the magnetic field. Black lines indicate a produced magnetic field without Mu-metal shielding at a horizontal distance from the centre of the active coil. Red line shows the magnetic field in correspondence with a Mu-metal shielding at 35 mm from the coil. Magnetic field intensity is concentrated by Mu-metal, leading to complete shielding with no detectable magnetic field at adjacent cultures (> 60 mm distance (small inset)).

magnetic fields. Results show that at 85 mm distance between the two target tissues the influence of the adjacent magnetic fields was negligible (< 11 μT) being less than the earth's magnetic field (25-65 μT;(Hulot, Finlay, Constable, Olsen, & Mandea, 2010)). Hence, two explants were cultured within one plate, but they were always stimulated simultaneously with the same frequency (Fig 3.1).

To further increase the usage of available incubator space, we employed Mu-metal (Magnetic Shields Limited, Tonbridge, UK) to shield adjacent culture plates from each other. FEMM was used to determine the required height and thickness of Mu-metal shields. Results showed that adequate Mu-metal shielding required a minimal sheet thickness of 1 mm, with a height of 100 mm to adequately shield adjacent culture plates separated by only 35 mm (Fig 3.8). Each shelf within the incubator was fully covered with sheets of Mu-metal. Moreover, we ensured that there was no direct contact between coils and Mu-metal to prevent attenuation of the magnetic field strength from Mu-metal influence.

Control and adjustability of the stimulation device

Using *in vitro* tissue to research the effects of magnetic stimulation has the advantage of precise control and isolation of experimental variables, increasing standardization and reproducibility of results and the possibility of comparison between studies. Therefore, to increase its applicability to different culture settings, this stimulation device was designed to be as adjustable as possible for parameters such as pulse waveform, frequency and field intensity.

To be able to systematically assess the effects of different magnetic stimulation frequencies the inter-pulse interval (*t*2, Fig 3.2) needs to be clearly defined and easily adjustable. This was achieved by using a programmable microcontroller card (Max 32, Chipkit), where the desired frequency can be programmed precisely (C-based code), specifying when to switch the circuit ON and OFF at any desired time-point to set total duration of stimulation, with a maximal stimulation frequency of ~5 kHz. Moreover, timing parameters influencing the pulse waveform are also easily adjustable, although decreasing the rise/fall times increases the maximum range of stimulation frequency. The rise-time (t_{rise}) is adaptable by changing the inductance L (e.g. changing the coil wire) and resistor R, while keeping Tau (τ) constant. The voltage-limit of the zener diode can be used to adjust the fall-time of the pulse waveform. Variations of the intensity and direction of the magnetic field $\overrightarrow{B}$ can be achieved by varying coil design and power supply voltage, compatible with the current electronic circuit. Moreover, simple movement of the target tissue along the vertical or horizontal axis of $\overrightarrow{B}$ modifies the magnetic field intensity $\overrightarrow{B}$ at the location of the target, depending on experimental requirements.

The advantage of this apparatus is that these changes are relatively easy and fast to accomplish, and do not require altering the main basic design of the electronic circuit, thus increasing its applicability to different experimental requirements, e.g. organotypic culture of the cerebellum, cortico-striatal circuits or hippocampus. In addition, to increase reproducibility and applicability, this device was designed to be as cost-efficient and mobile as possible, by operating automatically (no necessity to be connected to a dedicated computer once the microcontroller card is programmed) and without the requirement of amplifier set-ups and waveform generators.

DISCUSSION

Here we present the design of a novel *in vitro* magnetic stimulation device specifically constructed to respond to the requirements of organotypic culture, in order to examine the cellular effects of different magnetic stimulation parameters on neural tissue. Such investigation is necessary to identify parameters to optimize and tailor treatment of neurological disorders.

Importance of experimental (animal/cell) models

It is generally proposed that the effects of magnetic stimulation are due to the electric current induced in the conductive target tissue and its subsequent up- and down-stream neural circuit effects (Quentin, Chanes, Migliaccio, Valabrègue, & Valero-Cabré, 2013; Volz, Hamada, Rothwell, & Grefkes, 2014). While computational models have sought to understand the interactions between electromagnetic stimulation and neurons (Dmochowski et al., 2012; Joucla & Yvert, 2012; Modolo et al., 2013; Roth & Basser, 1990; Roth, Amir, Levkovitz, & Zangen, 2007), they can only predict outcomes based on particular assumptions (such as tissue resistance), thus systematic research in animal/cell models is needed to confirm their predictions.

However, before such fundamental research *in vivo* or *in vitro* can be undertaken, the experimental requirements particular to each *in vivo*/*in vitro* system need to be addressed: type of target tissue (isolated neurons vs 3 dimensional organotypic culture), its distance from coil, the presence of confounders such as eddy currents from surrounding magnetic fields as well as coil temperature. Here we describe the design of a stimulation device tailor-made for our specific *in vitro* set-up, which is

automated and freely programmable for pulse waveform (rise/fall-times and length), magnetic field intensity and direction so that it can be widely applicable to different experimental requirements.

Choosing Stimulation Parameters to Obtain a Defined Magnetic field

Magnetic stimulation is thought to act via the electric current generated in the tissue. Direction and strength of the electric current, depends on the conductivity (Wagner et al., 2014) of the tissue and the induced electric field (Pell et al 2011). The electric field strength and shape is defined by the intensity and direction of the magnetic field and its waveform. In addition, stimulation frequency and duration further modify its effect on tissues (Pell et al., 2011). Importantly, there is no single parameter combination to produce a specific magnetic and thus electric field; our device allows the selection of different combinations of stimulation parameters (frequency, wave-form, and magnetic field intensity) to obtain the required electric field in the tissue.

The direction of the magnetic field is an important parameter that needs to be controlled because it determines the intensity of the induced electric current, which in turn influences the neuronal populations that are activated (Volz et al., 2014). Our system allowed the development of a coil that produces an almost homogeneous vertical magnetic field at the location of the organotypic culture, which ensured the most efficient induction of an electric current along the horizontal plane of the target tissue.

Another parameter that influences the magnetic field is the shape of the pulse. Currently, commercially available stimulation devices are based on oscillatory circuits

producing sinusoidal pulses (Goetz et al., 2012; Goetz et al., 2013b) that cannot be altered by the user and which are based more on availability than consideration for optimal neuronal activation (Goetz et al., 2013b). Thus the only modifiable magnetic field parameter is amplitude. Unfortunately, as only about 1% of the electric pulse energy is transferred to the target (Hsu et al., 2003) with the rest being dissipated as coil heat (Goetz et al., 2013b), increasing magnetic field amplitude will require frequent pauses within high frequency pulse trains to avoid excess heating. Our new apparatus allows the choice of pulse waveform, so that we generated a trapezoidal pulse as being the most appropriate for our experimental requirements in terms of magnetic field intensity without excessive coil heating. This approach of using alternative pulse waveforms is consistent with studies (Havel et al., 1997; Peterchev et al., 2011; Sommer et al., 2006), which show that non-sinusoidal waveforms increase energy efficiency and decrease coil heating, while inducing neuronal depolarisation (Peterchev et al., 2011).

Coils specific to experimental requirements

While our new stimulation device permits definition of specific stimulation parameters, they depend on an appropriate coil to deliver them to the tissue. Given that the efficiency of electromagnetic induction varies according to the relative size of coil and target tissue (Deng et al., 2013; Weissman et al., 1992), the effects of large human stimulation coils cannot be assumed to generate the same fields in animals or in small culture dishes as in the human brain.

Recent studies have started to address the problem of coil size, stimulation focus and intensity in animal models, wherein small coil size renders high intensity stimulation

difficult to maintain due to thermal and mechanical stress (Bonmassar et al., 2012; Park et al., 2013; Rotem et al., 2014; Tischler et al., 2011). For high intensity stimulation, technical advances include coil-cooling chambers (Tischler et al., 2011), double-crossed coils to produce a smaller central stimulation focus (Rotem et al., 2014) or implantable submillimeter-coils (Bonmassar et al., 2012; Park et al., 2013), although their comparability to clinical human applications remains to be explored. In contrast, we recently created a small stimulation coil that is scaled to have a similar coil-to-brain ratio as in human stimulation (Weissman et al., 1992) and deliver lower intensity focal stimulation to awake mice *in vivo* (Rodger et al., 2012).

Likewise *in vitro*, the target tissue is usually small and stimulated in its entirety including its tissue boundaries which may impede circulation of the induced secondary current. Thus, size-specific, tailored stimulation coils and defined stimulation parameters (e.g. a homogenous magnetic field), which will decrease the effect of tissue boundaries in small *in vivo/in vitro* targets, are essential to interpret the effects of magnetic stimulation on neural tissue. Defined homogenous magnetic fields can be achieved by placing the target tissue within the axis of a Helmholtz coil solenoid (Montgomery, 1969) and the effects of different frequencies evaluated (Meyer et al., 2009). Nonetheless, Helmholtz coils are physically large and thus not well adapted for use in the limited space of an incubator, especially if multiple stimulation protocols are to be tested, where the fields induced by multiple proximate coils will interact, constraining the development of multi-channel stimulation systems (Han et al., 2004). The current study describes how incubator space usage can be further maximised by application of small single coils, separated by Mu-metal shielding, while maintaining a homogenous magnetic field.

Effective Biological Stimulation: Stimulation Intensity vs Frequency

Magnetic field intensity is one of the most manipulated and reported parameters in the literature. Human rTMS is generally applied at high intensities (~ 1-2.5 Tesla) around the threshold of motor cortex neuronal activation (Pell et al., 2011), as only high intensity suprathreshold stimulation that induces immediate behavioural effect (e.g. muscle contraction) can be directly measured in humans. However, rTMS induces currents not only beneath the site of maximum stimulation but also in surrounding brain regions at lower (subthreshold) intensities and little is known about the contribution of this broader stimulation to overall outcome, nor the minimum intensities required to elicit relevant neural changes. It has been shown that low intensity stimulation in the mT range, well below action potential threshold (Chan & Nicholson, 1986) shows pronounced, neurological effects (Cook et al., 2004; Mattsson & Simkó, 2012; Pessina et al., 2001; Robertson et al., 2010; Rodger et al., 2012; Sherafat et al., 2012). As the underlying mechanisms are not clearly defined, examination of the effects of defined stimulation parameters, such as can be produced by our *in vitro* system, is required.

Unlike intensity, the effects of which are not well understood from human studies, stimulation frequency has been extensively studied. For high intensity stimulation, frequencies ≥ 3 Hz are generally considered to have excitatory, while frequencies ≤ 1Hz exhibit inhibitory effects on cortical excitability (Fitzgerald et al., 2006; Lang et al., 2006). However, patterned high frequencies (e.g. theta burst stimulation) have more complex excitatory or inhibitory effects, which persist beyond the stimulation period (Hoogendam et al., 2010; Huang et al., 2005), are sensitive to intensity (McAllister,

Rothwell, & Ridding, 2009) and total stimulation duration (Gamboa et al., 2010), without increasing adverse effects (e.g. seizures). The exact cellular mechanisms induced by these differing temporal effects are still unknown and systematic investigation, such as is possible with our flexible system, is imperative to better tailor therapeutic applications. Recently, we have shown effects of stimulation frequency on neuronal structure, survival and gene expression, without induction of action potential firing (Grehl et al., 2015). This illustrates that investigation into the therapeutic potential of higher range complex frequencies delivered at lower stimulation intensities is essential, thus highlighting the requirement for stimulation devices that are tailored to specific experimental conditions to deliver defined magnetic field parameters in a controlled and systematic manner. Here we describe the manufacture of an adjustable automated device that can deliver pulses at up to 5 kHz.

CONCLUSION

Custom made stimulation devices will help to systematically investigate and understand the underlying effects of magnetic stimulation on biological tissue. Where a better understanding of magnetic stimulation effects will help to guide optimization of therapeutic application and increase the possibility to custom-tailor magnetic stimulation in the clinical setting.

ACKNOWLEDGEMENTS

This research was funded by the Institut pour la Recherche sur la Moelle épinière et l'Encéphale and a CNRS PICS grant (#121859) to support the international collaboration. SG was funded by UIS and SIRF grants, University of Western Australia, Perth, Australia.

Chapter 4

4 Investigating the effects of LI-rMS on neural circuits at a range of frequencies: anatomical and molecular changes.

We showed stimulation-specific effects of multi-session LI-rMS on cellular morphology and survival and associated underlying mechanisms in Chapter 2. Our results showed that repeated application of 1 Hz inhibited neuronal outgrowth and branching in conjunction with a relative increase in the number of CaBP immunoreactive interneurons in culture, suggesting an overall inhibitory effect of 1Hz stimulation on structural plasticity. Further, LI-rMS induced calcium release from intracellular stores and stimulation-specific changes in gene expression.

Thus, after investigating effects of LI-rMS on the single cell level, we subsequently wanted to examine the effects of LI-rMS at the neural circuit level. LI-rMS has been shown to have neurorehabilitative effects after injury, though studies using models of the CNS system are few and differ widely in the stimulation parameters applied. Hence, to better understand the fundamental effects of LI-rMS on neural circuits and its potential for repair we applied LI-rMS to an organotypic model of axonal injury, the olivo-cerebellar explant.

To systematically investigate stimulation-specific effects on repair at the system level, we delivered long-term stimulation with three frequencies identified from our previous study (Chapter 2) and measured survival and reinnervation of cerebellar Purkinje cells after climbing fibre denervation. To understand the underlying

mechanism of reinnervation, we measured changes of target gene expression after long-term LI-rMS. Further, to identify the cell population that was activated by the LI-rMS stimulation, we labelled explants with the early response gene marker c-fos after one stimulation session.

This axonal lesion model has been thoroughly characterized in our laboratories, where it has been shown that treatment with BDNF can induce functionally beneficial reinnervation to cerebellar Purkinje cells after denervation; results that have been replicated in the *in vitro* organotypic model examined in this study. To contrast effects of LI-rMS with BDNF induced reinnervation and to investigate effects of treatment combination, some explants were treated with BDNF alone or in combination with LI-rMS.

In this chapter we show that LI-rMS induces reinnervation and changes associated gene expression levels in a stimulation-specific manner. LI-rMS induced reinnervation was similar to BDNF induced reinnervation and no additive effect of stimulation was observed. We show that LI-rMS activated certain cellular subpopulations within the cerebellum 3.5 hours after one LI-rMS session and had no detrimental effect on neuronal survival.

Article 3

Grehl S., Goyenvalle C., Dunlop SA., Rodger J. & Sherrard RM. (2015). Low intensity repetitive magnetic stimulation induces olivo-cerebellar reinnervation. *Results compiled for publication.*

SG contribution: 95 %

Low intensity repetitive magnetic stimulation induces olivo-cerebellar reinnervation

Stephanie Grehl [1,2], Catherine Goyenvalle [2], Sarah A Dunlop [1], Jennifer Rodger [1] and Rachel M Sherrard [2]

(1) Experimental and Regenerative Neuroscience, School of Animal Biology, University of Western Australia, Perth, Australia. (2) Sorbonne Universités, UPMC-Univ P6 and CNRS, IBPS, UMR8256 Adaptation Biologique et Vieillissement, Paris, France.

Corresponding author:

Rachel M Sherrard

UMR 8256 Biological Adaptation and Ageing

Brain Development, Repair and Aging (BDRA)

Boite 14, University P. and M. Curie

9 Quai St Bernard, 75005, Paris

email: rachel.sherrard@upmc.fr

INTRODUCTION

Injury to the central nervous system resulting from traumatic brain injury, stroke or degenerative disease can lead to severe and lasting cognitive and functional deficits. Even though neurorehabilitation of the mature CNS is limited as lost cells are typically not replaceable (Horner & Gage, 2000), the brain maintains a high amount of plasticity to reconnect surviving cells (Nudo, 2013). Hence, therapies are focussed on preventing further cell death and subsequently to increase neuroplasticity *via* axonal regeneration, heterologous terminal sprouting and/or collateral reinnervation of the denervated cells (Kleim, 2011; Nudo, 2013). Neuronal plasticity is promoted by network activation, which can be difficult to induce in the injured system due to loss of connectivity and the presence of inhibitory signals (Butz et al., 2009; Carmichael, 2006).

Repetitive transcranial magnetic stimulation (rTMS) is used to non-invasively stimulate the brain. It has shown to have long-term effects on cortical excitability (Fitzgerald et al., 2006), modulate synaptic and structural plasticity (Vlachos et al., 2012) and to be beneficial for the treatment of neurological disorders such as stroke (Adeyemo et al., 2012; Kim et al., 2014; Schulz et al., 2013). Though outcomes are variable (Wassermann & Zimmermann, 2012).

rTMS is commonly applied *via* a figure-of-eight shaped coil to produce a focal high-intensity field that depolarises neurons in limited region of the cortex underlying the intersection of the two loops (Fatemi-Ardekani, 2008; Thielscher & Kammer, 2004). However, this centre is surrounded by a weaker magnetic field, such that a large

volume of adjacent cortical and sub-cortical tissue is also stimulated, albeit at a lower intensity (Cohen et al., 1990; Deng et al., 2013).

Lower intensity rTMS in humans (mT range) has been shown to modify cortical function (Capone et al., 2009; Robertson et al., 2010) brain oscillations (Cook et al., 2004) and be beneficial to the treatment of depression (Martiny et al., 2010). Moreover, animal studies show improvement of function and neuronal survival after traumatic brain injury (Yang et al., 2012) and peripheral nerve damage (De Pedro et al., 2005; Markov, 2007; Siebner & Rothwell, 2003; Walker et al., 1994) and alternation of the structure and function of abnormal neural circuits (Rodger et al., 2012). Low intensity repetitive magnetic stimulation *in vitro* (LI-rMS) has been shown to increase neuronal survival (Boland et al., 2002; Di Loreto et al., 2009; Kaszuba-Zwoinska J et al., 2010; Sherafat et al., 2012; Stratton et al., 2013), and to modulate mechanism involved in neuroplasticity such as increasing myelin repair (Gunay & Mert, 2011; Sherafat et al., 2012), modulate cAMP (Hogan & Wieraszko, 2004) and BDNF-TrkB (Di Loreto et al., 2009) expression in addition to calcium signalling (Barbier et al., 1996; Grassi et al., 2004; Grehl et al., 2015; Piacentini et al., 2008; Sawaguchi, 1997).

However, the effects of LI-rMS on neural plasticity, in particular in conjunction with different stimulation frequencies, have not been systematically investigated. At high intensities low frequency rTMS (< 1 Hz) is considered to have inhibitory effects, while high frequency (> 3 Hz) stimulation induces facilitatory effects (Fitzgerald et al., 2006; Hoogendam et al., 2010; Huerta & Volpe, 2009). Though patterned stimulation frequencies based on endogenous patterns of brain activity, such as theta-burst stimulation, have been shown to result in either excitatory or inhibitory effects

(Hoogendam et al., 2010; Huang et al., 2005). To date the effects of different frequencies at low intensity on biological tissue remain unknown.

To address this, we assessed the effects of different low intensity magnetic stimulation frequencies on neural circuit repair using the mouse olivo-cerebellar projection model of axonal injury. This model has been thoroughly characterized in our laboratories (Dixon et al., 2005; Fournier et al., 2005; Letellier et al., 2007; Lohof et al., 2005) and has the advantage of being organized with precise topography, displaying a one to one relationship between the afferent climbing fibre axons (CF) and the target Purkinje cell (PC) (Eccles et al., 1966; Fournier et al., 2005; Lohof et al., 2005). Reinnervation of denervated PCs after unilateral transection of the olivo-cerebellar pathway in the mature system has been shown to be induced *via* injection of brain derived neurotrophic factor (BDNF) (Dixon & Sherrard, 2006; Sherrard & Bower, 2001) leading to functional and cognitive benefits in rats (Willson et al., 2007; Willson et al., 2008).

To investigate defined LI-rMS effects on reinnervation, we used the optimized *in vitro* olivo-cerebellar system (explant) (Letellier et al., 2009) which resembles closely the *in vivo* system during normal development and postlesion reinnervation, and is thus highly suitable to investigate and optimize LI-rMS parameters. We stimulated olivo-cerebellar explants for 14 days after axonal denervation with either 1 Hz, 10 Hz or a biomimetic high frequency stimulation (BHFS) and assessed PC survival and reinnervation. We further investigated mechanisms underlying reinnervation: gene expression and c-fos activation.

METHODS

Animals

Timed pregnant Swiss mice were purchased from Janvier-Labs (Villejuif, France). Animal housing and all procedures followed guidelines established by le Comité National d'Ethique pour les Sciences de la Vie et de la Santé, in accordance with the European Communities Council Directive 2010/63/EU.

Organotypic Cultures and cerebellar denervation

Hindbrain explants were cultured from Swiss mice at embryonic day 15 (E15) as previously described (Chedotal et al., 1997; Letellier et al., 2009). E0 was the mating day. Briefly, anaesthetised dams were culled by cervical dislocation, the embryos removed and their brains were quickly dissected in ice-cold Gey's balanced salt solution (Eurobio) containing 5 mg/mL glucose. The hindbrain, including the cerebellar anlage and inferior olive nucleus, was isolated and the meninges removed. The right and left cerebella plates were separated at the midline (Fig 4.1A-C) and the explants transferred onto 30 mm Millicell membranes (pore size 0.4µm, Millipore; Fig 4.1D) and cultured at 35°C with medium containing 50 % basal medium with Earle's salts (Gibco), 2.5 % Hank's Balance Salt Solution (Gibco), 25 % horse serum (Gibco), 1 mM L-glutamine (Gibco), and 5 mg/mL glucose at 35°C in humidified air with 5 % CO_2. The culture day was designated 0 days *in vitro* (DIV). The medium was replaced every 2–3 days.

To denervate (Dx) cerebellar tissue and induce olivo-cerebellar reinnervation, the cerebella plates were removed from their explant brainstem at *DIV 23* (equivalent to

P17) and cocultured (graft) adjacent to the cerebellar tissue of an intact explant (host) (Fig 4.2A,B). Twenty-four hours after coculture some cerebella plates were treated (DxB) with 1µl (4µM) recombinant human brain derived neurotrophic factor (hBDNF; Alomone, 0.1 % BSA in H_2O), which induces climbing fibre reinnervation *in vivo* (Dixon & Sherrard, 2006; Sherrard & Bower, 2001).

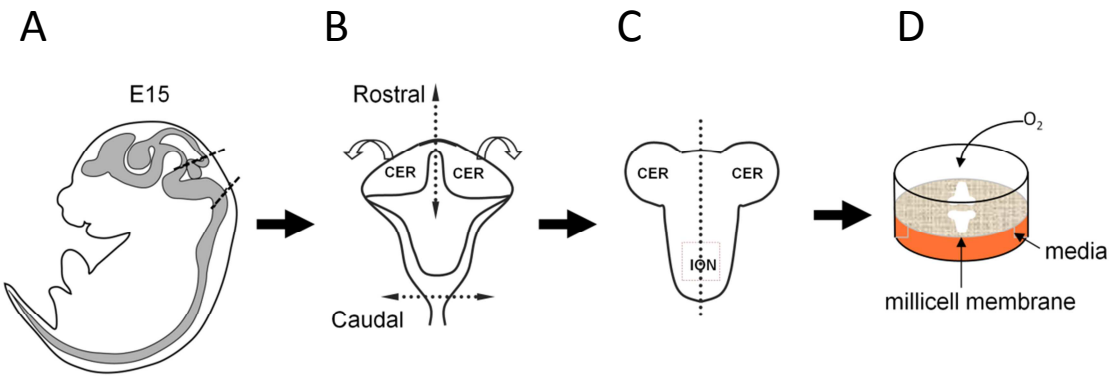

Figure 4.1 Cerebellar murine explants cultures at E15. The dashed lines with arrows indicate cuts. The hindbrain containing the cerebellum and the brainstem was dissected out (A), and the cerebellar plates folded outwards (open arrows B,C) to that the explant could be cultured flat with the dorsal surface on the Millicell membrane. Images partially modified from Chédotal et al. (1997); Letellier et al. (2009).

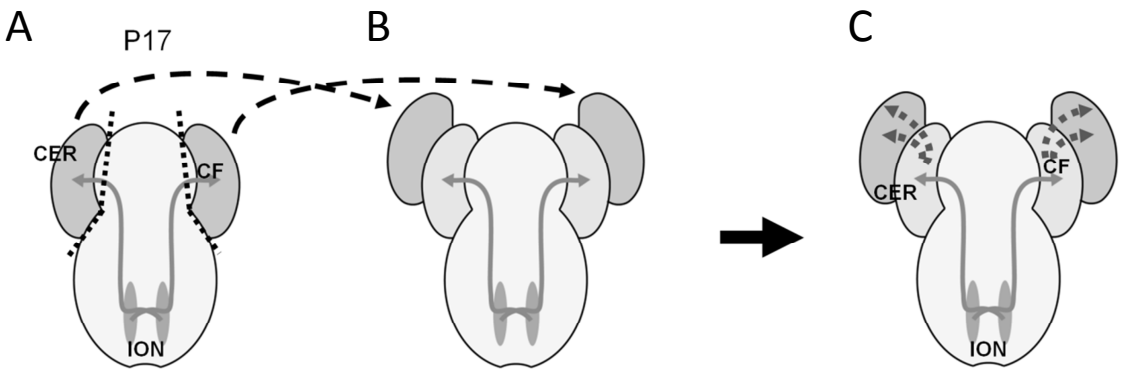

Figure 4.2 Cerebellar denervation (Dx), coculture and reinnervation. The dotted lines indicate cuts. Isolated cerebella plates at P17 (A) were cocultured adjacent to intact cerebellar hemispheres (B) to allow olivo-cerebellar reinnervation of PCs by CFs (C).

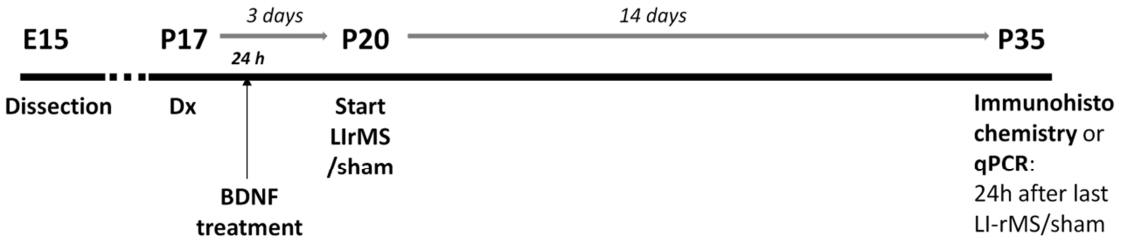

Figure 4.3 Timeline of explant procedure and treatment for reinnervation/PC survival or PCR analysis, using equivalent postnatal ages for simplicity. Explants are dissected from E15 mouse embryos and cultured until the start of denervation and coculture at 22 DIV (~P17). Some explants are treated with BDNF or Vehicle 24h after denervation (Dx). Magnetic stimulation (or control-sham) started 72h after coculture (~P20) 10 min a day for 14 days. 24h after last stimulation (~P35) explants were sampled and processed for analysis.

Magnetic stimulation

To evaluate whether magnetic stimulation can induce olivo-cerebellar reinnervation, Dx explants were stimulated for 10 min per day for 14 days starting at 3 days-post Dx (Fig 4.3), i.e. at 25 DIV (equivalent to P20). Magnetic stimulation was delivered with a custom-built stimulation machine and coil (Chapter 3), which had an outer diameter of 26 mm, an inner diameter of 10 mm, and 119 turns of 0.4 mm diameter copper wire (11.6 Ω). Coils were located immediately beneath the 6 well plate, 4 mm below the explants and the magnetic field strength was 10 mT at the location of explants (Chapter 3). Coil temperature did not rise above 35°C. To ensure that explants were not affected by the magnetic field of neighbouring stimulation, those within the same plate were cultured in the two most separated wells (Fig 4.4B) and different plates were separated by Mu-metal. Computational modelling and Hall effect measurements verified no spill-over of eddy currents between explants (Chapter 3).

A

Frequency	***1 Hz***	***10 Hz***	***BHFS***
Total pulses delivered in 10 minutes	600	6,000	109,000

B

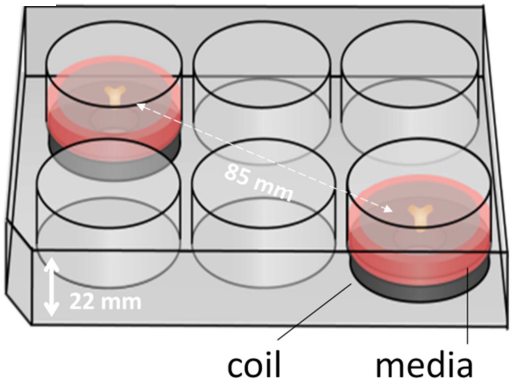

Figure 4.4 Culture set-up and pulse delivery. Number of pulses delivered per 10 min stimulation session (A) and schematic view of *in vitro* culture set-up for stimulation (B). B) Coils were centered below the well of a 6 well plate resulting in 4 mm distance from the centre plane of the explant located on the Millicell membrane.

Stimulation was delivered using a trapezoidal magnetic pulse with a rise/fall-time of 100 µs (Chapter 3) at frequencies of 1 Hz (Dx+1Hz), 10 Hz (Dx+10Hz) or biomimetic high frequency stimulation (Dx+BHFS: 62.6 ms trains of 20 pulses, repeated at 6.55 Hz for 1 min, followed by 9.75 Hz for 8 min and then 6.15 Hz for 1 min). The BHFS pattern was designed on electro-biomimetic principles (Martiny et al., 2010), based on our previous study (Rodger et al., 2012) which was modelled on endogenous patterns of electrical fields around activated nerves during exercise (patent PCT/AU2007/000454, Global Energy Medicine).

The total number of pulses delivered for each frequency is shown in Figure 4.4A. For all experiments, stimulation controls (sham) were treated identically but the coils were not activated. Some intact non-lesioned, non-cocultured explants of the same age and procedures are referred to as Control-intact.

Immunohistochemistry and Histological Analysis

The effects of different LI-rMS protocols on olivo-cerebellar reinnervation and the cell populations activated by the stimulation were evaluated by immunohistochemistry. In all experimental groups explants were fixed with 4 % paraformaldehyde for 4h at 4°C, rinsed 3x5 min in phosphate buffered saline (PBS) containing 0.25 % TritonX (PBS-T) and blocked in 20 % donkey serum for 2h at RT prior to incubation overnight at 4°C in primary antibody diluted in PBS-TG (PBS-T containing 0.2 % gelatine and 0.018 g/ml L-Lysine). The next day explants were washed 3x5 min in PBS-T and labelling was visualised with fluorescent-conjugated secondary antibodies in PBS-TG for 2h at RT. Finally, explants were rinsed and mounted in Mowiol.

To identify ***PC survival and CF reinnervation*** explants (~P35) were processed 24h after the last (14^{th}) stimulation. Purkinje cells were labelled with rabbit anti-calbindin-28k (CaBP) antibody ((Celio, 1990); 1:3000; Swant) and CF terminals with monoclonal mouse anti-VGLUT2 antibody ((Hioki et al., 2003; Letellier et al., 2009); 1:2000, Millipore). Primary antibodies were visualised using Cy3-conjugated donkey anti-mouse and Alexa Fluor (AF) 488-conjugated donkey anti-rabbit (both 1:200; Jackson Laboratories). Labelled explants were examined using epifluorescence microscopy (Eclipse E800; Nikon) and the total number of CaBP-positive PCs per cerebellar hemisphere was counted. Cocultured cerebella hemispheres were systematically examined (Fig 4.5A) for VGLUT2/CaBP colocalisation indicating PC reinnervation by CF. The number of CaBP-positive PCs (soma and primary dendrites) colocalised with VGLUT2 (Fig 4.5B,C) was counted per field of view (grid) and expressed as percentage PCs per field.

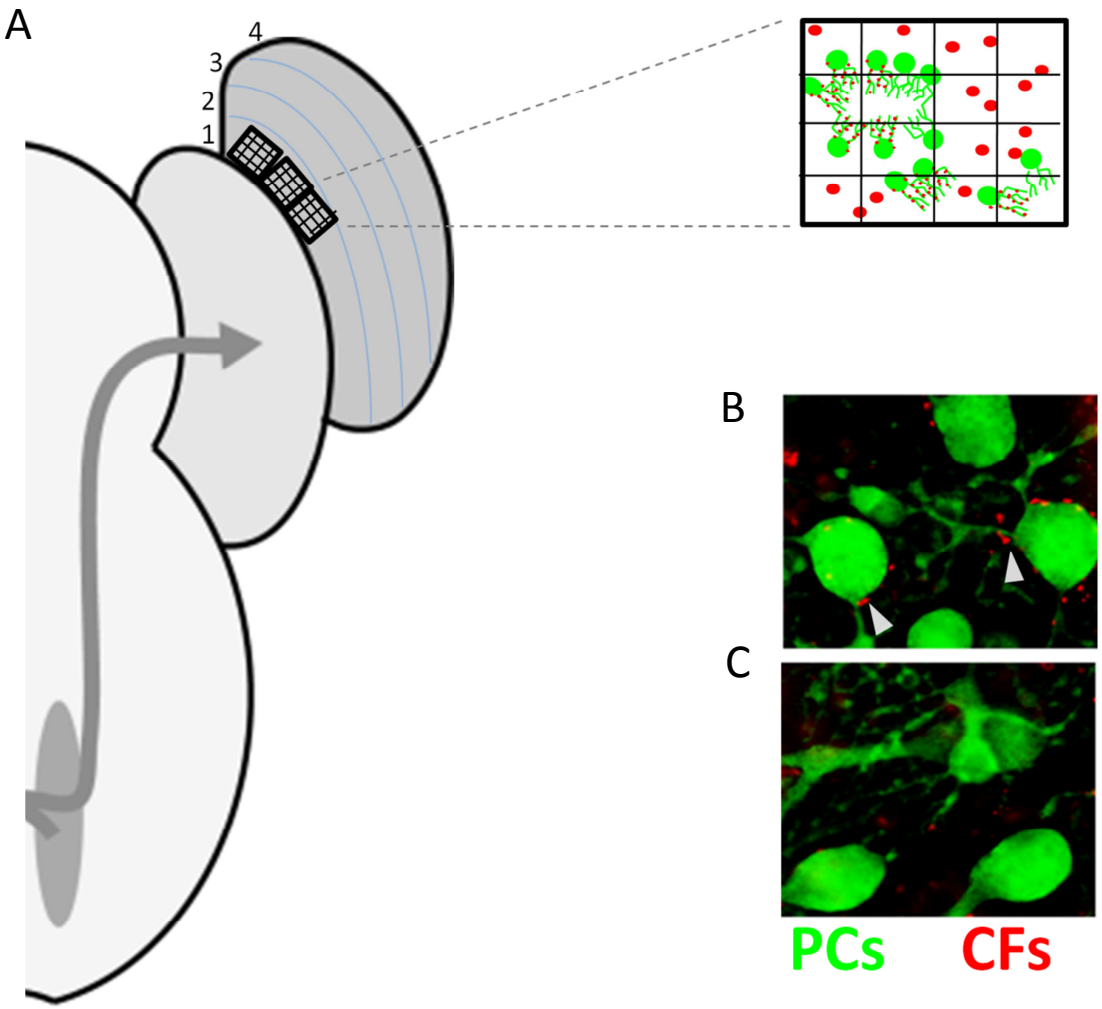

Figure 4.5 Climbing fibre reinnervation analysis. A) Cerebellar plates were divided into rows (1-4) starting parallel to host –graft border. Moving along each row, PCs (green) within an ocular grid field were investigated for reinnervation (red). B,C) Confocal image showing CaBP positive PC (green) and VGLUT2 positive labelling of CFs (fine red dots) and mossy fibres (larger red labelled terminals not associated with PCs, in background). For positive reinnervated cells (B) and non-reinnervated cells (C). Arrowheads show VGLUT2-positive CF terminals on PCs.

To identify which ***cells were activated*** by the magnetic stimulation we labelled c-fos 1.5h or 3.5h (Hausmann et al., 2001) after a single 10 min stimulation session at P20 (72h after Dx to investigate acute effects on stimulation day 1). Fixed explants were labelled with rabbit anti c-fos (Santa Cruz, 1:750) plus one of 4 different antibodies to label specific cell populations (Celio, 1990; Weyer & Schilling, 2003): PCs with

monoclonal mouse anti-CaBP-28k (1:2000; Swant), GABAergic interneurons with goat anti-Parvalbumin (PV, 1:3000; Swant), granule cells with monoclonal mouse anti-NeuN ((Weyer & Schilling, 2003); 1:200; Millipore) or astrocytes with monoclonal mouse anti-GFAP (1:500; Sigma). Primary antibody binding was visualised using fluorescently labelled secondary antibodies Cy3-conjugated donkey anti-rabbit, AF488 conjugated donkey anti-mouse and AMCA conjugated donkey anti-goat (all 1:200; Jackson Laboratories). Explants were examined using epifluorescence microscopy (DM 6000B; Leica): z-stacks were taken at 3 semi-randomly selected sites for each cocultured cerebellar hemisphere. Total c-fos positive staining was counted per image and double-labelled profiles were quantified visually for co-labelling. c-fos and CaBP positive cells were counted per image to identify the proportion that were activated by LI-rMS.

qRT-PCR

RNA preparation

To identify possible mechanisms underlying the effect of LI-rMS in olivo-cerebellar culture, RNA was extracted from either the cerebellar hemisphere or the inferior olivary region of Dx (LI-rMS/sham) explants 24h after last stimulation (~P35). Tissue from 5 cerebella plates and inferior olive regions were pooled for RNA. Total RNA was extracted using Trizol (Life Technologies) according to manufacturer's instructions (Chomczynski & Sacchi, 1987) and RNA concentration was measured by a NanoDrop 1000 Spectrophotometer (Thermo Scientific, Waltham, MA, USA) before being stored at -80°C.

200ng of total RNA was reverse transcribed in a 20µl reaction using a High Capacity cDNA Reverse Transcription Kit (Applied Biosystems). cDNA was amplified on a LightCycler® 480 (Roche Applied Bioscience, USA) for 10 µl reaction volume using SYBR Green I Master Mix (annealing temperature 58°C, 50 cycles). Housekeeper primers were derived from mouse-reference gene panel (Tataa Biocenter, Sweden): Glyceraldehyde 3-phosphate dehydrogenase (GAPDH), peptidylprolyl isomerase A (PPIA), Beta-2 microglobulin (B2M) and hypoxanthine phosphoribosyltransferase 1 (HPRT 1). Primer sequences of target genes were designed as follows (TM = 59.0 – 59.6): **BDNF:** Forward TCACTGGCTGACACTTTTGAGCA, Reverse CGCCGAACCCTCATAGACATGTTT*;* **Pax3:** Forward AGCAAACCCAAGCAGGTGACA, Reverse AGGATGCGGCTGATAGAACTCACT; **ST8SiaII:** Forward AGCACAATGAACGTGTCCCAGAA, Reverse GAGCCAGGTTGCACCTTATGACA; **ST8SiaIV:** Forward TTCCGGCATTCTGCTAGACAGTG, Reverse CGAAAGCCTCCAAATGCTCTTTGC.

Raw data were pre-processed with Lightcycler 480 software (Roche Applied Bioscience, USA). Target gene expression was normalised to appropriate housekeeper genes. All expressions were replicated in triplicate and the mean was used to calculate gene expression in each tissue sample. Normalized mean expression (log2(2-ΔCt)) (Livak & Schmittgen, 2001)) was used to determine differentially expressed genes between each group.

Statistical Analysis

All data were explored for normality, outliers and fulfilment of statistical test assumptions in SPSS 20 (IBM).

Reinnervation percentages were transformed with the ArcSin transformation to be analysed with Repeated Measures ANOVA (F) (row x stimulation). Univariate ANOVA per row was performed where RMAnova revealed significance for further tests. Dunnet-T3 post-doc comparisons were performed where appropriate. CaBP positive PC counts (CaBP) were analysed with Univariate ANOVA.

C-fos activation and CaBP/c-fos percentages was analysed with Kruskal-Wallis one-way analysis of variance (H) and Mann-Whitney (U) pairwise comparisons with Bonferroni-Dunn correction. Gene expression levels were compared by independent sample *t*-test. All values are expressed as mean ± SEM and considered significant at $p < 0.05$.

RESULTS

The aim of this study was to evaluate whether LI-rMS could induce reinnervation of denervated neurons using PC denervation in the olivo-cerebellar projection model of axonal injury. We assessed if LI-rMS affects neuronal survival and induction of axonal outgrowth and reinnervation of denervated Purkinje cells in the maturing cerebellum.

LI-rMS does not affect PC survival

To verify that LI-rMS does not have detrimental effects on denervated, and therefore potentially vulnerable PCs, we investigated the effect of LI-rMS on PC survival. Some explants were treated with BDNF, a known survival factor for PCs (Morrison & Mason, 1998) (N: $Control_{intact} = 6$, Dx-sham = 12, DxB = 10, Dx+1Hz = 8, Dx+10Hz =8, Dx+BHFS = 8). First, all PCs displayed a large branched dendritic tree, as has been previously described in explants (Letellier et al., 2009), confirming that PCs have matured in the explant environment. Moreover, LI-rMS does not have detrimental effects on

vulnerable neurons in Dx cerebella, with no difference in the total number of CaBP labelled PCs per cerebellar hemisphere between intact, LI-rMS or sham treated and Dx-BDNF treated groups (Fig 4.6) and an average CaBP pos cell count of 341 ± 32 across all groups. In addition, stimulation of non-lesioned explants with either 1 Hz or BHFS for 2 weeks/10min a day (N: Control-intact + 1 Hz = 5 and Control-intact+ BHFS = 5) had no effect on cell survival in the mature non-lesioned system (average CaBP count: 381 ± 40).

LI-rMS induces PC reinnervation

We investigated the effect of magnetic stimulation on climbing fibre reinnervation to denervated PCs (N: Dx-sham = 12, Dx+1Hz = 7, Dx+10Hz =7, Dx+BHFS = 7). In addition, as BDNF is upregulated by magnetic stimulation (Gersner et al., 2011; Ma et al., 2013; Yoon et al., 2011) and induces CF-PC reinnervation *in vivo* (Dixon & Sherrard, 2006; Willson et al., 2008), we used BDNF treatment of denervated cocultured explants (N: DxB = 10) to provide a comparator to LI-rMS-induced reinnervation. Our data show that in all explant cocultures there is a small amount of spontaneous ingrowth of VGLUT2-positive terminals, consistent with previous studies (Letellier et al 2009). Furthermore, consistent with *in vivo* studies (Dixon & Sherrard, 2006; Willson et al., 2008), BDNF induced the growth of VGLUT2-labelled terminals into the denervated cerebellar hemisphere, which localised around the PC somata and primary dendrites (Fig 4.5B). In the DxB cerebellar plates, the overall percentage of PCs that co-localised with VGLUT2 labelling (12.0 % ± 1.1) was greater than sham Dx explants (7.0 % ± 0.5) (Fig 4.7A,B).

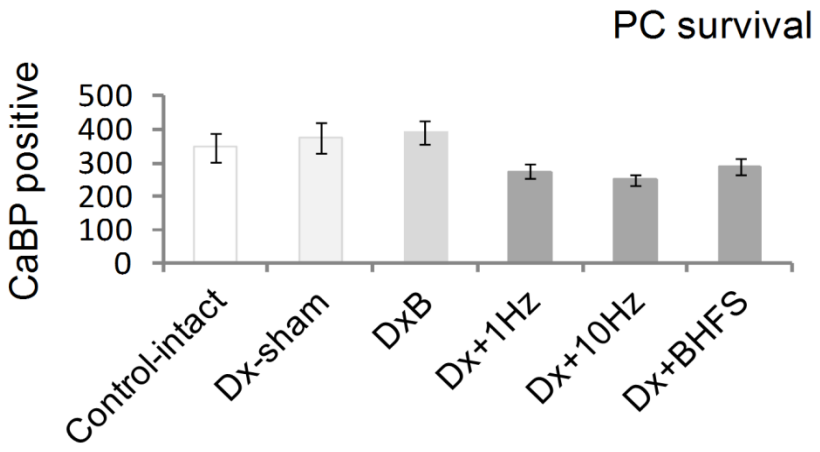

Figure 4.6 Total amount of PCs (CaBP positive cells) counted per cerebellar hemisphere. There was no difference of CaBP positive cells between any stimulation group ($F = 1.94$, $p = 0.062$).

In addition, 14 days of 10 min/day LI-rMS also induced PC reinnervation, but in a stimulation-specific manner. We showed that, in comparison to Dx-sham explants, BHFS treatment significantly increased the amount of VGLUT2 labelling in grafted cerebellar hemispheres with 19.5 % ± 3.1 PCs contacting VGLUT2-positive terminals. In contrast, LI-rMS at 1 Hz or 10 Hz suggested a smaller intermediate increase of VGLUT2-contacted PCs (11.7 % ± 1.7 and 8.9 % ± 1.0 respectively), which was not significant (Fig 4.7A). Moreover, pre-treatment with BDNF and subsequent 14-daily stimulations with 1 Hz or BHFS resulted in significant VGLUT2-positive PC reinnervation (19.4 % ± 3.2 and 16.0 % ± 2.6 PCs respectively) in comparison with Dx-sham (Fig 4.7B); but there was no additive effect of the 2 treatments.

The presence of VGLUT2-labelled terminals on PC somata and dendrites was most noticeable close to the host-graft junction and decreased linearly with distance into

the cerebellar hemisphere (Fig 4.7C). Therefore, the percentage of VGLUT2-contacted PCs was evaluated in rows with increasing distance from the Dx interface. Quantitatively, for those groups in which a significant amount of VGLUT2 reinnervation was induced, inter-group differences in VGLUT2-labelled reinnervation were only significant in the two first rows closest to the Dx (Row 1 and Row 2, Fig 4.7C), with the greatest amount of reinnervation being observed in Row 1.

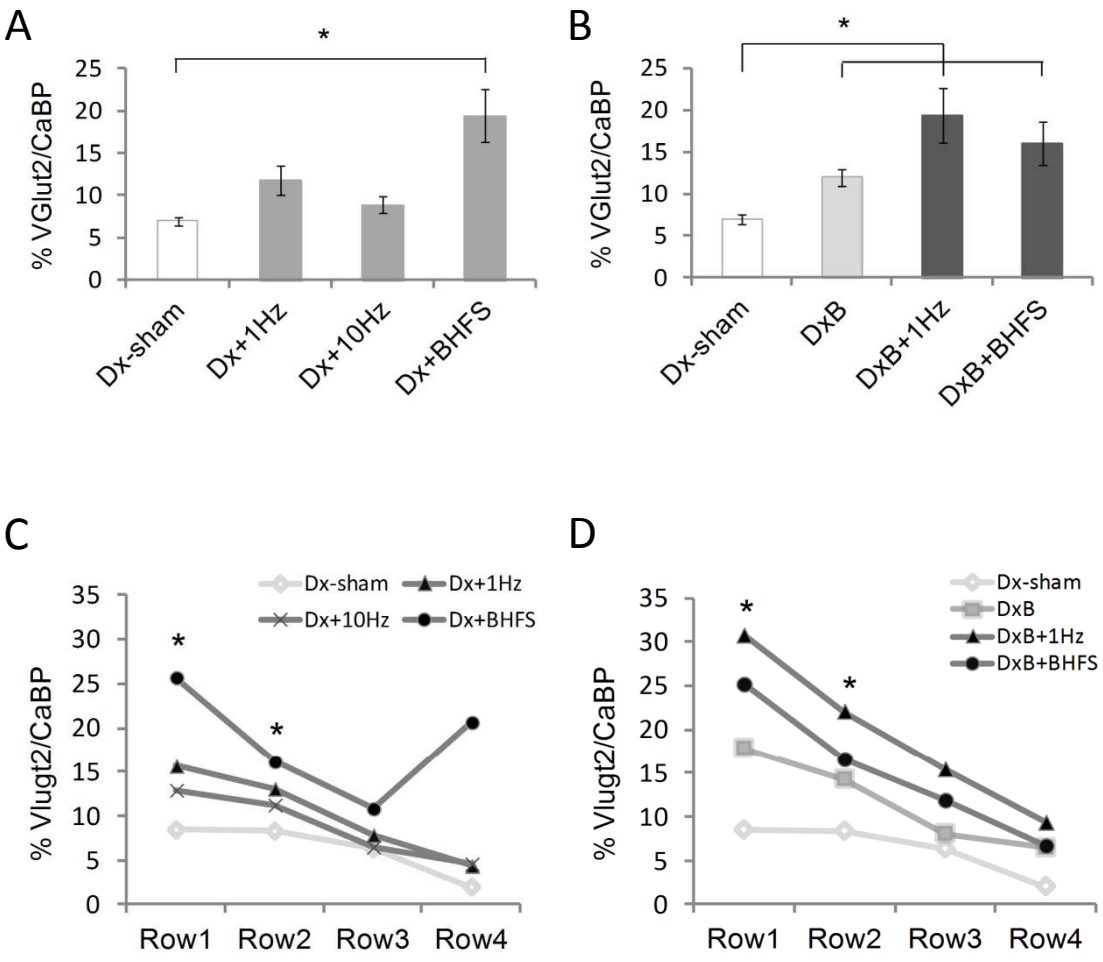

Figure 4.7 Cerebellar reinnervation, as shown by % CaBP-positive PCs colocalised with VGLUT2 terminals (see Fig 4.5), induced by LI-rMS alone (A,C) or in combination with BDNF (B,D). A, B) Total reinnervation per cerebellar hemisphere; C, D) CaBP-VGLUT2 colocalisation with increasing distance into the cerebellar hemisphere, Row1-4 (host-graft junction = Row 1). Single treatment with BDNF or BHFS, and BDNF plus 1 Hz or BHFS induces VGLUT2-positive reinnervation of denervated PCs ($F = 9.49$, $p < 0.00$), which is densest in the first two rows closest to the host-graft cerebellar hemisphere junction. Significant differences from Dx-sham: * $p < 0.05$; ** $p < 0.01$; *** $p < 0.001$.

qPCR

To understand mechanisms underlying LI-rMS induced CF-PC reinnervation, we measured changes of gene expression 24h after the last LI-rMS treatment (1 Hz, 10 Hz or BHFS or Dx-sham). We examined 4 candidate genes, BDNF, Pax3, Sia2 and Sia4, which are associated with olivo-cerebellar development (Sherrard et al., 2009) and neural plasticity (Rutishauser, 2008). After 14 days LI-rMS there was stimulation-specific modulation of gene expression (Fig 4.8). 1 Hz LI-rMS overall downregulated gene expression: in the cerebellar plates BDNF ($p = 0.018$) and Sia4 ($p = 0.042$); and in the inferior olive Pax3 ($p = 0.042$). 10 Hz showed a tissue related effect: decreasing gene expression in the cerebellar hemisphere (Pax3, $p=0.02$ and Sia4, $p= 0.004$) and increasing Sia2 expression in the inferior olive ($p=0.018$). BHFS upregulated BDNF expression, significantly in the inferior olive ($p=0.042$) and showed downregulatory effects on Pax3 ($p=0.047$) and Sia4 ($p=0.009$) expression in cerebella plates.

LI-rMS activates cerebellar cells

We show that LI-rMS induced CF-PC reinnervation in a stimulation-specific manner; only BHFS significantly increased reinnervation. To understand which cell populations were involved in this response, we labelled explants for the early response gene c-fos. We counted the number of c-fos labelled cells after a single 10 min BHFS stimulation 1.5h or 3.5h after stimulation. The total number of c-fos positive cells increased 3.5h after BHFS (338.7 ± 20.0) in comparison to non-stimulated DX-sham explants (262.7 ± 13.2, $p = 0.041$) and to 1.5h after stimulation (267.8 ± 28.8, $p = 0.021$) (Fig 4.9A).

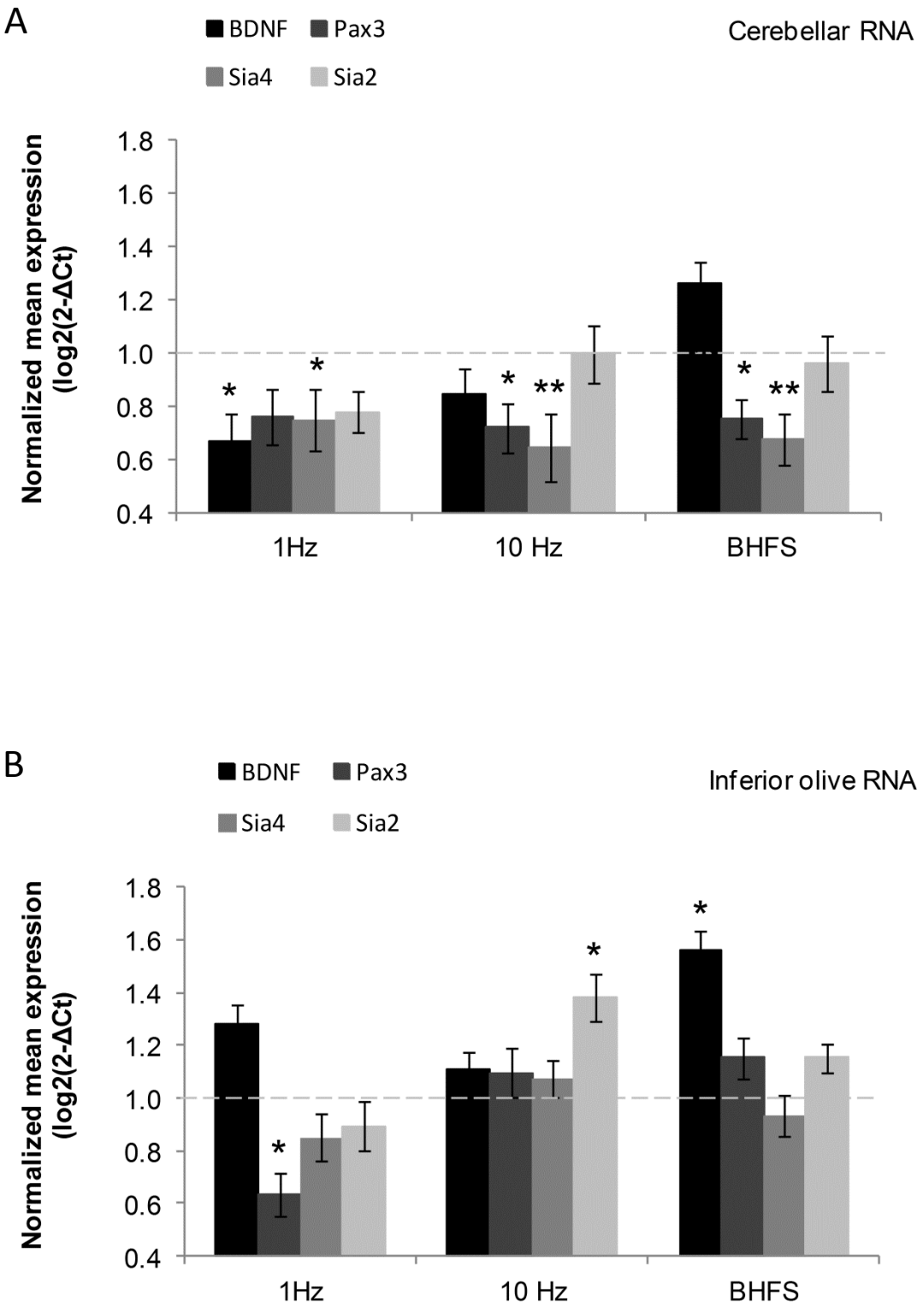

Figure 4.8 Normalized mean RNA expression (log2(2-ΔCt)) for grafted cerebellar hemisphere (A) and inferior olive region (B). Explants were stimulated for 14 days/10 min daily from ~P20 on. 24h after last stimulation cerebellar and ION tissue was sampled. Horizontal dashed lines (log2(2-ΔCt) = 1) is the normalised gene expression for sham-stimulated tissue. Significance of independent *t*-test: *$p < 0.05$, ** $p < 0.01$, *** $p \leq 0.000$.

It has been proposed that human cerebellar rTMS activates Purkinje cells in the cerebellar cortex (Koch, 2010). Moreover, PCs are the target of CF reinnervation. Hence, we examined PC activation by LI-rMS by counting the total number of c-fos, CaBP and double-labelled neurons per co-cultured cerebellar hemisphere. ~10-12 % of c-fos labelled cells co-localized with CaBP positive labelling (Fig 4.9B) and this did not change after LI-rMS. However, the percentage of PCs that were also c-fos positive (ratio CaBP:c-fos/CaBP) increased from 60 % in Dx-sham to 75 % 3.5h after BHFS stimulation (Fig 4.9B), albeit non-significant ($p = 0.38$).

To identify which other cell populations were activated by LI-rMS, we co-localised c-fos labelling with GFAP (astrocytes), parvalbumin (GABAergic interneurons) or NeuN (granule neurons) labelling. Qualitatively, there was no evidence of c-fos colocalisation with either GFAP-positive glia or parvalbumin-positive interneurons. While there was co-localization of Neu-N and c-fos, due to the small size of granule cells and their high density, this could not be quantified within the time constraints of this thesis.

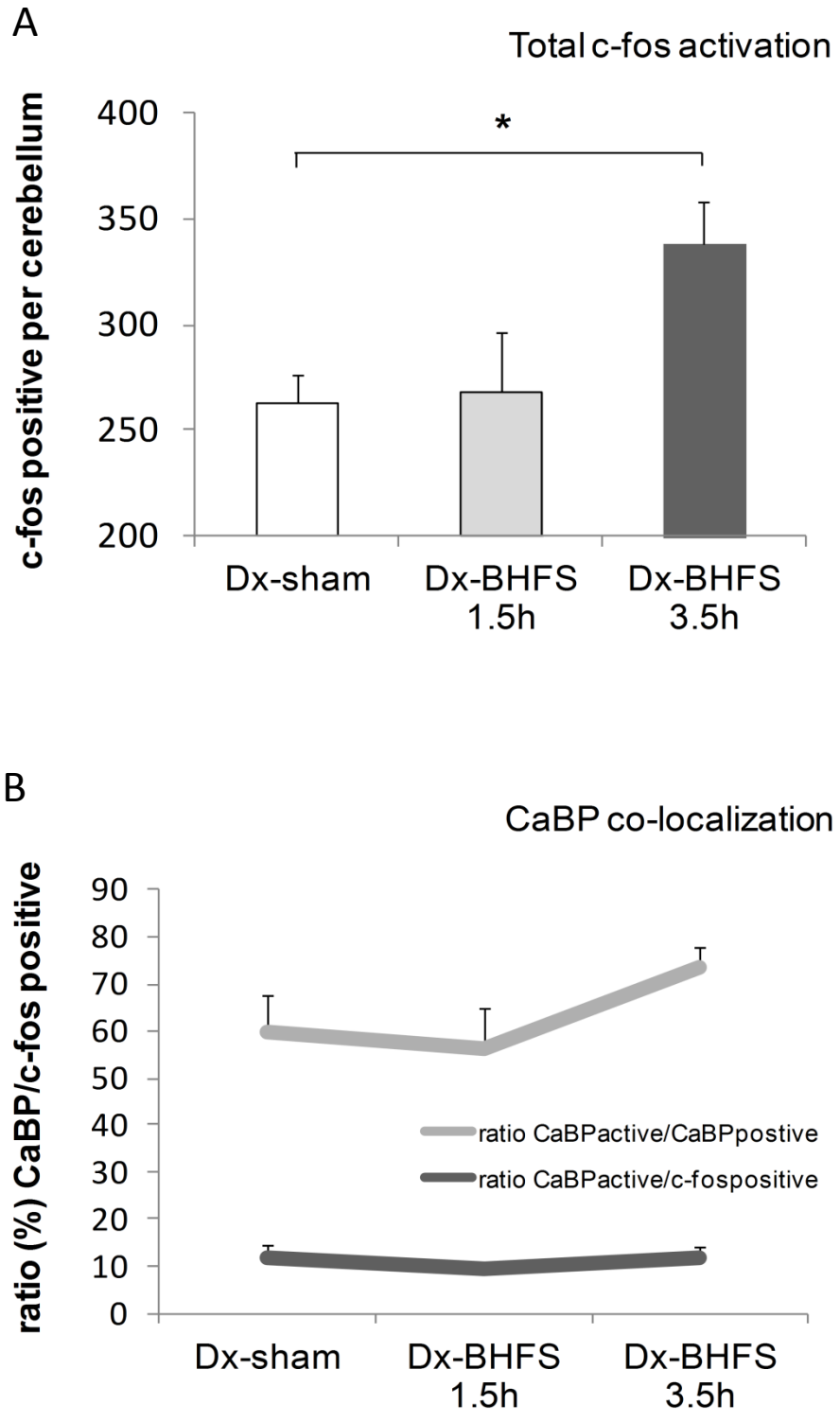

Figure 4.9 c-fos activation in cerebellar Dx hemispheres. A) Mean number of c-fos positive cells per denervated cerebellar hemisphere either 1.5 hours (Dx–BHFS 1.5h) or 3.5 hours (Dx–BHFS 3.5h) after one 10 min BHFS session or no stimulation (Dx-sham). C-fos labelling increased 3.5h after BHFS stimulation in contrast to 1.5h and Control ($H = 8.28$ $p = 0.016$; Dx-sham – Dx-BHFS3.5h: $U = -14.14$, $p=0.021$ and Dx-sham – Dx-BHFS1.5h: $U = -12.91$, $p = 0.8$). B) Proportion of c-fos positive PCs (ratio CaBP:c-fos/CaBP) and the percentage of all c-fos positive cells which were PCs (ratio CaBP:c-fos/c-fos). The proportion of c-fos labelled cells that were PCs remained stable following LI-rMS ($H = 0.99$, $p = 0.61$). Although the percentage of PCs that were c-fos positive increased this was not significant ($H = 1.95$, $p = 0.38$).

DISCUSSION

To investigate the fundamental effects of LI-rMS on neural circuit repair, we applied different protocols of LI-rMS to the olivo-cerebellar projection model of axonal injury (Letellier et al., 2009). Using the whole circuit organotypic model, which is both highly reproducible and readily manipulated, we systematically investigated the effects of different stimulation on the survival and reinnervation of PCs after CF denervation, as well as the underlying cellular and molecular mechanisms.

The effect of LI-rMS on PC survival

In our model of olivo-cerebellar denervation no significant decrease of PC survival was observed. To be able to reinnervate a denervated neuron, the cell must survive (Horner & Gage, 2000). Moreover, CF deprivation influences normal PC function (Rossi & Strata, 1995) and hence CF denervation might lead to higher PCs vulnerability and stresses (Sarna & Hawkes, 2003). Studies have shown that induction of cellular stress such as excessive increase of nitric oxide (NO) can result in detrimental effects on neuronal survival (Boland et al., 2002), where LI-rTMS has been shown to increase levels of NO in the rodent cerebellum (Chu et al., 2011) and cortical areas (Cho et al., 2012). Here we investigate for the first time the effect of LI-rMS on PC survival and show that LI-rMS treatment does not have detrimental effects on the survival of denervated PCs. Though a trend of an overall slight decrease of number of PC cells in the denervated cerbellum after LI-rMS can be argued, this non-significant pattern was not associated with stimulation-specific levels of reinnervation. This is in line with other experimental models, where studies have shown pro-survival to neutral effects on neuronal viability, both in *in vivo* models of stroke (Bates et al., 2012; Yang et al.,

2012) and in *in vitro* cultures (Boland et al., 2002; Di Loreto et al., 2009). Nonetheless, non-standardization of explant size might underestimate the underlying effect size. Further standardization of PC density per hemisphere would be beneficial to decrease variability and increase statistical power.

Patterned high frequency stimulation induces neural circuit repair

We investigated the amount of CF-PC reinnervation after LI-rMS with or without BDNF. Here we show for the first time that repeated LI-rMS induces olivo-cerebellar axonal outgrowth and target neuronal reinnervation after lesion of a normal neural circuit.

14 days 10min/day stimulation with patterned high frequency BHFS showed a significant overall increase in the amount of reinnervation of denervated PCs (20 %). All explants showed a small amount of spontaneous axonal sprouting (7 %) and no overall increase by straight 1 Hz or 10 Hz frequencies were observed. This is in contrast with studies of high intensity rTMS suggesting overall inhibitory effect of low frequency stimulation (≤ 1 Hz) (Fitzgerald et al., 2006; Lang et al., 2006). We have previously shown that 1 Hz LI-rMS decreases structural complexity in neurons, however did not affect general neurite outgrowth (Grehl et al., 2015). This suggests a more complex effect on neuronal structure of 1 Hz stimulation at lower intensities that requires further investigation.

In addition, we have recently shown that high frequency, patterned LI-rMS changes BDNF expression to induce structural plasticity in an abnormal neural circuit (Rodger et al., 2012). Treatment of explants with BDNF show a significant amount of reinnervation closest to the host-graft junction (18 %), similar to BHFS induced

reinnervation (26 %), which is consistent with previous studies *in vivo* showing BDNF induced reinnervation of PCs of 22 % (Willson et al., 2008). Interestingly pre-treatment with BDNF and subsequent LI-rMS did not induce additional amounts of reinnervation by BHFS, however it did induce reinnervation after 1 Hz stimulation (30 %). This suggests that BDNF mechanisms involved in LI-rMS/BDNF induced olivo-cerebellar reinnervation might underlie similar signalling pathways. It remains to be determined electrophysiologically if CF-PC synapses are functionally active and induce normal PC responses. However, previous studies *in vitro* have shown that mature CF-PC reinnervation result in mono-innervation (Letellier et al., 2007). Furthermore, studies *in vivo* have shown that even a small amount of reinnervation (22 %) can compensate functional deficits of complex motor and spatial skills (Willson et al., 2008).

BHFS stimulation activates Purkinje Cells

To understand cellular mechanisms underlying BHFS-induced CF reinnervation in the denervated cerbellum, we first identified which cerebellar cell populations were activated after one application of BHFS.

We show for the first time that low intensity magnetic stimulation increases c-fos, an early marker of cell activation (Bullitt, 1990; Herrera & Robertson, 1996) 3.5h after the end of stimulation. That is in accordance with previous findings showing increased expression of c-fos 3h but not 1.5h after high intensity rTMS in organotypic slice cultures of similar age (P25) (Hausmann et al., 2001). There, c-fos expression was dependent on sodium channel activity, suggesting membrane depolarization to the extent of sodium channel opening (Hausmann et al., 2001). Based on computational modelling of the electric field that showed below action potential threshold intensity

(Chapter 3), in addition to our previous study in single neurons showing release of calcium from intracellular stores during LI-rMS (Grehl et al., 2015), it suggests that our LI-rMS application does not induce depolarization to the extent of membrane channel opening, but is based on subcellular mechanisms such as changes in calcium concentration *via* intracellular stores (Grehl et al., 2015).

It has been suggested that cerebellar rTMS at high intensities can activate Purkinje cells in the cerebellar cortex (Koch, 2010). We investigated the amount of PCs activation after LI-rMS. A slight trend, similar to the observed increase of overall cellular activation, might be argued 3.5h after last stimulation. However, PC activation accounts for around 12 % of overall cellular activation by LI-rMS, suggesting that other non-identified cell types are also activated in the cerebellar plates after BHFS application. Our results suggest that PV expressing interneurons and glia are not stimulated by BHFS stimulation. In contrast, glutamatergic granule cells, which could not be quantified in this study, are the most likely candidate cells to account for c-fos activation as they are the most abundant cell type of the cerebellar cortex (Apps & Garwicz, 2005). Further investigation is necessary to identify the level of granule cell activation after LI-rMS.

Formation of CF-PC pathways is dependent on a variety of signalling interactions between CF and PCs during development (Watanabe & Kano, 2011), where PC state has been shown to be crucial to the control of CF-PC synapse formation (Letellier et al., 2007). Hence, the demonstration of PC activity is the first step underlying mechanisms of plasticity promoting mechanism of reinnervation in the mature olivo-cerebellar circuit.

Gene expression

For a neuron to be reinnervated after denervation, there needs to be an increase in growth permissive molecules and/or a decrease of growth inhibitory molecules of the cellular environment, as well as the ability to activate genetic programs for axonal growth (Dusart et al., 2005). To better understand possible long-term mechanisms underlying LI-rMS induced CF-PC reinnervation, we investigated the effects of LI-rMS on the expression of 4 candidate genes, all of which are involved in olivo-cerebellar development (Morrison & Mason, 1998; Sherrard & Bower, 2001; Sherrard et al., 2009; Sherrard et al., 2013) or neural plasticity (Rutishauser, 2008).

Although it has been shown that magnetic stimulation differentially alters gene expression in different neuronal populations (Funke & Benali, 2011; Ma et al., 2013; Vlachos et al., 2012) we show for the first time stimulation-specific effects of LI-rMS on cerebellar and inferior olive tissue. Here we show that LI-rMS induced stimulation-specific changes in BDNF gene expression. Only BHFS resulted in increased levels of BDNF expression in both cerebellar and inferior olive tissue, which accords with BDNF upregulation by high and low intensity magnetic stimulation (Gersner et al., 2011; Ma et al., 2013; Rodger et al., 2012; Zhang et al., 2007). In contrast, 1 Hz stimulation downregulated BDNF in cerebellar tissue, while 10 Hz showed no overall effect on BDNF expression. These expression changes are directly paralleled by CF-PC reinnervation: increased BDNF in reinnervating (ION) and target (cerebellar) tissue is associated with CF-PC reinnervation (BHFS), whereas when BDNF expression was unchanged or reduced (1 Hz and 10 Hz), there was no reinnervation. Given its pivotal role in many aspects of growth cone motility, neurite extension and synaptic and

structural plasticity (Lu et al., 2013; Tuttle & O'Leary, 1998) and the involvement of BDNF-TrkB signalling in olivo-cerebellar development (Sherrard et al., 2009) and cerebellar cortical plasticity (Carter, Chen, Schwartz, & Segal, 2002; Tanaka, Sekino, & Shirao, 2000), failure of BDNF upregulation in the inferior olive and near CF-PC synapses in the cerebellum is consistent with insufficient cues for CF growth and synapse induction, thus providing a potential mechanism underlying the observed differences in amount reinnervation between LI-rMS frequencies.

BDNF induced reinnervation has been shown to be dependent on polysialylated neural cell adhesion molecule (PSA-NCAM) (Sherrard et al., 2013), a growth-permissive cell surface molecule that can facilitate BDNF-TrkB interaction (Muller et al., 2000a) and is modulated during post-lesion axonal sprouting in the adult cerebellum (Dusart et al., 1999). Binding of PSA to NCAM is mediated *via* Sia4 and Sia2 (Angata & Fukuda, 2003), while transcription factor Pax3 expression has been shown to increase with NCAM polysialylation and BDNF levels, targeting downstream transcription of Sia2 (Angata & Fukuda, 2003; Kioussi & Gruss, 1994; Mayanil et al., 2001). It has been shown that upregulation of Sia2/4 after injury results in increased PSA-NCAM expression and greater axonal sprouting and axonal outgrowth through an injury scar (El Maarouf, Petridis, & Rutishauser, 2006). We suggest for the first time the involvement of Sia4, Sia2 and Pax3 in relation to stimulation induced structural plasticity in the mature olivo-cerebellar system. Further investigation of genes involved in response to short-term and long-term LI-rMS is necessary to reveal signalling and axonal transport mechanism underlying CF-PC reinnervation.

The influence of stimulation load

Here we show for the first time that long-term LI-rMS stimulation induces changes in structural plasticity after injury of a normal neural circuit. This study investigated the effects of total stimulation load of multiple LI-RMS for a unit time (10 min), based on previous stimulation durations (Rodger et al., 2012) and studies of biological relevance of timing (Angelov et al., 2007). Observed reinnervation effects might underlie an effect of total stimulation load (pulses/unit time). Though, our results indicate that dose and effect are not simply linearly related between number of pulses and reinnervation ($p = 0.15$). 10 min application of BHFS frequency delivers comparatively 18x larger number of pulses (Fig 4.3A) than 10 Hz stimulation, while 10 Hz stimulation delivers 10x larger amount of pulses in contrast to 1 Hz stimulation, within the same amount of time. However, 1 Hz and 10 Hz did not result in significant increases of reinnervation (10 Hz < 1 Hz), opposite to BHFS stimulation (Fig 4.7A). Suggesting a more complex relationship of stimulation parameters underlying observed LI-rMS effects. Studies in humans (Gamboa et al., 2010; Nettekoven et al., 2014) and animal (Volz et al., 2013) also suggest a non-linear relation between dose and effect. Further investigation is needed to identify the unique effects of different stimulation parameter, to optimize and better tailor magnetic stimulation in the clinic.

CONCLUSION

We investigated the effect of different LI-rMS stimulation on neural circuit repair. We show for the first time that low intensity, patterned biomimetic high frequency stimulation (BHFS) induces axonal reinnervation after injury. It is suggested that BDNF modulation underlies stimulation-specific effects of stimulation, where further

investigation is needed to reveal precise mechanism involved in the effects of LI-rMS on neural circuit repair.

Taken together, the results of this study and previous work in our laboratory (Grehl et al., 2015; Rodger et al., 2012) show that LI-rMS as a by-product of high intensity rTMS coils cannot be disregarded. Further understanding of the fundamental effects of LI-rMS on biological tissue is essential to better tailor future therapeutic application of rTMS and explore the therapeutic potential of LI-rMS.

ACKNOWLEDGEMENTS

We are grateful to Juan Sebastián Jara and Natalie Morellini for technical assistance and Caroline Dubacq and Samuel Bornens for scientific advice. This research was funded by a French CNRS PICS grant to support the international collaboration, SG was funded by UIS and SIRF grants, University of Western Australia, Perth, Australia.

Chapter 5

5 GENERAL DISCUSSION

5.1 What's new

The aim of this PhD was to provide a framework of fundamental molecular and cellular mechanisms underlying low intensity magnetic stimulation at different frequencies in normal CNS tissue in both single cells and neural-circuits. We show that LI-rMS affects structural complexity and cell survival at the single cortical cell level and induces outgrowth of axon collaterals in a lesioned neuronal network. Furthermore, here we demonstrate for the first time a possible mechanism of activation that might underlie the effects of low intensity magnetic stimulation.

5.2 Theory of mechanism

5.2.1 Calcium hypothesis

As described in detail in chapter 1, the calcium dependent theory of activation illustrates how increases in intracellular calcium concentration lead to second messenger effects on diverse neuronal functions (Fung & Robinson, 2013; Thickbroom, 2007). Intracellular calcium induced changes can range from calcium dependent cellular events all the way down the signalling cascade to gene expressions that modulate molecular, anatomical or functional plasticity (Berridge et al., 2000).

High intensity stimulation has been shown to induce intracellular calcium influx *via* the opening of membrane channels (Pell et al., 2011; Ziemann, Hallett, & Cohen, 1998), leading to sufficient depolarization of the membrane potential to the threshold of

inducing an action potential (Pell et al., 2011). Because low intensity stimulation at the mT level is not expected to result in sufficient membrane depolarization for ion channel opening and action potential induction, its effects have often been disregarded. Here we demonstrate for the first time that low intensity magnetic stimulation increases neuronal calcium concentration from intracellular stores only, without opening membrane channels such as would occur during an action potential. Calcium is a particularly versatile signalling ion (Berridge et al., 2000), because of its complex activation mechanism, wide range of signalling components and interaction with other signalling pathways. We propose that the release of calcium from intracellular stores as a general mechanism might underlie effects of low intensity magnetic stimulation on single cellular processes and neuroplasticity within brain tissue.

5.2.1.1 Applied calcium hypothesis

Changes in membrane potential can lead to activation of membrane channels/receptors such as G-protein coupled receptors, enzyme linked receptors and TRP channels (Mori et al., 2002), activating further second messenger cascades, leading to calcium release from intracellular stores, the endoplasmic reticulum and to a lesser extent the mitochondria (Berridge et al., 2000).

One possible mechanism of how these changes might lead to observed cellular and circuit effects is the activation of the PLC signalling pathway. This pathway has been shown to be activated *via* G protein-coupled receptor activation in the membrane. Activation results in increase of cytoplasmic calcium concentration by calcium release from intracellular stores of the endoplasmic reticulum *via* activation of the inositol

1,4,5-trisphosphate receptor (IP3R) (Foskett, White, Cheung, & Mak, 2007), which is expressed widely in the brain with particular abundance in the cerebellum (Furuichi, Shiota, & Mikoshiba, 1990). Alternatively, direct changes in endoplasmic reticulum membrane potential might directly influence ryanodine receptor (RyR) activity, previously shown to be voltage sensitive (De Crescenzo et al., 2006; Neves et al., 2002). Moreover, increases in intracellular calcium or direct membrane potential change can further influence mitochondrial calcium uptake and release (Santo-Domingo & Demaurex, 2010; Valsecchi et al., 2013). In addition, PLC pathway activity and increased intracellular calcium concentration lead to activation of PKC, which subsequently phosphorylates other molecules, further activating different signalling cascades (Tanaka & Nishizuka, 1994), including regulation of c-fos gene expression (Trejo & Brown, 1991).

5.2.1.2 Mechanism of stimulation-specific effects: cellular death

Our results suggest that low intensity magnetic stimulation at some frequencies induces slight detrimental effects on cellular survival. However, at the single cell level that effect was limited to straight high-frequency stimulation, while low-frequency straight and high-frequency patterned stimulation did not show such an effect. Decreases in cellular survival were associated with the upregulation of pro-apoptotic and downregulation of anti-apoptotic genes. In contrast, stimulation which did not induce apoptosis showed survival-promoting gene expression changes. This suggest a survival-promoting effect of patterned stimulation based on associated gene expression change.

One possible mechanism underlying the effect is stimulation-specific regulation of calcium buffering mechanism. Increases in intracellular calcium become toxic to the cell at prolonged high concentrations (Arundine & Tymianski, 2003). Hence control of free calcium within the cell is vital for the survival of the neuron through a combination of calcium sequestration (re-uptake into organelles such as mitochondria), calcium efflux (removal to the extracellular domain *via* pumps) and calcium binding (*via* calcium buffers, such as calretinin, parvalbumin and calbindin) (Chard et al., 1993; Gilabert, 2012).

Regulation of calcium sequestration in response to different stimulation frequencies might underlie stimulation-specific effects observed. One study has shown LI-rMS decreases mitochondrial membrane potential (Morabito et al., 2010b), though the effects on intracellular calcium levels were not investigated. Furthermore, other studies applying magnetic stimulation at high intensity show frequency-specific effects on parvalbumin and calbindin expressing interneurons (Benali et al., 2011), which suggests a possible involvement of calcium buffer regulation in frequency-specific magnetic stimulation effects, such as cellular death. In their study Benali et al., (2011) did not show an increase of cellular death in connection with changes in PV and CaBP expression after one session of high intensity rTMS at 1 Hz or TBS (i+c). Few other studies have reported effects of high intensity magnetic stimulation on cellular survival, though some studies investigating effects after injury show general pro-survival tendencies after higher frequency stimulation (Post, Müller, Engelmann, & Keck, 1999; Yoon et al., 2011). However, due to heating of the coils, in both human and animal application, higher frequencies (> 3 Hz) at high stimulation levels commonly require cooling intervals resulting in an overall patterned stimulation. This leads to the

suggestion that patterned waveforms may induce more intricate and biologically safe changes compared to straight frequencies (Hoogendam et al., 2010; Martiny et al., 2010), i.e. less stressful levels of intracellular calcium. This is in accordance with our data showing that cTBS and BHFS stimulation, did not decrease cellular survival, even though associated with as high an increase (at nM levels equivalent to those observed following action potential induction (Helmchen et al., 1997; Liao & Lien, 2009)) in intracellular calcium as 10 Hz and 100 Hz. While 1 Hz, even though applied as a straight frequency, increased levels of intracellular calcium to a lesser extend than all other frequencies without effecting cellular survival.

Further investigation is needed to test the calcium hypothesis on single cell and neural network level. First, identification of intracellular calcium stores involved in the calcium release during LI-rMS is necessary. Application of pharmacological agents blocking RyR (Ryanodine) and IP3 (Xestospongin C) receptors activity is the first step to better understand the nature of calcium release from intracellular stores during LI-rMS. Furthermore, systematic investigation of calcium sequestration responses to different magnetic stimulation parameters and subsequently activation of different signalling pathways will promote insight into the underlying mechanism of LI-rMS effects and associated neuroplastic changes between different neuronal subtypes and networks.

5.2.1.3 Neural circuit-specific effects

The use of the olivo-cerebellar explant as a model of neural circuit and axonal sprouting has the advantage over brain slice preparations that cellular connections are left intact within the olivo-cerebellar microcircuit and only cortical and spinal afferents are disconnected. In this model, no significant decrease of PC survival was observed,

though a trend of an overall slight detrimental effect of all LI-rMS frequencies can be argued, where 10 Hz stimulation showed the lowest amount of PC numbers in the denervated cerebellum, in contrast to clear differences in single cortical cells. This difference might be based on the influence from any combination of these four factors: experimental model (single cell – neural network), cell properties (cortical cell – cerebellar PC), stimulation duration (4 vs 14 days) and induced electrical current (waveform divergence). Further investigation is necessary to identify the specific involvement of each factor and the effect on neuronal survival.

However, different stimulation frequencies did result in differing amounts of axonal sprouting. High frequency patterned application resulted in significantly higher axonal ingrowth in constrast to straight low and high frequency stimulation. Like many brain networks, olivary and cerebellar neurons exhibit an oscillatory pattern of activation. Olivary neurons have been shown to oscillate between 2-8 Hz (Devor & Yarom, 2002). While the cerebellum shows a wide range of oscillatory activities covering both the lower-frequency and the higher-frequency ranges of delta, theta, beta, (high) gamma band or an even higher range at 160 – 260 Hz (De Zeeuw, Hoebeek, & Schonewille, 2008). Due to this typical state of activation, oscillating networks might be more responsive to patterned stimulation in general than to straight frequencies.

Consequently, this preference might be connected to the ability of a cell to control relatively large rises in intracellular calcium. While we could not directly measure intracellular calcium levels in cerebellar cells due to technical limitations, we showed that one LI-rMS session can significantly activate cerebellar neurons 3.5h after stimulation, a time-frame shown to be the optimal for detection of c-fos protein

upregulation (Hausmann et al., 2001). In contrast, we did not observe changes in c-fos RNA expression in our model of dissociated single cells 5 hours after one LI-rMS session, possibly based on an overall late suboptimal time-point for detection of c-fos RNA regulation (Appendix B, (Sheng & Greenberg, 1990)). Furthermore, our results intimates that the most abundant cerebellar cellular activation possibly involves glutaminergic granule neurons, while our dissociated cell culture model is comprised of predominantly inhibitory neurons.

However, the exact mechanisms underlying LI-rMS induced olivo-cerebellar reinnervation remain to be determined. The intracellular calcium receptor IP3 is particularly abundant in the cerebellum and along PC dendrites and has been shown to be crucial to changes in synaptic plasticity in the cerebellum (Furuichi et al., 1990; Rose & Konnerth, 2001). It has been shown that subthreshold electrical stimulation at proximal dendrites induces compartmentalized synaptic plasticity in cerebellar PCs (Eilers, Augustine, & Konnerth, 1995) and hippocampal neurons (Hulme et al., 2012). One possible mechanism underlying intercellular signalling in the mammalian brain involves electrical synapses (gap junctions). Electrical synapses, comprise clusters of connexin (Cx) containing channels, often interconnecting membranes of neurons of similar type, size and input resistance and are proposed to underlie oscillatory synchronization between connected cells (Connors & Long, 2004). Electrical synapses are widely expressed in the mammalian brain, and have shown to occur between olivary neurons (Mathy, Clark, & Häusser, 2014) and between PCs - Bergmann glia (Pakhotin & Verkhratsky, 2005). They are permeable to large ions such as calcium, and large molecules such as cAMP and IP3 depending on transjunctional voltage between cells and are modified by connected kinase phosphorylation (Connors & Long, 2004).

Increases in intracellular calcium can modulate permeability of electrical synapses at high concentration (Connors & Long, 2004), though the exact mechanisms are still unknown. Electrical synapses provide a direct mechanism of intercellular signalling *via* bi-directional exchange of ionic molecules without the release of neurotransmitter and provide a candidate mechanism of how regulation of signalling molecules (i.e. BDNF) can influence neuronal plasticity.

Studies are needed to identify a potential role of electrical synapses in subthreshold intercellular signalling, where existing mouse models of connexin knockout (KO), such as the Cx36-KO with associated elimination of electrical synapses (De Zeeuw et al., 2003), could be of great advantage to understand the neuroplastic effects of magnetic stimulation.

5.2.2 Stimulation load

In our studies we investigated the effects of total stimulation load (pulse density/unit time (10 min)), based on previous stimulation durations (Rodger et al., 2012) and studies of biological relevance of timing (Angelov et al., 2007), in addition to compatibility of application in the clinical setting where heating of the coil and associated cooling intervals alters the overall stimulation load. Effects of changes in stimulation load comprise three aspects of stimulation parameter: temporal pulse-spacing (frequency), rhythm of delivery (straight vs patterned) and dose (total number of pulses). In our system with mT intensity stimulation, obligatory cooling intervals due to coil heating were not necessary, leaving the possibility to investigate entirely straight patterns. Our results indicate that dose and effect are not simply linearly related and suggest an overall importance of stimulation load (pulse density/ unit

time). This is in accordance with studies in humans (Gamboa et al., 2010; Nettekoven et al., 2014) and animal research (Volz et al., 2013), showing that dose and effect are not simply linearly related and is in line with the theory of non-linear calcium activation (Fung & Robinson, 2013). Taken together our results suggest that LI-RMS has stimulation-specific effects on cellular/molecular mechanism and neural circuit repair. However, further investigation is needed to identify the unique influence of different stimulation parameters per stimulation load, together with optimizing stimulation duration for therapeutic benefits.

5.3 Stimulation delivery

Another important parameter in addition to stimulation load is how the stimulation is delivered to biological tissue. Magnetic stimulation effects are based on how the created secondary current interacts with the cell. The creation of the secondary electric current is dependent on the strength and direction of the electrical field, in addition to the inherent conductivity/impedance of the medium (i.e. brain). Estimation of inherent conductivities and hence precise prediction of the secondary electric current is not possible; however, precise description of the induced electric field is easily obtainable. This is essential to better understand magnetic stimulation effects and to be able to compare between outcomes of different studies. The induced electrical field is determined by magnetic field strength and pulse waveform (rise-time/fall-time, number of cycles) and its orientation within the biological tissue.

Studies in humans have shown outcome measurements to be dependent on the general direction of the created electric current inside the brain (Volz et al., 2014) and amount of reversal of this current (mono vs bi/polyphasic pulses) (Arai et al., 2005;

Maccabee et al., 1998; Sommer et al., 2006; Sommer et al., 2002), thought to be based on preferentially affecting specific cellular (sub)types and/or segments of a neuron (Esser, Hill, & Tononi, 2005; Maccabee et al., 1998; Ni et al., 2011; Pashut et al., 2011). Furthermore, it has been shown that different stimulation devices can deliver slightly differing waveforms under the same settings, resulting in slightly diverging cortical effects (Kammer et al., 2001; Thielscher & Kammer, 2004). Hence a large amount of variability can be induced just within the stimulation set-up on top of additional factors such as inter-subject variability. Thus to really further the understanding of magnetic stimulation effects at the tissue level, the stimulation, and therefore the generated field, needs to be clearly defined.

5.3.1 Stimulation delivery in our specific in vitro set-ups

The first set-up, provided for use in the first experiment (Chapter 2), produced a defined magnetic field in 24 well *in vitro* plates. Stimulation was delivered *via* a near-triangular pulse that produced an electric field with a maximum intensity of ~ 0.4 V/m (Appendix C).

However, subsequent work using organotypic cultures in 6 well plates (Chapter 4) required different magnetic waveform rto deliver a particular magnetic and electric field within the target tissue. The amplitude of the induced electric field is dependent not only on the amplitude of the magnetic field, but also on its direction (axial components), the more uniform the direction, the more efficient the stimulation. Furthermore, it has been shown that a uniform magnetic field influences cortical neuronal subpopulations differentially (Radman et al., 2009), with asymmetrically shaped cells being affected optimally by a homogenous electric field. Based on the

theory that magnetic stimulation affects PC cells (Koch, 2010; Pope & Miall, 2014), a highly asymmetric neuron, a uniform magnetic field was specifically required. Furthermore, to control for effects of the induced electric field direction, we designed near identical rise and fall-times of the trapezoidal, magnetic waveform to produce uniplanar, opposite electric field directions. Here, we show the design of a magnetic stimulation device that delivers precise magnetic stimulation according to our specific *in vitro* set-up requirements. We show that this low intensity magnetic stimulation activates cerebellar cells and has the potential to induce axonal sprouting in an established model of axonal injury.

Taken together it is apparent that a wide set of parameters influences the effects of magnetic stimulation, where effects on biological tissue seem to be dependent on the particular interaction of the induced electric field with the biological tissue. Thus, systematic control and clear description of the stimulation parameters is necessary. The description of the induced electric field appears to be the most optimal requirement to enable comparison of results between studies derived from different stimulation set-ups and thus to promote better understanding of the effects of magnetic stimulation at the cellular level.

5.4 Why does it all matter?

It is important to consider the different contexts in which magnetic stimulation research is designed and applied. Firstly, clinical rTMS is based on the drive to help patients now. However, in the last years progress towards more reliable and reproducible rTMS effects in therapeutic application has become controversial (Ridding & Rothwell, 2007; Wassermann & Zimmermann, 2012), due to its high

outcome variability. As human application is driven by patient care, though with limited outcome measurements as investigation of cellular/molecular mechanism is ethically and hence technically limited, optimization and standardization of magnetic stimulation is to a large extent impossible in a human research setting. Effects of magnetic stimulation are based on an enormous number of parameters. The influences of these parameters can only be assessed by systematically acquiring data under highly controlled and standardized experimental conditions. The greatest control of variability in parameters of both magnetic stimulation delivery and biological tissue manipulation is achieved in *in vitro* set-ups. Nonetheless, it has to be taken into account that the *in vitro* experimental paradigm, especially single neurons that are maintained in culture are relatively immature, albeit fully differentiated, and not integrated within functioning neural networks. Thus their response to magnetic fields may be modified by different receptor and calcium-buffering capacities to adult neurons in whole *in vivo* neural networks, especially in the absence of normal glial metabolic regulation and afferent activity. This, in turn, may make these neurons more susceptible to the low-intensity stimulation we induced in a manner that would not occur in the adult human brain even to higher intensity stimulation. However, the fundamental, bottom-up approach of *in vitro* paradigm provides a practical and theoretical framework to more efficiently direct investigation in more complex models (i.e. animals *in vivo*) and ultimately lead to (re-)interpretation of results obtained in human rTMS research.

Here we reveal for the first time a fundamental cellular mechanism of non-depolarising magnetic fields on neurons, which in the *in vivo* context would underlie any trans-synaptic, neural circuit or cell environment responses. This could only be

achieved by the application of a defined magnetic field to isolated cortical neurons, thus removing the confounding effects of glial responses and neuronal circuit activity from the observed outcomes. Furthermore, this approach identified potentially deleterious effects of 10 minutes continuous stimulation (slight increase in neuronal apoptosis) even at low intensity. Although such continuous pulse trains are not given in current human rTMS, our data has pertinence to potential future human high intensity stimulation protocols as advances in coil-cooling technology may remove the requirement for short stimulation trains interspersed with stimulation-free pauses.

Taken together, we provide a framework of fundamental investigation of molecular and cellular mechanisms underlying low intensity magnetic stimulation at different frequencies in normal CNS tissue, both in the single cell and neural circuits. Our results reveal a novel cell-intrinsic mechanism for low intensity magnetic field stimulation of neurons. Importantly, this mechanism may also be evoked during high intensity stimulation, thus potentially working together with previously described metabolic and synaptic plasticity mechanisms of human rTMS (Allen et al., 2007; Gersner et al., 2011; Vlachos et al., 2012).

CONCLUSION

We show that low intensity magnetic stimulation has profound effects on normal brain tissue, from genetic through molecular to complex circuit levels. Furthermore, we describe for the first time a feasible mechanism underlying the effects of low intensity magnetic stimulation and provide a framework of how to deliver low intensity magnetic stimulation to neural tissue in a systematic way. These results form the basis to better understand the complexity of magnetic stimulation, direct investigation in more complex models and establish the groundwork to confirm or reinterpret magnetic stimulation data derived in the clinic (Müller-Dahlhaus & Vlachos, 2013). Ultimately, better knowledge of electric field parameters and their interplay with molecular and cellular mechanism gained from *in vitro* and *in vivo* studies will be translated into the clinical setting to optimize efficiency and specificity of non-invasive neural stimulation in humans.

REFERENCES

Adeyemo, B. O., Simis, M., Macea, D., & Fregni, F. (2012). Systematic Review of Parameters of Stimulation: Clinical Trial Design Characteristics and Motor Outcomes in Noninvasive Brain Stimulation in Stroke. *Frontiers in Psychiatry, 3*(88). doi: 10.3389/fpsyt.2012.00088

Afifi, L., Jarrett Rushmore, R., & Valero-Cabré, A. (2013). Benefit of multiple sessions of perilesional repetitive transcranial magnetic stimulation for an effective rehabilitation of visuospatial function. *European Journal of Neuroscience, 37*(3), 441-454. doi: 10.1111/ejn.12055

Agarwal, R., & Agarwal, P. (2012). Glaucomatous neurodegeneration: An eye on tumor necrosis factor-alpha. *Indian J Ophthalmol, 60*, 255-261. doi: 10.4103/0301-4738.98700

Ahmed, Z., & Wieraszko, A. (2006). Modulation of learning and hippocampal, neuronal plasticity by repetitive transcranial magnetic stimulation (rTMS). *Bioelectromagnetics, 27*(4), 288-294. doi: 10.1002/bem.20211

Alberts, B., Johnson, A., Lewis, J., Raff, M., Roberts, K., et al. (Eds.). (2002). *Molecular biology of the cell* (4th ed.). New York: Garland Science.

Aldinucci, C., Palmi, M., Sgaragli, G., Benocci, A., Meini, A., et al. (2000). The effect of pulsed electromagnetic fields on the physiologic behaviour of a human astrocytoma cell line. *Biochimica et Biophysica Acta (BBA) - Molecular Cell Research, 1499*(1–2), 101-108. doi: 10.1016/s0167-4889(00)00111-7

Alho, H., Ferrarese, C., Vicini, S., & Vaccarino, F. (1988). Subsets of GABAergic neurons in dissociated cell cultures of neonatal rat cerebral cortex show co-localization with specific modulator peptides. *Brain Res, 467*(2), 193-204.

Allen, E. A., Pasley, B. N., Duong, T., & Freeman, R. D. (2007). Transcranial Magnetic Stimulation Elicits Coupled Neural and Hemodynamic Consequences. *Science, 317*(5846), 1918-1921. doi: 10.1126/science.1146426

Angata, K., & Fukuda, M. (2003). Polysialyltransferases: major players in polysialic acid synthesis on the neural cell adhesion molecule. *Biochimie, 85*(1-2), 195-206. doi: 10.1016/S0300-9084(03)00051-8

Angelov, D. N., Ceynowa, M., Guntinas-Lichius, O., Streppel, M., Grosheva, M., et al. (2007). Mechanical stimulation of paralyzed vibrissal muscles following facial nerve injury in adult rat promotes full recovery of whisking. *Neurobiology of Disease, 26*(1), 229-242. doi: 10.1016/j.nbd.2006.12.016

Apps, R., & Garwicz, M. (2005). Anatomical and physiological foundations of cerebellar information processing. *Nature Reviews Neuroscience, 6*(4), 297 - 311. doi: 10.1038/nrn1646

Arai, N., Okabe, S., Furubayashi, T., Terao, Y., Yuasa, K., et al. (2005). Comparison between short train, monophasic and biphasic repetitive transcranial magnetic stimulation (rTMS) of the human motor cortex. *Clinical Neurophysiology, 116*(3), 605-613. doi: 10.1016/j.clinph.2004.09.020

Arundine, M., & Tymianski, M. (2003). Molecular mechanisms of calcium-dependent neurodegeneration in excitotoxicity. *Cell Calcium, 34*(4–5), 325-337. doi: 10.1016/S0143-4160(03)00141-6

Ash, M., Martin, B., Edward, E., Kuo-Chen, C., Matthew S., G., et al. (2009). Steps to the clinic with ELF EMF. *Natural Science, 1*(3), 157-165. doi: 10.4236/ns.2009.13020

Aydin-Abidin, S., Moliadze, V., Eysel, U. T., & Funke, K. (2006). Effects of repetitive TMS on visually evoked potentials and EEG in the anaesthetized cat: dependence on stimulus

frequency and train duration. *The Journal of Physiology, 574*(2), 443-455. doi: 10.1113/jphysiol.2006.108464

Aydin-Abidin, S., Trippe, J., Funke, K., Eysel, U., & Benali, A. (2008). High- and low-frequency repetitive transcranial magnetic stimulation differentially activates c-Fos and zif268 protein expression in the rat brain. *Experimental Brain Research, 188*(2), 249-261. doi: 10.1007/s00221-008-1356-2

Bailey, C. J., Karhu, J., & Ilmoniemi, R. J. (2001). Transcranial magnetic stimulation as a tool for cognitive studies. *Scandinavian Journal of Psychology, 42*(3), 297-306. doi: 10.1111/1467-9450.00239

Baptista, A. F., Goes, B. T., Menezes, D., Gomes, F. C. A., Zugaib, J., et al. (2009). PEMF fails to enhance nerve regeneration after sciatic nerve crush lesion. *Journal of the Peripheral Nervous System, 14*(4), 285-293. doi: 10.1111/j.1529-8027.2009.00240.x

Barbier, E., Veyret, B., & Dufy, B. (1996). Stimulation of Ca2+ influx in rat pituitary cells under exposure to a 50 Hz magnetic field. *Bioelectromagnetics, 17*(4), 303-311. doi: 10.1002/(sici)1521-186x(1996)17:4<303::aid-bem6>3.0.co;2-7

Barker, A. T., Jalinous, R., & Freeston, I. L. (1985). NON-INVASIVE MAGNETIC STIMULATION OF HUMAN MOTOR CORTEX. *The Lancet, 325*(8437), 1106-1107. doi: 10.1016/S0140-6736(85)92413-4

Basham, E., Zhi, Y., & Wentai, L. (2009). Circuit and Coil Design for In-Vitro Magnetic Neural Stimulation Systems. *Biomedical Circuits and Systems, IEEE Transactions on, 3*(5), 321-331. doi: 10.1109/tbcas.2009.2024927

Bates, K. A., Clark, V. W., Meloni, B. P., Dunlop, S. A., & Rodger, J. (2012). Short-term low intensity PMF does not improve functional or histological outcomes in a rat model of transient focal cerebral ischemia. *Brain Research, 1458*(0), 76-85. doi: 10.1016/j.brainres.2012.04.006

Battocletti, J. H., Macias, M. Y., Pintar, F. A., Maiman, D. J., & Sutton, C. H. (2000). A box coil for the stimulation of biological tissue and cells in vitro and in vivo by pulsed magnetic fields. *Biomedical Engineering, IEEE Transactions on, 47*(3), 402-408. doi: 10.1109/10.827309

Beaudoin, G. M. J., Lee, S.-H., Singh, D., Yuan, Y., Ng, Y.-G., et al. (2012). Culturing pyramidal neurons from the early postnatal mouse hippocampus and cortex. *Nature Protocols, 7*(9), 1741 - 1754. doi: 10.1038/nprot.2012.099

Becchetti, A., & Whitaker, M. (1997). Lithium blocks cell cycle transitions in the first cell cycles of sea urchin embryos, an effect rescued by myo-inositol. *Development, 124*(6), 1099-1107.

Benali, A., Trippe, J., Weiler, E., Mix, A., Petrasch-Parwez, E., et al. (2011). Theta-Burst Transcranial Magnetic Stimulation Alters Cortical Inhibition. *The Journal of Neuroscience, 31*(4), 1193-1203. doi: 10.1523/jneurosci.1379-10.2011

Berardelli, A., Inghilleri, M., Rothwell, J. C., Romeo, S., Currà, A., et al. (1998). Facilitation of muscle evoked responses after repetitive cortical stimulation in man. *Experimental Brain Research, 122*(1), 79-84. doi: 10.1007/s002210050493

Berridge, M. J., Lipp, P., & Bootman, M. D. (2000). The versatility and universality of calcium signalling. *Nature Reviews Molecular Cell Biology, 1*, 11-21. doi: 10.1038/35036035

Bijsterbosch, J. D., Barker, A. T., Lee, K.-H., & Woodruff, P. W. R. (2012). Where does transcranial magnetic stimulation (TMS) stimulate? Modelling of induced field maps for some common cortical and cerebellar targets. *Medical & Biological Engineering & Computing, 50*(7), 671-681. doi: 10.1007/s11517-012-0922-8

Binder, D. K., & Scharfman, H. E. (2004). Mini Review: Brain-derived Neurotrophic Factor. *Growth Factors, 22*(3), 123-131. doi: 10.1080/08977190410001723308

Boland, A., Delapierre, D., Mossay, D., Dresse, A., & Seutin, V. (2002). Effect of intermittent and continuous exposure to electromagnetic fields on cultured hippocampal cells. *Bioelectromagnetics, 23*(2), 97-105. doi: 10.1002/bem.102

Bonfanti, L. (2006). PSA-NCAM in mammalian structural plasticity and neurogenesis. *Progress in Neurobiology, 80*(3), 129-164. doi: 10.1016/j.pneurobio.2006.08.003

Bonmassar, G., Lee, S. W., Freeman, D. K., Polasek, M., Fried, S. I., et al. (2012). Microscopic magnetic stimulation of neural tissue. *Nature Communications, 3*(921), 1-10. doi: 10.1038/ncomms1914

Bramham, C. R., & Messaoudi, E. (2005). BDNF function in adult synaptic plasticity: The synaptic consolidation hypothesis. *Progress in Neurobiology, 76*(2), 99-125. doi: 10.1016/j.pneurobio.2005.06.003

Brederode van, J. F. M., Helliesen, M. K., & Hendrickson, A. E. (1991). Distribution of the calcium-binding proteins parvalbumin and calbindin-D28k in the sensorimotor cortex of the rat. *Neuroscience, 44*(1), 157-171. doi: 10.1016/0306-4522(91)90258-P

Bronaugh, E. L. (1995). *Helmholtz coils for calibration of probes and sensors: limits of magnetic field accuracy and uniformity.* Paper presented at the Electromagnetic Compatibility, 1995. Symposium Record., 1995 IEEE International Symposium on.

Bullitt, E. (1990). Expression of C-fos-like protein as a marker for neuronal activity following noxious stimulation in the rat. *The Journal of Comparative Neurology, 296*(4), 517-530. doi: 10.1002/cne.902960402

Butz, M., Wörgötter, F., & van Ooyen, A. (2009). Activity-dependent structural plasticity. *Brain Research Reviews, 60*(2), 287-305. doi: 10.1016/j.brainresrev.2008.12.023

Capone, F., Dileone, M., Profice, P., Pilato, F., Musumeci, G., et al. (2009). Does exposure to extremely low frequency magnetic fields produce functional changes in human brain? *Journal of Neural Transmission, 116*(3), 257-265. doi: 10.1007/s00702-009-0184-2

Carlson, C., & Devinsky, O. (2009). The excitable cerebral cortex: Fritsch G, Hitzig E. Über die elektrische Erregbarkeit des Grosshirns. Arch Anat Physiol Wissen 1870;37:300–32. *Epilepsy & Behavior, 15*(2), 131-132. doi: 10.1016/j.yebeh.2009.03.002

Carmichael, S. T. (2006). Cellular and molecular mechanisms of neural repair after stroke: Making waves. *Annals of Neurology, 59*(5), 735-742. doi: 10.1002/ana.20845

Carter, A. R., Chen, C., Schwartz, P. M., & Segal, R. A. (2002). Brain-Derived Neurotrophic Factor Modulates Cerebellar Plasticity and Synaptic Ultrastructure. *The Journal of Neuroscience, 22*(4), 1316-1327. doi: 0270-6474/02/221316-12

Celio, M. R. (1990). Calbindin D-28k and parvalbumin in the rat nervous system. *Neuroscience, 35*(2), 375-475. doi: 10.1016/0306-4522(90)90091-H

Chan, C. Y., & Nicholson, C. (1986). Modulation by applied electric fields of Purkinje and stellate cell activity in the isolated turtle cerebellum. *The Journal of Physiology, 371*(1), 89-114.

Chard, P. S., Bleakman, D., Christakos, S., Fullmer, C. S., & Miller, R. J. (1993). Calcium buffering properties of calbindin D28k and parvalbumin in rat sensory neurones. *The Journal of Physiology, 472*(1), 341-357.

Chedotal, A., Bloch-Gallego, E., & Sotelo, C. (1997). The embryonic cerebellum contains topographic cues that guide developing inferior olivary axons. *Development, 124*(4), 861-870.

Cho, S. I., Nam, Y. S., Chu, L. Y., Lee, J. H., Bang, J. S., et al. (2012). Extremely low-frequency magnetic fields modulate nitric oxide signaling in rat brain. *Bioelectromagnetics, 33*(7), 576-584. doi: 10.1002/bem.21715586-574

Chomczynski, P., & Sacchi, N. (1987). Single-step method of RNA isolation by acid guanidinium thiocyanate-phenol-chloroform extraction. *Analytical Biochemistry, 162*(1), 156-159. doi: 10.1016/0003-2697(87)90021-2

Chu, L. Y., Lee, J. H., Nam, Y. S., Lee, Y. J., Park, W.-H., et al. (2011). Extremely low frequency magnetic field induces oxidative stress in mouse cerebellum. *General Physiology and Biophysics, 30*(4), 415-421. doi: 10.4149/gpb_2011_04_415

Ciampi de Andrade, D., Mhalla, A., Adam, F., Texeira, M. J., & Bouhassira, D. (2014). Repetitive transcranial magnetic stimulation induced analgesia depends on N-methyl-d-aspartate glutamate receptors. *Pain, 155*(3), 598-605. doi: 10.1016/j.pain.2013.12.022

Cohen, L. G., Roth, B., Nilsson, J., Nguyet, D., Panizza, M., et al. (1990). Effects of coil design on delivery of focal magnetic stimulation. Technical considerations. *Electroencephalography and clinical Neurophysiology, 75*, 50-357.

Connors, B. W., & Long, M. A. (2004). ELECTRICAL SYNAPSES IN THE MAMMALIAN BRAIN. *Annual Review of Neuroscience, 27*(1), 393-418. doi: 10.1146/annurev.neuro.26.041002.131128

Cook, C. M., Thomas, A. W., & Prato, F. S. (2004). Resting EEG is affected by exposure to a pulsed ELF magnetic field. *Bioelectromagnetics, 25*(3), 196-203. doi: 10.1002/bem.10188

Cracco, R. Q., Cracco, J. B., Maccabee, P. J., & Amassian, V. E. (1999). Cerebral function revealed by transcranial magnetic stimulation. *Journal of Neuroscience Methods, 86*(2), 209-219. doi: 10.1016/S0165-0270(98)00167-8

Cunha, C., Brambilla, R., & Thomas, K. L. (2010). A simple role for BDNF in learning and memory? *Frontiers in Molecular Neuroscience, 3*(1), 1-14. doi: 10.3389/neuro.02.001.2010

Cuypers, K., Thijs, H., & Meesen, R. L. J. (2014). Optimization of the Transcranial Magnetic Stimulation Protocol by Defining a Reliable Estimate for Corticospinal Excitability. *PLoS ONE, 9*(1), e86380. doi: 10.1371/journal.pone.0086380

Daskalakis, Z. J. (2014). Theta-burst transcranial magnetic stimulation in depression: when less may be more. *Brain, In press*. doi: 10.1093/brain/awu123

De Crescenzo, V., Fogarty, K. E., ZhuGe, R., Tuft, R. A., Lifshitz, L. M., et al. (2006). Dihydropyridine Receptors and Type 1 Ryanodine Receptors Constitute the Molecular Machinery for Voltage-Induced Ca2+ Release in Nerve Terminals. *The Journal of Neuroscience, 26*(29), 7565-7574. doi: 10.1523/jneurosci.1512-06.2006

De Pedro, J. A., Pérez-Caballer, A. J., Dominguez, J., Collía, F., Blanco, J., et al. (2005). Pulsed electromagnetic fields induce peripheral nerve regeneration and endplate enzymatic changes. *Bioelectromagnetics, 26*(1), 20-27. doi: 10.1002/bem.20049

De Zeeuw, C. I., Chorev, E., Devor, A., Manor, Y., Van Der Giessen, R. S., et al. (2003). Deformation of Network Connectivity in the Inferior Olive of Connexin 36-Deficient Mice Is Compensated by Morphological and Electrophysiological Changes at the Single Neuron Level. *The Journal of Neuroscience, 23*(11), 4700-4711. doi: 0270-6474/03/234700-12

De Zeeuw, C. I., Hoebeek, F. E., & Schonewille, M. (2008). Causes and Consequences of Oscillations in the Cerebellar Cortex. *Neuron, 58*(5), 655-658. doi: 10.1016/j.neuron.2008.05.019

De Zeeuw, C. I., Hoogenraad, C. C., Koekkoek, S. K. E., Ruigrok, T. J. H., Galjart, N., et al. (1998). Microcircuitry and function of the inferior olive. *Trends in Neurosciences, 21*(9), 391-400. doi: 10.1016/S0166-2236(98)01310-1

DeFelipe, J. (1997). Types of neurons, synaptic connections and chemical characteristics of cells immunoreactive for calbindin-D28K, parvalbumin and calretinin in the neocortex. *Journal of chemical neuroanatomy, 14*(1), 1-19. doi: 10.1016/S0891-0618(97)10013-8

Deng, Z.-D., Lisanby, S. H., & Peterchev, A. V. (2013). Electric field depth–focality tradeoff in transcranial magnetic stimulation: Simulation comparison of 50 coil designs. *Brain Stimulation, 6*(1), 1-13. doi: 10.1016/j.brs.2012.02.005

Devor, A., & Yarom, Y. (2002). Generation and Propagation of Subthreshold Waves in a Network of Inferior Olivary Neurons. *Journal of Neurophysiology, 87*(6), 3059-3069. doi: 10.1152/jn.00736.2001

Di Lazzaro, V., Capone, F., Apollonio, F., Borea, P. A., Cadossi, R., et al. (2013). A Consensus Panel Review of Central Nervous System Effects of the Exposure to Low-Intensity

Extremely Low-Frequency Magnetic Fields. *Brain Stimulation, 6*(4), 469-476. doi: 10.1016/j.brs.2013.01.004

Di Lazzaro, V., Oliviero, A., Pilato, F., Mazzone, P., Insola, A., et al. (2003). Corticospinal volleys evoked by transcranial stimulation of the brain in conscious humans. *Neurological Research, 25*, 143-150. doi: 10.1179/016164103101201292

Di Lazzaro, V., Oliviero, A., Pilato, F., Saturno, E., Dileone, M., et al. (2004). The physiological basis of transcranial motor cortex stimulation in conscious humans. *Clinical Neurophysiology, 115*(2), 255-266. doi: 10.1016/j.clinph.2003.10.009

Di Loreto, S., Falone, S., Caracciolo, V., Sebastiani, P., D'Alessandro, A., et al. (2009). Fifty hertz extremely low-frequency magnetic field exposure elicits redox and trophic response in rat-cortical neurons. *Journal of Cellular Physiology, 219*(2), 334-343. doi: 10.1002/jcp.21674

Dixon, K. J., Hilber, W., Speare, S., Willson, M. L., Bower, A. J., et al. (2005). Post-lesion transcommissural olivocerebellar reinnervation improves motor function following unilateral pedunculotomy in the neonatal rat. *Experimental Neurology, 196*(2), 254-265. doi: 10.1016/j.expneurol.2005.07.018

Dixon, K. J., & Sherrard, R. M. (2006). Brain-derived neurotrophic factor induces post-lesion transcommissural growth of olivary axons that develop normal climbing fibers on mature Purkinje cells. *Experimental Neurology, 202*(1), 44-56. doi: 10.1016/j.expneurol.2006.05.010

Dmochowski, J. P., Bikson, M., Datta, A., Richardson, J., Fridriksson, J., et al. (2012,). *On the role of electric field orientation in optimal design of transcranial current stimulation.* Paper presented at the Engineering in Medicine and Biology Society (EMBC), 2012 Annual International Conference of the IEEE.

Dusart, I., Ghoumari, A., Wehrle, R., Morel, M. P., Bouslama-Oueghlani, L., et al. (2005). Cell death and axon regeneration of Purkinje cells after axotomy: Challenges of classical hypotheses of axon regeneration. *Brain Research Reviews, 49*(2), 300-316. doi: 10.1016/j.brainresrev.2004.11.007

Dusart, I., Morel, M. P., Wehrlé, R., & Sotelo, C. (1999). Late axonal sprouting of injured Purkinje cells and its temporal correlation with permissive changes in the glial scar. *The Journal of Comparative Neurology, 408*(3), 399-418. doi: 10.1002/(sici)1096-9861(19990607)408:3<399::aid-cne7>3.0.co;2-2

Eccles, J. C., Ilinas, R., & Sasaki, K. (1966). The excitatory synaptic action of climbing fibres on the Purkinje cells of the cerebellum. *The Journal of Physiology, 182*, 268-296.

Eilers, J., Augustine, G. J., & Konnerth, A. (1995). Subthreshold synaptic Ca2+ signalling in fine dendrites and spines of cerebellar Purkinje neurons. *Nature, 373*(155-158). doi: 10.1038/373155a0

El Maarouf, A., Petridis, A. K., & Rutishauser, U. (2006). Use of polysialic acid in repair of the central nervous system. *Proceedings of the National Academy of Sciences, 103*(45), 16989-16994. doi: 10.1073/pnas.0608036103

Esser, S. K., Hill, S. L., & Tononi, G. (2005). Modeling the Effects of Transcranial Magnetic Stimulation on Cortical Circuits. *Journal of Neurophysiology, 94*(1), 622-639. doi: 10.1152/jn.01230.2004

Fatemi-Ardekani, A. (2008). Transcranial Magnetic Stimulation: Physics, Electrophysiology, and Applications. *Critical Reviews in Biomedical Engineering, 36*(5-6), 375-412. doi: 10.1615/CritRevBiomedEng.v36.i5-6.30

Fitzgerald, J., & Fawcett, J. (2007). Repair in the central nervous system. *Journal of Bone & Joint Surgery, British Volume, 89-B*(11), 1413-1420. doi: 10.1302/0301-620x.89b11.19651

Fitzgerald, P. B., Fountain, S., & Daskalakis, Z. J. (2006). A comprehensive review of the effects of rTMS on motor cortical excitability and inhibition. *Clinical Neurophysiology, 117*(12), 2584-2596. doi: 10.1016/j.clinph.2006.06.712

Fleischmann, A., Hvalby, O., Jensen, V., Strekalova, T., Zacher, C., et al. (2003). Impaired Long-Term Memory and NR2A-Type NMDA Receptor-Dependent Synaptic Plasticity in Mice Lacking c-Fos in the CNS. *The Journal of Neuroscience, 23*(27), 9116-9122. doi: 0270-6474/03/239116-07

Foskett, J. K., White, C., Cheung, K.-H., & Mak, D.-O. D. (2007). Inositol Trisphosphate Receptor Ca2+ Release Channels. *Physiological Reviews, 87*(2), 593-658. doi: 10.1152/physrev.00035.2006

Fournier, B., Lohof, A. M., Bower, A. J., Mariani, J., & Sherrard, R. M. (2005). Developmental modifications of olivocerebellar topography: The granuloprival cerebellum reveals multiple routes from the inferior olive. *The Journal of Comparative Neurology, 490*(1), 85-97. doi: 10.1002/cne.20648

Frahm, J., Mattsson, M.-O., & Simkó, M. (2010). Exposure to ELF magnetic fields modulate redox related protein expression in mouse macrophages. *Toxicology Letters, 192*(3), 330-336. doi: 10.1016/j.toxlet.2009.11.010

Freedman, N. J., Liggett, S. B., Drachman, D. E., Pei, G., Caron, M. G., et al. (1995). Phosphorylation and Desensitization of the Human β1-Adrenergic Receptor. *Journal of Biological Chemistry, 270*(30), 17953-17961. doi: 10.1074/jbc.270.30.17953

Fung, P. K., & Robinson, P. A. (2013). Neural field theory of calcium dependent plasticity with applications to transcranial magnetic stimulation. *Journal of Theoretical Biology, 324*(0), 72-83. doi: 10.1016/j.jtbi.2013.01.013

Funke, K., & Benali, A. (2011). Modulation of cortical inhibition by rTMS – findings obtained from animal models. *The Journal of Physiology, 589*(18), 4423-4435. doi: 10.1113/jphysiol.2011.206573

Furuichi, T., Shiota, C., & Mikoshiba, K. (1990). Distribution of inositol 1,4,5-trisphosphate receptor mRNA in mouse tissues. *FEBS Letters, 267*(1), 85-88. doi: 10.1016/0014-5793(90)80294-S

Galvani, L. (1791). De viribus electricitatis in mot u musculari.

Gamboa, O. L., Antal, A., Laczo, B., Moliadze, V., Nitsche, M. A., et al. (2011). Impact of repetitive theta burst stimulation on motor cortex excitability. *Brain Stimulation, 4*(3), 145-151. doi: 10.1016/j.brs.2010.09.008

Gamboa, O. L., Antal, A., Moliadze, V., & Paulus, W. (2010). Simply longer is not better: reversal of theta burst after-effect with prolonged stimulation. *Experimental Brain Research, 204*(2), 181-187. doi: 10.1007/s00221-010-2293-4

Gao, F., Wang, S., Guo, Y., Wang, J., Lou, M., et al. (2010). Protective effects of repetitive transcranial magnetic stimulation in a rat model of transient cerebral ischaemia: a microPET study. *European Journal of Nuclear Medicine and Molecular Imaging, 37*(5), 954-961. doi: 10.1007/s00259-009-1342-3

Gascon, E., Vutskits, L., Jenny, B., Durbec, P., & Kiss, J. Z. (2007). PSA-NCAM in postnatally generated immature neurons of the olfactory bulb: a crucial role in regulating p75 expression and cell survival. *Development, 134*(6), 1181-1190. doi: 10.1242/dev.02808

Gaujoux, R., & Seoighe, C. (2010). A flexible R package for nonnegative matrix factorization. *BMC Bioinformatics, 11*(1), 367. doi: 10.1186/1471-2105-11-367

George, M. S., Taylor, J. J., & Short, E. B. (2013). The expanding evidence base for rTMS treatment of depression. *Current Opinion in Psychiatry, 26* (1), 13-18.

Gerschlager, W., Christensen, L. O. D., Bestmann, S., & Rothwell, J. C. (2002). rTMS over the cerebellum can increase corticospinal excitability through a spinal mechanism involving activation of peripheral nerve fibres. *Clinical Neurophysiology, 113*(9), 1435-1440. doi: 10.1016/S1388-2457(02)00156-6

Gerschlager, W., Siebner, H. R., & Rothwell, J. C. (2001). Decreased corticospinal excitability after subthreshold 1 Hz rTMS over lateral premotor cortex. *Neurology, 57*(3), 449-455. doi: 10.1016/S1053-8119(01)92490-5

Gersner, R., Kravetz, E., Feil, J., Pell, G., & Zangen, A. (2011). Long-Term Effects of Repetitive Transcranial Magnetic Stimulation on Markers for Neuroplasticity: Differential Outcomes in Anesthetized and Awake Animals. *The Journal of Neuroscience, 31*(20), 7521-7526. doi: 10.1523/jneurosci.6751-10.2011

Gilabert, J. A. (2012). Cytoplasmic Calcium Buffering. In M. S. Islam (Ed.), *Calcium Signaling*. London: Springer

Ginty, D. D., Bonni, A., & Greenberg, M. E. (1994). Nerve growth factor activates a Ras-dependent protein kinase that stimulates c-fos transcription via phosphorylation of CREB. *Cell, 77*(5), 713 - 725. doi: 10.1016/0092-8674(94)90055-8

Goetz, S., Helling, F., & Weyh, T. (2013a). P 232. Leaving the beaten track of TMS waveform restrictions: Concepts and prototype for a 'convertible' stimulator that can generate almost every type of existing and future waveform. *Clinical Neurophysiology, 124*(10), e177. doi: 10.1016/j.clinph.2013.04.309

Goetz, S., Pfaeffl, M., Huber, J., Singer, M., Marquardt, R., et al. (2012, Aug. 28 2012-Sept. 1 2012). *Circuit topology and control principle for a first magnetic stimulator with fully controllable waveform.* Paper presented at the Engineering in Medicine and Biology Society (EMBC), 2012 Annual International Conference of the IEEE.

Goetz, S., Truong, C. N., Gerhofer, M. G., Peterchev, A. V., Herzog, H.-G., et al. (2013b). Analysis and Optimization of Pulse Dynamics for Magnetic Stimulation. *PLoS ONE, 8*(3), e55771. doi: 10.1371/journal.pone.0055771

Grassi, C., D'Ascenzo, M., Torsello, A., Martinotti, G., Wolf, F., et al. (2004). Effects of 50 Hz electromagnetic fields on voltage-gated Ca2+ channels and their role in modulation of neuroendocrine cell proliferation and death. *Cell Calcium, 35*(4), 307-315. doi: 10.1016/j.ceca.2003.09.001

Grehl, S., Viola, H. M., Fuller-Carter, P. I., Carter, K. W., Dunlop, S. A., et al. (2015). Cellular and Molecular Changes to Cortical Neurons Following Low Intensity Repetitive Magnetic Stimulation at Different Frequencies. *Brain Stimulation, 8*(1), 114-123. doi: 10.1016/j.brs.2014.09.012

Gunay, I., & Mert, T. (2011). Pulsed magnetic fields enhance the rate of recovery of damaged nerve excitability. *Bioelectromagnetics, 32*(3), 200-208. doi: 10.1002/bem.20629

Gutierrez, H., & Davies, A. M. (2007). A fast and accurate procedure for deriving the Sholl profile in quantitative studies of neuronal morphology. *Journal of Neuroscience Methods, 163*(1), 24-30. doi: 10.1016/j.jneumeth.2007.02.002

Hallett, M. (2007). Transcranial Magnetic Stimulation: A Primer. *Neuron, 55*(2), 187-199. doi: DOI: 10.1016/j.neuron.2007.06.026

Halliwell, B., & Whiteman, M. (2004). Measuring reactive species and oxidative damage in vivo and in cell culture: how should you do it and what do the results mean? *British Journal of Pharmacology, 142*(2), 231-255. doi: 10.1038/sj.bjp.0705776

Han, B. H., Chun, I. K., Lee, S. C., & Lee, S. Y. (2004). Multichannel magnetic stimulation system design considering mutual couplings among the stimulation coils. *Biomedical Engineering, IEEE Transactions on, 51*(5), 812-817. doi: 10.1109/tbme.2004.824123

Harvey, A. R., Ooi, J. W. W., & Rodger, J. (2012). Chapter One - Neurotrophic Factors and the Regeneration of Adult Retinal Ganglion Cell Axons. In L. G. Jeffrey & F. T. Ephraim (Eds.), *International Review of Neurobiology* (Vol. Volume 106, pp. 1-33): Academic Press.

Hatten, M. E. (1985). Neuronal regulation of astroglial morphology and proliferation in vitro. *The Journal of Cell Biology, 100*(2), 384-396. doi: 10.1083/jcb.100.2.384

Hattori, T., Takei, N., Mizuno, Y., Kato, K., & Kohsaka, S. (1995). Neurotrophic and neuroprotective effects of neuron-specific enolase on cultured neurons from embryonic rat brain. *Neuroscience Research, 21*(3), 191-198. doi: 10.1016/0168-0102(94)00849-B

Hausmann, A., Marksteiner, J., Hinterhuber, H., & Humpel, C. (2001). Magnetic stimulation induces neuronal c-fos via tetrodotoxin-sensitive sodium channels in organotypic cortex brain slices of the rat. *Neuroscience Letters, 310*(2–3), 105-108. doi: 10.1016/S0304-3940(01)02073-0

Hausmann, A., Weis, C., Marksteiner, J., Hinterhuber, H., & Humpel, C. (2000). Chronic repetitive transcranial magnetic stimulation enhances c-fos in the parietal cortex and hippocampus. *Molecular Brain Research, 76*(2), 355-362. doi: 10.1016/S0169-328X(00)00024-3

Havel, W. J., Nyenhuis, J. A., Bourland, J. D., Foster, K. S., Geddes, L. A., et al. (1997). Comparison of rectangular and damped sinusoidal dB/dt waveforms in magnetic stimulation. *Magnetics, IEEE Transactions on, 33*(5), 4269-4271. doi: 10.1109/20.619732

He, Y.-L., Liu, D.-D., Fang, Y.-J., Zhan, X.-Q., Yao, J.-J., et al. (2013). Exposure to Extremely Low-Frequency Electromagnetic Fields Modulates Na+ Currents in Rat Cerebellar Granule Cells through Increase of AA/PGE2 and EP Receptor-Mediated cAMP/PKA Pathway. *PLoS ONE, 8*(1), e54376. doi: 10.1371/journal.pone.0054376

Hellmann, J., Jüttner, R., Roth, C., Bajbouj, M., Kirste, I., et al. (2012). Repetitive magnetic stimulation of human-derived neuron-like cells activates cAMP-CREB pathway. *European Archives of Psychiatry and Clinical Neuroscience, 262*(1), 87-91. doi: 10.1007/s00406-011-0217-3

Hellström, M., & Harvey, A. R. (2014). Cyclic AMP and the regeneration of retinal ganglion cell axons. *The International Journal of Biochemistry & Cell Biology, In Press, Corrected Proof* doi: 10.1016/j.biocel.2014.04.018

Helmchen, F., Borst, J. G., & Sakmann, B. (1997). Calcium dynamics associated with a single action potential in a CNS presynaptic terminal. *Biophysical Journal, 72*(3), 1458-1471. doi: 10.1016/S0006-3495(97)78792-7

Hernández-Hernández, H., Cruces-Solis, H., Elías-Viñas, D., & Verdugo-Díaz, L. (2009). Neurite Outgrowth on Chromaffin Cells Applying Extremely Low Frequency Magnetic Fields by Permanent Magnets. *Archives of Medical Research, 40*(7), 545-550. doi: 10.1016/j.arcmed.2009.10.002

Herrera, D. G., & Robertson, H. A. (1996). Activation of c-fos in the brain. *Progress in Neurobiology, 50*(2–3), 83-107. doi: 10.1016/S0301-0082(96)00021-4

Hioki, H., Fujiyama, F., Taki, K., Tomioka, R., Furuta, T., et al. (2003). Differential distribution of vesicular glutamate transporters in the rat cerebellar cortex. *Neuroscience, 117*(1), 1-6. doi: 10.1016/S0306-4522(02)00943-0

Hodgkin, A. L., & Huxley, A. F. (1952). A quantitative description of membrane current and its application to conduction and excitation in nerve. *The Journal of Physiology, 117*(4), 500-544.

Hogan, M. V., & Wieraszko, A. (2004). An increase in cAMP concentration in mouse hippocampal slices exposed to low-frequency and pulsed magnetic fields. *Neuroscience Letters, 366*(1), 43-47. doi: 10.1016/j.neulet.2004.05.006

Hoogendam, J. M., Ramakers, G. M. J., & Di Lazzaro, V. (2010). Physiology of repetitive transcranial magnetic stimulation of the human brain. *Brain Stimulation, 3*(2), 95-118. doi: 10.1016/j.brs.2009.10.005

Hoppenrath, K., & Funke, K. (2013). Time-course of changes in neuronal activity markers following iTBS-TMS of the rat neocortex. *Neuroscience Letters, 536*(0), 19-23. doi: 10.1016/j.neulet.2013.01.003

Horner, P. J., & Gage, F. H. (2000). Regenerating the damaged central nervous system. *Nature, 407*(6807), 963-970. doi: 10.1038/35039559

Hsu, K.-H., Nagarajan, S. S., & Durand, D. M. (2003). Analysis of efficiency of magnetic stimulation. *Biomedical Engineering, IEEE Transactions on, 50*(11), 1276-1285. doi: 10.1109/tbme.2003.818473

Huang, J., Ye, Z., Hu, X., Lu, L., & Luo, Z. (2010). Electrical stimulation induces calcium-dependent release of NGF from cultured Schwann cells. *Glia, 58*(5), 622-631. doi: 10.1002/glia.20951

Huang, Y.-Z., Edwards, M. J., Rounis, E., Bhatia, K. P., & Rothwell, J. C. (2005). Theta Burst Stimulation of the Human Motor Cortex. *Neuron, 45*(2), 201-206. doi: 10.1016/j.neuron.2004.12.033

Huang, Y.-Z., & Rothwell, J. C. (2004). The effect of short-duration bursts of high-frequency, low-intensity transcranial magnetic stimulation on the human motor cortex. *Clinical Neurophysiology, 115*(5), 1069-1075. doi: 10.1016/j.clinph.2003.12.026

Huerta, P., & Volpe, B. (2009). Transcranial magnetic stimulation, synaptic plasticity and network oscillations. *Journal of NeuroEngineering and Rehabilitation, 6*(1), 7. doi: 10.1186/1743-0003-6-7

Hulme, S. R., Jones, O. D., Ireland, D. R., & Abraham, W. C. (2012). Calcium-Dependent But Action Potential-Independent BCM-Like Metaplasticity in the Hippocampus. *The Journal of Neuroscience, 32*(20), 6785-6794. doi: 10.1523/jneurosci.0634-12.2012

Hulot, G., Finlay, C. C., Constable, C. G., Olsen, N., & Mandea, M. (2010). The Magnetic Field of Planet Earth. *Space Science Reviews, 152*(1-4), 159-222. doi: 10.1007/s11214-010-9644-0

Ikeda, T., Kurosawa, M., Uchikawa, C., Kitayama, S., & Nukina, N. (2005). Modulation of monoamine transporter expression and function by repetitive transcranial magnetic stimulation. *Biochemical and Biophysical Research Communications, 327*(1), 218-224. doi: 10.1016/j.bbrc.2004.12.009

Jackson, J. D. (1962). *Classical Electrodynamics*. New York: Wiley.

Jessen, K. R., & Mirsky, R. (1980). Glial cells in the enteric nervous system contain glial fibrillary acidic protein. *Nature, 286*(5774), 736 - 737. doi: 10.1038/286736a0

Joucla, S., & Yvert, B. (2012). Modeling extracellular electrical neural stimulation: From basic understanding to MEA-based applications. *Journal of Physiology-Paris, 106*(3–4), 146-158. doi: 10.1016/j.jphysparis.2011.10.003

Juszczak, K., Kaszuba-Zwoinska, J., & Thor, P. J. (2012). Pulsating electromagnetic field stimulation of urothelial cells induces apoptosis and diminishes necrosis: new insight to magnetic therapy in urology. *J Physiol Pharmacol, 63*(4), 397-401.

Kammer, T., Beck, S., Thielscher, A., Laubis-Herrmann, U., & Topka, H. (2001). Motor thresholds in humans: a transcranial magnetic stimulation study comparing different pulse waveforms, current directions and stimulator types. *Clinical Neurophysiology, 112*(2), 250-258. doi: 10.1016/S1388-2457(00)00513-7

Kaszuba-Zwoinska J, Wojcik K, B. M., Ziomber A, Pierzchalski P, Rokita E, et al. (2010). Pulsating electromagnetic field stimulation prevents cell death of puromycin treated U937 cell line. *Journal of Physiology and Pharmacology, 61*(2), 201-205.

Kim, W.-S., Jung, S. H., Oh, M. K., Min, Y. S., Lim, J. Y., et al. (2014). Effect of repetitive transcranial magnetic stimulation over the cerebellum on patients with ataxia after posterior circulation stroke: A pilot study. *Journal of Rehabilitation Medicine, 45*(5), 418-423. doi: 10.2340/16501977-1802

Kioussi, C., & Gruss, P. (1994). Differential induction of Pax genes by NGF and BDNF in cerebellar primary cultures. *The Journal of Cell Biology, 125*(2), 417-425. doi: 10.1083/jcb.125.2.417

Kleim, J. A. (2011). Neural plasticity and neurorehabilitation: Teaching the new brain old tricks. *Journal of Communication Disorders, 44*(5), 521-528. doi: 10.1016/j.jcomdis.2011.04.006

Knapska, E., & Kaczmarek, L. (2004). A gene for neuronal plasticity in the mammalian brain: Zif268/Egr-1/NGFI-A/Krox-24/TIS8/ZENK? *Progress in Neurobiology, 74*(4), 183 - 211. doi: 10.1016/j.pneurobio.2004.05.007

Koch, G. (2010). Repetitive transcranial magnetic stimulation: a tool for human cerebellar plasticity. *Functional Neurology, 25*(3), 159-163.

Koch, G., Mori, F., Marconi, B., Codecà, C., Pecchioli, C., et al. (2008). Changes in intracortical circuits of the human motor cortex following theta burst stimulation of the lateral cerebellum. *Clinical Neurophysiology, 119*(11), 2559-2569. doi: 10.1016/j.clinph.2008.08.008

Komuro, Y., Fahrion, J., Foote, K., Fenner, K., Kumada, T., et al. (2013). Granule Cell Migration and Differentiation. In M. Manto, J. Schmahmann, F. Rossi, D. Gruol & N. Koibuchi (Eds.), *Handbook of the Cerebellum and Cerebellar Disorders* (pp. 107-125): Springer Netherlands.

Kornhauser, J. M., Cowan, C. W., Shaywitz, A. J., Dolmetsch, R. E., Griffith, E. C., et al. (2002). CREB Transcriptional Activity in Neurons Is Regulated by Multiple, Calcium-Specific Phosphorylation Events. *Neuron, 34*(2), 221-233. doi: 10.1016/S0896-6273(02)00655-4

Kullmann, D. M., & Lamsa, K. (2008). Roles of distinct glutamate receptors in induction of anti-Hebbian long-term potentiation. *The Journal of Physiology, 586*(6), 1481-1486. doi: 10.1113/jphysiol.2007.148064

Labedi, A., Benali, A., Mix, A., Neubacher, U., & Funke, K. (2014). Modulation of Inhibitory Activity Markers by Intermittent Theta-burst Stimulation in Rat Cortex is NMDA-receptor Dependent. *Brain Stimulation, 7*(3), 394-400. doi: 10.1016/j.brs.2014.02.010

Lang, N., Harms, J., Weyh, T., Lemon, R. N., Paulus, W., et al. (2006). Stimulus intensity and coil characteristics influence the efficacy of rTMS to suppress cortical excitability. *Clinical Neurophysiology, 117*(10), 2292-2301. doi: 10.1016/j.clinph.2006.05.030

Lee, S. W., Oh, B.-M., Kim, S., & Paik, N.-J. (2014). The molecular evidence of neural plasticity induced by cerebellar repetitive transcranial magnetic stimulation in the rat brain: a preliminary report. *Neuroscience Letters, 575*, 47-52. doi: 10.1016/j.neulet.2014.05.029

Lee, Y.-S., Lin, C.-Y., Robertson, R. T., Hsiao, I., & Lin, V. W. (2004). Motor Recovery and Anatomical Evidence of Axonal Regrowth in Spinal Cord-Repaired Adult Rats. *Journal of Neuropathology & Experimental Neurology, 63*(3), 233-245.

Letellier, M., Bailly, Y., Demais, V., Sherrard, R. M., Mariani, J., et al. (2007). Reinnervation of Late Postnatal Purkinje Cells by Climbing Fibers: Neosynaptogenesis without Transient Multi-Innervation. *The Journal of Neuroscience, 27*(20), 5373-5383. doi: 10.1523/jneurosci.0452-07.2007

Letellier, M., Wehrlé, R., Mariani, J., & Lohof, A. M. (2009). Synapse elimination in olivo-cerebellar explants occurs during a critical period and leaves an indelible trace in Purkinje cells. *Proceedings of the National Academy of Sciences, 106*(33), 14102-14107. doi: 10.1073/pnas.0902820106

Lezoualc'h, F., Engert, S., Berning, B., & Behl, C. (2000). Corticotropin-Releasing Hormone-Mediated Neuroprotection against Oxidative Stress Is Associated with the Increased Release of Non-amyloidogenic Amyloid β Precursor Protein and with the Suppression of Nuclear Factor-κB. *Molecular Endocrinology, 14*(1), 147-159. doi: 10.1210/me.14.1.147

Li, C.-T., Chen, M.-H., Juan, C.-H., Huang, H.-H., Chen, L.-F., et al. (2014). Efficacy of prefrontal theta-burst stimulation in refractory depression: a randomized sham-controlled study. *Brain, 137*(7), 2088-2098. doi: 10.1093/brain/awu109

Li, S., Liu, B. P., Budel, S., Li, M., Ji, B., et al. (2004). Blockade of Nogo-66, Myelin-Associated Glycoprotein, and Oligodendrocyte Myelin Glycoprotein by Soluble Nogo-66 Receptor Promotes Axonal Sprouting and Recovery after Spinal Injury. *The Journal of Neuroscience, 24*(46), 10511-10520. doi: 10.1523/jneurosci.2828-04.2004

Liao, C. W., & Lien, C. C. (2009). Estimating intracellular Ca2+ concentrations and buffering in a dendritic inhibitory hippocampal interneuron. *Neuroscience, 164*(4), 1701-1711. doi: 10.1016/j.neuroscience.2009.09.052

Livak, K. J., & Schmittgen, T. D. (2001). Analysis of Relative Gene Expression Data Using Real-Time Quantitative PCR and the 2−ΔΔCT Method. *Methods, 25*(4), 402-408. doi: 10.1006/meth.2001.1262

Lohof, A. M., Mariani, J., & Sherrard, R. M. (2005). Afferent–target interactions during olivocerebellar development: transcommissural reinnervation indicates interdependence of Purkinje cell maturation and climbing fibre synapse elimination. *European Journal of Neuroscience, 22*(11), 2681-2688. doi: 10.1111/j.1460-9568.2005.04493.x

Lu, B., Nagappan, G., Guan, X., Nathan, P. J., & Wren, P. (2013). BDNF-based synaptic repair as a disease-modifying strategy for neurodegenerative diseases. *Nature Reviews Neuroscience, 14*(6), 401-416. doi: 10.1038/nrn3505

Ma, J., Zhang, Z., Su, Y., Kang, L., Geng, D., et al. (2013). Magnetic stimulation modulates structural synaptic plasticity and regulates BDNF–TrkB signal pathway in cultured hippocampal neurons. *Neurochemistry International, 62*(1), 84-91. doi: 10.1016/j.neuint.2012.11.010

Maccabee, P. J., Nagarajan, S. S., Amassian, V. E., Durand, D. M., Szabo, A. Z., et al. (1998). Influence of pulse sequence, polarity and amplitude on magnetic stimulation of human and porcine peripheral nerve. *The Journal of Physiology, 513*(2), 571-585. doi: 10.1111/j.1469-7793.1998.571bb.x

Majewska, A. K., Newton, J. R., & Sur, M. (2006). Remodeling of Synaptic Structure in Sensory Cortical Areas In Vivo. *The Journal of Neuroscience, 26*(11), 3021-3029. doi: 10.1523/jneurosci.4454-05.2006

Makowiecki, K., Harvey, A. R., Sherrard, R. M., & Rodger, J. (2014). Low-Intensity Repetitive Transcranial Magnetic Stimulation Improves Abnormal Visual Cortical Circuit Topography and Upregulates BDNF in Mice. *The Journal of Neuroscience, 34*(32), 10780-10792. doi: 10.1523/jneurosci.0723-14.2014

Malik, A. R., Urbanska, M., Gozdz, A., Swiech, L. J., Nagalski, A., et al. (2013). Cyr61, a Matricellular Protein, Is Needed for Dendritic Arborization of Hippocampal Neurons. *Journal of Biological Chemistry, 288*(12), 8544-8559. doi: 10.1074/jbc.M112.411629

Markov, M. S. (2007). Expanding Use of Pulsed Electromagnetic Field Therapies. *Electromagnetic Biology and Medicine, 26*(3), 257-274. doi: 10.1080/15368370701580806

Martiny, K., Lunde, M., & Bech, P. (2010). Transcranial Low Voltage Pulsed Electromagnetic Fields in Patients with Treatment-Resistant Depression. *Biological Psychiatry, 68*(2), 163-169. doi: 10.1016/j.biopsych.2010.02.017

Mathy, A., Clark, B. A., & Häusser, M. (2014). Synaptically Induced Long-Term Modulation of Electrical Coupling in the Inferior Olive. *Neuron, 81*(6), 1290-1296. doi: 10.1016/j.neuron.2014.01.005

Mattsson, M.-O., & Simkó, M. (2012). Is there a relation between extremely low frequency magnetic field exposure, inflammation and neurodegenerative diseases? A review of in vivo and in vitro experimental evidence. *Toxicology, 301*(1–3), 1-12. doi: 10.1016/j.tox.2012.06.011

Mayanil, C. S. K., George, D., Freilich, L., Miljan, E. J., Mania-Farnell, B., et al. (2001). Microarray Analysis Detects Novel Pax3 Downstream Target Genes. *Journal of Biological Chemistry, 276*(52), 49299-49309. doi: 10.1074/jbc.M107933200

Mayanil, C. S. K., George, D., Mania-Farnell, B., Bremer, C. L., McLone, D. G., et al. (2000). Overexpression of Murine Pax3 Increases NCAM Polysialylation in a Human Medulloblastoma Cell Line. *Journal of Biological Chemistry, 275*(30), 23259-23266.

McAllister, S. M., Rothwell, J. C., & Ridding, M. C. (2009). Selective modulation of intracortical inhibition by low-intensity Theta Burst Stimulation. *Clinical Neurophysiology, 120*(4), 820-826. doi: 10.1074/jbc.M002975200

McCreary, C. R., Dixon, S. J., Fraher, L. J., Carson, J. J. L., & Prato, F. S. (2006). Real-time measurement of cytosolic free calcium concentration in Jurkat cells during ELF magnetic field exposure and evaluation of the role of cell cycle. *Bioelectromagnetics, 27*(5), 354-364. doi: 10.1002/bem.20248

McIntyre, C. C., & Grill, W. M. (2002). Extracellular Stimulation of Central Neurons: Influence of Stimulus Waveform and Frequency on Neuronal Output. *Journal of Neurophysiology, 88*(4), 1592-1604. doi: 10.1152/jn.00147.2002

Meberg, P. J., & Miller, M. W. (2003). Culturing Hippocampal and Cortical Neurons. *Methods in Cell Biology, 71*, 111-127. doi: 10.1016/S0091-679X(03)01007-0

Meloni, B. P., Majda, B. T., & Knuckey, N. W. (2001). Establishment of neuronal in vitro models of ischemia in 96-well microtiter strip-plates that result in acute, progressive and delayed neuronal death. *Neuroscience, 108*(1), 17-26. doi: 10.1016/s0306-4522(01)00396-7

Meyer, J. F., Wolf, B., & Gross, G. W. (2009). Magnetic Stimulation and Depression of Mammalian Networks in Primary Neuronal Cell Cultures. *Biomedical Engineering, IEEE Transactions on, 56*(5), 1512-1523. doi: 10.1109/tbme.2009.2013961

Modolo, J., Thomas, A. W., & Legros, A. (2013). Neural mass modeling of power-line magnetic fields effects on brain activity. *Frontiers in Computational Neuroscience, 7*. doi: 10.3389/fncom.2013.00034

Montgomery, D. B. (1969). *Solenoid magnet design : the magnetic and mechanical aspects of resistive and superconducting systems*. New York: Wiley Interscience.

Morabito, C., Guarnieri, S., Fanograve, G., & Mariggi, M. A. (2010a). Effects of Acute and Chronic Low Frequency Electromagnetic Field Exposure on PC12 Cells during Neuronal Differentiation. *Cellular Physiology and Biochemistry, 26*(6), 947-958. doi: 10.1159/000324003

Morabito, C., Rovetta, F., Bizzarri, M., Mazzoleni, G., Fanò, G., et al. (2010b). Modulation of redox status and calcium handling by extremely low frequency electromagnetic fields in C2C12 muscle cells: A real-time, single-cell approach. *Free Radical Biology and Medicine, 48*(4), 579-589. doi: 10.1016/j.freeradbiomed.2009.12.005

Morgado-Valle, C., Verdugo-Díaz, L., García, D. E., Morales-Orozco, C., & Drucker-Colín, R. (1998). The role of voltage-gated Ca2+ channels in neurite growth of cultured chromaffin cells induced by extremely low frequency (ELF) magnetic field stimulation. *Cell and Tissue Research, 291*(2), 217-230. doi: 10.1007/s004410050992

Mori, Y., Wakamori, M., Miyakawa, T., Hermosura, M., Hara, Y., et al. (2002). Transient Receptor Potential 1 Regulates Capacitative Ca2+ Entry and Ca2+ Release from Endoplasmic Reticulum in B Lymphocytes. *The Journal of Experimental Medicine, 195*(6), 673-681. doi: 10.1084/jem.20011758

Morrison, M. E., & Mason, C. A. (1998). Granule Neuron Regulation of Purkinje Cell Development: Striking a Balance Between Neurotrophin and Glutamate Signaling. *The Journal of Neuroscience, 18*(10), 3563-3573. doi: 0270-6474/98/183563-11

Müller-Dahlhaus, F., & Vlachos, A. (2013). Unraveling the cellular and molecular mechanisms of repetitive magnetic stimulation. *Frontiers in Molecular Neuroscience, 6*. doi: 10.3389/fnmol.2013.00050

Muller, D., Djebbara-Hannas, Z., Jourdain, P., Vutskits, L., Durbec, P., et al. (2000a). Brain-derived neurotrophic factor restores long-term potentiation in polysialic acid-neural cell adhesion molecule-deficient hippocampus. *Proceedings of the National Academy of Sciences, 97*(8), 4315-4320. doi: 10.1073/pnas.070022697

Muller, M. B., Toschi, N., Kresse, A. E., Post, A., & Keck, M. E. (2000b). Long-Term Repetitive Transcranial Magnetic Stimulation Increases the Expression of Brain-Derived Neurotrophic Factor and Cholecystokinin mRNA, but not Neuropeptide Tyrosine mRNA in Specific Areas of Rat Brain. *Neuropsychopharmacology, 23*(2), 205-215. doi: 10.1016/S0893-133X(00)00099-3

Muller, P. A., Dhamne, S. C., Vahabzadeh-Hagh, A. M., Pascual-Leone, A., Jensen, F. E., et al. (2014). Suppression of Motor Cortical Excitability in Anesthetized Rats by Low Frequency Repetitive Transcranial Magnetic Stimulation. *PLoS ONE, 9*(3), e91065. doi: 10.1371/journal.pone.0091065

Mungrue, I. N., & Bredt, D. S. (2004). nNOS at a glance: implications for brain and brawn. *Journal of Cell Science, 117*(13), 2627-2629. doi: 10.1242/jcs.01187

Muralidharan-Chari, V., Clancy, J. W., Sedgwick, A., & D'Souza-Schorey, C. (2010). Microvesicles: mediators of extracellular communication during cancer progression. *Journal of Cell Science, 123*(10), 1603-1611. doi: 10.1242/jcs.064386

Nettekoven, C., Volz, L. J., Kutscha, M., Pool, E.-M., Rehme, A. K., et al. (2014). Dose-Dependent Effects of Theta Burst rTMS on Cortical Excitability and Resting-State Connectivity of the Human Motor System. *The Journal of Neuroscience, 34*(20), 6849-6859. doi: 10.1523/jneurosci.4993-13.2014

Neves, S. R., Ram, P. T., & Iyengar, R. (2002). G Protein Pathways. *Science, 296*(5573), 1636-1639. doi: 10.1126/science.1071550

Nguyen, D., & Xu, T. (2008). The expanding role of mouse genetics for understanding human biology and disease. *Disease Models & Mechanisms, 1*(1), 56-66. doi: 10.1242/dmm.000232

Ni, Z., Charab, S., Gunraj, C., Nelson, A. J., Udupa, K., et al. (2011). Transcranial Magnetic Stimulation in Different Current Directions Activates Separate Cortical Circuits. *Journal of Neurophysiology, 105*(2), 749-756. doi: 10.1152/jn.00640.2010

Nudo, R. J. (2013). Recovery after brain injury: mechanisms and principles. *Frontiers in Human Neuroscience 7*(887), 1-24. doi: 10.3389/fnhum.2013.00887

Pakhotin, P., & Verkhratsky, A. (2005). Electrical synapses between Bergmann glial cells and Purkinje neurones in rat cerebellar slices. *Molecular and Cellular Neuroscience, 28*(1), 79-84. doi: 10.1016/j.mcn.2004.08.014

Park, H.-J., Bonmassar, G., Kaltenbach, J. A., Machado, A. G., Manzoor, N. F., et al. (2013). Activation of the central nervous system induced by micro-magnetic stimulation. *Nature Communications, 4*, 1-9. doi: 10.1038/ncomms3463

Pascual-Leone, A. (2006). Disrupting the brain to guide plasticity and improve behavior. In R. M. Aage (Ed.), *Progress in Brain Research* (Vol. 157, pp. 315-404): Elsevier.

Pascual-Leone, A., Bartres-Faz, D., & Keenan, J. P. (1999). Transcranial magnetic stimulation: studying the brian-behaviour relationship by induction of 'virtual lesions'. *Philosophical Transactions of the Royal Society, 354*, 1229-1238. doi: 10.1098/rstb.1999.0476

Pascual-Leone, A., Freitas, C., Oberman, L., Horvath, J., Halko, M., et al. (2011). Characterizing Brain Cortical Plasticity and Network Dynamics Across the Age-Span in Health and Disease with TMS-EEG and TMS-fMRI. *Brain Topography, 24*(3-4), 302-315. doi: 10.1007/s10548-011-0196-8

Pascual-Leone, A., Walsh, V., & Rothwell, J. (2000). Transcranial magnetic stimulation in cognitive neuroscience - virtual lesion, chronometry, and functional connectivity. *Current Opinion in Neurobiology, 10*, 232 - 237. doi: 10.1016/S0959-4388(00)00081-7

Pashut, T., Wolfus, S., Friedman, A., Lavidor, M., Bar-Gad, I., et al. (2011). Mechanisms of Magnetic Stimulation of Central Nervous System Neurons. *PLoS Comput Biol, 7*(3), e1002022. doi: 10.1371/journal.pcbi.1002022

Pell, G. S., Roth, Y., & Zangen, A. (2011). Modulation of cortical excitability induced by repetitive transcranial magnetic stimulation: Influence of timing and geometrical parameters and underlying mechanisms. *Progress in Neurobiology, 93*(1), 59-98. doi: 10.1016/j.pneurobio.2010.10.003

Pessina, G. P., Aldinucci, C., Palmi, M., Sgaragli, G., Benocci, A., et al. (2001). Pulsed electromagnetic fields affect the intracellular calcium concentrations in human astrocytoma cells. *Bioelectromagnetics, 22*(7), 503-510. doi: 10.1002/bem.79

Peterchev, A. V., Murphy, D. L., & Lisanby, S. H. (2011). Repetitive transcranial magnetic stimulator with controllable pulse parameters. *Journal of Neural Engineering, 8*(3), 2922-2926. doi: 10.1109/IEMBS.2010.5626287

Piacentini, R., Ripoli, C., Mezzogori, D., Azzena, G. B., & Grassi, C. (2008). Extremely low-frequency electromagnetic fields promote in vitro neurogenesis via upregulation of Cav1-channel activity. *Journal of Cellular Physiology, 215*(1), 129-139. doi: 10.1002/jcp.21293

Platz, T., & Rothwell, J. C. (2010). Brain stimulation and brain repair – rTMS: from animal experiment to clinical trials – what do we know? *Restorative Neurology and Neuroscience, 28*(4), 387-398. doi: 10.3233/rnn-2010-0570

Ponti, G., Peretto, P., & Bonfanti, L. (2006). A subpial, transitory germinal zone forms chains of neuronal precursors in the rabbit cerebellum. *Developmental Biology, 168-180*. doi: 10.1016/j.ydbio.2006.02.037

Pope, P. A., & Miall, C. R. (2014). Restoring cognitive functions using non-invasive brain stimulation techniques in patients with cerebellar disorders. *Frontiers in Psychiatry 5*(33), 1-7. doi: DOI=10.3389/fpsyt.2014.00033

Post, A., Müller, M. B., Engelmann, M., & Keck, M. E. (1999). Repetitive transcranial magnetic stimulation in rats: evidence for a neuroprotective effect in vitro and in vivo. *European Journal of Neuroscience, 11*(9), 3247-3254. doi: 10.1046/j.1460-9568.1999.00747.x

Queiroz de, A. C. M. (2005). Mutual Inductance and Inductance Calculations by Maxwell's Method. http://www.coe.ufrj.br/~acmq/tesla/maxwell.pdf

Quentin, R., Chanes, L., Migliaccio, R., Valabrègue, R., & Valero-Cabré, A. (2013). Fronto-tectal white matter connectivity mediates facilitatory effects of non-invasive neurostimulation on visual detection. *NeuroImage, 82*(0), 344-354. doi: 10.1016/j.neuroimage.2013.05.083

Radman, T., Ramos, R. L., Brumberg, J. C., & Bikson, M. (2009). Role of cortical cell type and morphology in subthreshold and suprathreshold uniform electric field stimulation in vitro. *Brain Stimulation, 2*(4), 215-228. doi: 10.1016/j.brs.2009.03.007

Ravera, S., Bianco, B., Cugnoli, C., Panfoli, I., Calzia, D., et al. (2010). Sinusoidal ELF magnetic fields affect acetylcholinesterase activity in cerebellum synaptosomal membranes. *Bioelectromagnetics, 31*(4), 270-276. doi: 10.1002/bem.20563

Reeber, S. L., White, J. J., George-Jones, N. A., & Sillitoe, R. V. (2013). Architecture and development of olivocerebellar circuit topography *Frontiers in Neural Circuits 6*(115), 1-14. doi: 10.3389/fncir.2012.00115

Reichert, W. M. (Ed.). (2008). *Indwelling neural implants; strategies for contending with the in vivo environment* (Vol. 32). Portland: Book News, Inc.

Ridding, M. C., & Rothwell, J. C. (2007). Is there a future for therapeutic use of transcranial magnetic stimulation? *Nature Reviews Neuroscience, 8*(7), 559-567. doi: 10.1038/nrn2169

Robert, F., Cloix, J.-F., & Hevor, T. (2012). Ultrastructural characterization of rat neurons in primary culture. *Neuroscience, 200*, 248-260. doi: 10.1016/j.neuroscience.2011.10.002

Robertson, J. A., Théberge, J., Weller, J., Drost, D. J., Prato, F. S., et al. (2010). Low-frequency pulsed electromagnetic field exposure can alter neuroprocessing in humans. *Journal of The Royal Society Interface, 7*(44), 467-473. doi: 10.1098/rsif.2009.0205

Rodger, J., Mo, C., Wilks, T., Dunlop, S. A., & Sherrard, R. M. (2012). Transcranial pulsed magnetic field stimulation facilitates reorganization of abnormal neural circuits and corrects behavioral deficits without disrupting normal connectivity. *The FASEB Journal, 26*(4), 1593-1606. doi: 10.1096/fj.11-194878

Rohan, M. L., Yamamoto, R. T., Ravichandran, C. T., Cayetano, K. R., Morales, O. G., et al. (2014). Rapid Mood-Elevating Effects of Low Field Magnetic Stimulation in Depression. *Biological Psychiatry, 76*(3), 186-193. doi: 10.1016/j.biopsych.2013.10.024

Rose, C. R., & Konnerth, A. (2001). Stores Not Just for Storage: Intracellular Calcium Release and Synaptic Plasticity. *Neuron, 31*(4), 519-522. doi: 10.1016/S0896-6273(01)00402-0

Rossi, F., & Strata, P. (1995). Reciprocal trophic interactions in the adult climbing fibre—Purkinje cell system. *Progress in Neurobiology, 47*(4–5), 341-369. doi: 10.1016/0301-0082(95)80006-T

Rossini, P. M., Barker, A. T., Berardelli, A., Caramia, M. D., Caruso, G., et al. (1994). Non-invasive electrical and magnetic stimulation of the brain, spinal cord and roots: basic principles and procedures for routine clinical application. Report of an IFCN committee. *Electroencephalography and clinical Neurophysiology, 91*(2), 79-92.

Rossini, P. M., Berardelli, A., Deuschl, G., Hallett, M., Maertens de Noordhout, A. M., et al. (1999). Applications of magnetic cortical stimulation. *Electroencephalography and Clinical Neurophysiology, 52(Suppl)*(171-185).

Rotem, A., & Moses, E. (2008). Magnetic Stimulation of One-Dimensional Neuronal Cultures. *Biophysical Journal, 94*(12), 5065-5078. doi: 10.1529/biophysj.107.125708

Rotem, A., Neef, A., Neef, N. E., Agudelo-Toro, A., Rakhmilevitch, D., et al. (2014). Solving the Orientation Specific Constraints in Transcranial Magnetic Stimulation by Rotating Fields. *PLoS ONE, 9*(2), e86794. doi: 10.1371/journal.pone.0086794

Roth, B. J., & Basser, P. J. (1990). A model of the stimulation of a nerve fiber by electromagnetic induction. *Biomedical Engineering, IEEE Transactions on, 37*(6), 588-597. doi: 10.1109/10.55662

Roth, Y., Amir, A., Levkovitz, Y., & Zangen, A. (2007). Three-Dimensional Distribution of the Electric Field Induced in the Brain by Transcranial Magnetic Stimulation Using Figure-8 and Deep H-Coils. *Journal of Clinical Neurophysiology, 24*(1), 31-38.

Rothwell, J. C., Day, B. L., Thompson, P. D., Dick, J. P., & Marsden, C. D. (1987). Some experiences of techniques for stimulation of the human cerebral motor cortex through the scalp. *Neurosurgery, 20*(1), 156-163.

Roy Choudhury, K., Boyle, L., Burke, M., Lombard, W., Ryan, S., et al. (2011). Intra subject variation and correlation of motor potentials evoked by transcranial magnetic stimulation. *Irish Journal of Medical Science, 180*(4), 873-880. doi: 10.1007/s11845-011-0722-4

Ruohonen, J., & Ilmoniemi, R. J. (1999). Modeling of the stimulating field generation in TMS. *Electroencephalogr Clin Neurophysiol Suppl, 51*, 30-40.

Rutishauser, U. (2008). Polysialic acid in the plasticity of the developing and adult vertebrate nervous system. *Nat Rev Neurosci, 9*(1), 26-35. doi: 10.1038/nrn2285

Salinas, F. S., Lancaster, J. L., & Fox, P. T. (2009). 3D modeling of the total electric field induced by transcranial magnetic stimulation using the boundary element method. *Physics in Medicine and Biology, 54*(12), 3631-3647. doi: 10.1088/0031-9155/54/12/002

Santo-Domingo, J., & Demaurex, N. (2010). Calcium uptake mechanisms of mitochondria. *Biochimica et Biophysica Acta (BBA) - Bioenergetics, 1797*(6-7), 907-912. doi: 10.1016/j.bbabio.2010.01.005

Sarna, J. R., & Hawkes, R. (2003). Patterned Purkinje cell death in the cerebellum. *Progress in Neurobiology, 70*(6), 473-507. doi: 10.1016/S0301-0082(03)00114-X

Sawaguchi, T. (1997). Attenuation of Preparatory Activity for Reaching Movements by a D1-Dopamine Antagonist in the Monkey Premotor Cortex. *J Neurophysiol, 78*(4), 1769-1774.

Schmahmann, J. D., & Caplan, D. (2006). Cognition, emotion and the cerebellum. *Brain, 129*(2), 290-292. doi: 10.1093/brain/awh729

Schulz, R., Gerloff, C., & Hummel, F. C. (2013). Non-invasive brain stimulation in neurological diseases. *Neuropharmacology, 64*, 579-587. doi: 10.1016/j.neuropharm.2012.05.016

Schutter, D. J. L. G., & van Honk, J. (2006). An electrophysiological link between the cerebellum, cognition and emotion: Frontal theta EEG activity to single-pulse

cerebellar TMS. *NeuroImage, 33*(4), 1227-1231. doi: 10.1016/j.neuroimage.2006.06.055

Seo, Y.-W., Shin, J. N., Ko, K. H., Cha, J. H., Park, J. Y., et al. (2003). The Molecular Mechanism of Noxa-induced Mitochondrial Dysfunction in p53-Mediated Cell Death. *Journal of Biological Chemistry, 278*(48), 48292-48299. doi: 10.1074/jbc.M308785200

Sheng, M., & Greenberg, M. E. (1990). The regulation and function of c-fos and other immediate early genes in the nervous system. *Neuron, 4*(4), 477-485. doi: 10.1016/0896-6273(90)90106-P

Sherafat, M., Heibatollahi, M., Mongabadi, S., Moradi, F., Javan, M., et al. (2012). Electromagnetic Field Stimulation Potentiates Endogenous Myelin Repair by Recruiting Subventricular Neural Stem Cells in an Experimental Model of White Matter Demyelination. *Journal of Molecular Neuroscience, 48*(1), 144-153. doi: 10.1007/s12031-012-9791-8

Sherrard, R. M., & Bower, A. J. (2001). BDNF and NT3 extend the critical period for developmental climbing fibre plasticity. *NeuroReport, 12*(13), 2871-2874. doi: 10.1097/00001756-200109170-00023

Sherrard, R. M., Dixon, K. J., Bakouche, J., Rodger, J., Lemaigre-Dubreuil, Y., et al. (2009). Differential expression of TrkB isoforms switches climbing fiber-Purkinje cell synaptogenesis to selective synapse elimination. *Developmental Neurobiology, 69*(10), 647-662. doi: 10.1002/dneu.20730

Sherrard, R. M., Letellier, M., Lohof, A. M., & Mariani, J. (2013). Formation and Reformation of Climbing Fibre Synapses in the Cerebellum: a Similar Story? *The Cerebellum, 12*(3), 319-321. doi: 10.1007/s12311-012-0443-x

Shimizu, H., Tsuda, T., Shiga, Y., Miyazawa, K., Onodera, Y., et al. (1999). Therapeutic Efficacy of Transcranial Magnetic Stimulation for Hereditary Spinocerebellar Degeneration. *The Tohoku Journal of Experimental Medicine, 189*(3), 203-211. doi: 10.1620/tjem.189.203

Shupak, N. M., Prato, F. S., & Thomas, A. W. (2004). Human exposure to a specific pulsed magnetic field: effects on thermal sensory and pain thresholds. *Neuroscience Letters, 363*(2), 157-162. doi: 10.1016/j.neulet.2004.03.069

Siebner, H. R., Hartwigsen, G., Kassuba, T., & Rothwell, J. C. (2009). How does transcranial magnetic stimulation modify neuronal activity in the brain? - Implications for studies of cognition. *Cortex, 45*(9), 1035-1045. doi: 10.1016/j.cortex.2009.02.007

Siebner, H. R., & Rothwell, J. (2003). Transcranial magnetic stimulation: new insights into representational cortical plasticity. *Experimental Brain Research, 148*(1), 1-16. doi: 10.1007/s00221-002-1234-2

Simpson, J., Lane, J., Immer, C., & Youngquist, R. (2001). Simple Analytic Expressions for the Magnetic Field of a Circular Current Loop. *NASA Technical Documents*. http://ntrs.nasa.gov/archive/nasa/casi.ntrs.nasa.gov/20010038494.pdf

Sommer, M., Alfaro, A., Rummel, M., Speck, S., Lang, N., et al. (2006). Half sine, monophasic and biphasic transcranial magnetic stimulation of the human motor cortex. *Clinical Neurophysiology, 117*(4), 838-844. doi: 10.1016/j.clinph.2005.10.029

Sommer, M., Lang, N., Tergau, F., & Paulus, W. (2002). Neuronal tissue polarization induced by repetitive transcranial magnetic stimulation? *NeuroReport, 13*(6), 809-811. doi: 10.1097/00001756-200205070-00015

Stagg, C. J., Wylezinska, M., Matthews, P. M., Johansen-Berg, H., Jezzard, P., et al. (2009). Neurochemical Effects of Theta Burst Stimulation as Assessed by Magnetic Resonance Spectroscopy. *Journal of Neurophysiology, 101*(6), 2872-2877. doi: 10.1152/jn.91060.2008

Stratton, D., Lange, S., & Inal, J. M. (2013). Pulsed extremely low-frequency magnetic fields stimulate microvesicle release from human monocytic leukaemia cells. *Biochemical and Biophysical Research Communications, 430*(2), 470-475. doi: 10.1016/j.bbrc.2012.12.012

Sugihara, I. (2005). Microzonal projection and climbing fiber remodeling in single olivocerebellar axons of newborn rats at postnatal days 4–7. *The Journal of Comparative Neurology, 487*(1), 93-106. doi: 10.1002/cne.20531

Sugihara, I., Lohof, A. M., Letellier, M., Mariani, J., & Sherrard, R. M. (2003). Post-lesion transcommissural growth of olivary climbing fibres creates functional synaptic microzones. *European Journal of Neuroscience, 18*(11), 3027-3036. doi: 10.1111/j.1460-9568.2003.03045.x

Talelli, P., Greenwood, R. J., & Rothwell, J. C. (2007). Exploring Theta Burst Stimulation as an intervention to improve motor recovery in chronic stroke. *Clinical Neurophysiology, 118*(2), 333-342. doi: 10.1016/j.clinph.2006.10.014

Tanaka, C., & Nishizuka, Y. (1994). The Protein Kinase C Family for Neuronal Signaling. *Annual Review of Neuroscience, 17*(1), 551-567. doi: 10.1146/annurev.ne.17.030194.003003

Tanaka, S., Sekino, Y., & Shirao, T. (2000). The effects of neurotrophin-3 and brain-derived neurotrophic factor on cerebellar granule cell movement and neurite extension in vitro. *Neuroscience, 97*(4), 727-734. doi: 10.1016/S0306-4522(00)00049-X

Tao, X., Finkbeiner, S., Arnold, D. B., Shaywitz, A. J., & Greenberg, M. E. (1998). Ca2+ Influx Regulates BDNF Transcription by a CREB Family Transcription Factor-Dependent Mechanism. *Neuron, 20*(4), 709-726. doi: 10.1016/S0896-6273(00)81010-7

Tasset, I., Medina, F. J., Jimena, I., Agüera, E., Gascón, F., et al. (2012). Neuroprotective effects of extremely low-frequency electromagnetic fields on a Huntington's disease rat model: effects on neurotrophic factors and neuronal density. *Neuroscience, 209*(0), 54-63. doi: 10.1016/j.neuroscience.2012.02.034

Thangaraju, M., Kaufmann, S. H., & Couch, F. J. (2000). BRCA1 Facilitates Stress-induced Apoptosis in Breast and Ovarian Cancer Cell Lines. *Journal of Biological Chemistry, 275*(43), 33487-33496. doi: 10.1074/jbc.M005824200

Thickbroom, G. (2007). Transcranial magnetic stimulation and synaptic plasticity: experimental framework and human models. *Experimental Brain Research, 180*(4), 583-593. doi: 10.1007/s00221-007-0991-3

Thielscher, A., & Kammer, T. (2002). Linking Physics with Physiology in TMS: A Sphere Field Model to Determine the Cortical Stimulation Site in TMS. *NeuroImage, 17*(3), 1117-1130. doi: 10.1006/nimg.2002.1282

Thielscher, A., & Kammer, T. (2004). Electric field properties of two commercial figure-8 coils in TMS: calculation of focality and efficiency. *Clinical Neurophysiology, 115*(7), 1697-1708. doi: 10.1016/j.clinph.2004.02.019

Thomas, W. E. (1985). Synthesis of acetylcholine and γ-aminobutyric acid by dissociated cerebral cortical cells in vitro. *Brain Research, 332*(1), 79-89. doi: 10.1016/0006-8993(85)90391-9

Tischler, H., Wolfus, S., Friedman, A., Perel, E., Pashut, T., et al. (2011). Mini-coil for magnetic stimulation in the behaving primate. *Journal of Neuroscience Methods, 194*(2), 242-251. doi: 10.1016/j.jneumeth.2010.10.015

Tofts, P. S. (1990). The distribution of induced currents in magnetic stimulation of the nervous system. *Physics in Medicine and Biology, 35*(8), 1119-1128. doi: 10.1088/0031-9155/35/8/008

Trejo, J., & Brown, J. H. (1991). c-fos and c-jun are induced by muscarinic receptor activation of protein kinase C but are differentially regulated by intracellular calcium. *Journal of Biological Chemistry, 266*(12), 7876-7882.

Trillenberg, P., Bremer, S., Oung, S., Erdmann, C., Schweikard, A., et al. (2012). Variation of stimulation intensity in transcranial magnetic stimulation with depth. *Journal of Neuroscience Methods, 211*(2), 185-190. doi: 10.1016/j.jneumeth.2012.09.007

Trippe, J., Mix, A., Aydin-Abidin, S., Funke, K., & Benali, A. (2009). Theta burst and conventional low-frequency rTMS differentially affect GABAergic neurotransmission in the rat

cortex. *Experimental Brain Research, 199*(3-4), 411-421. doi: 10.1007/s00221-009-1961-8

Tuttle, R., & O'Leary, D. D. M. (1998). Neurotrophins Rapidly Modulate Growth Cone Response to the Axon Guidance Molecule, Collapsin-1. *Molecular and Cellular Neuroscience, 11*(1-2), 1-8. doi: 10.1006/mcne.1998.0671

Urban, N. N., & Barrionuevo, G. (1996). Induction of Hebbian and Non-Hebbian Mossy Fiber Long-Term Potentiation by Distinct Patterns of High-Frequency Stimulation. *The Journal of Neuroscience, 16*(13), 4293-4299. doi: 0270-6474/96/164293-07

Valero-Cabré, A., Payne, B., Rushmore, J., Lomber, S., & Pascual-Leone, A. (2005). Impact of repetitive transcranial magnetic stimulation of the parietal cortex on metabolic brain activity: a 14C-2DG tracing study in the cat. *Experimental Brain Research, 163*(1), 1-12. doi: 10.1007/s00221-004-2140-6

Valsecchi, F., Ramos-Espiritu, L. S., Buck, J., Levin, L. R., & Manfredi, G. (2013). cAMP and Mitochondria. *Physiology, 28*(3), 199-209. doi: 10.1152/physiol.00004.2013

Vincent, A. M., Russell, J. W., Sullivan, K. A., Backus, C., Hayes, J. M., et al. (2007). SOD2 protects neurons from injury in cell culture and animal models of diabetic neuropathy. *Experimental Neurology, 208*(2), 216-227. doi: 10.1016/j.expneurol.2007.07.017

Viola, H. M., Arthur, P. G., & Hool, L. C. (2007). Transient Exposure to Hydrogen Peroxide Causes an Increase in Mitochondria-Derived Superoxide As a Result of Sustained Alteration in L-Type Ca2+ Channel Function in the Absence of Apoptosis in Ventricular Myocytes. *Circulation Research, 100*(7), 1036-1044. doi: 10.1161/01.res.0000263010.19273.48

Vlachos, A., Müller-Dahlhaus, F., Rosskopp, J., Lenz, M., Ziemann, U., et al. (2012). Repetitive Magnetic Stimulation Induces Functional and Structural Plasticity of Excitatory Postsynapses in Mouse Organotypic Hippocampal Slice Cultures. *The Journal of Neuroscience, 32*(48), 17514-17523. doi: 10.1523/jneurosci.0409-12.2012

Volz, L. J., Benali, A., Mix, A., Neubacher, U., & Funke, K. (2013). Dose-Dependence of Changes in Cortical Protein Expression Induced with Repeated Transcranial Magnetic Theta-Burst Stimulation in the Rat. *Brain Stimulation, 6*(4), 598-606. doi: 10.1016/j.brs.2013.01.008

Volz, L. J., Hamada, M., Rothwell, J. C., & Grefkes, C. (2014). What Makes the Muscle Twitch: Motor System Connectivity and TMS-Induced Activity. *Cerebral Cortex, Epub*. doi: 10.1093/cercor/bhu032

Wagner, T., Eden, U., Rushmore, J., Russo, C. J., Dipietro, L., et al. (2014). Impact of brain tissue filtering on neurostimulation fields: A modeling study. *NeuroImage, 85*(3), 1048-1057. doi: 10.1016/j.neuroimage.2013.06.079

Walker, J. L., Evans, J. M., Resig, P., Guarnier, S., Meade, P., et al. (1994). Enhancement of Functional Recovery Following a Crush Lesion to the Rat Sciatic Nerve by Exposure to Pulsed Electromagnetic Fields. *Experimental Neurology, 125*(2), 302-305. doi: 10.1006/exnr.1994.1033

Walsh, V. (2003). *Transcranial magnetic stimulation : a neurochronometrics of mind*. Cambridge, Mass.: Cambridge, Mass. : MIT Press.

Walsh, V., & Rushworth, M. (1999). A primer of magnetic stimulation as a tool for neuropsychology *Neuropsychologia, 37*, 125 - 135.

Wang, F., Geng, X., Tao, H.-Y., & Cheng, Y. (2010). The Restoration After Repetitive Transcranial Magnetic Stimulation Treatment on Cognitive Ability of Vascular Dementia Rats and Its Impacts on Synaptic Plasticity in Hippocampal CA1 Area. *Journal of Molecular Neuroscience, 41*(1), 145-155. doi: 10.1007/s12031-009-9311-7

Wang, H.-Y., Crupi, D., Liu, J., Stucky, A., Cruciata, G., et al. (2011). Repetitive Transcranial Magnetic Stimulation Enhances BDNF–TrkB Signaling in Both Brain and Lymphocyte. *The Journal of Neuroscience, 31*(30), 11044-11054. doi: 10.1523/jneurosci.2125-11.2011

Wassermann, E. M., Epstein, C. M., Ziemann, U., Walsh, V., Paus, T., et al. (2008). *The Oxford Handbook of TRANSCRANIAL STIMULATION*. Oxford: Oxford University Press.

Wassermann, E. M., & Zimmermann, T. (2012). Transcranial magnetic brain stimulation: Therapeutic promises and scientific gaps. *Pharmacology & Therapeutics, 133*(1), 98-107. doi: 10.1016/j.pharmthera.2011.09.003

Watanabe, M., & Kano, M. (2011). Climbing fiber synapse elimination in cerebellar Purkinje cells. *European Journal of Neuroscience, 34*(10), 1697-1710. doi: 10.1111/j.1460-9568.2011.07894.x

Wei, J., Davis, K. M., Wu, H., & Wu, J.-Y. (2004). Protein Phosphorylation of Human Brain Glutamic Acid Decarboxylase (GAD)65 and GAD67 and Its Physiological Implications†. *Biochemistry, 43*(20), 6182-6189. doi: 10.1021/bi0496992

Weissman, J. D., Epstein, C. M., & Davey, K. R. (1992). Magnetic brain stimulation and brain size: relevance to animal studies. *Electroencephalography and clinical Neurophysiology, 85*(3), 215-219. doi: 10.1016/0168-5597(92)90135-X

Weitzman, J. B., Fiette, L., Matsuo, K., & Yaniv, M. (2000). JunD Protects Cells from p53-Dependent Senescence and Apoptosis. *Molecular Cell, 6*(5), 1109-1119. doi: 10.1016/S1097-2765(00)00109-X

Weyer, A., & Schilling, K. (2003). Developmental and cell type-specific expression of the neuronal marker NeuN in the murine cerebellum. *Journal of Neuroscience Research, 73*(3), 400-409. doi: 10.1002/jnr.10655

Wigström, H., & Gustafsson, B. (1986). Postsynaptic control of hippocampal long-term potentiation. *Journal de physiologie, 81*(4), 228-236.

Willson, M. L., Bower, A. J., & Sherrard, R. M. (2007). Developmental neural plasticity and its cognitive benefits: olivocerebellar reinnervation compensates for spatial function in the cerebellum. *European Journal of Neuroscience, 25*(5), 1475-1483. doi: 10.1111/j.1460-9568.2007.05410.x

Willson, M. L., McElnea, C., Mariani, J., Lohof, A. M., & Sherrard, R. M. (2008). BDNF increases homotypic olivocerebellar reinnervation and associated fine motor and cognitive skill. *Brain, 131*(4), 1099-1112. doi: 10.1093/brain/awn024

Yadollahpour, A., Firouzabadi, S. M., Shahpari, M., & Mirnajafi-Zadeh, J. (2014). Repetitive transcranial magnetic stimulation decreases the kindling induced synaptic potentiation: Effects of frequency and coil shape. *Epilepsy Research, 108*(2), 190-201. doi: 10.1016/j.eplepsyres.2013.11.023

Yang, Y., Li, L., Wang, Y.-G., Fei, Z., Zhong, J., et al. (2012). Acute neuroprotective effects of extremely low-frequency electromagnetic fields after traumatic brain injury in rats. *Neuroscience Letters, 516*(1), 15-20. doi: 10.1016/j.neulet.2012.03.022

Yong, Y., Ming, Z. D., Feng, L., Chun, Z. W., & Hua, W. (2014). Electromagnetic fields promote osteogenesis of rat mesenchymal stem cells through the PKA and ERK1/2 pathways. *Journal of Tissue Engineering and Regenerative Medicine, in press*. doi: 10.1002/term.1864

Yoon, K., Lee, Y.-T., & Han, T. (2011). Mechanism of functional recovery after repetitive transcranial magnetic stimulation (rTMS) in the subacute cerebral ischemic rat model: neural plasticity or anti-apoptosis? *Experimental Brain Research, 214*(4), 549-556. doi: 10.1007/s00221-011-2853-2

Yuasa, S., Kawamura, K., Ono, K., Yamakuni, T., & Takahashi, Y. (1991). Development and migration of Purkinje cells in the mouse cerebellar primordium. *Anatomy and Embryology, 184*(3), 195-212. doi: 10.1007/bf01673256

Zhang, B., Kirov, S., & Snoddy, J. (2005). WebGestalt: an integrated system for exploring gene sets in various biological contexts. *Nucleic Acids Research, 33*(suppl 2), W741-W748. doi: 10.1093/nar/gki475

Zhang, L., Liu, W., Szumlinski, K. K., & Lew, J. (2012). p10, the N-terminal domain of p35, protects against CDK5/p25-induced neurotoxicity. *Proceedings of the National Academy of Sciences, 109*(49), 20041-20046. doi: 10.1073/pnas.1212914109

Zhang, X., Mei, Y., Liu, C., & Yu, S. (2007). Effect of transcranial magnetic stimulation on the expression of c-Fos and brain-derived neurotrophic factor of the cerebral cortex in rats with cerebral infarct. *Journal of Huazhong University of Science and Technology, 27*(4), 415-418. doi: 10.1007/s11596-007-0416-3

Ziemann, U., Hallett, M., & Cohen, L. G. (1998). Mechanisms of Deafferentation-Induced Plasticity in Human Motor Cortex. *The Journal of Neuroscience, 18*(17), 7000-7007. doi: 0270-6474/98/187000-08

Ziemann, U., Paulus, W., Nitsche, M. A., Pascual-Leone, A., Byblow, W. D., et al. (2008). Consensus: Motor cortex plasticity protocols. *Brain Stimulation, 1*(3), 164-182. doi: 10.1016/j.brs.2008.06.006

APPENDIX

A. Data not shown (Chapter 2): PI

Neuronal viability following a single session of LI-rMS stimulation *via* propidium iodide (PI) 10µl/ml addition to the imaging media (5-10 min incubation time after cease of stimulation). In total, two neurons were excluded from analysis due to PI positive staining after one single LI-rMS session after 1Hz and TBS respectively. No other frequency resulted in PI positive staining post-stimulation.

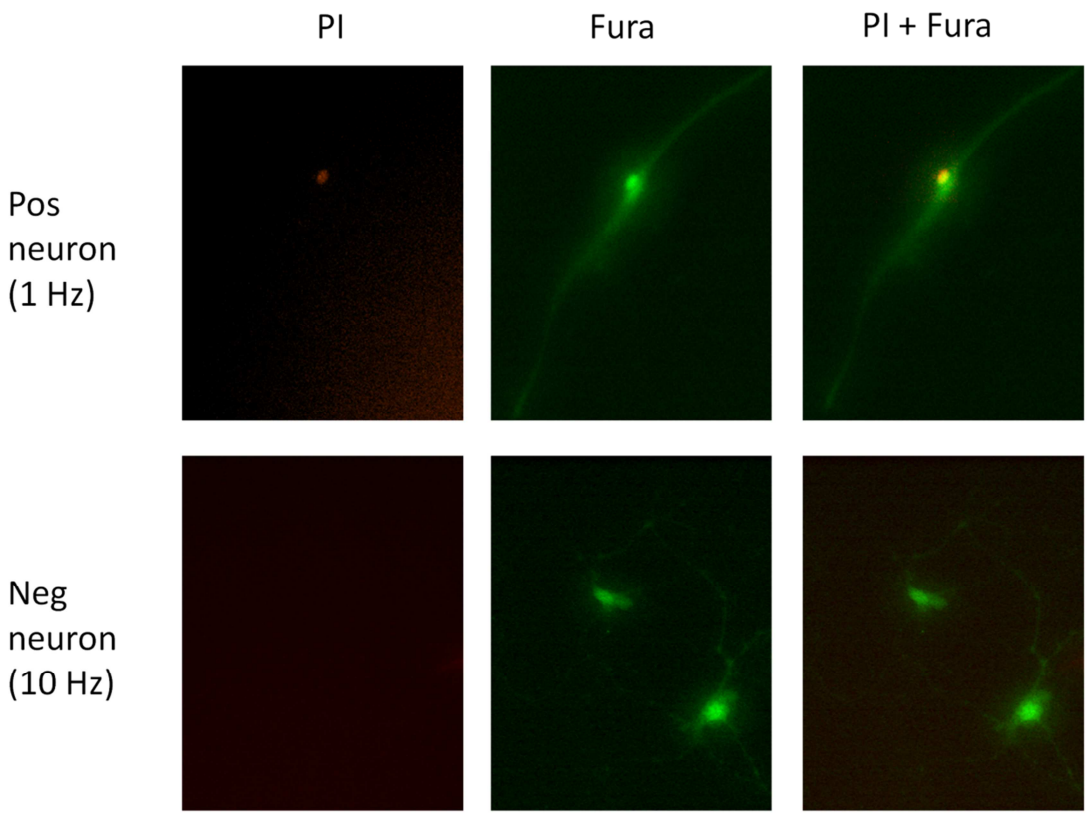

Figure A.1 Propidium iodide (PI) fluorescence images. Fluorescence images captured with a Hamamatsu Orca ER digital camera attached to an inverted Nikon TE2000-U microscope during real-time calcium imaging experiment. PI was added at 10 µl/ml 5-10 min after stimulation had creased, incubated for 1min before image capture. PI and Fura-2 images were overlaid in Adobe Photoshop CS2 and inspected for co-localization. PI positive neurons (N = 2 - 1Hz and TBS) were excluded from analysis. No other neurons showed PI positive staining.

B. Data not shown (Chapter 2): Gene list

rtPCR cAMP / Ca2+ Signaling PathwayFinder PCR Array (Qiagen)

Gene regulation 5 hours after one stimulation with 1 Hz, 10 Hz or BHFS frequency or Control. This time-point was chosen as averaged optimal time-point for RNA regulation across all genes and thus leaves some individual regulation time-points to be suboptimal, e.g. early transcription factors family (SRE)

Genes not shown in Chapter2/paper were not significantly regulated

Sterol regulatory element (SRE) or SRE-like Enhancer Sequences:

Cnn1, Cyr61, Egr1, Egr2, Fos, Fosb, Hspa4 (Hsp70), Junb, Scg2, Srf, Thbs1 (TSP-1), Vcl.

CRE Enhancer Sequence: **Neuropeptides/Neurotransmitters:** Adrb1, Cga, Chga, Gcg, Inhba, Kcna5 (KV1.5), Krtap14, Nos2 (iNOS), Penk, Prl, S100a8, S100a9, S100g, Scg2, Slc18a1, Sst, Sstr2, Tacr1, Th, Vip.

Cell Cycle, Cell Survival, & DNA Repair: Bcl2, Brca1, Ccna1, Ccnd1, Cdk5, Cdkn2b (p15Ink4b), Gem, Nf1, Pcna, Pmaip1 (NoxA), Ppp1r15a (Gadd34), Rb1.

Growth Factors: Areg, Bdnf, Crh, Fgf6, Tgfb3, Tnf.

Signaling: Dusp1 (Ptpn16), Hspa5 (Grp78), Pln, Ppp2ca, Prkar1a, Sgk1.

Transcription: Atf3, Creb1, Crem, Egr1, Egr2, Fos, Jund, Maf, Per1, Pou1f1 (Pit1), Pou2af1 (OCA-B), Stat3.

Metabolism: Ahr, Amd1, Eno2, Hk2, Ldha, Pck2, Sod2.

Immune Regulation: Il2, Il6, Mif, Ptgs2 (Cox2).

Other Ca2+ Responsive Elements: Calb1, Calb2, Calcrl, Calm1, Calr, Ddit3 (Gadd153/Chop), Ncam1, Npy, Plat (tPA)

Table B.1: Raw fold changes per gene compared to Control

	1Hz	10Hz	BHFS
	Fold Change	Fold Change	Fold Change
Adrb1	1.0116	1.1207	1.1087
Ahr	1.2283	1.574	0.8364
Amd1	0.7937	0.923	0.823
Areg	0.8586	1.3054	1.0085
Atf3	0.5561	1.0677	0.9497
Bcl2	0.9548	1.1496	0.8639
Bdnf	0.8706	1.1846	0.692
Brca1	1.1975	1.5416	1.0709
Calb1	1.0994	1.1956	0.8659
Calb2	1.4914	1.2435	0.9992
Calcrl	0.7253	0.9734	0.6778
Calm1	0.0321	0.9712	0.5792
Calr	1.1329	1.0652	1.191
Ccna1	0.408	1.5631	1.0441
Ccnd1	0.816	0.8377	0.8135
Cdk5	0.9727	0.9667	0.8173
Cdkn2b	1.162	1.2551	0.9259
Cga	2.6208	1.053	1.6383
Chga	0.8104	0.6804	0.9431
Cnn1	0.4108	1.1984	1.9892
Creb1	1.2924	1.8589	0.7486
Crem	0.8746	0.9802	0.7417
Crh	0.6492	0.6218	0.6669
Cyr61	1.2864	1.3734	1.4099
Ddit3	0.9287	1.0554	0.8659
Dusp1	0.8645	0.8875	0.9832
Egr1	1.3134	1.2904	0.9969
Egr2	1.234	1.0457	1.0345
Eno2	0.3869	0.3672	0.3911
Fgf6	0.839	1.2874	2.1819
Fos	1.0968	0.9847	0.9453
Fosb	0.9461	1.0054	0.9563
Gcg	0.6522	0.4833	0.6295
Gem	0.9548	0.9061	0.752
Hk2	1.3566	1.2874	0.9152
Hspa4	0.7405	0.7852	0.6208
Hspa5	0.9417	1.0652	0.8042
Il2	2.0093	1.1819	5.3848
Il6	1.7736	0.6175	1.423
Inhba	1.3819	1.7791	0.9674
Junb	0.4293	0.3766	0.5367
Jund	0.5129	0.4008	0.7696
Kcna5	1.0329	0.7093	1.7887
Krtap14	1.9141	0.8338	2.8002
Ldha	1.3044	1.0505	1.1164
Maf	1.0046	1.0726	0.6487

Mif	0.9794	0.923	0.9152
Ncam1	1.0234	1.1874	0.8759
Nf1	0.7828	0.9019	0.5983
Nos2	0.4373	0.5413	0.8364
Npy	0.9266	0.8916	0.7986
Pck2	0.9504	0.8936	0.8599
Pcna	1.0401	1.0701	0.8923
Penk	0.9439	0.9446	0.9174
Per1	0.6256	0.4018	0.7678
Plat	0.9977	0.6348	1.1855
Pln	0.8066	0.7708	0.7503
Pmaip1	1.977	2.8768	1.6158
Pou1f1	0.4043	0.5695	0.3104
Pou2af1	1.0968	1.3766	0.6654
Ppp1r15a	1.4208	1.0876	4.4864
Ppp2ca	0.9439	1.0008	0.8154
Prkar1a	0.8766	0.8712	0.8882
Prl	0.3439	0.4811	0.9652
Ptgs2	0.6015	1.0826	1.1425
Rb1	1.1045	1.2321	0.7643
S100a8	1.1329	1.0951	1.3905
S100a9	1.162	0.7834	1.4099
S100g	1.1892	0.811	1.3064
Scg2	0.8048	0.8454	0.7366
Sgk1	0.9593	0.8148	0.9259
Slc18a1	2.3187	2.4928	3.6525
Sod2	0.7649	0.9209	0.6324
Srf	1.1594	1.0361	0.9585
Sst	0.9526	0.9556	0.8422
Sstr2	0.9482	0.9381	1.0132
Stat3	0.7055	0.6915	0.8116
Tacr1	1.5801	1.204	1.3808
Tgfb3	0.7974	1.2292	1.2677
Th	0.6862	0.7907	0.9787
Thbs1	1.203	1.3483	0.775
Tnf	0.6227	0.4208	0.8619
Vcl	1.234	1.2435	0.9855
Vip	0.8274	0.923	0.8042
Actb	1.0473	0.8712	0.8383
B2m	1.0693	1.0901	0.9674
Gapdh	1.203	1.1053	0.9674
Gusb	0.9013	0.8338	0.9585
Hsp90ab1	0.9223	1.0851	1.0784
MGDC	1.5619	1.2407	2.031
RTC	1.3044	0.9359	1.365
RTC	1.2716	0.923	1.3338
RTC	0.0392	0.987	1.2973
PPC	0.0164	0.9402	1.5111
PPC	0.0162	0.9424	1.2445
PPC	0.0115	0.811	1.0985

C. Induced electric field of coil used for 24 well plate set-up (Chapter 2)

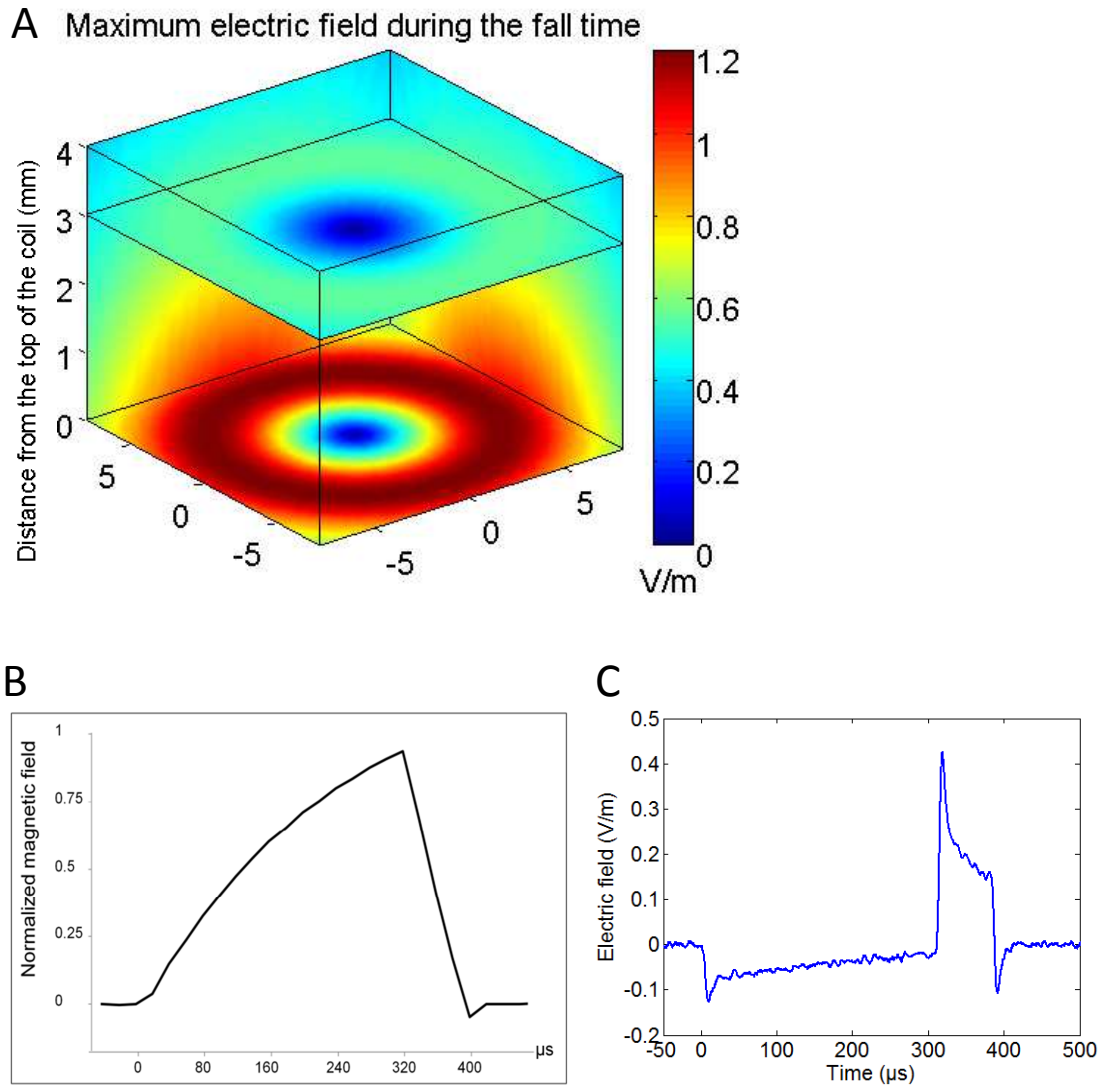

Figure C.1 Magnetic waveform and modelled electric field induced by 24 well coil (Chapter 2). A) Modelled 3D overview of the induced electric field from the top of the coil wiring (horizontal plane at 0 mm). Plane at 3 mm corresponds to average horizontal location of target cells. Colours indicate the electric field strength (V/m). B) Single magnetic pulse waveform in normalized units measured *via* hall effect. The stimulation device was programmed to cease current flow at 300 µs (pulse ON) but due to technical imprecision, pulse ceased at 320 µs. C) Modelled induced electric field strength during one pulse in a round conductor at a radius of 4.5 mm from the central axis and 3 mm vertical distance from top of the coils wiring. Maximum electric field strength at target cells ~ 0.4 V/m during down time of pulse waveform.

D. Coil vibration measurements

All vibration were measured with a single point vibrometer: http://www.polytec.com/us/products/vibration-sensors/single-point-vibrometers/modular-systems/ofv-534-compact-sensor-head

1. Coil used for 24 well plate set-up (Chapter 2)

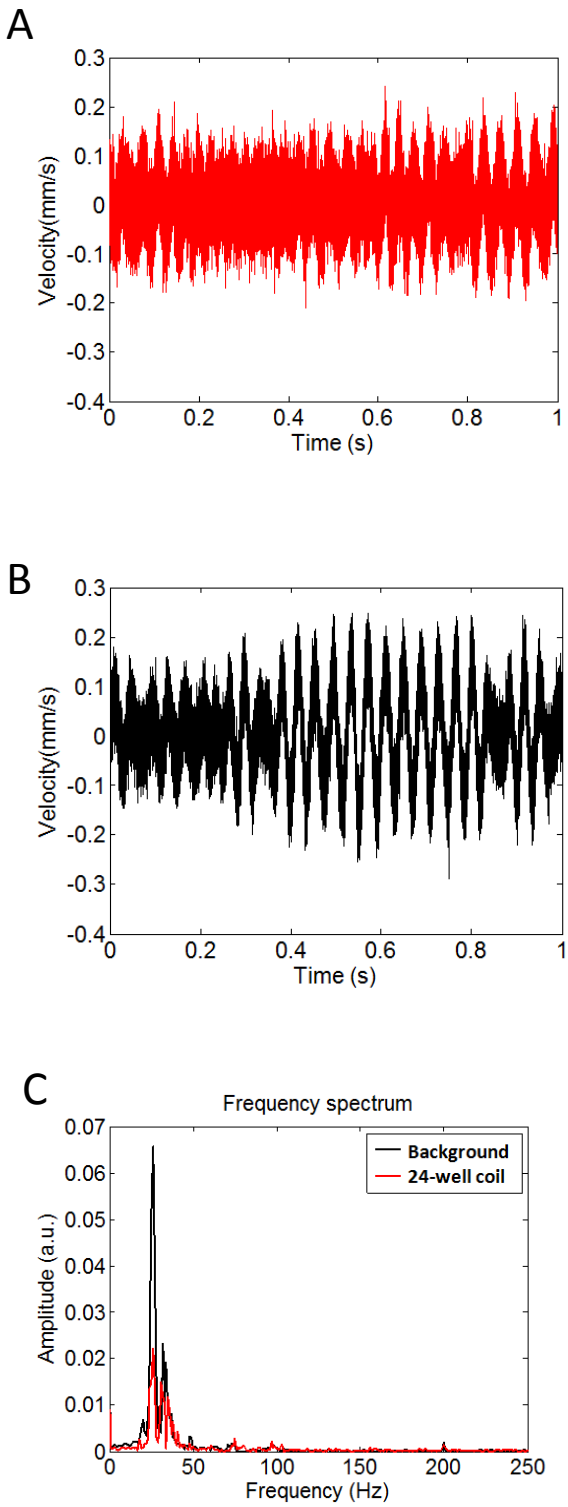

Figure D.1 Vibration measurements of the 24 well coil (A, red) and background surface (B, black) in mm/s as measured by a single point vibrometer with OFV-534 compact sensor head for high optical sensitivity. Vibration velocity of coil is below background vibration. C) Fourier transform of the frequency spectrum, confirming below background amplitude vibrations as shown in Chapter 2/article for publication).

2. Coil used for 6 well plate set-up (Chapter 3+4)

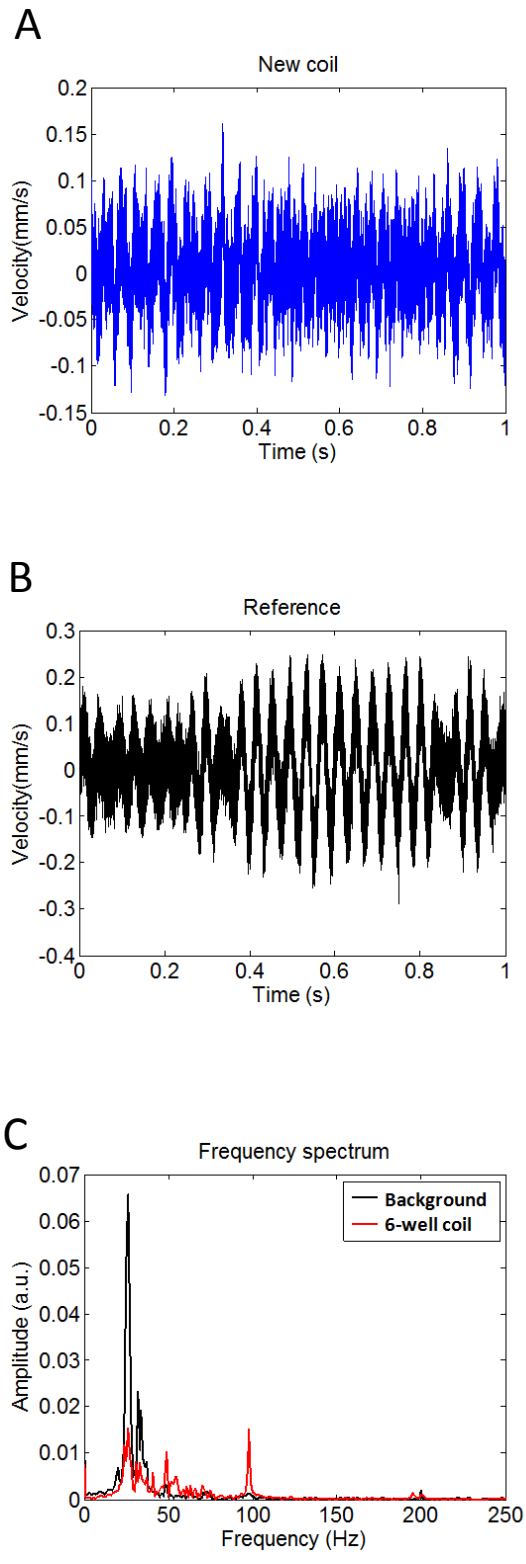

Figure D.2 Vibration measurement of the 6 well coil (A, blue) and background surface (B, black) in mm/s as measured by a single point vibrometer with OFV-534 compact sensor head for high optical sensitivity. Vibration velocity of coil is below background vibration. C) Fourier transform of the frequency spectrum confirming total below background amplitude vibrations.

E. Published manuscript + supplementary material

Grehl, S., Viola, H. M., Fuller-Carter, P. I., Carter, K. W., Dunlop, S. A., Hool, L. C., Sherrard, R.M., Rodger, J. (2015). Cellular and Molecular Changes to Cortical Neurons Following Low Intensity Repetitive Magnetic Stimulation at Different Frequencies. Brain Stimulation, 8(1), 114-123.

Brain Stimulation 8 (2015) 114–123

Contents lists available at ScienceDirect

Brain Stimulation

journal homepage: www.brainstimjrnl.com

Cellular and Molecular Changes to Cortical Neurons Following Low Intensity Repetitive Magnetic Stimulation at Different Frequencies

Stephanie Grehl [a,d], Helena M. Viola [b], Paula I. Fuller-Carter [a], Kim W. Carter [c], Sarah A. Dunlop [a], Livia C. Hool [b], Rachel M. Sherrard [b,d,1], Jennifer Rodger [a,*,1]

[a] School of Animal Biology, University of Western Australia, Perth, Australia
[b] School of Anatomy, Physiology and Human Biology, University of Western Australia, Perth, Australia
[c] Telethon Institute for Child Health Research, Centre for Child Health Research, University of Western Australia, Perth, Australia
[d] Sorbonne Universités, UPMC Univ Paris 06 & CNRS, IBPS-B2A UMR 8256 Biological Adaptation and Ageing, Paris, France

ARTICLE INFO

Article history:
Received 9 February 2014
Received in revised form
5 September 2014
Accepted 21 September 2014
Available online 23 October 2014

Keywords:
Pulsed magnetic fields
Repetitive transcranial magnetic stimulation
rTMS
Cortical neurons
Calcium signaling

ABSTRACT

Background: Repetitive transcranial magnetic stimulation is increasingly used as a treatment for neurological dysfunction. Therapeutic effects have been reported for low intensity rTMS (LI-rTMS) although these remain poorly understood.
Objective: Our study describes for the first time a systematic comparison of the cellular and molecular changes in neurons *in vitro* induced by low intensity magnetic stimulation at different frequencies.
Methods: We applied 5 different low intensity repetitive magnetic stimulation (LI-rMS) protocols to neuron-enriched primary cortical cultures for 4 days and assessed survival, and morphological and biochemical change.
Results: We show pattern-specific effects of LI-rMS: simple frequency pulse trains (10 Hz and 100 Hz) impaired cell survival, while more complex stimulation patterns (theta-burst and a biomimetic frequency) did not. Moreover, only 1 Hz stimulation modified neuronal morphology, inhibiting neurite outgrowth. To understand mechanisms underlying these differential effects, we measured intracellular calcium concentration during LI-rMS and subsequent changes in gene expression. All LI-rMS frequencies increased intracellular calcium, but rather than influx from the extracellular milieu typical of depolarization, all frequencies induced calcium release from neuronal intracellular stores. Furthermore, we observed pattern-specific changes in expression of genes related to apoptosis and neurite outgrowth, consistent with our morphological data on cell survival and neurite branching.
Conclusions: Thus, in addition to the known effects on cortical excitability and synaptic plasticity, our data demonstrate that LI-rMS can change the survival and structural complexity of neurons. These findings provide a cellular and molecular framework for understanding what low intensity magnetic stimulation may contribute to human rTMS outcomes.

Introduction

Repetitive transcranial magnetic stimulation (rTMS) is used in clinical treatment to non-invasively stimulate the brain and promote long-term plastic change in neural circuit function [1,2], with benefits for a wide range of neurological disorders [3–5]. In addition, there is increasing evidence that low intensity magnetic stimulation (LI-rTMS) may also be therapeutic, particularly in mood regulation and analgesia [6–8]. Nonetheless, clinical outcomes of rTMS and LI-rTMS are variable [9] and greater knowledge of the mechanisms underlying different stimulation regimens is needed in order to optimize these treatments.

Investigating the mechanisms of both high and low intensity rTMS is important because most human rTMS protocols deliver a

Funded by an Australian Research Council Linkage grant LP110100201, the National Health and Medical Research Council Australia (Grant No. 634386), the Neurotrauma Program (State Government of Western Australia, funded through the Road Trauma Trust Account, but the project does not reflect views or recommendations of the Road Safety Council) and a French CNRS PICS grant to support the international collaboration. SG is funded by UIS and SIRF grants, University of Western Australia. HV is funded by the National Heart Foundation (Grant No. NHF PF 11P 6024). KWC is supported by the McCusker Charitable Foundation Bioinformatics Centre. LH is an ARC Future Fellow and honorary NHMRC Senior research fellow, JR is an NHMRC Senior Research Fellow and SAD an NHMRC Principal Research Fellow.

* Corresponding author. Experimental and Regenerative Neurosciences M317, School of Animal Biology, University of Western Australia, 35 Stirling Highway, Crawley, WA 6009, Australia. Tel.: +61 8 6488 2245.
E-mail address: jennifer.rodger@uwa.edu.au (J. Rodger).
[1] These two are co-senior authors.

http://dx.doi.org/10.1016/j.brs.2014.09.012
1935-861X/

range of stimulation intensities across and within the brain. Human rTMS is most commonly delivered using butterfly figure-of-eight shaped coils [10,11] to produce focal high-intensity fields that depolarize neurons in a small region of the cortex underlying the intersection of the 2 loops [10,11], which in turn can modulate activity in downstream neural centers [12,13]. However, this stimulation focus is surrounded by a weaker magnetic field such that a large volume of adjacent cortical and sub-cortical tissue is also stimulated, albeit at a lower intensity that is below activation threshold [14,15]. While the functional importance of this parafocal low-intensity stimulation in the context of human rTMS is unclear, low-intensity magnetic stimulation on its own modifies cortical function [7,16] and brain oscillations [17]. Moreover, animal and *in vitro* studies demonstrate that low-intensity stimulation alters calcium signaling [18,19], gene expression [20], neuroprotection [21] and the structure and function of neural circuits [22,23]. However, the mechanisms underlying outcomes of low-intensity magnetic stimulation, particularly in conjunction with different stimulation frequencies, have not been investigated.

To address this, we undertook a systematic investigation of the fundamental morphological and molecular effects of five repetitive low intensity magnetic stimulation (LI-rMS) protocols in a simple *in vitro* system with defined magnetic field parameters. We show for the first time that LI-rMS induces calcium release from intracellular stores. Moreover, we show specific effects of different stimulation protocols on neuronal survival and morphology and associated changes in expression of genes mediating apoptosis and neurite outgrowth. Taken together, our data demonstrate that even low intensity magnetic stimulation induces long-term modifications to neuronal structure, which might have implications for understanding the effects of high-intensity human rTMS in the whole brain.

Methods

Animals

C57Bl/6j mice pups were sourced from the Animal Resources Centre (Canning Vale, WA, Australia). Experimental procedures were approved by the UWA Animal Ethics Committee (03/100/957).

Tissue culture

To investigate changes in neuron biology following LI-rMS stimulation, we used neuronal enriched cultures from postnatal day 1 mouse cortex. Pups were euthanased by pentobarbitone sodium (150 mg/kg i.p.), decapitated and both cortices removed. Pooled cortical tissue was dissociated and prepared following standard procedures [24]. Cells were suspended in NB media (Neurobasal-A, 2% B27 (Gibco®), 0.6 mg/ml creatine, 0.5 mM L-glutamine, 1% Penicillin/Streptomycin, and 5 mM Hepes) and plated on round poly-D-lysine coated coverslips at a density of 75,000 cells/well (day 0 *in vitro*; DIV 0). On DIV 3, half the culture medium was removed and replaced with fresh media containing cytosine arabinofuranoside (6 μM; Sigma) to inhibit glial proliferation. Cells were grown at 37 °C in an incubator (5% CO_2 + 95% air) for 10 days and half the medium was replaced on DIV 6 and 9. To ensure that any experimental effects were not due to either different litters or culture sessions, plated coverslips from each litter were randomly allocated to stimulation groups. The whole culture-stimulation procedure was repeated 3 times.

Repetitive magnetic stimulation

LI-rMS stimulation was delivered to cells in the incubator with a custom built round coil (8 mm inside diameter, 16.2 mm outside diameter, 10 mm thickness, 0.25 mm copper wire, 6.1 Ω resistance, 462 turns) placed 3 mm from the coverslip (Fig. 1A) and driven by a 12 V magnetic pulse generator: a simple resistor-inductor circuit under control of a programmable (C-based code) micro-controller card (CardLogix, USA). The non-sinusoidal monophasic pulse [25] had a measured 320 μs rise time and generated an intensity of 13 mT as measured at the target cells by hall effect (ss94a2d, Honeywell, USA) and assessed by computational modeling using Matlab (Mathworks, USA; Fig. 1B,C). Coil temperature did not rise above 37 °C, ruling out confounding effects of temperature change. Vibration from the bench surface (background) and the top surface of the coil were measured at 10 Hz stimulation using a single-point-vibrometer (Polytec, USA); coil vibration was within vibration amplitude of background (Fig. 1D).

Stimulation was delivered for 10 continuous minutes per day at 1 of 5 frequencies: 1 Hz, which reduces, or 10 Hz which increases, cortical excitability in human rTMS [26,27]; we also used 100 Hz, consistent with very low intensity pulsed magnetic field stimulation [8,28], continuous theta burst stimulation (cTBS: 3 pulses at 50 Hz repeated at 5 Hz) showing inhibitory effects on cortical excitability post-stimulation in human rTMS [29,30] or biomimetic high frequency stimulation (BHFS: 62.6 ms trains of 20 pulses, repeated at 9.75 Hz). The BHFS pattern was designed on electro-biomimetic principles [6], based on the main parameter from our previous studies [22,23] which was modeled on endogenous patterns of electrical fields around activated nerves during exercise (patent PCT/AU2007/000454, Global Energy Medicine). The total number of pulses delivered for each stimulation paradigm is shown in Table 1. We chose a standard duration of stimulation of 10 min (rather than a standard number of pulses) because studies of brain plasticity reveal that 10 min of physical training or LI-rTMS is sufficient to induce functional and structural plasticity [22,23,31]. For all experiments, controls were treated identically but the coils were not activated. An overview of experiments and summary of experimental design is shown in Fig. 1E.

Immunohistochemistry

To investigate the influence of different stimulation frequencies at the cellular level, we used immunohistochemistry to examine neuronal survival and the prevalence of different cell types. Cells plated on glass coverslips were grown in 12 spatially separated wells of a 24 well plate to ensure no overlap of magnetic field. Wells were stimulated for 10 min daily from DIV 6–9 and cells were fixed with 4% paraformaldehyde 24 h after the last stimulation. Mouse anti-active Caspase-3 (1:50, Abcam) and TUNEL (DeadEnd™ Fluorometric TUNEL System, Promega) double labeling were carried out to identify apoptosis. Glia and neurons were labeled with rabbit anti-GFAP (1:500, Dako) or mouse anti-βIII Tubulin (1:500, Covance). Subpopulations of neurons were identified, using rabbit anti-calbindin D-28K (inhibitory and small excitatory neurons; 1:500, Chemicon [32]) or mouse anti-SMI-32 (excitatory neurons; 1:2000, Covance [33]). Antibody binding was visualized using fluorescently labeled secondary antibodies (Alexa Fluor 546 and Alexa Fluor 488; Invitrogen). Cell nuclei were labeled with either Hoechst (1:1000, Sigma Aldrich) or Dapi (DeadEnd™). Coverslips were mounted with Fluoromount-G.

Histological analysis

For each experimental group, histological analyses were performed blind to stimulation paradigm on 12–18 images containing cultured cells from 2 to 3 different litters. Five semi-randomly distributed images per immunostained coverslip were taken from locations underneath the desired magnetic field (13 mT), in order to

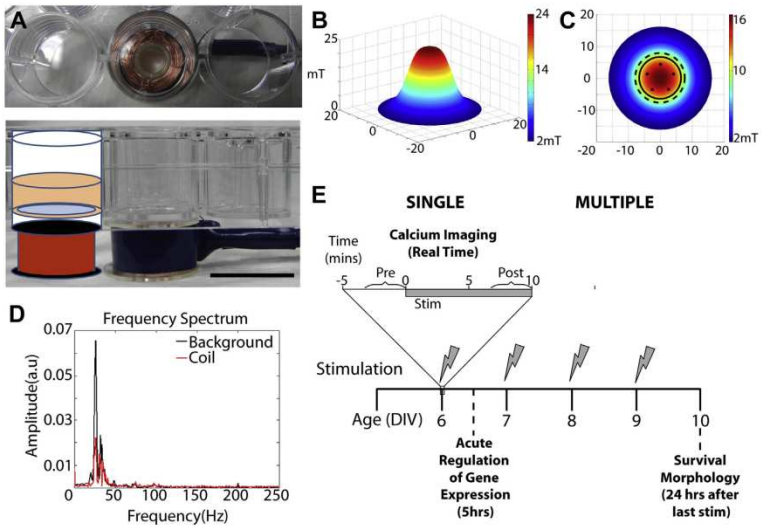

Figure 1. Stimulation apparatus and experimental design. A: photographs of an *in vitro* stimulation coil used in this study. Views are from the top (top panel) and side (bottom panel). The diagram in the bottom panel shows that the coil was placed beneath one well of a 24 well culture dish containing a coverslip (blue) with culture medium (pink). The coil (orange) was located at a distance of 3 mm from the coverslip because of the thickness of the plastic base of the culture dish (white). Note that neighboring wells did not contain coverslips to avoid interactions of magnetic fields from individual coils (compare extent of magnetic field and coverslip shown in C). B: Matlab software model representing the induced magnetic field at the level of the coil, distance in mm. C: Top view of modeled magnetic field strength at 3 mm from the base of the coil (position of the coverslip). Dashed circle represents the well and solid circle represents the edge of the coverslip (Ø = 13 mm). Black dots show the sampling locations for cell counts and morphological analysis. D: Fourier transform of the frequency spectrum of vibration measurement (mm/s) taken by a single-point-vibrometer placed either on the bench surface (background) or on top of the coil (in place of the culture plate as illustrated in A). Vibration measured from background surface (black) and the coil (red) confirms that the coil did not generate vibration above background levels. E: Timeline for our experimental design. We delivered multiple sessions of LI-rMS (DIV6-9) to see the cumulative effects on the survival and morphology of single neurons. Then in separate experiments we examined potential mechanisms underpinning these cellular effects by identifying acute changes induced by a single session of LI-rMS: (1) intracellular calcium during stimulation; (2) gene expression 5 h after stimulation, an interval necessary for transcriptional changes to have occurred. The inset shows the detailed timeframe for intracellular calcium imaging, and is an example for DIV 6. LI-rMS was delivered for 10 min (grey zone). Ratiometric fluorescent values recorded over the last 3 min of stimulation were averaged and reported as a percentage of pre-stimulation baseline. Scale bar (A): 15 mm. (For interpretation of the references to color in this figure legend, the reader is referred to the web version of this article.)

analyze cells that had received similar stimulation intensity. We counted cells labeled with the following antibody combinations: βIII Tubulin or GFAP (neurons/glia), Caspase-3 and TUNEL (apoptotic cells), or Calbindin or SMI-32 (inhibitory/excitatory neurons). Raw counts were normalized to the total cells numbers (Hoechst or DAPI labeled) in the analyzed field (FA). Cells that were not immunolabeled for either marker were identified as 'other' and included in the total cell count.

Morphometric analysis was undertaken on individually visualized neurons. Calbindin labeled neurons had weakly labeled processes thus neurite morphology could not be reliably distinguished. Thus, only SMI-32 positive cells were analyzed. For every cell, the longest neurite was traced and its total length calculated with Image J. To estimate neuronal morphology, fast Sholl analysis [34] was performed, using an Image-Pro®Plus (Media Cybernetics, Inc.) based macro (M. Doulazmi, UPMC).

Table 1
Total number of pulses delivered during 10 min for each frequency.

Frequency	Total pulses delivered in 10 min
1 Hz	600
10 Hz	6000
100 Hz	60,000
cTBS	7000
BHFS	120,000

Calcium imaging

To assess the mechanisms underlying LI-rMS effects, we measured real-time changes in intracellular calcium during stimulation. On DIV 6–10, cells were incubated in 1 μM Fura-2AM (Molecular Probes) supplemented media at 37 °C for 90–120 min. Immediately prior to experimentation, cells were transferred to Fura-2AM supplemented imaging solution containing: 140 mM NaCl, 5 mM KCl, 2.5 mM $CaCl_2$, 0.5 mM $MgCl_2$, 10 mM Glucose and 10 mM Hepes (pH 7.4). Intracellular calcium was assessed at 37 °C as described previously [35] to evaluate ratiometric change and estimate intracellular concentration $[Ca^{2+}]_i$ (nM). Fura-2 340/380 nm ratiometric fluorescence was captured using a Hamamatsu Orca ER digital camera attached to an inverted Nikon TE2000-U microscope (ex 340/380 nm, em 510 nm) and analyzed by manually tracing cells in MetaMorph® 6.3 (Molecular Devices).

Ratiometric fluorescent values were recorded from 5 min pre-stimulation to 5 min post-stimulation (or control) at 1 min time intervals. Analyses were made off-line such that the experimenter was blind to stimulation group. Ratiometric fluorescent values were averaged over the last 3 min of stimulation (μ_{Main}: minutes 8–10), and normalized to the pre-stimulation baseline (μ_{Pre}: minutes 3–5). Percentage Fura-2 ratiometric signal change ($Y_{\%change}$) was calculated ($Y_{\%change} = [(\mu_{Pre} - \mu_{Main})/\mu_{Main}) * 100]$ (Fig. 1E). Pilot experiments showed that there was no effect of culture age (DIV) on calcium responses, thus data were pooled across days.

Following each experiment, cells were fixed with 4% paraformaldehyde and immunostained for GFAP/βIII Tubulin/Hoechst, as described above, to confirm that imaged cells were neurons. Only data from βIII tubulin-positive neurons were included in the analysis.

To investigate the source of increased intracellular calcium, we assessed alterations in intracellular calcium when neurons were either placed in calcium-free imaging solution, or exposed to thapsigargin (3 μM, SIGMA) to deplete intracellular calcium stores. For calcium-free studies, cells were placed in calcium-free imaging solution (140 mM NaCl, 5 mM KCl, 0.5 mM $MgCl_2$, 10 mM HEPES, 10 mM Glucose, 3 mM EGTA, pH 7.4) immediately prior to experimentation. To confirm that results were not based on changes in ion concentration, in some experiments we compensated for the drop in Ca^{2+} with an equi-molar replacement of Mg^{2+} to keep a constant surface charge effect across the membrane. Results showed no difference between these 2 solutions. Thapsigargin studies (supplemented 10 min prior to experimentation) were performed in normal 2.5 mM calcium containing imaging solution. All imaging solutions were supplemented with 1 μM Fura-2AM. Cell viability was confirmed with propidium iodide (PI) post-stimulation and cells that were permeable to PI were excluded from subsequent analysis.

PCR array

To investigate the molecular events triggered by different frequency stimulation, changes in gene expression were examined in a separate series of cultures following a single stimulation at DIV 6. For each group (3 frequencies plus control), three replicates of ten wells underwent one stimulation session. Five hours after the end of stimulation, total RNA was extracted with Trizol (Life Technologies) followed by purification on RNeasy kit columns (Qiagen). cDNA was transcribed from 200 ng of total RNA using the RT^2 Easy First Strand cDNA Synthesis Kit (Qiagen). For each sample, 250 ng of cDNA was applied to the Mouse cAMP/Ca^{2+} Signaling Pathway Finder PCR Array and amplified on a Rotorgene 6000. Results were analyzed by a researcher (K Carter), who did not know the tissue groupings, on the Qiagen RT^2 Profiler PCR array data analysis (v3.5) using the geometric mean of housekeeping genes glyceraldehyde-3-phosphate dehydrogenase and glucuronidase beta. Normalized mean expression levels ($\log2(2 - \Delta Ct)$) were used to determine differentially expressed genes between each group and control. Changes in gene expression were analyzed further in R 3.0.1 using the NMF package [36], Ingenuity Pathways Analysis (IPA) and WebGestalt [37].

Statistical analysis

Data from all groups were explored for outliers and normal distribution with SPSS Statistics 20 (IBM). For cell survival and calcium imaging experiments, effects of frequency were analyzed with One-way Analysis of Variance (Kruskal–Wallis; H) and Mann–Whitney (*U*) pairwise comparisons with Bonferroni-Dunn correction where appropriate. Neurite length data was analyzed with Univariate ANOVA (F). Gene expression levels from the PCR array were compared by two sample *t*-test. All values are expressed as mean ± SEM and considered significant at $P < 0.05$.

Results

We delivered multiple sessions of LI-rMS (DIV6-9) to see the cumulative effects on the survival and morphology of single neurons. We then examined potential mechanisms underpinning these cellular effects by identifying acute changes induced by a single session of LI-rMS: (1) intracellular calcium during stimulation; (2) gene expression 5 h after a single stimulation session, an interval necessary for transcriptional changes to have occurred. The experimental design is summarized in Fig. 1E.

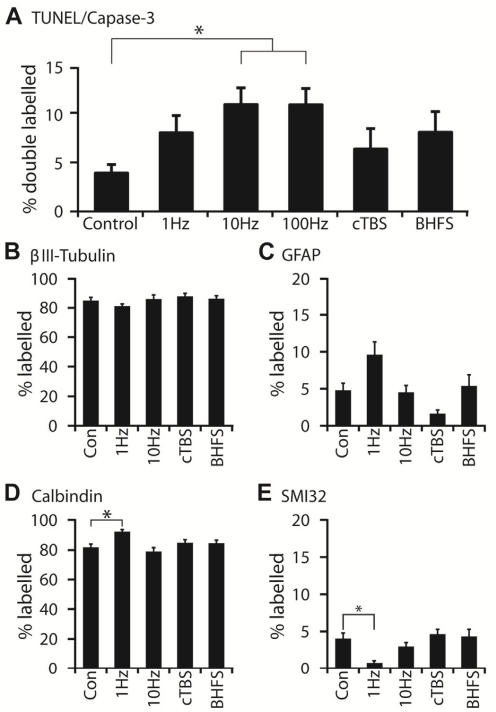

Figure 2. LI-rMS alters cell survival. A: Percentage cells double labeled for Caspase-3 and TUNEL were increased following 10 and 100 Hz compared to unstimulated controls ($H = 14.32$, $P = 0.014$. Pairwise comparisons Control-10 Hz: $U = -23.832$, $P = 0.036$ and Control-100 Hz: $U = -24.237$, $P = 0.044$). B, C: Percentage cells that were labeled with βIII Tubulin (neurons; B) or GFAP (glia; C) (Neuron: $H = 5.93$, $P = 0.204$, Glia: $H = 14.53$, $P = 0.006$. Pairwise comparisons (U): no significant difference to Control). D, E: Percentage cells that were labeled with Calbindin (D) or SMI-32 (E). 1 Hz increased the proportion of calbindin positive inhibitory neurons and decreased SMI-32 positive glutamatergic neurons compared to unstimulated controls ($H = 21.103$, $P = 0.000$. Pairwise comparisons Control-1 Hz: $U = -35.94$, $P = 0.001$. SMI-32: $H = 15.19$, $P = 0.004$. Pairwise comparisons Control-1 Hz: $U = 26.71$, $P = 0.029$). Error bars are standard error of the mean.

rMS stimulation-specific effects on neuronal survival and morphology

We first investigated whether low intensity LI-rMS had deleterious effects and induced apoptosis by counting cells double labeled for Caspase-3 and TUNEL ($N_{\text{fields analyzed (FA)}}$: Control = 22; 1 Hz = 10; 10 Hz = 10; 100 Hz = 9; cTBS = 10; BHFS = 10). While the great majority of cells (about 90%) continued growing normally, there was a small but significant increase of apoptotic cells in cultures stimulated at 10 Hz (11.11% ± 1.84) and 100 Hz (11.08% ± 1.79) compared to unstimulated controls (4.3% ± 0.9; $P = 0.036$ and 0.044 respectively, Fig. 2A). In contrast, stimulation by 1 Hz and complex frequencies did not significantly alter apoptosis (~4–7% cells in

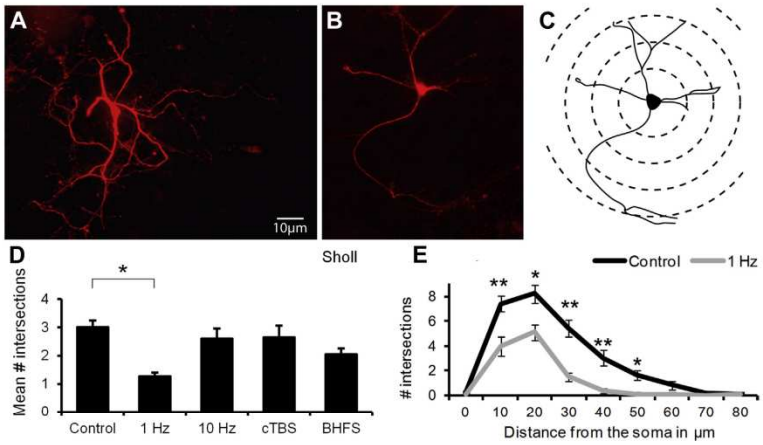

Figure 3. LI-rMS has stimulation pattern-specific effects on neuronal morphology. A, B: Representative neuronal morphology from control (A) and 1 Hz (B) stimulation. C: diagram illustrating Sholl analysis. D: mean number of dendrite intersections per neuron following LI-rMS (4 days, 10 min per day) at different frequencies ($H = 17.84$, $P = 0.001$. Pairwise comparisons Control-1 Hz: $U = 30.771$, $P = 0.001$). E: Number of intersections per concentric Sholl circle from 10 to 80 μm from the soma are decreased in 1 Hz stimulated samples compared to unstimulated controls (10 μm: $U = 7.13$, $P = 0.008$, 20 μm: $U = 5.94$, $P = 0.015$, 30 μm: $U = 7.86$, $P = 0.005$, 40 μm: $U = 6.84$, $P = 0.009$, 50 μm: $U = 5.29$, $P = 0.021$). Error bars are standard error of the mean.

each group). Because stimulation at 100 Hz did not induce more apoptosis than 10 Hz, it was not investigated further.

We next evaluated whether different LI-rMS patterns altered the proportions of neurons and glia in primary cortical cultures (N_{FA}: Control = 19; 1 Hz = 18; 10 Hz = 18; cTBS = 18; BHFS = 15). The ratio of neurons-to-glia following stimulation at any frequency was no different from unstimulated control cultures (Fig. 2B,C), suggesting that the small amount of apoptosis (~4–7%) involved all cell types equally. On average, pooled across all frequencies, we observed 85.6% ± 1.1 neurons, 5.1% ± 1.3 glia and 9.3% undefined cells in our cultures.

Because some studies have shown that magnetic fields differentially affect inhibitory and excitatory neurons [38,39] we quantified the proportions of two neuronal populations: calbindin D-28K-positive neurons, which are predominantly inhibitory [32], and SMI-32-labeled excitatory neurons (N_{FA}: Control = 24; 1 Hz = 13; 10 Hz = 25; cTBS = 16; BHFS = 14). The higher proportion of inhibitory neurons in early postnatal cultures is in line with previous studies [40]. Only 1 Hz stimulation altered the relative proportions by increasing that of calbindin positive neurons ($P = 0.001$), from 81.6% ± 1.8 in control cultures to 92.2% ± 1.7, while decreasing the percentage of SMI-32 positive neurons ($P = 0.029$), from 4.1% ± 0.8 in control cells to 0.8% ± 0.3 (Fig. 2D,E). This reduction in number of SMI-32 positive cells (3.3%) is within the 4–7% cell death observed in control and 1 Hz stimulated cultures (Fig. 2A) and suggests that LI-rMS at 1 Hz slightly impaired survival of SMI-32 positive excitatory neurons without increasing apoptosis overall.

We then investigated neurite branching and outgrowth from individual SMI-32 positive neurons (*N*: Control = 24; 1 Hz = 8; 10 Hz = 14; cTBS = 7; BHFS = 11). Stimulation at 1 Hz significantly reduced neurite branching and outgrowth by 60% compared to control neurons (Fig. 3A–E; $P = 0.001$). Sholl analysis revealed that changes occurred 10–50 μm from the soma (Fig. 3E). However, the length of the longest neurite of each SMI-32 positive neuron was not significantly different between stimulation frequencies ($F = 0.936$, $P = 0.45$).

LI-rMS releases calcium from intracellular stores

To identify mechanisms that may explain these morphological and cell survival data, we examined changes in intracellular calcium during stimulation. Compared to unstimulated controls, each of 10 Hz, cTBS and BHFS stimulation significantly increased Fura-2 ratiometric fluorescence ($P < 0.001$; Fig. 4A) by 11–13 % (Control: 2.1% ± 0.8; 10 Hz: 13.4% ± 2.3; cTBS: 15.0% ± 2.6 and BHFS: 15.1% ± 2.0). This is equivalent to an average change in intracellular Ca^{2+} from 34.31 nM ± 7.44 in control to 414.77 nM ± 41.52 after 10 min stimulation, a rise which is in the range of increased Ca^{2+} concentration following action potential induction [41,42]. In contrast, 1 Hz stimulation induced an intermediate increase (8.3% ± 1.1) in Fura-2 ratiometric fluorescence which was not significantly different from either unstimulated control or other stimulation frequencies (Fig. 4A). No impact on neuronal viability was observed following a single session of LI-rMS stimulation (data not shown).

To determine whether the increase in intracellular calcium originated from the extracellular milieu or intracellular stores, we stimulated neurons either in calcium-free imaging solution, or after thapsigargin treatment (Fig. 4B). Because of apparent equivalence of effect for cTBS and BHFS stimulation in previous experiments, pharmacological tests were carried out on 1 Hz, 10 Hz and BHFS frequencies. For all frequencies, the increase in neuronal Fura-2 ratiometric fluorescence under calcium-free conditions was not significantly different from that in normal imaging media (1 Hz: 10.7% ± 2.5; 10 Hz: 14.7% ± 1.8 and BHFS: 14.7% ± 1.7). In contrast, exposure of cells to thapsigargin resulted in strong attenuation of the Fura-2 signal during stimulation at all frequencies ($P < 0.05$; 1 Hz: 1.5% ± 1.4, 10 Hz: 4.6% ± 2.4 and BHFS: 0.4% ± 0.4). These data indicate that LI-rMS stimulation induces release of Ca^{2+} from intracellular stores rather than influx from the extracellular milieu (Fig. 4B).

LI-rMS changes expression of genes implicated in neuronal survival

To further understand how LI-rMS may lead to changes in cell survival and morphology, we examined the immediate up-and

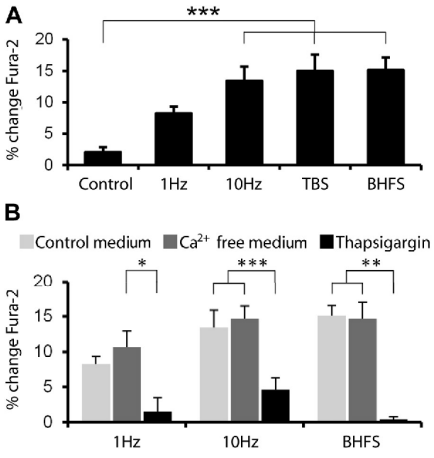

Figure 4. LI-rMS induces Ca^{2+} release from intracellular stores. Alterations in Fura-2 340/380 nm ratiometric fluorescence (% change Fura-2) in cortical neurons after a single 10 min stimulation with 1 Hz, 10 Hz, cTBS and BHFS frequencies. A: LI-rMS at each of 10 Hz, cTBS and BHFS increased intracellular calcium compared to unstimulated controls, while 1 Hz only generated an intermediate rise ($H = 20.7$, $P = 0.000$. Pairwise comparisons Control-10 Hz: $U = -27.97$, $P = 0.007$; Control-cTBS: $U = -32.48$, $P = 0.001$; Control-BHFS: $U = -38.03$, $P = 0.000$). B: LI-rMS induced similar increase in Fura-2 ratiometric fluorescence in normal imaging and calcium-free media but not in thapsigargin supplemented ($H = 20.89$, $P = 0.000$. Pairwise comparisons Normal-Thapsigargin: $U = 23.6$, $P = 0.000$; Ca^{2+} free − Thapsigargin: $U = 31.39$, $P = 0.000$). Error bars are standard error of the mean.

downregulation of genes associated with Ca^{2+} signaling, 5 h after a single session of stimulation at different frequencies. Raw data are provided on UWA's data sharing website (http://researchdataonline.research.uwa.edu.au/). We identified 16 genes (Table 2; Fig. 5A) for which expression changes were significantly different from unstimulated controls ($P < 0.05$) in at least one of the three experimental groups (Fig. 5B). Enrichment analysis on these 16 genes in IPA and gene ontology terms (Webgestalt; Supplementary Table 1) revealed that 15 of the 16 genes were significantly associated with two major biofunctions: 1) cell survival and apoptosis and 2) cell morphology and migration (Fig. 5C). The remaining gene, slc18a1 encodes a vesicular monoamine transporter and was significantly increased following stimulation with 10 Hz.

All LI-rMS frequencies induced changes in genes situated within neuronal survival or apoptosis pathways (Fig. 6A, B), of which some were common to all frequencies (ENO2 and CRH), and others pattern-specific (Figs. 5B and 6A, B; Table 2). 10 Hz stimulation, which was associated with apoptosis, upregulated pro-apoptotic genes (e.g. Pmaip1/Noxa, and BRCA1) and downregulated anti-apoptotic genes (e.g. JunD). In addition, stimulation by frequencies which did not induce apoptosis resulted in pro-survival changes to gene expression (e.g. 1 Hz upregulated hexokinase and BHFS downregulated cdk5 and Sod2). These data also show that although all our LI-rMS paradigms altered intracellular Ca^{2+}, the downstream effects on gene expression were specific for each stimulation frequency and rhythm.

Discussion

This study used cortical neuron cultures to identify cellular and molecular mechanisms underlying the outcomes of different low intensity magnetic stimulation parameters. Our data show differential effects of specific LI-rMS paradigms on neuronal survival and morphology. Furthermore, evidence for calcium release from intracellular stores and stimulation-specific regulation of gene expression identify a potential cellular and molecular framework for understanding what low intensity magnetic stimulation may contribute to rTMS outcomes in humans.

Paradigm-specific effects on neuronal survival: dose vs rhythm

Our study shows specific effects of different LI-rMS paradigms on neuronal survival, suggesting that the overall stimulation load (pulse

Table 2
List of genes that were significantly up or downregulated (Student *t*-test) 5 h after a single PMF stimulation at 1 Hz, 10 Hz or BHFS frequencies. Fold change (primary colors indicate upregulation and pastels indicate downregulation) and *P*-values are relative to unstimulated controls.

ID	Entrez Gene Name	1Hz p-value	1 Hz Log FC	10 Hz p-value	10Hz Log FC	BHFS p-value	BHFS Log FC	Function	Type(s)
Brca1	breast cancer 1, early onset	0.27	1.200	0.03	1.530	0.62	1.070	Cell survival	transcription regulator
Cdk5	cyclin-dependent kinase 5	0.75	-1.030	0.68	-1.040	0.03	-1.220	Cytoskeletal remodelling	Nuclear kinase
Cga	glycoprotein hormones, alpha polypeptide	0.20	2.620	0.75	1.050	0.04	1.640	Cell survival	hormone
Crh	corticotropin releasing hormone	0.01	-1.540	0.03	-1.620	0.003	-1.500	Cell survival	Extracellular cytokine
Cyr61	cysteine-rich, angiogenic inducer, 61	0.19	1.290	0.06	1.370	0.03	1.410	Cytoskeletal remodelling	Extracellular protein
Eno2	enolase 2 (gamma, neuronal)	0.04	-2.590	0.03	-2.740	0.03	-2.560	Cell survival	Cytoplasmic enzyme
Gem	GTP binding protein overexpressed in skeletal muscle	0.85	-1.050	0.33	-1.110	0.02	-1.330	apoptosis	Membrane enzyme
Hk2	hexokinase 2	0.04	1.360	0.14	1.280	0.57	-1.090	Cell survival	Cytoplasmic kinase
Hspa4	heat shock 70kDa protein 4	0.09	-1.350	0.08	-1.280	0.04	-1.610		Cytoplasmic protein
Junb	jun B proto-oncogene	0.04	-2.330	0.03	-2.670	0.08	-1.860	Cell survival	transcription regulator
Jund	jun D proto-oncogene	0.07	-1.950	0.007	-2.510	0.33	-1.300	Cell survival	transcription regulator
Pmaip1	phorbol-12-myristate-13-acetate-induced protein 1	0.31	1.980	0.03	2.860	0.30	1.620	apoptosis	Cytoplasmic protein
Pou1f1	POU class 1 homeobox 1	0.26	-2.470	0.10	-1.760	0.04	-3.220	Cell survival	transcription regulator
Slc18a1	solute carrier family 18 (vesicular monoamine), member 1	0.37	2.320	0.04	2.480	0.23	3.650		Membrane transporter
Sod2	superoxide dismutase 2, mitochondrial	0.22	-1.310	0.71	-1.090	0.03	-1.580	apoptosis	Cytoplasmic enzyme
Tnf	tumor necrosis factor	0.34	-1.610	0.04	-2.390	0.89	-1.160	Cell survival	Extracellular cytokine

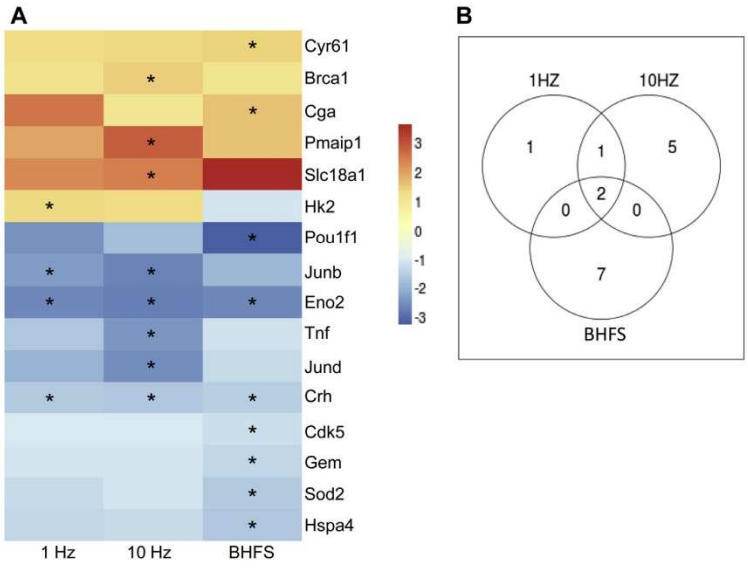

C

Molecules in Network	Focus Molecules	Top Functions
Brca1, Cdk5, Cga, Crh, Cyr61, Eno2, Gem, Hk2, Hspa4, Junb, Jund, Pmaip1, Pou1f1, Slc18a1, Sod2, Tnf, TSHB, GH2, Crhr	15	Cell Death and Survival, Cell Cycle, Cellular Development, Endocrine System Disorders, Cellular Growth and Proliferation, Hematological System Development and Function
Slc18	1	Cell-To-Cell Signaling and Interaction, Nervous System Development and Function, Cellular Growth and Proliferation

Figure 5. Changes in gene expression following different LI-rMS stimulation protocols. A: Heat map showing changes in expression (log_2 fold change) of the 16 genes that were significantly (asterisks) regulated following LI-rMS stimulation at one or more frequencies. B: Venn diagram showing number of changes in gene expression that are common to all frequencies and those that are specific to individual frequencies. C: Biofunctions of the 16 modulated genes as identified in Ingenuity Pathway analysis.

number and density) and/or rhythm of pulse delivery may be important. It has recently been proposed that there is no simple dose-dependent cumulative effect of rTMS on the cerebral cortex [43]. Our data on isolated cortical neurons, showing that several low-intensity stimulation paradigms induce similar changes to intracellular calcium concentration but different patterns of gene expression and cell survival, extend this hypothesis to suggest that pulse rhythm, i.e. the pattern of stimulation frequency, is a primary determinant.

Considering pulse trains delivered at simple frequencies, increasing stimulation load (pulses/unit time) is associated with an increase in intracellular Ca^{2+} and cell death. In the group that received the lowest number of pulses (1 Hz: 600 pulses), there was only an intermediate non-significant increase in intracellular Ca^{2+} and a level of apoptosis that was within the range observed in control cultures (4%). Moreover, increasing stimulation load with 10 and 100 Hz (6000 and 60,000 pulses within the 10 min stimulation period), significantly increased intracellular Ca^{2+} and overall cellular apoptosis, consistent with the deleterious effect of prolonged magnetic stimulation to human monocyte leukemia cells [44]. Such fundamental biological knowledge will be important to future human rTMS as advances in coil cooling will permit longer stimulation trains without frequent TMS-free pauses seen in current clinical practice [5]. In contrast, even higher stimulation load, but delivered with a complex biomimetic frequency (TBS: 7000 and BHFS: 120,000 pulses within 10 min) did not increase neuronal apoptosis despite rises in intracellular Ca^{2+} similar to those following 10 Hz. This not only confirms the hypothesis that dose and effect are not simply related [43,45], but suggests that the rhythm with which the pulses are delivered is fundamental to their effect. By mimicking endogenous patterns of neuronal firing, biomimetic complex waveforms may induce more intricate and biologically safe changes compared to simple frequencies [6,27]. One

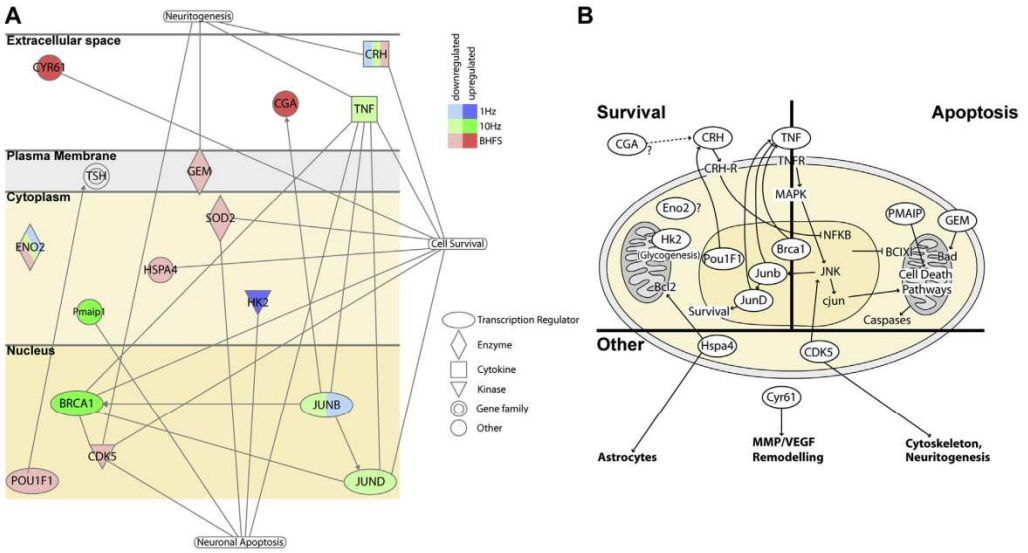

Figure 6. Representations of the relationships between 15 genes that were significantly regulated following LI-rMS stimulation. A: Pathway diagram obtained from Ingenuity Pathway Analysis showing the relationship between the genes examined following LI-rMS (blue = 1 Hz; green = 10 Hz and red = BHFS). Dark shading indicates upregulation and light shading indicates downregulation. B: Regulated genes (in ovals) are situated within the cell survival and cell death pathways (see also Table 2 and Fig. 5C). Non-regulated genes are included to provide context. (For interpretation of the references to color in this figure legend, the reader is referred to the web version of this article.)

possible mechanism underlying these observations is frequency- and pattern-specific regulation of calcium-buffering proteins [46–48], which is likely to contribute to the complex relationship between stimulation load, regulation of intracellular Ca^{2+} levels and cell viability. Indeed the promising therapeutic outcomes in human patients using TBS, albeit at high-intensity [49,50], would appear to support the hypothesis. Thus our data shows a complex interplay between pulse frequency, rhythm and outcome, confirms the recent suggestion that appropriately designed rTMS protocols may generate highly adaptable therapies to treat a wide range of neurological conditions [5].

The possibility that the effect of LI-rMS is determined by the number and/or rhythm of pulses was supported by our gene expression studies, which show that 1 Hz results in fewer gene-expression changes than 10 Hz and BHFS stimulation and BHFS alters a greater number of genes than 10 Hz. The majority of the regulated genes in our study were associated with cell survival and apoptosis pathways (Fig. 5C), consistent with evidence for pro-survival [21] or pro-apoptotic [44,51] effects of magnetic fields and our survival data (discussed above). All frequencies in our study downregulated neuron-specific enolase (ENO2) and corticotrophin-releasing hormone (CRH), both of which have neuroprotective properties [52,53]. However, in addition, we show paradigm-specific regulation of genes within neuronal survival and apoptosis pathways. Increased apoptosis after 10 Hz stimulation was associated with the upregulation of pro-apoptotic [54,55] and downregulation of anti-apoptotic genes [56,57]. In contrast, stimulation by frequencies which did not induce apoptosis showed survival-promoting gene expression changes [58,59]. Given that neuroprotective effects of rTMS remain controversial [60], further characterization of these gene expression changes at the protein and functional level could identify novel neuroprotective therapies for treatment of neurological disorders.

Stimulation-specific effects of LI-rMS on neuronal morphology: implications for reorganization of cortical circuits

In addition to effects on neuronal survival, our data also shows a stimulation pattern-specific effect on neuronal morphology. 1 Hz stimulation reduced neurite complexity of glutamatergic projection neurons, consistent with a recent study in hippocampal neurons *in vitro* demonstrating that 1 Hz magnetic stimulation reduced dendritic branching and damaged synaptic structure [61]. This suggests that the intermediate rise in Ca^{2+} following 1 Hz stimulation, although statistically non-significant, has biological relevance. In addition, 1 Hz-induced neurite regression would have the net effect of reducing excitatory connectivity within a cortical circuit, which is consistent with the LTD-like effects of 1 Hz rTMS on the human cortex [62]. However, we studied dissociated neurons, with minimal contact between neurites, suggesting that magnetic stimulation may directly alter neuronal structure beyond those changes (e.g. spines) associated with modulation from synaptic signaling [48,63,64].

Although we did not observe morphological changes when applying other frequencies, BHFS upregulated Cyr61, which is involved in the control of dendritic growth and has been associated with reorganization of neuronal projections [65] and in association with longer treatment may contribute to the reorganization of abnormal circuitry induced by LI-rTMS at BHFS frequency [22,23].

Intracellular Ca^{2+} increase: mechanism of cortical plasticity?

Changes in intracellular Ca^{2+} in response to magnetic fields have been demonstrated in a range of cells [18,66,67]. We show here for the first time that in neurons LI-rMS releases Ca^{2+} from intracellular stores. This provides a mechanism for LI-rMS induced cellular and molecular changes that is independent of action potential

induction, given that the stimulation was subthreshold, estimated to be 0.5 V/m [6], which is several orders of magnitude below the ~50 V/m that depolarizes neurons [43]. This concurs with our gene expression data in which markers of synaptic activity and action potential firing (e.g. CREB and BDNF) were not upregulated (data not shown). Importantly, calcium release from intracellular stores can modulate synaptic plasticity [68] even without action potential firing and associated calcium influx. Therefore our data provide a mechanism to explain the effects of low intensity magnetic stimulation on cortical neurons [16], and provides a cellular and molecular framework for understanding what low intensity magnetic stimulation may add to the altered calcium signaling induced by the high-intensity focus of human rTMS, and thus its potential contribution to human rTMS outcomes.

Elucidation of novel mechanisms: relevance of in vitro *low intensity LI-rMS to human rTMS*

As discussed above, we have identified changes to cell morphology, intracellular calcium flux and gene expression in isolated neurons stimulated by subthreshold low-intensity magnetic pulses. This experimental paradigm is *very different* from the peri-threshold high-intensity stimulation of whole neural networks in human rTMS; so what do our data contribute? First, our data reveal for the first time a fundamental cellular mechanism of non-depolarizing magnetic fields on neurons, which in the *in vivo* context would underlie any trans-synaptic, neural circuit or cell environment responses. This could only be achieved by the application of a defined magnetic field to isolated cortical neurons, thus removing the confounding effects of glial responses and neuronal circuit activity from the observed outcomes. However, neurons that are maintained in culture are relatively immature, albeit fully differentiated, and not integrated within functioning neural networks. Thus their response to magnetic fields may be modified by different receptor and calcium-buffering capacities to adult neurons, especially in the absence of normal glial metabolic regulation and afferent activity. This, in turn, may make these neurons more susceptible to the low-intensity stimulation we induced in a manner that would not occur in the adult human brain even to higher intensity stimulation. Second, we identified potentially deleterious effects of 10 min continuous stimulation (slight increase in neuronal apoptosis) even at low intensity. Although such continuous pulse trains are not given in current human rTMS, the concern our data raise has pertinence to potential future human rTMS protocols as advances in coil-cooling technology may remove the requirement for short stimulation trains interspersed with TMS-free pauses. Taken together, our data demonstrate a novel cell-intrinsic mechanism for low intensity magnetic field stimulation of neurons which provides new insights into the structural and functional plastic changes described following low intensity magnetic stimulation [8,16,22,23]. Importantly, this mechanism may also be evoked during high-intensity stimulation, thus potentially working together with previously described metabolic and synaptic plasticity mechanisms of human rTMS [12,61,64,69,70].

Conclusion

In summary, our data show that magnetic fields of different frequencies and rhythms alter intracellular calcium concentration and gene expression, which are consistent with long-term modulation of neuronal survival. The immediate modification of calcium levels and gene expression support the development of long-term changes following multiple stimulation sessions. Taken together with our previous study demonstrating that LI-rTMS can induce reorganization of neural circuits *in vivo* [22,23] our data indicate that effects of low intensity stimulation as a by-product of high-intensity rTMS coils cannot be disregarded. Although, our stimulation parameters did not directly mimic those used in human rTMS, the knowledge about mechanisms underlying the effects of different stimulation paradigms provided by this study will contribute to understanding magnetic stimulation outcomes and optimizing therapeutic application in humans.

Acknowledgments

We are grateful to Marissa Penrose and Michael Archer for technical assistance, Rob Woodward and Andrew Garrett for scientific advice and assistance and Mohamed Doulazmi for the fast Sholl Analysis program and scientific advice. Finally we would like to thank Global Energy Medicine Pty Ltd for the donation of stimulation devices.

Supplementary data

Supplementary data related to this article can be found at http://dx.doi.org/10.1016/j.brs.2014.09.012.

References

[1] Pell GS, Roth Y, Zangen A. Modulation of cortical excitability induced by repetitive transcranial magnetic stimulation: Influence of timing and geometrical parameters and underlying mechanisms. Prog Neurobiol 2011;93(1):59–98.
[2] Thickbroom G. Transcranial magnetic stimulation and synaptic plasticity: experimental framework and human models. Exp Brain Res 2007;180:583–93.
[3] Adeyemo BO, Simis M, Macea D, Fregni F. Systematic review of parameters of stimulation: clinical trial design characteristics and motor outcomes in noninvasive brain stimulation in stroke. Front Psychiatry 2012;3(88) [Review].
[4] George MS, Taylor JJ, Short EB. The expanding evidence base for rTMS treatment of depression. Curr Opin Psychiatry 2013;26:13–8.
[5] Daskalakis ZJ. Theta-burst transcranial magnetic stimulation in depression: when less may be more. Brain 2014;137:1860–2.
[6] Martiny K, Lunde M, Bech P. Transcranial low voltage pulsed electromagnetic fields in patients with treatment-resistant depression. Biol Psychiatry 2010;68:163–9.
[7] Robertson JA, Theberge J, Weller J, Drost DJ, Prato FS, Thomas AW. Low-frequency pulsed electromagnetic field exposure can alter neuroprocessing in humans. J R Soc Interface 2010 Mar 6;7(44):467–73.
[8] Di Lazzaro V, Capone F, Apollonio F, et al. A consensus panel review of central nervous system effects of the exposure to low-intensity extremely low-frequency magnetic fields. Brain Stimul 2013;6:469–76.
[9] Wassermann EM, Zimmermann T. Transcranial magnetic brain stimulation: therapeutic promises and scientific gaps. Pharmacol Ther 2012;133(1):98–107.
[10] Fatemi-Ardekani A. Transcranial magnetic stimulation: physics, electrophysiology, and applications. Crit Rev Biomed Eng 2008;36(5–6):375–412.
[11] Thielscher A, Kammer T. Electric field properties of two commercial figure-8 coils in TMS: calculation of focality and efficiency. Clin Neurophysiol 2004;115(7):1697–708.
[12] Valero-Cabre A, Payne BR, Rushmore J, Lomber SG, Pascual-Leone A. Impact of repetitive transcranial magnetic stimulation of the parietal cortex on metabolic brain activity: a 14C-2DG tracing study in the cat. Exp Brain Res 2005;163(1):1–12.
[13] Aydin-Abidin S, Trippe J, Funke K, Eysel UT, Benali A. High- and low-frequency repetitive transcranial magnetic stimulation differentially activates c-Fos and zif268 protein expression in the rat brain. Exp Brain Res 2008;188(2):249–61.
[14] Cohen LG, Roth B, Nilsson J, et al. Effects of coil design on delivery of focal magnetic stimulation. Technical considerations. Electroencephalogr Clin Neurophysiol 1990;75:350–7.
[15] Deng Z-D, Lisanby SH, Peterchev AV. Electric field depth–focality tradeoff in transcranial magnetic stimulation: simulation comparison of 50 coil designs. Brain Stimul 2013;6(1):1–13.
[16] Capone F, Dileone M, Profice P, et al. Does exposure to extremely low frequency magnetic fields produce functional changes in human brain? J Neural Transm 2009;116(3):257–65.
[17] Cook CM, Thomas AW, Prato FS. Resting EEG is affected by exposure to a pulsed ELF magnetic field. Bioelectromagnetics 2004;25(3):196–203.
[18] Pessina GP, Aldinucci C, Palmi M, et al. Pulsed electromagnetic fields affect the intracellular calcium concentrations in human astrocytoma cells. Bioelectromagnetics 2001;22(7):503–10.
[19] Piacentini R, Ripoli C, Mezzogori D, Azzena GB, Grassi C. Extremely low-frequency electromagnetic fields promote in vitro neurogenesis via upregulation of Cav1-channel activity. J Cell Physiol 2008;215(1):129–39.
[20] Mattsson M-O, Simkó M. Is there a relation between extremely low frequency magnetic field exposure, inflammation and neurodegenerative diseases? A

review of in vivo and in vitro experimental evidence. Toxicology 2012;301(1–3):1–12.
[21] Yang Y, Li L, Wang Y-G, et al. Acute neuroprotective effects of extremely low-frequency electromagnetic fields after traumatic brain injury in rats. Neurosci Lett 2012;516(1):15–20.
[22] Rodger J, Mo C, Wilks T, Dunlop SA, Sherrard RM. Transcranial pulsed magnetic field stimulation facilitates reorganization of abnormal neural circuits and corrects behavioral deficits without disrupting normal connectivity. FASEB J 2012;26(4):1593–606.
[23] Makowiecki K, Harvey A, Sherrard RM, Rodger J. Low-intensity repetitive transcranial magnetic stimulation improves abnormal visual cortical circuit topography and upregulates BDNF in mice. J Neurosci 2014;34:10780–92.
[24] Meloni BP, Majda BT, Knuckey NW. Establishment of neuronal in vitro models of ischemia in 96-well microtiter strip-plates that result in acute, progressive and delayed neuronal death. Neuroscience 2001;108(1):17–26.
[25] Peterchev AV, Murphy DL, Lisanby SH. Repetitive transcranial magnetic stimulator with controllable pulse parameters. J Neural Eng 2011;8(3):2922–6.
[26] Fitzgerald PB, Fountain S, Daskalakis ZJ. A comprehensive review of the effects of rTMS on motor cortical excitability and inhibition. Clin Neurophysiol 2006;117:2584–96.
[27] Hoogendam JM, Ramakers GMJ, Di Lazzaro V. Physiology of repetitive transcranial magnetic stimulation of the human brain. Brain Stimul 2010;3(2):95–118.
[28] Ash M, Martin B, Edward E, Kuo-Chen C, Matthew SG, Reba G. Steps to the clinic with ELF EMF. Nat Sci 2009;1(3):157–65.
[29] Gamboa OL, Antal A, Laczo B, Moliadze V, Nitsche MA, Paulus W. Impact of repetitive theta burst stimulation on motor cortex excitability. Brain Stimul 2011;4:145–51.
[30] Huang Y-Z, Edwards MJ, Rounis E, Bhatia KP, Rothwell JC. Theta burst stimulation of the human motor cortex. Neuron 2005;45(2):201–6.
[31] Angelov DN, Ceynowa M, Guntinas-Lichius O, et al. Mechanical stimulation of paralyzed vibrissal muscles following facial nerve injury in adult rat promotes full recovery of whisking. Neurobiol Dis 2007;26:229–42.
[32] Brederode van JFM, Helliesen MK, Hendrickson AE. Distribution of the calcium-binding proteins parvalbumin and calbindin-D28k in the sensorimotor cortex of the rat. Neuroscience 1991;44(1):157–71.
[33] DeFelipe J. Types of neurons, synaptic connections and chemical characteristics of cells immunoreactive for calbindin-D28K, parvalbumin and calretinin in the neocortex. J Chem Neuroanat 1997;14(1):1–19.
[34] Gutierrez H, Davies AM. A fast and accurate procedure for deriving the Sholl profile in quantitative studies of neuronal morphology. J Neurosci Methods 2007;163(1):24–30.
[35] Viola HM, Arthur PG, Hool LC. Transient exposure to hydrogen peroxide causes an increase in mitochondria-derived superoxide as a result of sustained alteration in L-type Ca^{2+} channel function in the absence of apoptosis in ventricular myocytes. Circ Res 2007;100:1036–44.
[36] Gaujoux R, Seoighe C. A flexible R package for nonnegative matrix factorization. BMC Bioinformatics 2010;11(1):367.
[37] Zhang B, Kirov S, Snoddy J. WebGestalt: an integrated system for exploring gene sets in various biological contexts. Nucleic Acids Res 2005;33(Suppl. 2):W741–8.
[38] Benali A, Trippe J, Weiler E, et al. Theta-burst transcranial magnetic stimulation alters cortical inhibition. J Neurosci 2011;31:1193–203.
[39] Meyer JF, Wolf B, Gross GW. Magnetic stimulation and depression of mammalian networks in primary neuronal cell cultures. IEEE Trans Biomed Eng 2009;56:1512–23.
[40] Alho H, Ferrarese C, Vicini S, Vaccarino F. Subsets of GABAergic neurons in dissociated cell cultures of neonatal rat cerebral cortex show co-localization with specific modulator peptides. Brain Res 1988 Apr 1;467(2):193–204.
[41] Liao CW, Lien CC. Estimating intracellular Ca2+ concentrations and buffering in a dendritic inhibitory hippocampal interneuron. Neuroscience 2009;164(4):1701–11.
[42] Helmchen F, Borst JG, Sakmann B. Calcium dynamics associated with a single action potential in a CNS presynaptic terminal. Biophys J 1997;72(3):1458–71.
[43] Volz LJ, Benali A, Mix A, Neubacher U, Funke K. Dose-dependence of changes in cortical protein expression induced with repeated transcranial magnetic theta-burst stimulation in the rat. Brain Stimul 2013;6(4):598–606.
[44] Stratton D, Lange S, Inal JM. Pulsed extremely low-frequency magnetic fields stimulate microvesicle release from human monocytic leukaemia cells. Biochem Biophys Res Commun 2013;430(2):470–5.
[45] Nettekoven C, Volz LJ, Kutscha M, et al. Dose-dependent effects of theta burst rTMS on cortical excitability and resting-state connectivity of the human motor system. J Neurosci 2014;34(20):6849–59.
[46] Gilabert JA. Cytoplasmic calcium buffering. In: Islam MS, editor. Calcium signaling. London: Springer; 2012.
[47] Chard PS, Bleakman D, Christakos S, Fullmer CS, Miller RJ. Calcium buffering properties of calbindin D28k and parvalbumin in rat sensory neurones. J Physiol 1993;472(1):341–57.
[48] Funke K, Benali A. Modulation of cortical inhibition by rTMS – findings obtained from animal models. J Physiol 2011;589(18):4423–35.
[49] Li C-T, Chen M-H, Juan C-H, et al. Efficacy of prefrontal theta-burst stimulation in refractory depression: a randomized sham-controlled study. Brain 2014;137(7):2088–98.
[50] Talelli P, Greenwood RJ, Rothwell JC. Exploring Theta Burst Stimulation as an intervention to improve motor recovery in chronic stroke. Clin Neurophysiol 2007;118(2):333–42.
[51] Juszczak K, Kaszuba-Zwoinska J, Thor PJ. Pulsating electromagnetic field stimulation of urothelial cells induces apoptosis and diminishes necrosis: new insight to magnetic therapy in urology. J Physiol Pharmacol 2012;63(4):397–401.
[52] Hattori T, Takei N, Mizuno Y, Kato K, Kohsaka S. Neurotrophic and neuroprotective effects of neuron-specific enolase on cultured neurons from embryonic rat brain. Neurosci Res 1995;21(3):191–8.
[53] Lezoualc'h F, Engert S, Berning B, Behl C. Corticotropin-releasing hormone-mediated neuroprotection against oxidative stress is associated with the increased release of non-amyloidogenic amyloid β precursor protein and with the suppression of nuclear factor-κB. Mol Endocrinol 2000;14(1):147–59.
[54] Seo Y-W, Shin JN, Ko KH, et al. The molecular mechanism of noxa-induced mitochondrial dysfunction in p53-mediated cell death. J Biol Chem 2003;278(48):48292–9.
[55] Thangaraju M, Kaufmann SH, Couch FJ. BRCA1 facilitates stress-induced apoptosis in breast and ovarian cancer cell lines. J Biol Chem 2000;275(43):33487–96.
[56] Agarwal R, Agarwal P. Glaucomatous neurodegeneration: an eye on tumor necrosis factor-alpha. Indian J Ophthalmol 2012;60:255–61.
[57] Weitzman JB, Fiette L, Matsuo K, Yaniv M. JunD protects cells from p53-dependent senescence and apoptosis. Mol Cell 2000;6(5):1109–19.
[58] Vincent AM, Russell JW, Sullivan KA, et al. SOD2 protects neurons from injury in cell culture and animal models of diabetic neuropathy. Exp Neurol 2007;208(2):216–27.
[59] Zhang L, Liu W, Szumlinski KK, Lew J. p10, the N-terminal domain of p35, protects against CDK5/p25-induced neurotoxicity. Proc Natl Acad Sci U S A 2012;109(49):20041–6.
[60] Bates KA, Clark VW, Meloni BP, Dunlop SA, Rodger J. Short-term low intensity PMF does not improve functional or histological outcomes in a rat model of transient focal cerebral ischemia. Brain Res 2012;1458(0):76–85.
[61] Ma J, Zhang Z, Su Y, et al. Magnetic stimulation modulates structural synaptic plasticity and regulates BDNF–TrkB signal pathway in cultured hippocampal neurons. Neurochem Int 2013;62(1):84–91.
[62] Gerschlager W, Siebner HR, Rothwell JC. Decreased corticospinal excitability after subthreshold 1 Hz rTMS over lateral premotor cortex. Neurology 2001;57(3):449–55.
[63] Majewska AK, Newton JR, Sur M. Remodeling of synaptic structure in sensory cortical areas in vivo. J Neurosci March 15, 2006;26(11):3021–9.
[64] Vlachos A, Müller-Dahlhaus F, Rosskopp J, Lenz M, Ziemann U, Deller T. Repetitive magnetic stimulation induces functional and structural plasticity of excitatory postsynapses in mouse organotypic hippocampal slice cultures. J Neurosci 2012;32(48):17514–23.
[65] Malik AR, Urbanska M, Gozdz A, et al. Cyr61, a matricellular protein, is needed for dendritic arborization of hippocampal neurons. J Biol Chem 2013;288(12):8544–59.
[66] Huang J, Ye Z, Hu X, Lu L, Luo Z. Electrical stimulation induces calcium-dependent release of NGF from cultured Schwann cells. Glia 2010;58(5):622–31.
[67] McCreary CR, Dixon SJ, Fraher LJ, Carson JJL, Prato FS. Real-time measurement of cytosolic free calcium concentration in Jurkat cells during ELF magnetic field exposure and evaluation of the role of cell cycle. Bioelectromagnetics 2006;27(5):354–64.
[68] Hulme SR, Jones OD, Ireland DR, Abraham WC. Calcium-dependent but action potential-independent BCM-like metaplasticity in the Hippocampus. J Neurosci 2012;32(20):6785–94.
[69] Gersner R, Kravetz E, Feil J, Pell G, Zangen A. Long-term effects of repetitive transcranial magnetic stimulation on markers for neuroplasticity: differential outcomes in anesthetized and awake animals. J Neurosci 2011;31(20):7521–6.
[70] Allen EA, Pasley BN, Duong T, Freeman RD. Transcranial magnetic stimulation elicits coupled neural and hemodynamic consequences. Science 2007;317(5846):1918–21.

Resumé

Les champs électromagnétiques sont couramment utilisés pour stimuler de manière non-invasive le cerveau humain soit à des fins thérapeutiques ou dans un contexte de recherche. Les effets de la stimulation magnétique varient en fonction de la fréquence et de l'intensité du champ magnétique. Les mécanismes mis en jeu restent inconnus, d'autant plus lors de stimulations à faible intensité.

Dans cette thèse, nous avons évalué les effets de stimulations magnétiques répétées à différentes fréquences appliqués à faible intensité (10-13 mT ; Low Intensity Repetitive Magnetic Stimulation : LI-rMS) *in vitro,* sur des cultures corticales primaires et sur des modèles de réparation neuronale. De plus, nous décrivons une méthodologie pour la construction d'un dispositif instrumental fait sur mesure pour stimuler des cultures cellulaires.

Les résultats montrent des effets dépendant de la fréquence sur la libération du calcium des stocks intracellulaires, sur la mort cellulaire, sur la croissance des neurites, sur la réparation neuronale, sur l'activation des neurones et sur l'expression de gènes impliqués.

En conclusion, nous avons montré pour la première fois un nouveau mécanisme d'activation cellulaire par les champs magnétiques à faible intensité. Cette activation se fait en l'absence d'induction de potentiels d'action. Les résultats soulignent l'importance biologique de la LI-rMS par elle-même mais aussi en association avec les effets de la rTMS à haute intensité. Une meilleure compréhension des effets fondamentaux de la LI-rMS sur les tissus biologiques est nécessaire afin de mettre au point des applications thérapeutiques efficaces pour le traitement des conditions neurologiques.

Mots clés : [stimulation magnétique, LI-rMS, neurones corticales, réparation neuronale, calcium intracellulaire, rTMS, in vitro, instrument]